

AD-A140 983

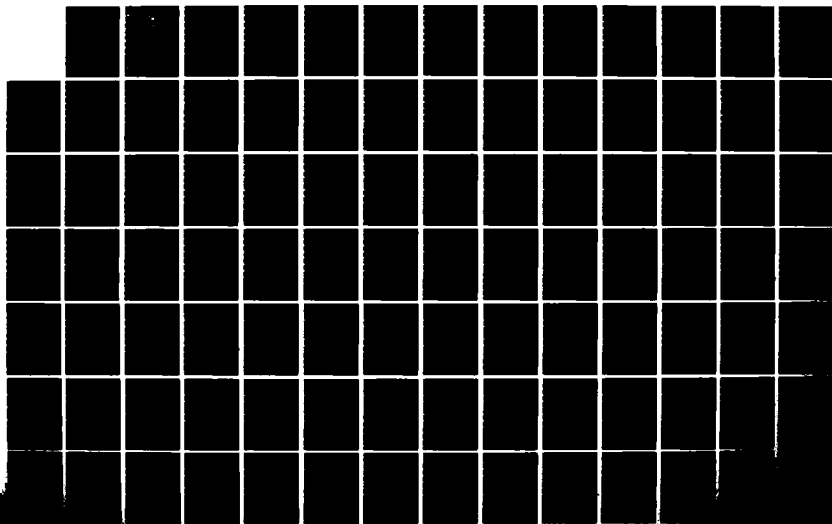
MULTIVARIABLE DIGITAL FLIGHT CONTROL DESIGN OF THE
X-29A(U) AIR FORCE INST OF TECH WRIGHT-PATTERSON AFB OH
SCHOOL OF ENGINEERING R S FELDMANN MAR 84
AFIT/GE/EE/84M-3

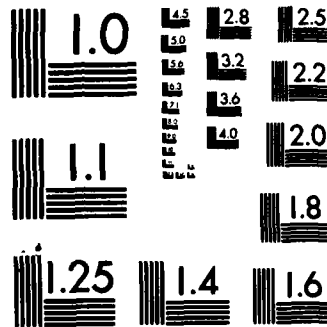
1/4

UNCLASSIFIED

F/G 1/3

NL





MICROCOPY RESOLUTION TEST CHART
NATIONAL BUREAU OF STANDARDS-1963-A

DDC ①

AD-A140 983



DESIGN OF THE X-29A

THESIS

AFIT/GE/EE/84M-3

Roger S Feldmann
2Lt USAF

DTIC FILE COPY

DTIC

MAY 15 84

DEPARTMENT OF THE AIR FORCE
AIR UNIVERSITY (ATC)

AIR FORCE INSTITUTE OF TECHNOLOGY

Wright-Patterson Air Force Base, Ohio

MULTIVARIABLE DIGITAL FLIGHT CONTROL

DESIGN OF THE X-29A

THESIS

AFIT/GE/EE/84M-3 Roger S Feldmann
 2Lt USAF

Approved for public release; distribution unlimited.

DTIC
GPO 1984

MULTIVARIABLE DIGITAL FLIGHT CONTROL DESIGN
OF THE X-29A

THESIS

Presented to the Faculty of the School of Engineering
of the Air Force Institute of Technology
Air University
in Partial Fulfillment of the
Requirements for the Degree of
Master of Science

by

Roger S. Feldmann

2Lt USAF

Graduate Engineering

March 1984

Accession For	
NTIS GSA&I	<input checked="" type="checkbox"/>
DTIC TAB	<input type="checkbox"/>
Unannounced	<input type="checkbox"/>
Justification	
BY _____	
Distribution/	
Availability Codes	
Dist _____	
A-1	

PREFACE

This thesis is an initial design attempt for the X-29A demonstrator aircraft. This thesis was sponsored by the Flight Control Laboratory.

I thank my thesis advisor, Dr. John J. D'Azzo, for his assistance and suggestions. I also wish to thank my colleagues Lt Jeffrey Simmers, Capt William Locken, Lt Marc Hoffman, and Lt Brian Mayhew who produced theses applying Porter's method also. Thanks also to Capt David Potts, Mr. Finley Barfield, Capt Stan Fuller, and others at the Air Force Flight Dynamics Laboratory's Flight Control Division. I wish to also thank Capt John West and others at NASA-DRYDEN at Edwards AFB.

Special thanks to my family for their encouragement and understanding.

2Lt Roger S. Feldmann

CONTENTS

Title	Page
Preface.....	ii
List of Figures.....	v
List of Tables.....	vii
Abbreviations and Symbols.....	x
Abstract.....	xi
 I. Introduction.....	 1
Background.....	1
Problem.....	3
Scope.....	3
Assumptions.....	4
Sequence of Presentation.....	4
 II. Multivariable Control Theory Using Singular Perturbation Methods.....	 6
Introduction.....	6
Known Plant- Regular Design.....	10
Known Plant- Irregular Design.....	15
 III. The X-29A Demonstrator.....	 21
Aerodynamics.....	21
Close-Coupled Canards.....	24
Strake-Flaps.....	25
Wing Composition and Shape.....	25
Variable Camber.....	26
Common Components.....	27
Fly-by-Wire.....	29
Relaxed Stability.....	29
Summary.....	31
 IV. Longitudinal Controller Designs.....	 33
Introduction.....	33
Description of Maneuvers.....	36
Development of Aircraft Model.....	39
Application of Porter's Method.....	45
Results.....	51
Summary.....	78

V.	Lateral Controller Designs.....	84
	Introduction.....	84
	Description of Maneuvers.....	85
	Application of Porter's Method.....	87
	Development of Minimum-Gain Robust Controller..	92
	Evaluation of Selected Design Parameters.....	95
	Beta-pointing.....	96
	Coordinated turn.....	111
	Summary.....	121
VI.	Conclusions and Recommendations.....	128
	General Comments.....	128
	Conclusions.....	134
	Recommendations.....	139
	Suggestions for improvements.....	139
	Design algorithms.....	142
	Future designs for the X-29A.....	148
	Bibliography.....	151
	Appendix A: Other Design Approaches.....	153
	Longitudinal Designs.....	153
	Lateral Designs.....	155
	Data set2.....	156
	Appendix B: Additional Longitudinal Results.....	157
	Direct Climb.....	157
	Direct Lift1.....	171
	Direct Lift2.....	183
	Pitch-Pointing.....	195
	Vertical Translation1.....	207
	Vertical Translation2.....	219
	Appendix C: Additional Lateral Results.....	226
	Beta-Pointing.....	231
	Coordinated Turn.....	247
	Appendix D: State-Space Matrices.....	266
	Appendix E: Design Parameters and Commanded Inputs....	274
	Appendix F: Controller Matrices.....	282
	Appendix G: Figures of Merit.....	290
	Appendix H: Control Input Rates.....	298
	Vita.....	307

LIST OF FIGURES

Figures	Title	Page
2-1	Proportional Plus Integral Controller	9
2-2	System Block Diagram-Continuous Design	17
2-3	System Block Diagram-Discrete Design	18
3-1	The X-29A, FSW Aircraft	22
3-2	Active Camber Increases FSW Longitudinal Static Stability	28
3-3	X-29A Longitudinal Stability	30
4-1	Direct Climb;1.2 Mach, 15 000 Feet	57
4-2	Direct Climb;1.2 Mach, 15 000 Feet	58
4-3	Direct Climb;1.2 Mach, 15 000 Feet	59
4-4	Direct Climb;1.2 Mach, 15 000 Feet	60
4-5	Direct Lift1;1.2 Mach, 15 000 Feet	63
4-6	Direct Lift1;1.2 Mach, 15 000 Feet	64
4-7	Direct Lift1;1.2 Mach, 15 000 Feet	65
4-8	Direct Lift2;1.2 Mach, 15 000 Feet	67
4-9	Direct Lift2;1.2 Mach, 15 000 Feet	68
4-10	Direct Lift2;1.2 Mach, 15 000 Feet	69
4-11	Pitch-Pointing;1.2 Mach, 15 000 Feet	71
4-12	Pitch-Pointing;1.2 Mach, 15 000 Feet	72
4-13	Pitch-Pointing;1.2 Mach, 15 000 Feet	73
4-14	Vertical Translation1;1.2 Mach,15 000 Feet	75
4-15	Vertical Translation1;1.2 Mach,15 000 Feet	76
4-16	Vertical Translation1;1.2 Mach,15 000 Feet	77
4-17	Vertical Translation2;1.2 Mach,15 000 Feet	79
4-18	Vertical Translation2;1.2 Mach,15 000 Feet	80
4-19	Vertical Translation2;1.2 Mach,15 000 Feet	81
5-1	Beta-Pointing;1.2 Mach, 15 000 Feet	102
5-2	Beta-Pointing;1.2 Mach, 15 000 Feet	103
5-3	Beta-Pointing;1.2 Mach, 15 000 Feet	105
5-4	Beta-Pointing;1.2 Mach, 15 000 Feet	106
5-5	Beta-Pointing;1.2 Mach, 15 000 Feet	108
5-6	Coordinated Turn;1.2 Mach, 15 000 Feet	113
5-7	Coordinated Turn;1.2 Mach, 15 000 Feet	114
5-8	Coordinated Turn;1.2 Mach, 15 000 Feet	115
5-9	Coordinated Turn;1.2 Mach, 15 000 Feet	117
5-10	Coordinated Turn;1.2 Mach, 15 000 Feet	119
5-11	Coordinated Turn;1.2 Mach, 15 000 Feet	120
6-1	System Block Diagram-Discrete Design With Sensor Noise	130
6-2	System Block Diagram-Discrete Design With State Noise	133

LIST OF FIGURES

(Continued)

Figures		Page
B-1 to B-14	Direct Climb;0.4 Mach, sea level;0.9 Mach 50 000 feet;0.7 Mach, 15 000 feet; 0.9 Mach, sea level	157 170
B-15 to B-26	Direct Lift1;0.4 Mach, sea level;0.9 Mach, 50 000 feet;0.7 Mach, 15 000 feet; 0.9 Mach, sea level	171 182
B-27 to B-38	Direct Lift2;0.4 Mach, sea level;0.9 Mach, 50 000 feet;0.7 Mach, 15 000 feet; 0.9 Mach, sea level	183 194
B-39 to B-50	Pitch-Pointing;0.4 Mach, sea level;0.9 Mach, 50 000 feet;0.7 Mach, 15 000 feet; 0.9 Mach, sea level	195 206
B-51 to B-62	Vertical Translation1;0.4 Mach, sea level; 0.9 Mach, 50 000 feet;0.7 Mach, 15 000 feet;0.9 Mach, sea level	207 218
B-63 to B-74	Vertical Translation2;0.4 Mach, sea level; 0.9 Mach, 50 000 feet;0.7 Mach, 15 000 feet;0.9 Mach, sea level	219 230
C-1 to C-16	Beta-Pointing;0.4 Mach, sea level;0.9 Mach, 50 000 feet;0.7 Mach, 15 000 feet;0.9 Mach, sea level	231 246
C-17 to C-35	Coordinated-Turn;0.4 Mach, sea level;0.9 Mach, 50 000 feet;0.7 Mach, 15 000 feet; 0.9 Mach, sea level	247 265

LIST OF TABLES

Table	Title	Page
2-1	Asymptotic Equations For Zero-B Form 2	13
2-1	Asymptotic Equations For Zero-B Form 2	14
4-1	Design Parameters	52
4-2	Controller Matrices	53
4-3	Figures Of Merit	54
4-4	Control Input Rates	55
5-1	Design Parameters	96
5-2	Controller Matrices	97
5-3	Figures Of Merit	98
5-4	Control Input Rates	99
D-1	Longitudinal State-Space Matrices; 0.4 Mach, sea level	266
D-2	Longitudinal State-Space Matrices; 0.9 Mach, 50 000 feet	267
D-3	Longitudinal State-Space Matrices; 0.7 Mach, 15 000 feet	268
D-4	Longitudinal State-Space Matrices; 0.9 Mach, sea level	269
D-5	Lateral State-Space Matrices; 0.4 Mach, sea level	270
D-6	Lateral State-Space Matrices; 0.9 Mach, 50 000 feet	271
D-7	Lateral State-Space Matrices; 0.7 Mach, 15 000 feet	272
D-8	Lateral State-Space Matrices; 0.9 Mach, sea level	273
E-1	Design Parameters and Commanded Inputs For Longitudinal Controller; 0.4 Mach, sea level	274
E-2	Design Parameters and Commanded Inputs For Longitudinal Controller; 0.9 Mach, 50 000 feet	275
E-3	Design Parameters and Commanded Inputs For Longitudinal Controller; 0.7 Mach, 15 000 feet	276
E-4	Design Parameters and Commanded Inputs For Longitudinal Controller; 0.9 Mach, sea level	277

LIST OF TABLES

(Continued)

Table		Page
E-5	Design Parameters and Commanded Inputs For Lateral Controller; 0.4 Mach, sea level	278
E-6	Design Parameters and Commanded Inputs For Lateral Controller; 0.9 Mach, 50 000 feet	279
E-7	Design Parameters and Commanded Inputs For Lateral Controller; 0.7 Mach, 15 000 feet	280
E-8	Design Parameters and Commanded Inputs For Lateral Controller; 0.9 Mach, sea level	281
F-1	Longitudinal Controller Matrices; 0.4 Mach, sea level	282
F-2	Longitudinal Controller Matrices; 0.9 Mach, 50 000 feet	283
F-3	Longitudinal Controller Matrices; 0.7 Mach, 15 000 feet	284
F-4	Longitudinal Controller Matrices; 0.9 Mach, sea level	285
F-5	Lateral Controller Matrices; 0.4 Mach, sea level	286
F-6	Lateral Controller Matrices; 0.9 Mach, 50 000 feet	287
F-7	Lateral Controller Matrices; 0.7 Mach, 15 000 feet	288
F-8	Lateral Controller Matrices; 0.9 Mach, sea level	289
G-1	Longitudinal Figures of Merit; 0.4 Mach, sea level	290
G-2	Longitudinal Figures of Merit; 0.9 Mach, 50 000 feet	291
G-3	Longitudinal Figures of Merit; 0.7 Mach, 15 000 feet	292
G-4	Longitudinal Figures of Merit; 0.9 Mach, sea level	293
G-5	Lateral Figures of Merit; 0.4 Mach, sea level	294
G-6	Lateral Figures of Merit; 0.9 Mach, 50 000 feet	295
G-7	Lateral Figures of Merit; 0.7 Mach, 15 000 feet	296
G-8	Lateral Figures of Merit; 0.9 Mach, sea level	297

LIST OF TABLES

(Continued)

Table		Page
H-0	Control Input Deflections and Rates	298
H-1	Longitudinal Control Input Rates; 0.4 Mach, sea level	299
H-2	Longitudinal Control Input Rates; 0.9 Mach, 50 000 feet	300
H-3	Longitudinal Control Input Rates; 0.7 Mach, 15 000 feet	301
H-4	Longitudinal Control Input Rates; 0.9 Mach, sea level	302
H-5	Lateral Control Input Rates; 0.4 Mach, sea level	303
H-6	Lateral Control Input Rates; 0.9 Mach, 50 000 feet	304
H-7	Lateral Control Input Rates; 0.7 Mach, 15 000 feet	305
H-8	Lateral Control Input Rates; 0.9 Mach, sea level	306

ABBREVIATIONS AND SYMBOLS

A	plant matrix
B	input matrix
C	output matrix
K, K_0, K_1	controller matrices
M	measurement
T	sampling period
$C A^{k-1} B$	k-th Markov parameter
$G(\lambda)$	system matrix
$\Gamma(\lambda)$	asymptotic transfer function matrix
e	error vector
f	sampling frequency
g	gain parameter
u	control input vector
v	command input vector
w	measurement vector
x	state vector
y	output vector
z	integral of error vector
m	number of inputs
n	number of states
p	number of outputs
Z_t	transmission zeros

ABSTRACT

✓ Multivariable design techniques developed by Professor Brian Porter of the University of Salford, England are applied to the X-29A forward swept-wing demonstrator. The aircraft model is in a linearized state-space form at a number of different flight conditions. The computer aided design program MULTI is used to develop the control laws.

Separate longitudinal and lateral controllers are developed for each of eight maneuvers of five different flight conditions: 0.4 Mach, 0k ft; 0.9 Mach, 50k ft; 1.2 Mach, 15k ft; 0.7 Mach, 15k ft; and 0.9 Mach, 0k ft. A universal lateral controller that is effective for all maneuvers at all flight conditions is developed. Finally, a universal lateral controller requiring only three distinct gains is developed. This minimum gain universal lateral controller produces minimal degradation of response, while permitting the elimination of gain scheduling usually required of digital flight controllers. In addition, maximum possible maneuvers are performed without exceeding control input limitations.

Suggestions for improving MULTI to allow artificial intelligence algorithms are discussed. These would enable the designer to determine the number of point designs required to satisfactorily cover the flight envelope, and at the same time provide the designer with the capability of designing for many points with minimal effort.

CHAPTER I

INTRODUCTION

Background

Future aircraft will probably use digital computers for a number of functions. Integrated fire/flight control, navigation, threat assessment/management, and weapons delivery are areas which show great promise. Digital computers offer reduced weight and cost with improved performance. Future aircraft will use more control inputs in order to achieve greater maneuverability. An increase in the number of control surfaces means an increase in pilot workload that can be eased with digital flight control.

Future fighters will achieve this greater maneuverability only with a corresponding decline in static stability. This means that, without proper control, future fighters will be unstable. Since no pilot can continuously provide compensating inputs to an inherently unstable aircraft, digital computers will have to control the aircraft for him. The ability of computers to solve complicated algorithms in a short time also offers the opportunity for new maneuvers, called control-configured vehicle (CCV) maneuvers, that are now possible with multiple control surfaces.

Since computers, or controllers, will stabilize and control the aircraft, the question arises as to the best method

for designing these complex flight-control algorithms. Classical control theory designs, which examine single-input/single-output systems (SISO), are ill-suited for multiple-input/multiple-output systems. As more and more inputs are added more trial and error is required in the design. Linear quadratic gaussian (LQG) techniques can be applied to MIMO systems, but the states must be known or estimated. Unfortunately, no known algorithms exist for choosing the proper weighting elements, and much trial-and-error and insight obtained from experience must be employed.

Professor Brian Porter of the University of Salford, U. K. has developed a design method that can synthesize digital flight controllers. Porter's method decouples the outputs while minimizing the trial-and-error or tuning required. This thesis is a third generation attempt to apply Porter's method to aircraft. Many improvements and refinements are added to the computer-aided-design (CAD) program MULTI. This thesis suggests a number of future possible improvements to MULTI that would eliminate most of the trial-and-error presently required. This would change the design engineer's role to that of selecting the best computer-generated designs, rather than trying to generate them himself. These algorithms offer the ability for a single design engineer to synthesize a longitudinal/lateral controller with sensors, actuators, and lags for the entire flight envelope within a short time period.

Grumman Aerospace Corporation is developing a demonstrator aircraft under the auspices of the Defense Advanced Research

Projects Agency (DARPA). The demonstrator, the X-29A, incorporates a number of advanced technology features. These features include composite materials, variable camber wings, forward swept wings, fly-by-wire, and close-coupled canards.

Problem

This thesis first develops a controller using Porter's method for each of six longitudinal maneuvers at five flight conditions. Next, a controller for each of two lateral maneuvers at five flight conditions is developed. A robust controller, capable of producing good responses for both lateral maneuvers at all flight conditions, is developed. Finally, a robust lateral controller requiring only three distinct gains is developed. The outputs, control surface deflections, control surface rates, and states of interest are examined and compared for different flight conditions and controllers. The flight conditions chosen are 0.4 Mach, 0k feet; 0.9 Mach, 50k feet; 1.2 Mach, 15k feet; 0.7 Mach, 15k feet; and 0.9 Mach, 0k feet. The longitudinal maneuvers performed are direct climb, two direct lifts, pitch-pointing, and two vertical translations. The lateral maneuvers performed are beta-pointing and coordinated turn. In each case the maximum possible maneuver without exceeding control input limits is performed.

Scope

Lastly, this thesis incorporates improvements made to MULTI. Because of the large number of maneuvers and flight conditions, the models used do not include sensors, actuators, lags, or control input rate limitations. However, these improvements can easily be added by using MULTI to adjust the

controller to accomodate these refinements. Since the ability to determine easily the input rates was not added to MULTI until after the design work was completed, the controller and maximum inputs were not adjusted. The rates are presented, though, and where they exceed allowable maximums, can be decreased by reducing the maximum steady-state input or lengthening the time the aircraft has to perform the maneuver. This is easily done and does not require retuning the controller. Because of limited time, no attempt was made to develop a robust longitudinal controller, but the data necessary to do so are included.

Assumptions

Grumman developed a nonlinear simulation program for the X-29A. Linearized data in state-space form at five flight conditions is used. Specifically, "data set #3", first promulgated in August 1983 is used.

The controllers synthesized in this thesis are developed using the latest MULTI version released in August 1983. MULTI is written in FORTRAN and is run on the CDC-6600 computer system at AFIT. Calcomp plotters are used to produce the plots in this thesis, although plots at the terminal are also available. Note that MULTI is an interactive design tool, allowing the engineer many design iterations in a short span of time.

Sequence of Presentation

Chapter II briefly describes the theory used to develop MULTI and provides a list of references for the serious inte-

rested industrious reader. Chapter III describes the X-29A. Chapter IV details the design process for the longitudinal controllers and presents results. Chapter V details the design process for the lateral controllers and presents results. In addition a single robust lateral controller requiring only three gains is obtained for all maneuvers at all five flight conditions. Chapter VI summarizes the results achieved in the thesis, gives recommendations for future work, and details a class of future possible additions to MULTI to improve results and greatly improve productivity.

CHAPTER II

MULTIVARIABLE CONTROL LAWS USING SINGULAR PERTURBATION METHODS

Introduction

The designs presented in Chapters IV and V are obtained using the interactive computer-aided-design (CAD) tool MULTI. MULTI implements the multivariable control laws developed by Professor Brian Porter of the University of Salford, England. This chapter gives a brief introduction to two of the design methods used to obtain high performance tracking systems for the X-29A.

It should be noted that the continuous-time methods have a corresponding discrete-time method with no loss of generality. It is advantageous to examine the designs in the continuous-time method because it is conceptually easier to consider pole and transmission zero locations in the s -plane than the z -plane. Before accepting the discrete design, sampling effects and time delays must be considered (Ref 1:58-77).

The state and output equations are described by first-order linear differential equations written in state-space format:

$$\dot{\underline{x}} = \underline{Ax} + \underline{Bu} \quad (2-1)$$

$$\underline{y} = \underline{Cx} \quad (2-2)$$

where

A = the continuous-time plant matrix ($n \times n$)

B = the continuous-time control matrix ($n \times m$)

C = the continuous-time output matrix ($p \times n$)

x = state vector ($n \times 1$)

y = output vector ($p \times 1$)

u = control input vector ($m \times 1$)

Note that Porter's method does not allow a feedforward matrix (D). For systems containing a D matrix, a satisfactory equivalent representation may be obtained by redefining the control inputs as states. This imbeds the D matrix into the C matrix and causes the actuator inputs to become the new control inputs. This transformation is often necessary for systems that have accelerations as outputs.

The proportional plus integral (PI) cascade compensator performs both tracking and disturbance rejection. The results in this thesis are obtained using a discrete-time PI implementation in MULTI. The equivalent digital equations are:

$$\underline{x}[(k+1)T] = \exp\{\underline{A}T\} * \underline{x}(kT) + \int_0^T \exp\{\underline{A}T\} * \underline{B}dt * \underline{u}(kT) \quad (2-3)$$

$$\underline{y}[kT] = \underline{C} * \underline{x}(kT) \quad (2-4)$$

where

$\exp\{\underline{A}T\}$ = sampled data plant matrix

$\int_T^0 \exp\{\underline{A}T\} * \underline{B}dt$ = sampled data control matrix

\underline{C} = sampled data output matrix

T = sampling period

Since $u(kT)$ is piecewise constant over the sample period, it may be moved outside of the integral (Ref 2:7-24). Figure

2-1 shows the PI controller. MULTI implements two samplers, one in the feedback loop from the plant, and the other in the commanded input. The single sampler shown in Figure 2-1 is equivalent to the other two implemented in MULTI.

The A, B, and C matrices are partitioned in the following manner:

$$\begin{bmatrix} \dot{\underline{x}}_1 \\ \dot{\underline{x}}_2 \end{bmatrix} = \begin{bmatrix} \underline{A}_{11} & \underline{A}_{12} \\ \underline{A}_{21} & \underline{A}_{22} \end{bmatrix} \begin{bmatrix} \underline{x}_1 \\ \underline{x}_2 \end{bmatrix} + \begin{bmatrix} \underline{B}_1 \\ \underline{B}_2 \end{bmatrix} \underline{u} \quad (2-5)$$

$$\underline{y} = \begin{bmatrix} \underline{C}_1 & \underline{C}_2 \end{bmatrix} \begin{bmatrix} \underline{x}_1 \\ \underline{x}_2 \end{bmatrix} \quad (2-6)$$

where \underline{A}_{11} is a matrix of order $((n-m) \times (n-m))$

where \underline{A}_{22} , \underline{C}_2 , and \underline{B}_2 are matrices of order $(m \times m)$

(Ref 3:39).

A restriction of Porter's method is that the number of inputs must be equal to the number of outputs. Control inputs for the X-29A aircraft model refer to canards, symmetrical flaperons, strake-flaperons, thrust, rudder, and differential flaperons. Outputs for the X-29A are selected states.

Two design methods, Regular and Irregular, are presented. The Regular design method is applied to the longitudinal state-space equations while the Irregular de-

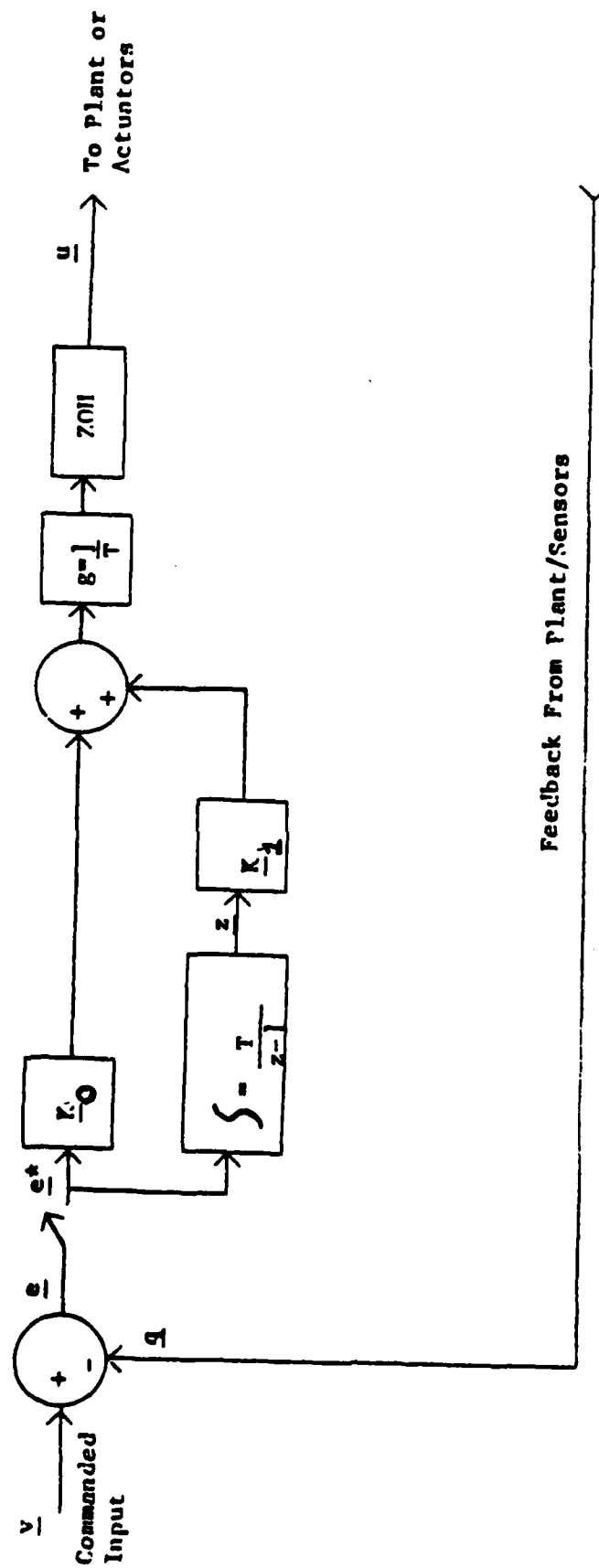


Figure 2-1 Proportional Plus Integral (PI) Controller

sign method is applied to the lateral state-space equations.

A major advantage of Porter's method is that output feedback is used. Consequently, not all the states must be known, just those selected in an Irregular design.

Known Plant- Regular Design

A Regular system has the product $[CB]$ equal to the number of outputs. Thus the system has a first Markov parameter of maximal rank and minimum phase. $[CB]$ must have full rank (be nonsingular) so that it is invertible (Ref 3:7).

A requirement of Porter's method is that the system be controllable (A, B a controllable pair) and observable (A, C an observable pair). In addition, the matrix

$$\underline{P} = \begin{bmatrix} \underline{A} & \underline{B} \\ -\underline{C} & \underline{0} \end{bmatrix} \quad (2-7)$$

must have full rank to assure controllability using the PI controller.

The control law for the digital controller is given by:

$$\underline{u}(kT) = (1/T) \left[\underline{K}_0 \underline{e}(kT) + \underline{K}_1 \underline{z}(kT) \right] \quad (2-8)$$

where

\underline{K}_0 is the proportional gain matrix for the error signal $\underline{e}(kT)$

\underline{K}_1 is the gain matrix for the backward difference of the error signal, which is designated as $\underline{z}(kT)$.

Equivalently, in the continuous case:

$$\underline{u} = g(\underline{K}_0 \underline{e} + \underline{K}_1 \int \underline{e} dt) \quad (2-9)$$

where

g is the forward path gain

\underline{K}_0 is the proportional gain for the error signal

\underline{K}_1 is the gain for the integral for the error signal.

For the discrete case:

$$\underline{e}(kT) = \underline{v}(kT) - \underline{y}(kT) \quad (2-10)$$

$$\underline{z}[(k+1)T] = \underline{z}(kT) + T \underline{e}(kT) \quad (2-11)$$

The controller matrices are as follows:

$$\underline{K}_0 = \underline{A}(\underline{C}_2 \underline{B}_2)^{-1} \underline{\Sigma} \quad (2-12)$$

$$\underline{K}_1 = (\underline{C}_2 \underline{B}_2)^{-1} \underline{\Sigma} \quad (2-13)$$

where

$$\underline{\Sigma} = \text{diagonal matrix } \{\sigma_1, \sigma_2, \dots, \sigma_p\}$$

Note that the cascade vector integrator drives the steady state error vector to zero for a constant command input vector. The state derivative is driven to zero for all cases except where an output is the derivative of one of the states. For example, in the longitudinal mode if pitch rate q is commanded as a step then the state derivative of pitch angle will reach the commanded value. This causes a transmission zero at the origin. For this case, if an Irregular design is used, the state derivative must not be chosen to be fed back.

When Porter's method is applied, it may be desirable but

not necessary for the B matrix in equation (2-4) to be in the form $\begin{bmatrix} 0 \\ \underline{B} \\ -2 \end{bmatrix}$. MULTI accepts either form.

For the continuous case, as the gain factor g increases to infinity in the limit, the system transfer matrix given as follows:

$$\underline{G}(s) = \underline{C}(s\underline{I} - \underline{A})^{-1}\underline{B} \quad (2-14)$$

assumes an asymptotic form

$$\underline{\Gamma}(\lambda) = \tilde{\underline{\Gamma}}(\lambda) + \hat{\underline{\Gamma}}(\lambda) \quad (2-15)$$

where

$\tilde{\underline{\Gamma}}(\lambda)$ is the "slow" transfer function matrix

$\hat{\underline{\Gamma}}(\lambda)$ is the "fast" transfer function matrix

The roots of these transfer functions are grouped into three categories as Z_1 , Z_2 , and Z_3 . The slow modes are the roots in Z_1 and Z_2 . As the gain factor increases in the limit, the poles of Z_1 become uncontrollable while the poles of Z_2 become unobservable. As this occurs, the fast modes corresponding to Z_3 increasingly dominate the system response. Expressions for the asymptotic modes are given in Table 2-1 (Ref 1:69-70). Therefore, as the sampling period T approaches zero, the closed-loop transfer function becomes:

Table 2-1

Asymptotic Equations for Zero-B₂ Form

System is represented by:

$$\begin{bmatrix} \dot{x}_1 \\ \dot{x}_2 \end{bmatrix} = \begin{bmatrix} \hat{A}_{11} & \hat{A}_{12} \\ \hat{A}_{21} & \hat{A}_{22} \end{bmatrix} \begin{bmatrix} x_1 \\ x_2 \end{bmatrix} + \begin{bmatrix} 0 \\ \hat{B}_2 \end{bmatrix} u \quad \text{and} \quad y = \begin{bmatrix} \hat{C}_1 & \hat{C}_2 \end{bmatrix} \begin{bmatrix} x_1 \\ x_2 \end{bmatrix}$$

Continuous Case

Gain Factor = g

(Poles are in the s-plane)

$$\tilde{r}(\lambda) = C_0(\lambda I_n - A_0)^{-1} B_0 = 0$$

$$\hat{r}(\lambda) = (\lambda I_m + g \hat{C}_2 \hat{B}_2 K_0)^{-1} g \hat{C}_2 \hat{B}_2 K_0$$

(Finite roots)

$$Z_1 = \{ |\lambda K_0 + K_1| = 0 \}$$

$$Z_2 = \{ |\lambda I_{n-m} - \hat{A}_{11} + \hat{A}_{12} \hat{C}_2^{-1} \hat{C}_1| = 0 \}$$

(Infinite roots)

$$Z_3 = \{ |\lambda I_m + g \hat{C}_2 \hat{B}_2 K_0| = 0 \}$$

Discrete Case

Gain Factor = 1/T

(Poles are in the z-plane)

$$\tilde{r}(\lambda) = C_0(\lambda I_n - A_0)^{-1} B_0$$

$$\hat{r}(\lambda) = (\lambda I_m - I_m + \hat{C}_2 \hat{B}_2 K_0)^{-1} \hat{C}_2 \hat{B}_2 K_0$$

$$Z_1 = \{ |\lambda I_m - I_m + T K_0^{-1} K_1| = 0 \}$$

$$Z_2 = \{ |\lambda I_{n-m} - T \hat{A}_{11} + \hat{A}_{12} \hat{C}_2^{-1} \hat{C}_1| = 0 \}$$

$$Z_3 = \{ |\lambda I_m - I_m + \hat{C}_2 \hat{B}_2 K_0| = 0 \}$$

Table 2-1(continued)

where:

$$\underline{A}_0 = \left[\begin{array}{c|c} -\underline{K}_0^{-1} \underline{K}_1 & 0 \\ \hline \underline{A}_{12} \underline{C}_2^{-1} \underline{K}_0^{-1} \underline{K}_1 & \underline{A}_{11} - \underline{A}_{12} \underline{C}_2^{-1} \underline{C}_1 \end{array} \right]$$

$$\underline{B}_0 = \left[\begin{array}{c|c} 0 & \\ \hline \underline{A}_{12} \underline{C}_2^{-1} & \end{array} \right]$$

$$\underline{C}_0 = [\underline{K}_0^{-1} \underline{K}_1 \mid 0]$$

$$\underline{\Gamma}(\lambda) = \underline{\Gamma}(\lambda) = (\lambda \underline{I}_p - \underline{I}_p + \frac{C}{2} \frac{B}{2} \frac{K}{0})^{-1} \frac{C}{2} \frac{B}{2} \frac{K}{0} \quad (2-16)$$

Thus if $\frac{K}{0}$ is chosen as follows:

$$\frac{C}{2} \frac{B}{2} \frac{K}{0} = \text{diagonal matrix } \{\sigma_1, \sigma_2, \dots, \sigma_p\} = \underline{\Sigma}$$

then

$$\underline{\Gamma}(\lambda) = \text{diagonal matrix } \{\sigma_1 / (\lambda - 1 + \sigma_1), \dots, \sigma_p / (\lambda - 1 + \sigma_p)\} \quad (2-17)$$

The fast mode roots and the transmission zeros must lie within the unit circle in the z-plane (discrete) for the system to be stable. The transmission zeros are a subset of the slow modes and can be calculated from the equation in Table 2-1 since $Z_t = Z_2$.

From equation (2-17) it can be seen that decoupling is achieved as the sampling period goes to zero. If the transmission zeros are not in the stable region, then the output matrix C must be changed. Alternately, a lower limit on the sample period may be acceptable. If not, the different set of outputs requires that a new design be attempted.

Known Plant- Irregular Design

When the product [CB] is rank deficient, then an Irregular design must be used. Extra output measurements are required. The new feedback vector is given as follows:

$$\underline{w}(t) = \begin{bmatrix} \frac{C}{1} + \frac{MA}{11} & \frac{C}{2} + \frac{MA}{12} \end{bmatrix} \begin{bmatrix} \underline{x}_1(t) \\ \underline{x}_2(t) \end{bmatrix} \quad (2-18)$$

$$= \begin{bmatrix} \underline{F}_1 & \underline{F}_2 \end{bmatrix} \begin{bmatrix} \underline{x}_1(t) \\ \underline{x}_2(t) \end{bmatrix} \quad (2-19)$$

where

\underline{M} is of order $(p \times (n-p))$

\underline{F}_1 is of order $(p \times (n-p))$

\underline{F}_2 is of order $(p \times p)$

The system is shown in Figures 2-2 and 2-3. The elements of the measurement matrix \underline{M} are selected so that the matrix $[\underline{F}]$ has full rank. Thus the F matrix replaces the C matrix in the design method. The control law equation (2-8) is unchanged, but the error vector is redefined as:

$$\underline{e}(kT) = \underline{v}(kT) - \underline{w}(kT) \quad (2-20)$$

Since the command input $v(t)$ is a constant vector

$$\lim_{t \rightarrow \infty} \dot{\underline{x}}_1(t) = \lim_{t \rightarrow \infty} \left[\underline{A}_{11} \underline{x}_1(t) + \underline{A}_{12} \underline{x}_2(t) \right] = 0$$

then

$$\begin{aligned} \lim_{k \rightarrow \infty} \underline{e}(kT) &= \lim_{k \rightarrow \infty} \{ \underline{v}(kT) - \underline{y}(kT) - \underline{M} [\underline{A}_{11} \underline{x}_1(kT) + \underline{A}_{12} \underline{x}_2(kT)] \} \\ &= \lim_{k \rightarrow \infty} \{ \underline{v}(kT) - \underline{y}(kT) \} \\ &= \underline{0} \end{aligned} \quad (2-21)$$

Thus the error vector is driven to zero in the steady state for a constant command input vector.

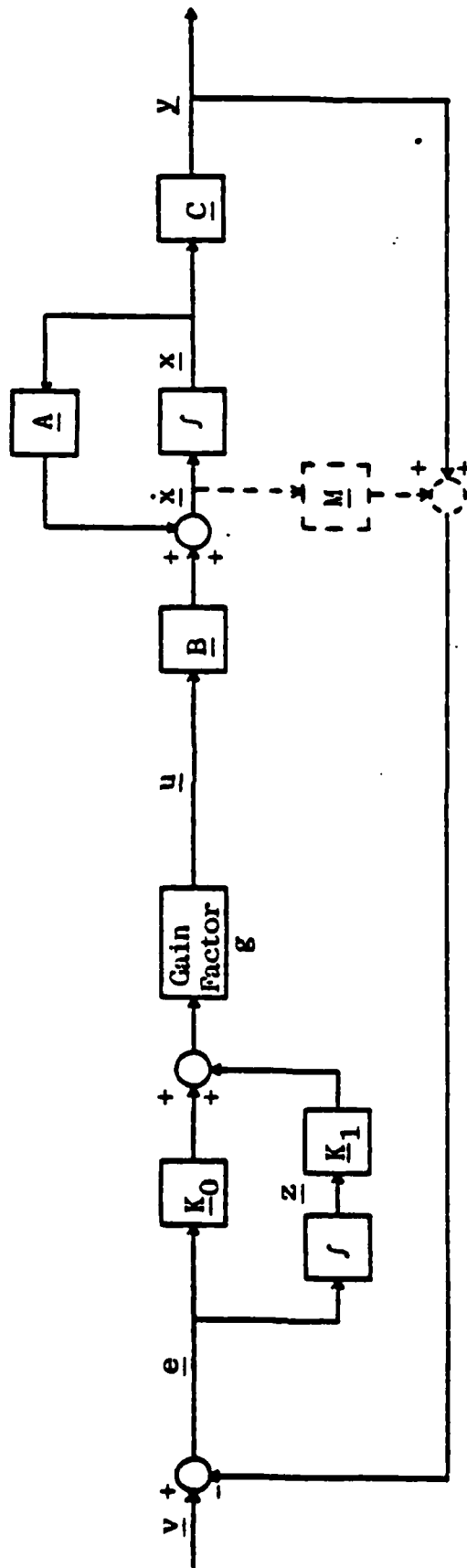


Figure 2-2 System Block Diagram - Continuous Design

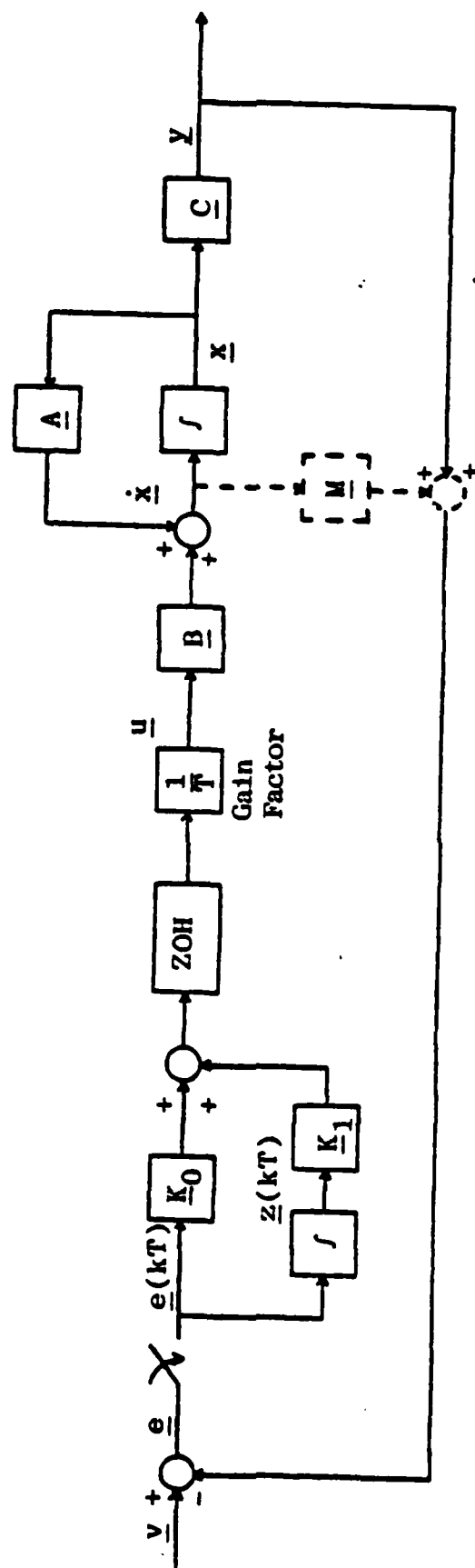


Figure 2-3 System Block Diagram - Discrete Design

For an Irregular design, the closed-loop transfer function matrix of equation (2-15) approaches an asymptotic value as the sampling period goes to zero (Ref 3:121-122):

$$\underline{\Gamma}(\lambda) = (\underline{C}_1 - \underline{C}_2 \underline{F}_2^{-1} \underline{F}_1) (\lambda \underline{I}_{n-p} - \underline{I}_{n-p} - \underline{TA}_{11} + \underline{TA}_{12} \underline{F}_2^{-1} \underline{F}_1)^{-1} (\underline{TA}_{12} \underline{F}_2^{-1})$$

$$\underline{\Gamma}(\lambda) = \underline{C}_2 \underline{F}_2^{-1} (\lambda \underline{I}_p - \underline{I}_p + \underline{F}_2 \underline{B}_2 \underline{K}_0)^{-1} \underline{F}_2 \underline{B}_2 \underline{K}_0 \quad (2-22)$$

The transmission zeros are determined as for a Regular system, except that the F matrix is substituted for the C matrix. The resulting transmission zeros must be in the open left half s-plane (continuous case) or within the unit circle in the z-plane (discrete case).

For an Irregular design, as the gain factor goes to infinity, the slow modes corresponding to the poles Z_1 become uncontrollable. The fast modes corresponding to the poles of Z_3 remain controllable and observable as the gain $1/T$ goes to infinity. However, unlike a Regular design, the slow modes corresponding to the poles of Z_2 remain both observable and controllable. Thus the slow transfer function matrix does not approach zero as the sampling period is reduced to zero. Therefore the slow and fast transfer matrices given in (2-22) must be diagonal for decoupling to take place in the limit.

The measurement matrix M is chosen such that:

1. M is as sparse as possible.

2. $\underline{F} \underline{B}$ has full rank.
 $\begin{matrix} 2 & 2 \end{matrix}$

3. The resulting transmission zeros must be in the stable region. Otherwise, there is a lower limit on the sampling period.

4. Decoupling of outputs in the limit as the sampling frequency goes to infinity is guaranteed only if the product

$\underline{C} \underline{F}^{-1}$ is a diagonal matrix.
 $\begin{matrix} 2 & 2 \end{matrix}$

5. The system has closed-loop roots in the stable region.

The controller matrices must be chosen such that:

$$\underline{K}_0 = \alpha \underline{K}_1 = \alpha (\underline{F} \underline{B})^{-1} \text{diag}\{\sigma_1, \sigma_2, \dots, \sigma_p\} \quad (2-23)$$

CHAPTER III

THE X-29A DEMONSTRATOR

Aerodynamics

The X-29A demonstrator aircraft integrates several different advanced technologies of aircraft design (see Figure 3-1). This chapter discusses forward-swept wings, close-coupled canards, strake-flaps, variable camber, fly-by-wire, relaxed stability, and the interactions between them. Although no knowledge of the actual aircraft design is needed to apply Porter's method, it is often helpful to gain some insight into how the aircraft "should" behave.

In general, swept wings, fore and aft, help to move the aircraft through the air more efficiently by reducing compressibility drag. Drag slows the aircraft by transferring energy from the aircraft to surrounding air. As a wing travels through air, it compresses the air in front of it, creating compressibility drag (Ref 4). As the aircraft increases speed, compressibility drag increases. By sweeping the wings at an angle nonperpendicular to the forward velocity of the aircraft, the velocity component of the airstream perpendicular to the leading edge of the aircraft is less than that of the aircraft itself. This causes the air to move along the length of wing, instead of just from leading edge to trailing edge.

As the aircraft enters supersonic speeds, wave drag also occurs. In the subsonic region, the pressure wave created by the wing pushes air out of the way. But in the supersonic

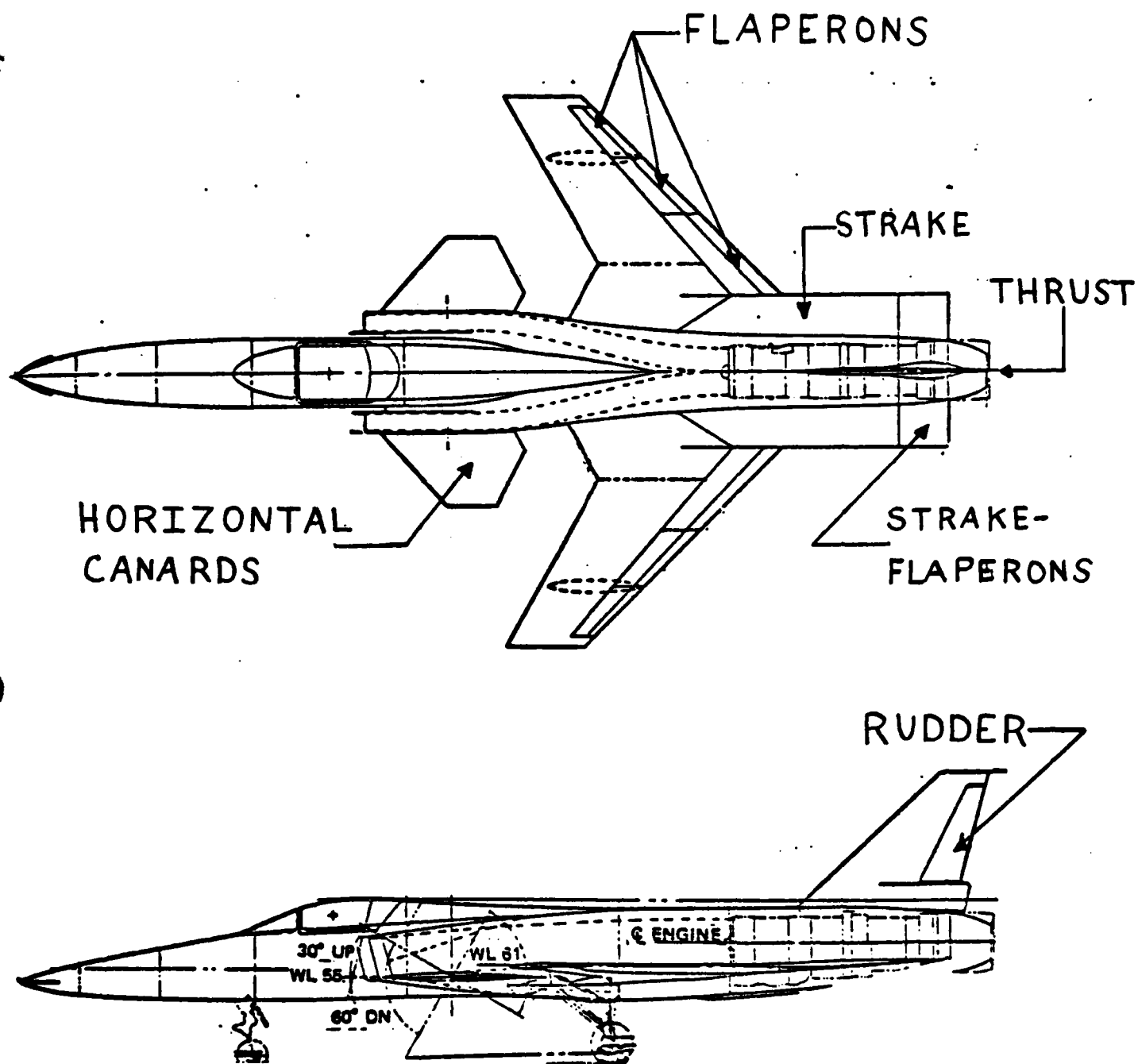


Fig. 3-1. The X-29, FSW Aircraft.

region the pressure wave, which only travels at the speed of sound, is overtaken by the aircraft which is traveling faster than the speed of sound. These differences in speed, and hence pressure, cause a sonic boom. This sonic boom is caused by a transfer of energy from the aircraft to the surrounding airstream. This wave drag can be minimized by presenting a smooth minimized cross-sectional area of the aircraft to the oncoming airstream. Forward-swept wings have a much smoother cross-sectional area than aft-swept wings, and hence have less wave drag.

Forward-swept wings are placed further back along the fuselage, further away from the center of gravity, than aft-swept wings. In order to minimize pitching moment, the payload of the aircraft is placed at the center of gravity of the aircraft. Aft-swept wings, being close to the center of gravity of the aircraft, present a dilemma for the designer. If the fuselage is "pinched-in" to present a smooth cross-sectional area, then payload is reduced. If payload capability is not reduced, then the resulting uneven cross-sectional area increases the wave drag at supersonic speeds.

Forward-swept wings have an important advantage over aft-swept wings in "stall-progression". In order to generate more lift for the aircraft the angle of attack (between the wing and the airstream) is increased. As this happens, the air passing across the top of the wing speeds up. By Bernoulli's principle, this difference in speeds causes a pressure differential that causes lift. If, however, the angle of attack

becomes too great then the airstream can not follow the contour of the wing, causing stall. Stall progression occurs in the opposite direction of airflow. Thus stall progression moves from trailing edge to leading edge of the wing and along the wing from the aft-most part of the wing to the fore-most part of the wing. In aft-swept wings, the aft-most part of the wing is at its tips, where the ailerons are located. This means that the ailerons are no longer effective and control is lost. In forward-swept wings the aft-most part of the wing is at its root, or the part of the wing that is attached to the fuselage. Thus stall first occurs away from the ailerons. Moving the ailerons to the root for aft-swept wings is not feasible since this would reduce the roll moment by decreasing the lever arm. These advantages allow the X-29A to fly at angles of attack of up to 70 degrees. Present aircraft without vectored thrust cannot fly at angles of attack greater than 30 degrees or stall occurs.

Close-Coupled Canards

Close-coupled canards, located in front of the forward-swept wings, can be used to channel air to the root of the wing in order to resist stall. This further increases the capability of the X-29A to fly at greater angles of attack before stall is induced.

In statically stable aircraft, the lift vector is located aft of the center of gravity. This means that the aircraft tends to have a nose-down pitching moment. In conventional aft-swept wing aircraft, this is countered by placing a rear horizontal stabilizer to provide a downward force to counter

wing lift. While this cancels out the pitching moments about the center of gravity, it also reduces the total lift of the aircraft. In forward-swept wing aircraft the horizontal stabilizers, or canards, are placed in front of the center of gravity. Thus while it still cancels out the pitching moment about the center of gravity, it now adds to total lift. With the lift vectors from the wings and canards on opposite sides of the center of gravity, the center of gravity can be moved around, permitting much greater flexibility in payload distribution.

Strake-Flaps

Strakes, horizontal surfaces attached to the fuselage from the wings to the tail, have flaps attached at the tail to provide a nose-down pitching moment at high angles of attack. (Ref 5). The strakes also aid in increasing pitch damping by resisting movement as the rear of the fuselage moves up and down (Ref 4). The strakes can be moved in concert with the close-coupled canards and symmetrical flaps on the wings to obtain optimal air flow as the airstream passes from front to back of the aircraft.

Wing Composition and Shape

Past applications of forward-swept wings have been limited to small sweep angles because of structural divergence of the wings. As the angle of attack of the wing increases, the wing is twisted. In aft-swept aircraft, the leading edge of the wing twists downwards, thus relieving the load by decreasing the angle of attack. In forward-swept wing aircraft,

however, the wing is twisted upwards, increasing the angle of attack. This leads to even greater twisting of the wing until the structure cannot bear the load and could be torn away.

Grumman has been able to overcome this problem by using a process known as "aeroelastic tailoring". In aeroelastic tailoring, composite materials, such as boron fiber and graphite in a plastic matrix, are used to produce a nonmetallic wing that is 30% lighter than a metal wing of the same strength. In addition, the wing structure is optimized by varying the direction and thickness of the layers of bonded fiber composite material. This layering effectively distributes the twisting load, which is greatest at the wingtips, over the entire wing.

The X-29A uses supercritical wings to increase its critical Mach number. The critical Mach number is the speed at which the aircraft can fly before the air hitting the front of its wings increases to the speed of sound. As the air passes over the top of the wing it slows down, producing a shock wave. This phenomenon, known as the Bernoulli effect, increases drag and decreases lift. Supercritical wings have a greater leading edge radius of curvature and a flatter surface top. This causes the air to reach supersonic speeds earlier and sustains the supersonic speed further along the wing. This pushes the shock wave to the trailing edge of the wing, where drag is much less and lift is not decreased as much.

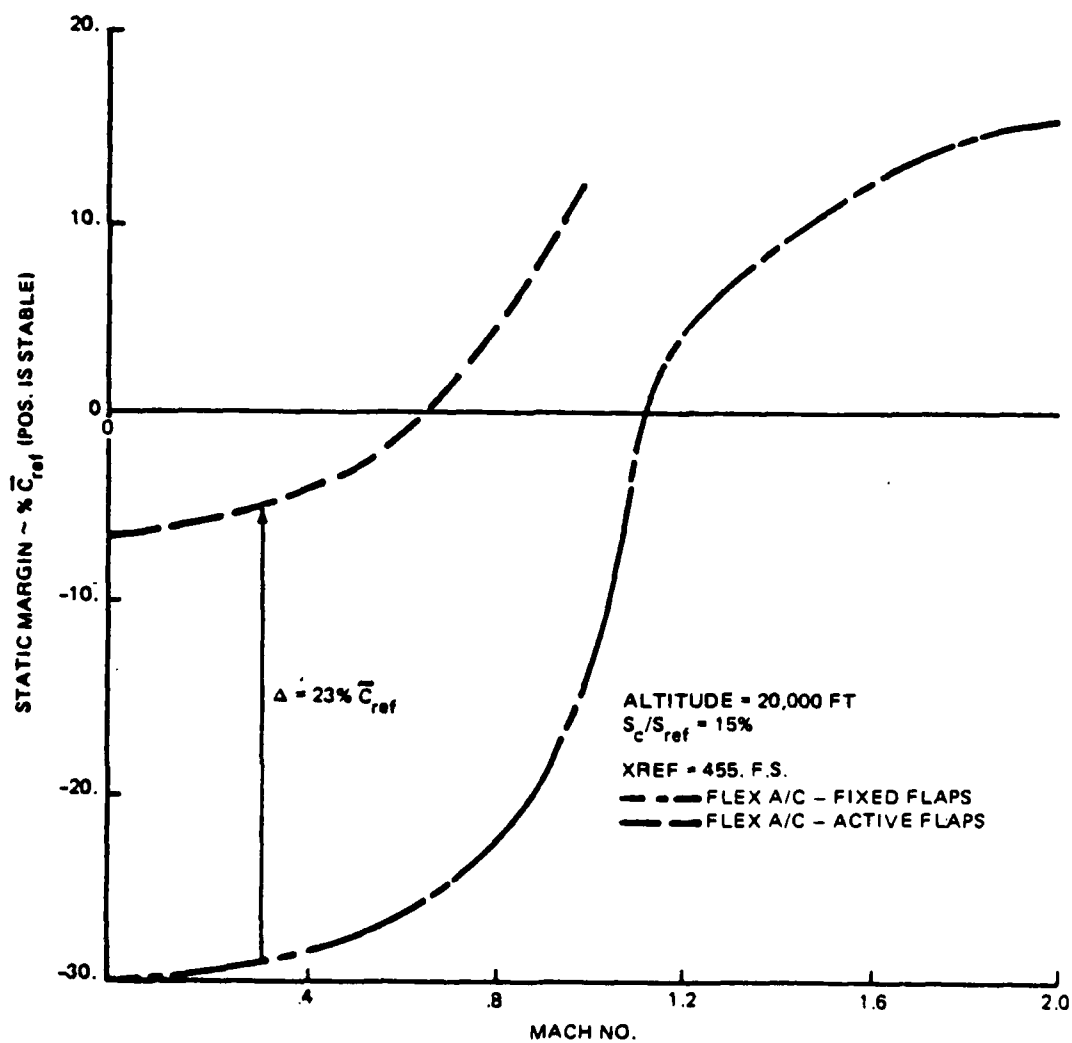
Variable Camber

The X-29A uses trailing edge surfaces to vary the camber of the wing to provide the optimal wing shape over differing

flight conditions. The surfaces are composed of three parts along the wing. The outermost part, called the outboard flaperon, is the equivalent of an aileron which is used to provide roll control. The inboard flaperon, composed of two parts, is similar to a traditional flap to provide additional lift during landing. The trailing edge control surfaces are separated into three parts to combat aerodynamic flutter. The inboard flaperon uses one actuator to move both trailing edge surfaces. This is done because of weight and space constraints. Both actuators are moved together. Independent movement of the inboard and outboard flaperons is not possible because of nonlinearities in the actuators. Thus all three parts move together as symmetrical flaperons to provide variable camber and as differential flaperons to perform lateral maneuvers. This results in increased maneuverability and reduced drag throughout the flight envelope (See Figure 3-2). An integrated flight control computer is used to automatically control optimum wing shape during steady level flight. To provide variable camber, the flaperons are moved as a function of canard displacement. If the pilot wishes to use the symmetrical flaperons to perform a maneuver, he must switch to manual camber control.

Common Components

In order to minimize cost, 56% by weight of the X-29A consists of components which are common to existing aircraft. The forward fuselage and cockpit area are from the F-5A fighter; the main landing gear, control surface actuators, auxilia-



0694-353W

Figure 3-2 Active Camber Increases FSW Longitudinal Static Stability

ry power system, and engine accessory drive are from the F-16; and the engine is a GE F404 turbofan that is from the F-18.

Fly-by-Wire

Past aircraft have used mechanical inputs from the pilot to power hydraulic actuators which move the control surfaces. The X-29A uses electric signals from the pilot, called "fly-by-wire", to activate the hydraulic actuators that move the control surfaces. This advanced technology reduces weight and space and may provide increased reliability through multiple redundancy and distributed processing. Future aircraft might possibly be "all-electric", in which not only the signals from the pilot will be electric, but the actuators that move the control surfaces will be electrically powered as well. This has the additional advantage of greatly reducing the "dead-zone", the lag in time between when the inputs are commanded and when the control surfaces actually start to move. Future technology might also provide fiber-optic links to the hydraulic system. In addition to further reducing weight and space, such circuits are less vulnerable than electric circuits are to "EMP" (electromagnetic pulse).

Relaxed Stability

The X-29A is statically unstable at subsonic speeds (see Figure 3-3). Since an uncompensated perturbation in the longitudinal plane would cause the X-29A to go unstable in a fraction of a second, digital flight control computers must provide "artificial stability" for the aircraft. This has the advantage that smaller and lighter flight control surfaces are

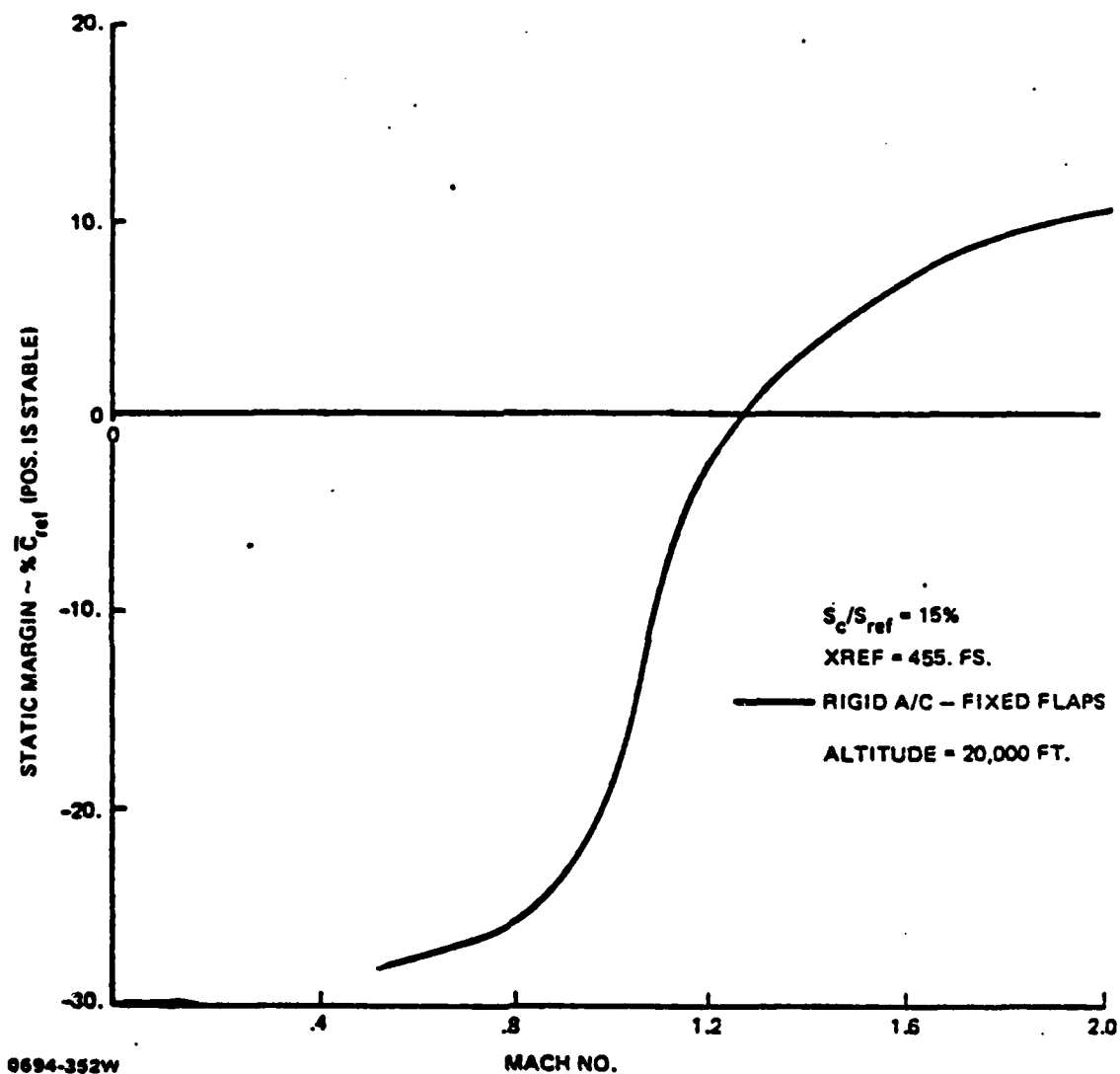


Fig. 3-3 X-29 Longitudinal Stability.

needed. But this also has the disadvantage that if the computer hardware should fail, or if the software of the controller is faulty, then the pilot will be unable to recover the aircraft. Hardware failure risk is minimized by providing a backup power supply and redundant digital computers. Software failure risk is guarded against by providing a backup "analog reversion-mode" system that enables the pilot to recover the aircraft. But this adds weight and cost to the aircraft.

At supersonic speeds the center of pressure (point at which the lift vector of the aircraft is applied) moves back towards the center of gravity of the aircraft. The aircraft is then neutrally stable and smaller control surface deflections are needed to stabilize and maneuver the aircraft. This decreases drag since every time a control surface is moved, a transfer in energy from the aircraft to the surrounding airstream occurs.

Summary

Since the X-29A's aerodynamics enable it to move more efficiently through air, less fuel is required to fly it than a conventional aircraft of similar size. Smaller weight and size also permit a reduction in cost of building the X-29A. Thus fixed and marginal costs are kept to a minimum. The "lift-to-trim" canards offer the advantage of freedom of payload distribution. The reduction in size offers increased survivability, since smaller aircraft are harder to detect. Relaxed stability permits greater maneuverability, and hence greater survivability and mission effectiveness. Digital

flight control systems may also offer better performance when battle damage is sustained by permitting reconfiguration of the control laws.

Unfortunately, this increase in performance must be paid for with increased complexity in design.

CHAPTER IV

LONGITUDINAL CONTROLLER DESIGNS

Introduction

This chapter presents the results of the longitudinal controller designs for the five flight conditions for each of six maneuvers. A sample flight condition, 1.2 Mach at 15 000 feet, is presented. Although each flight condition is discussed, supporting state-space matrices, design parameters, commanded inputs, controller matrices, figures of merit, and plots for the other four flight conditions are included in the appendices.

Grumman Aerospace Corporation developed a nonlinear simulation computer program for the X-29A demonstrator aircraft at different flight conditions. From this program linearized data in state-space form at five flight conditions is obtained. Many design methods, including Porter's method, assume linear behavior in order to achieve mathematically tractable results. While the simplification of linearized performance of the X-29A for small perturbations about the chosen flight condition is a good one, it becomes less valid the greater the perturbations become. The usual remedy is to design controllers at many flight conditions, and then use gain-scheduling between the discrete design points. This approach requires that the design method lend itself readily to development of many controllers with minimum effort.

In order to further simplify the model, the longitudinal and lateral controllers are developed separately. This is

possible in the X-29A because no cross-coupling occurs. If this were not the case, though, this would be a good first approach. After separate designs are obtained, the complete longitudinal/lateral controller could be retuned to accommodate cross-coupling. If the cross-coupling is too great, however, then the controller would have to be designed using the full model. This increases complexity, though, and does not allow the advantage of separate design teams for the longitudinal and lateral controllers (Ref 6). Decoupling also permits separate computers for the longitudinal and lateral controllers.

In order to further simplify the model, a reduced number of states is used in the Grumman model. The states used are q , pitch rate; θ , pitch angle; α , angle-of-attack; and $VTOT$, total velocity. This controller design further assumes that $VTOT$ is approximated by U , forward velocity. Note that since the model used assumes steady level flight as the initial condition, U can be replaced with u , the change in forward velocity.

Symmetrical flaperons, thrust, canards, and strake-flaperons (strakes) are the available longitudinal inputs. Since the X-29A uses variable camber, this initial design attempt uses only thrust, canards, and strakes as control inputs. This allows a separate controller to be designed to adjust the symmetrical flaperons to provide variable camber.

Porter's method requires that the number of inputs be equal to the number of outputs. It is difficult to command

four separate outputs that do not conflict with one another. If all four inputs are used, then all four states can be controlled as outputs. Since commanding q and θ is redundant, a transmission zero at the origin occurs. This signifies that redundant inputs are present. Even though the outputs commanded are redundant, the required maneuver can now be performed with four control surfaces.

Thus all of the longitudinal maneuvers performed understate the actual longitudinal performance capabilities of the X-29A. Future designs should use two separate longitudinal controllers for the X-29A. One design would treat the canards, symmetrical flaperons, and strakes as one control input in order to minimize drag. This design would more properly model aerodynamic effects, since changes in the canard affect the airflow over the inboard flaperons. Changes in the inboard flaperons, which occur with active variable camber, in turn affect the airflow passing over the strakes. Thus movement of the flaperons would be a function of canard movement, while movement of the strakes would be a function of flaperons or canards. This controller would be used all of the time and would be the only controller used when the X-29A is cruising. Since the number of independent control inputs is reduced to only two (canards, flaperons, and strakes; thrust), only two outputs could be controlled. The other longitudinal controller would treat all the control inputs as independent inputs, permitting maximum performance. This controller would enable the aircraft to achieve maximum maneuverability, and would be activated by the pilot when he wished to perform a

maneuver, or when an automatic set of pre-programmed maneuvers was initiated, as in integrated fire/flight control. The second controller would take precedence over the first, since this controller would be used in combat. When absolute maximum maneuvers were not being used, then the first controller's inputs would be added to the second controller's inputs in order to perform the desired maneuvers with the greatest efficiency.

The outputs chosen to be controlled are the states q , u , and α . It is extremely important that the same output (C) matrix be used for all of the maneuvers. Otherwise, the pilot would have to flip a switch to tell the aircraft what maneuver he was about to command. In addition, different output matrices make attainment of a universal, or robust controller, extremely doubtful. Lastly, the advent of digital flight control permits automatic maneuvering while in combat. This occurs when the pilot has maneuvered the aircraft within close proximity to the target, and gives authority to the controller to take over. Different output matrices can be accommodated by a digital flight control system that uses a predetermined set of maneuvers, but now the problem of large gain transients in switching back and forth to different controllers must be overcome.

Description of Maneuvers

Controllers are designed for six longitudinal maneuvers at each of the five flight conditions. The initial design attempts used a different controller for each maneuver, for a

total of forty controllers. However, it is noticed that performance is only slightly degraded by using the same controller for three of the maneuvers, another controller for two of the maneuvers, and a separate controller for the remaining maneuver. In keeping with the overall goal of obtaining a robust controller, this reduces the total number of controllers to fifteen longitudinal controllers.

Note that all outputs must be commanded to some value; no output is allowed to "float". Since the X-29A is a new aircraft, maximum possible maneuvers are commanded. Note that in many instances transient responses are degraded in order to obtain maximum performance. The maximum possible maneuver is determined by simply increasing the commanded inputs until input limits are met. MULTI allows input limits to be reached, but not exceeded during a simulation, and notifies the designer. This frees the design engineer from having to determine these maximums by using a rigorous a-priori aerodynamic analysis. Since the option to easily determine control input rates was not added to MULTI until after design work was completed, control input rates are exceeded for some maneuvers. Where the rates are exceeded, the maximum commanded steady-state input need only be reduced or the maneuver time lengthened, but the controller does not have to be refined. In order to facilitate easy comparison of aircraft capabilities at different flight conditions, each longitudinal maneuver was commanded over the same time duration. Different flight conditions performed different maneuvers better than others, and flight condition number three, at 1.2 Mach at 15

000 feet is a good representative. One of the additions to MULTI that this thesis makes is to incorporate a prefilter of the pilot's commanded inputs. The prefilter allows an increase of approximately three percent in the commanded steady-state value of the maximum maneuver. This is traded off against a degradation in settling time values, however.

The six longitudinal maneuvers designed for are direct climb, direct lift1, direct lift2, pitch-pointing, vertical translation1, and vertical translation2. One controller is used for direct climb, direct lift1, and direct lift2 at each flight condition. In direct climb, q is commanded as a pulse, u is ramped-up and held to a steady-state value, and α is commanded to zero. This maneuver allows the pilot to point the nose of the aircraft at a target and increase the airspeed in order to chase it. In direct lift1, q is commanded as a pulse of 0.7 seconds duration, while u and α are commanded to zero. This gives an indication of how well the aircraft can change its pitch in a short time. In direct lift2, q is commanded as a pulse of 3.2 seconds duration, while again u and α are commanded to zero. Note that since α is commanded to zero, the flight-path angle γ is now equal to θ . θ can be calculated by taking the integral of the commanded q input.

A single controller is used for pitch-pointing at each flight condition. In pitch-pointing, q is commanded to a value that produces a pitch angle, θ , equal to the commanded value of α . U is commanded to zero. This maneuver

is of greatest benefit to aircraft that cannot fly at large angles of attack. Pitch-pointing, also called fuselage-pointing, allows the aircraft to increase its pitch angle without increasing its flight path angle, γ . γ is held to zero since θ and α are kept equal.

A single controller is used for vertical translation¹ and vertical translation². In vertical translation¹, q and u are commanded to zero while α is commanded as a pulse. This maneuver moves the aircraft upwards a fixed distance. This maneuver is useful for refueling and positioning the aircraft within a formation. In vertical translation², q and u are again commanded to zero, but this time α is commanded to ramp-up and hold a steady-state value. This maneuver causes the aircraft to rise at a fixed velocity while keeping the pitch angle zero.

Development of Aircraft Model

The first step in digital flight control design is the development of the aircraft equations of motion based upon certain assumptions (Ref 7). Such assumptions may include:

1. The X and Z axes lie in the longitudinal plane with the center of the chosen axis system at the center of gravity of the aircraft.
2. The mass of the aircraft is constant. Although much fuel may be expended (up to 23.8% by weight of the X-29A) during a mission, the amount of fuel expended during a 16 second maneuver can be safely disregarded.
3. The earth is an inertial reference. For an aircraft this is a good assumption.

4. The perturbations from equilibrium (steady level flight) are small.

5. Quasisteady flow occurs. This assumes that the airstream surrounding the X-29A changes instantaneously when the aircraft is disturbed from equilibrium. Although at higher Mach numbers (transonic and above) compressibility drag renders this a less satisfactory assumption, it is a good first approximation.

6. The aircraft is a rigid body. After the design is completed, a bending mode analysis can be completed to see if this is a valid assumption.

Next, the equations of motion must be used to develop a nonlinear simulation program. Typically, an aerodynamicist develops the equations of motion and aircraft model computation program for the digital flight control engineer. Note that a limited nonlinear simulation capability has been added to another program supporting MULTI (Ref 8). In this thesis, the linearized data received from NASA are assumed to be correct since the equations of motion are not made available. After transforming the linearized data containing the plant (A matrix) and inputs (B matrix) into state-space form, the designer must decide what outputs (C matrix) will be used. For certain outputs a feedforward (D matrix) term may also have to be added. The outputs chosen will determine whether a Regular or Irregular design method is first attempted. A Regular design offers three advantages. First, a Regular design requires fewer gains than an Irregular design does.

Second, a Regular design offers the possibility of faster performance since some slow modes become uncontrollable in an Regular design. Lastly, other things being equal, a Regular design is easier since fewer parameters must be chosen.

The design of the longitudinal controllers in this thesis uses a Regular design with a constant C matrix with q, u, and alpha as outputs. After obtaining the A, B, C, and D matrices it is next necessary to determine the transmission zeros and to be sure that there are no decoupling zeros by using the computer program ZERO (Ref 9). Alternately, decoupling zeros may be determined by examining the system matrix P (Ref 10). The system is controllable and observable if P has full rank. (see equation 4-3). A third method of checking controllability is to examine the M_c and M_o matrices.

$$\underline{M}_c = \begin{bmatrix} \underline{B} & \underline{A} & \underline{B} & \dots & \underline{A}^{n-1} & \underline{B} \end{bmatrix} \quad (4-1)$$

$$\underline{M}_o = \begin{bmatrix} \underline{C} & \underline{C} \underline{A} & \dots & \underline{C} \underline{A}^{n-1} \end{bmatrix}^T \quad (4-2)$$

\underline{M}_c must have full rank for the system to be controllable.

\underline{M}_o must have full rank for the system to be observable.

After entering the data in state-space form, the program gives the decoupling and transmission zeros. There must be no input-decoupling zeros, otherwise the system is uncontrollable. If the system is uncontrollable because B does not have full rank, then redundant controls are present. The B matrix

can be made to have full rank by combining the linearly dependent columns so that all columns are linearly independent. Output-decoupling zeros, which determine observability, possibly can be removed with an Irregular design. If the system is unobservable because C is rank deficient, then additional measurements must be added to the system. This is done by adding an M, or measurement matrix in an Irregular design. Transmission zeros must be in the closed left-half plane. If not, they possibly can be moved from the right-half plane to the left-half plane by using an Irregular design.

If the product of the C and B matrices has full rank, then a Regular design may be attempted if no transmission zeros are in the right-half plane. Although a design may be possible, good results are not guaranteed. If it appears that only designs excessively requiring large inputs (e. g., too large a canard deflection) resulting from large controller gains are possible, then the singular decomposition of P (Ref 11) must be examined. The singular decomposition is a measure of the singularity of a matrix. If P is barely nonsingular, then large gains will be required to stabilize the aircraft. This can only be remedied by changing the system. The easiest way to do this is to change the C and D matrices by choosing different outputs. Changing the B matrix requires a change in control inputs, while changing the A matrix requires a modified aircraft.

$$\underline{P} = \begin{bmatrix} -\underline{A} & \underline{B} \\ -\underline{C} & \underline{D} \end{bmatrix} \quad (4-3)$$

The closed-loop roots can be determined by calculating the closed loop transfer matrix $G(s)$:

$$\underline{G}(s) = \underline{C}[\underline{sI} - \underline{A}]^{-1} \underline{B} \quad (4-4)$$

Calculation of the final transmission zeros (those obtained after the system model, design parameters, and sampling period are chosen) provides a theoretical limit to the performance of the system with the chosen design. As the sampling period approaches zero in the limit, the sampling frequency approaches infinity. As the sampling frequency approaches infinity, some of the closed-loop eigenvalues asymptotically approach the transmission zeros.

In order to calculate the theoretical limit the \underline{B} matrix is transformed into $\begin{bmatrix} \underline{0} \\ \underline{B}_2 \end{bmatrix}$ form. The \underline{B}_2 matrix is square and has as

many rows as system inputs. If enough zero rows already exist, then the order of the state equations is changed to place the zero rows on top. If not, then a transformation matrix \underline{T} must be found to change \underline{B} into the required form. As the sampling frequency approaches infinity, the closed-loop roots are driven to the final transmission zeros. Note that this analysis only applies to the limits of performance, not to the actual performance itself.

$$\begin{bmatrix} \underline{0} \\ \underline{B}_2 \end{bmatrix} = \underline{T}\underline{B} \quad (4-5)$$

Transforming the \underline{B} matrix has three advantages. First, the transmission zeros can be calculated by hand, thus

validating the results obtained from the computer program ZERO. Second, in the limit as the sampling frequency goes to infinity, decoupling of outputs is guaranteed. Lastly, for Irregular designs, algorithms exist for picking M (measurement matrix) elements. Unfortunately, these algorithms may not select M elements that produce good results, and the designer may have to resort to guessing which elements to pick.

Matrix manipulation can be facilitated with the use of MATLAB, a computer program developed by Cleve Moler at the University of New Mexico.

Next, the design parameters specifying the digital controller are selected.

Finally, steady-state analysis of performance can be accomplished by using $G(s)$ and $R(s)$ (formed from the commanded inputs). Transient analysis is evaluated using control rate limits.

To summarize, preparation for selection of design parameters (steps 1-5), design (step 6), and evaluation (steps 7-10) require the following:

1. Validation of the aircraft model (A, B, C , and D matrices).
2. Selection of outputs (C matrix).
3. Determination of Regular or Irregular design.
4. Check of the controllability (B and A matrices) and observability (C and A matrices) of the system. This may be accomplished by using a computer program, examining P , or examining M and M .
5. Determination and evaluation of the transmission zeros using a computer program. Note that Porter's method works

equally well for both analog and digital systems. However, the discrete time transmission zeros are also affected by the sampling period. As the sampling period approaches zero, increasingly tight tracking occurs.

6. Calculation of $G(s)$. (A, B, and C matrices)

7. Transformation of the B matrix using a T matrix to obtain transmission zeros, guaranteed decoupling of outputs, and algorithms for picking M elements (M matrix only used for Irregular design). (If possible, not required).

8. Selection of design parameters (see Application of Porter's Method). Evaluation of singularity using singular decomposition if required.

9. Evaluation of steady-state performance using $G(s)$ and commanded inputs $R(s)$.

10. Evaluation of transient performance based upon control rate limitations.

Application of Porter's Method

The state and output equations for flight condition number three (1.2 Mach at 15 000 feet) are:

$$\dot{\underline{x}} = \begin{bmatrix} \dot{\theta} \\ \dot{u} \\ \dot{\alpha} \\ \dot{q} \end{bmatrix} = \begin{bmatrix} 0 & 0 & 0 & 1 \\ -32.13 & -.08695 & -25.86 & -.3359 \\ .3301E-06 & -.5869E-04 & -2.468 & .993 \\ 0 & -.01025 & 18.79 & -.934 \end{bmatrix} \begin{bmatrix} \theta \\ u \\ \alpha \\ q \end{bmatrix} + \begin{bmatrix} 0 & 0 & 0 \\ -.6313 & -.08545 & 107.9 \\ -.00361 & -.6837E-03 & -.003212 \\ .3912 & -.1231 & -.7639 \end{bmatrix} \begin{bmatrix} \delta_c \\ \delta_s \\ \delta_r \end{bmatrix} \quad (4-6)$$

$$\dot{\underline{x}} = \underline{Ax} + \underline{Bu}$$

$$\underline{Y} = \underline{C}\underline{x} = \begin{bmatrix} q \\ u \\ \alpha \end{bmatrix} = \begin{bmatrix} 0 & 0 & 0 & 1 \\ 0 & 1 & 0 & 0 \\ 0 & 0 & 1 & 0 \end{bmatrix} \begin{bmatrix} \theta \\ u \\ \alpha \\ q \end{bmatrix} \quad (4-7)$$

Using the computer program ZERO to obtain the decoupling and transmission zeros yields:

1. There are no decoupling zeros.
2. A transmission zero exists at (0,0). This is expected since the number of transmission zeros should be equal to the number of states minus the number of inputs (Ref 12).
3. The above values are obtained for the other four flight conditions as well.

Note that the state-space equations have $\begin{bmatrix} \underline{0} \\ \underline{B} \\ 2 \end{bmatrix}$ form.

The resulting product below is recognized as having full rank.

$$\underline{CB} = \underline{C} \frac{\underline{B}}{2} \quad (4-8)$$

Thus a Regular design is permitted. Since \underline{A}_{12} and \underline{A}_{21} have full rank, it is seen that the \underline{P} matrix in equation (4-1) is non-singular. Therefore, the system is controllable and observable, verifying the results obtained from the program ZERO.

The plant matrix can be partitioned into the form:

$$\underline{A} = \begin{bmatrix} \underline{A}_{11} & \underline{A}_{12} \\ \underline{A}_{21} & \underline{A}_{22} \end{bmatrix} \quad (4-9)$$

where \underline{A}_{11} is (n-m) x (n-m) with n=number of states and m=number of inputs.

Note that no transmission zeros are in the right-half plane. Therefore, a regular design is permitted.

Since the B matrix could not be easily transformed, a T matrix is not explicitly determined. MULTI uses any form of the B matrix when the controller matrices are computed.

Next it is necessary to choose the best set of design parameters to obtain a controller that gives the best performance. For both Regular and Irregular designs the following parameters must be chosen:

1. ALPHA- Proportion of integral to direct feedback such that $\underline{K}_0 = \text{ALPHA} * \underline{K}_1$. A special incentive exists to try to

achieve a design with ALPHA equal to one since this reduces the required gains by half. Using "cache-memory", controller gains can be stored in registers (Ref 14). Since \underline{K}_0 and \underline{K}_1 are

equal when ALPHA is one, the number of required registers is reduced by a factor of two. Heuristically, ALPHA should be greater than zero and less than two.

2. EPSILON- Sigma matrix multiplier. Heuristically, EPSILON should be greater than zero and less than four.

3. SIGMA weighting matrix- SIGMA has p weighting diagonal entries. The individual SIGMA elements correspond to the respective commanded inputs and outputs. Because the SIGMA matrix is diagonal, the outputs can be decoupled.

4. SAMPLE PERIOD- This thesis uses 0.025 seconds. The SAMPLE PERIOD should be greater than 0.01 seconds and less than 0.10 seconds. As the SAMPLE PERIOD is reduced, the

closed-loop roots of the model migrate to the transmission zeros. If transmission zeros should exist in the right-half plane, then there is a lower limit on the allowable value of the SAMPLE PERIOD.

5. Commanded inputs are initially set to some maneuver values that the designer is sure the aircraft can perform. The magnitude of the steady-state control inputs u_{ss} to the aircraft for a desired maneuver y_{ss} can be computed from the open-loop aircraft transfer function $G(s)$ by using:

$$u_{ss} = [\underline{G}(0)]^{-1} y_{ss} \quad (4-10)$$

To start, the design parameters ALPHA, EPSILON, and SIGMA are set equal to one. Then the \underline{K} matrices, or controllers, are examined. In general, the entries of the \underline{K} matrices should have orders of magnitude greater than or equal to negative two and less than or equal to two. In addition to most designs being in this general area, the dynamic range of the elements is minimized. This aids in producing computationally correct results.

The following is a suggested design procedure for using the computer-aided-design tool MULTI. It should be noted that no unique solution exists to the design process. Tradeoffs are made between transient and steady-state response, between maximum commanded inputs and control input responses, and between length of maneuver time and control input rates. Additional tradeoffs must be made in the search for a robust

controller. The design parameters affect one another, with the greatest coupling between ALPHA and EPSILON, and among the SIGMA elements.

1. Aircraft model:

Enter the A, B, C, and D matrices in state-space form. For an initial design attempt, no sensors or actuators are used.

2. Simulation parameters:

Set the state and integrator initial values, $X(0)$ and $Z(0)$. Since the aircraft data provided are for steady level trimmed flight, these vectors are set to zero. Since only perturbations are of interest, the trim values of alpha and theta do not affect the simulation. However, it should be noted that if these trim values are large, the results could show that additional increments are possible when in fact they would exceed the allowable values.

Set the commanded inputs that correspond to the maneuver to be performed. Choose a sampling period (e. g., .025 seconds). Set the simulation time (for this thesis 16 seconds) to be at least as long as the commanded input. Next, set the calculation step size in time equal to the sampling period.

For an initial design attempt no lags are used. The lag capability in MULTI models the synchronous analog-to-digital delay. The computation delay, which is asynchronous, is usually much shorter than the analog-to-digital delay. The digital-to-analog delay is negligible. No capability currently exists in MULTI for modeling input "dead-zones", the delay between the commanded start of the control input and when the

control inputs actually start to respond. For example, without afterburners, the dead-zone for thrust is approximately 0.5 seconds.

Lastly, set the control input limits:

Canards (-60,30) degrees

Strakes (-19.5,13) degrees

Thrust (-14782,2000) pounds

Note that these limits are set from trim values. Since 14 782 pounds are required to achieve steady level flight, total thrust may be decreased by the same amount.

3. Design parameters:

Initially, ALPHA, EPSILON, and SIGMA are set to one. If all of the entries of the controller matrices exceed the specified orders of magnitude, then EPSILON, the multiplier of these entries, is adjusted in the opposite direction. Next, the entries of each column in the controller matrix are examined. Again, if the entries in a particular column exceed the heuristically determined controller limits, the corresponding SIGMA element is adjusted. Once the controller entries are adjusted to a best initial guess, a simulation is run. MULTI alerts the designer if control inputs are exceeded.

If control inputs are exceeded, the designer should make sure that the maneuver commanded is one the aircraft is capable of performing. If so, the design parameters should be adjusted by small increments, and the simulation rerun. Once the simulation produces inputs that are within limits, the outputs should be examined.

The outputs are quickly examined using the option that provides figures of merit. Design parameters are retuned until the best figures of merit are obtained. Next, plots of outputs, states, and inputs are examined at the terminal. If satisfactory, the commanded inputs are increased until control input limits are reached in order to determine the largest allowable command. Lastly, tradeoffs are made between design objectives. Note that overshoots can sometimes be reduced by increasing ALPHA. When a satisfactory design is achieved, calcomp plots are generated.

Results

The design parameters and maximum commanded inputs selected are presented in Table 4-1. The controller matrices resulting from the selected design parameters are presented in Table 4-2. Figures of merit are provided in Table 4-3. Control rates are provided in Table 4-4. Calcomp plots of outputs, commanded inputs, control inputs, theta, and flight-path angle are provided in Figures 4-1 to 4-19. Note that only nonzero commanded inputs are plotted. Similar information is provided for the other four flight conditions in appendices B, D, E, F, G, and H.

The first longitudinal maneuver, direct climb, is best performed by the flight condition at 1.2 Mach, 15 000 feet. A smoothed pulse pitch rate of approximately 47 degrees/second is commanded and closely followed (see Figure 4-1). The

TABLE 4-1

DESIGN PARAMETERS AND COMMANDED INPUTS FOR LONGITUDINAL CONTROLLER

Flight Condition - 1.2 Mach, 15 000 feet

Maneuver	Command Vector \underline{v}	ALPHA	EPSILON	SIGMA (Diagonal values)
	*			
Direct Climb	1.2, .8, 2, 3.2 1.2, 405, 16, 16 0, 0, 0, 0	1.1	0.9	2, 1, 0
Direct Lift1	.2, .45, .5, .7 0, 0, 0, 0 0, 0, 0, 0			
Direct Lift2	1.6, .72, 2.4, 3.2 0, 0, 0, 0 0, 0, 0, 0			
Pitch-Pointing	.8, .0225, 1.2, 1.6 0, 0, 0, 0 .8, .0225, 16, 16	1.1	0.9	2, 1, .15
Vertical Translation1	0, 0, 0, 0 0, 0, 0, 0 1.8, .027, 3.2, 4.5	.82	.9	1.5, 1., .067
Vertical Translation2	0, 0, 0, 0 0, 0, 0, 0 0.8, .024, 16, 16			

*Note: Each pulse entry in \underline{v} has four parts:

- 1) The time (seconds) the input reached steady-state,
- 2) steady-state value (angles are in radians),
- 3) the time the input leaves steady-state and starts to return to zero,
- 4) and the time the input returns to zero.

TABLE 4-2
CONTROLLER MATRICES

Flight Condition - 1.2 Mach, 15 000 feet

Maneuver	Command Vector <u>y</u>	ALPHA	** K		
	*		0		
Direct Climb	1.2, .8, 2, 3.2 1.2, 405, 16, 16 0, 0, 0, 0	1.1			
Direct Lift1	.2, .45, .5, .7 0, 0, 0, 0 0, 0, 0, 0		.1902E+01 .1630E-02 0 -.1006E+02 -.5156E-01 0 .3164E-02 .9144E-02 0		
Direct Lift2	1.6, .72, 2.4, 3.2 0, 0, 0, 0 0, 0, 0, 0				
Pitch-Pointing	.8, .0225, 1.2, 1.6 0, 0, 0, 0 .8, .0225, 16, 16	1.1	.1902E+1 .1630E-2 -.2572E2 -.1006E2 -.5156E-1 -.8040E2 .3164E-2 .9144E-2 -.2141		
Vertical Translation1	0, 0, 0, 0 0, 0, 0, 0 1.8, .027, 3.2, 4.5	.82	.1064E1 .1215E-2 -.8563E1 -.5624E1 -.3844E-1 -.2677E2 .1769E-2 .6816E-2 -.713E-1		
Vertical Translation2	0, 0, 0, 0 0, 0, 0, 0 0.8, .024, 16, 16				

*Note: Each pulse entry in y has four parts:

- 1) The time (seconds) the input reached steady-state,
- 2) steady-state value (angles are in radians),
- 3) the time the input leaves steady-state and starts to return to zero,
- 4) and the time the input returns to zero.

**Note: $\underline{K}_0 = \text{ALPHA} * \underline{K}_1$

TABLE 4-3

LONGITUDINAL FIGURES OF MERIT

Flight Condition - 1.2 Mach, 15 000 feet

Maneuver	Command Vector \underline{v}	t * s	t ** p	M *** p
Direct Climb	1.2, .8, 2, 3.2 1.2, 405, 16, 16 0, 0, 0, 0	15 1.35 8.70	1.65 1.5 2.1	.8113 408.6827 .3000
Direct Lift1	.2, .45, .5, .7 0, 0, 0, 0 0, 0, 0, 0	15 15 15	.45 12.15 .6	.4689 4.00E-8 .1227
Direct Lift2	1.6, .72, 2.4, 3.2 0, 0, 0, 0 0, 0, 0, 0	15 15 15	1.95 2.55 2.4	.7501 -.5716 .2888
Pitch-Pointing	.8, .0225, 1.2, 1.6 0, 0, 0, 0 .8, .0225, 16, 16	15 15 4.8	1.05 1.2 15	.0255 -.0196 .02250
Vertical Translation1	0, 0, 0, 0 0, 0, 0, 0 1.8, .027, 3.2, 4.5	15 15 15	1.95 1.95 3.3	.0033 -.0089 .0230
Vertical Translation2	0, 0, 0, 0 0, 0, 0, 0 0.8, .024, 16, 16	15 15 6.15	1.05 1.2 15	.0037 -.0094 .0240

*Note: settling time in seconds

**Note: peak time in seconds

***Note: peak value (greatest magnitude), angles in radians

Note: commanded inputs are smoothed

Note: commanded inputs in order are - pitch rate, change in velocity, and angle-of-attack

TABLE 4-4

LONGITUDINAL CONTROL INPUT RATES

Flight Condition - 1.2 Mach, 15 000 feet

Maneuver	Command Vector \underline{v}	* $\dot{\delta}_c$	** $\dot{\delta}_s$	*** $\dot{\delta}_t$
Direct Climb	1.2, .8, 2, 3.2 1.2, 405, 16, 16 0, 0, 0, 0	13.8	-174	21
Direct Lift1	.2, .45, .5, .7 0, 0, 0, 0 0, 0, 0, 0	-32	167	0.2
Direct Lift2	1.6, .72, 2.4, 3.2 0, 0, 0, 0 0, 0, 0, 0	16	-86	.25
Pitch-Pointing	.8, .0225, 1.2, 1.6 0, 0, 0, 0 .8, .0225, 16, 16	-18	-58	-.15
Vertical Translation1	0, 0, 0, 0 0, 0, 0, 0 1.8, .027, 3.2, 4.5	7	18	.05
Vertical Translation2	0, 0, 0, 0 0, 0, 0, 0 0.8, .024, 16, 16	-9.5	-28	-.08

*Note: maximum canard rate (magnitude) in degrees/second

**Note: maximum strake rate (magnitude) in degrees/second

***Note: maximum thrust rate (magnitude) in hundreds of lbs./second

Note: commanded inputs are smoothed

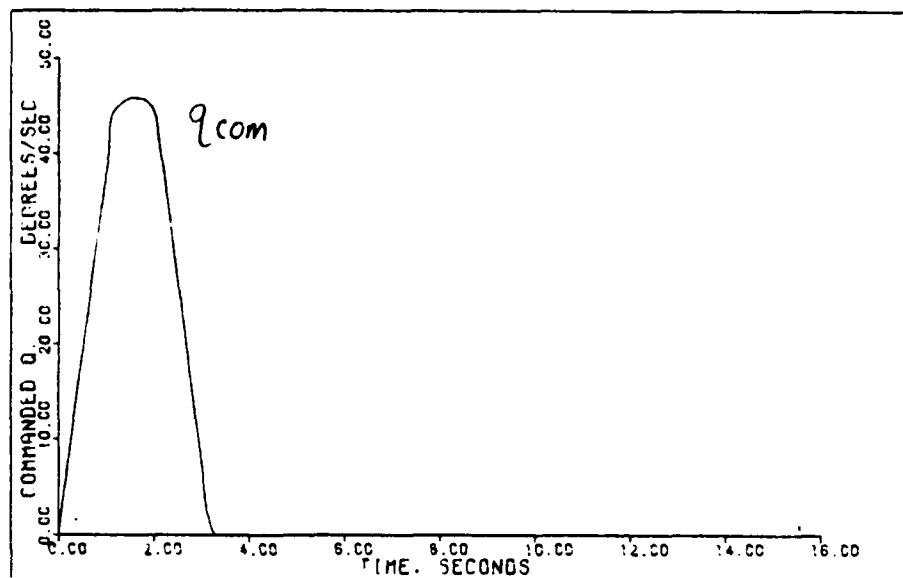
Note: commanded inputs in order are - pitch rate, change in velocity, and angle-of-attack

forward velocity is increased by 405 feet/second and held. The commanded u input and output are indistinguishable (see Figure 4-2). The largest maximum commanded inputs (in decreasing order) are at 1.2 Mach, 15 000 feet; 0.9 Mach, sea level; 0.4 Mach, sea level; 0.7 Mach, 15 000 feet; and 0.9 Mach, 50 000 feet.

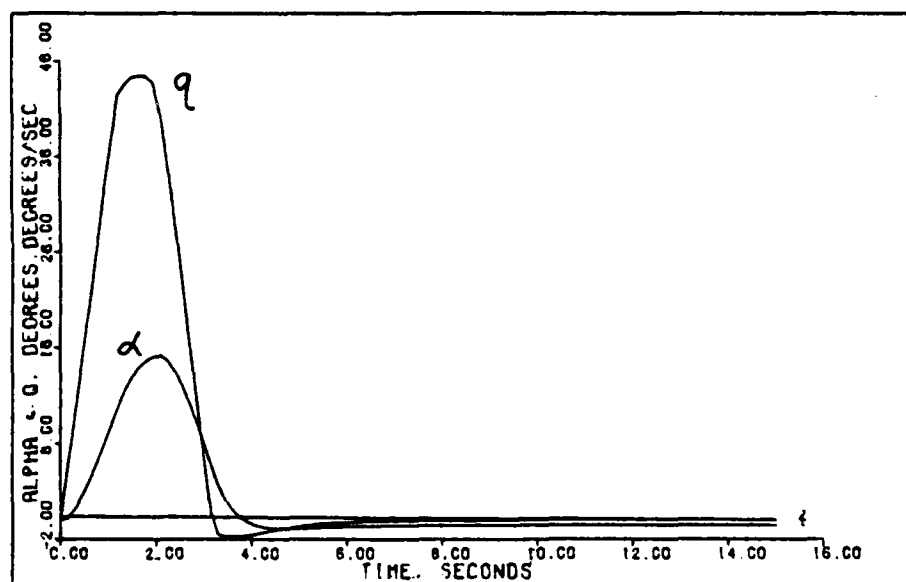
Since thrust is an input, velocity control is excellent for all maneuvers performed. The additional thrust required to increase velocity ranges from 320 pounds at 0.4 Mach, sea level, to 1000 pounds at 0.9 Mach, sea level. At 1.2 Mach, 15 000 feet, 340 additional pounds of thrust is required (see Figure 4-3). The limiting input for direct climb is the strakes (see Figure 4-3). The direct climb maneuver commands α to zero, so flight-path angle should equal θ in the steady-state since:

$$\gamma = \theta - \alpha \quad (4-11)$$

An examination of the γ and θ plots reveals that after an initial transient, γ does indeed track θ closely (see Figure 4-4). The best steady-state tracking (performance is presented in decreasing order) is performed by 1.2 Mach, 15 000 feet; 0.9 Mach, sea level; 0.7 Mach, 15 000 feet; 0.9 Mach, 50 000 feet; and 0.4 Mach, sea level. The best transient response is provided by 0.9 Mach, sea level; 1.2 Mach, 15 000 feet; 0.7 Mach, 15 000 feet; 0.4 Mach, sea level; and 0.9 Mach, 50 000 feet. Steady-state γ varies from 90 degrees (more could have been commanded, but the assumption of small perturbations is stretched here at best)



COMMANDED Q INPUT TO DIRECT CLIMB: 1.2M, 15K FT



ALPHA & Q OUTPUTS TO DIRECT CLIMB: 1.2M, 15K FT

Figure 4-1

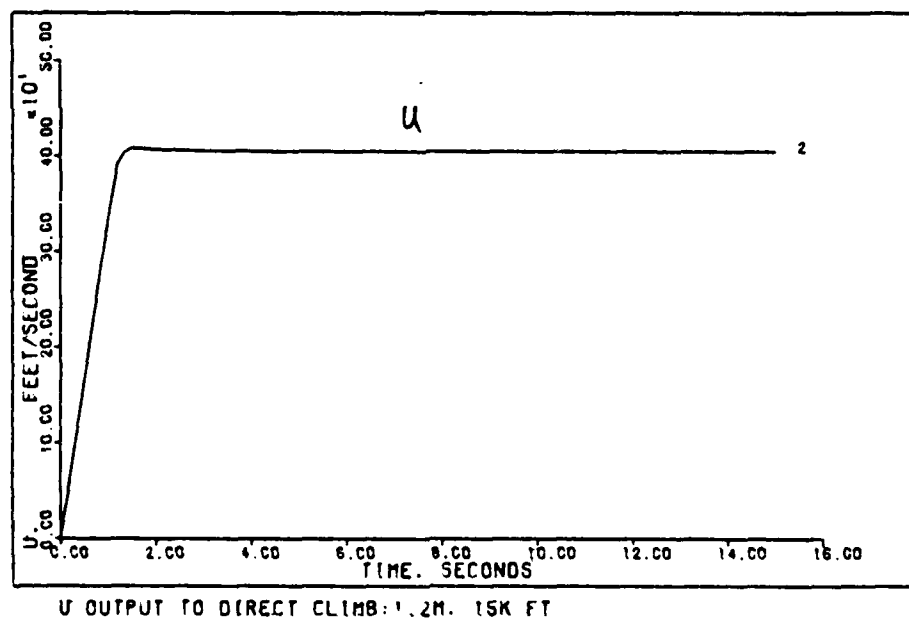
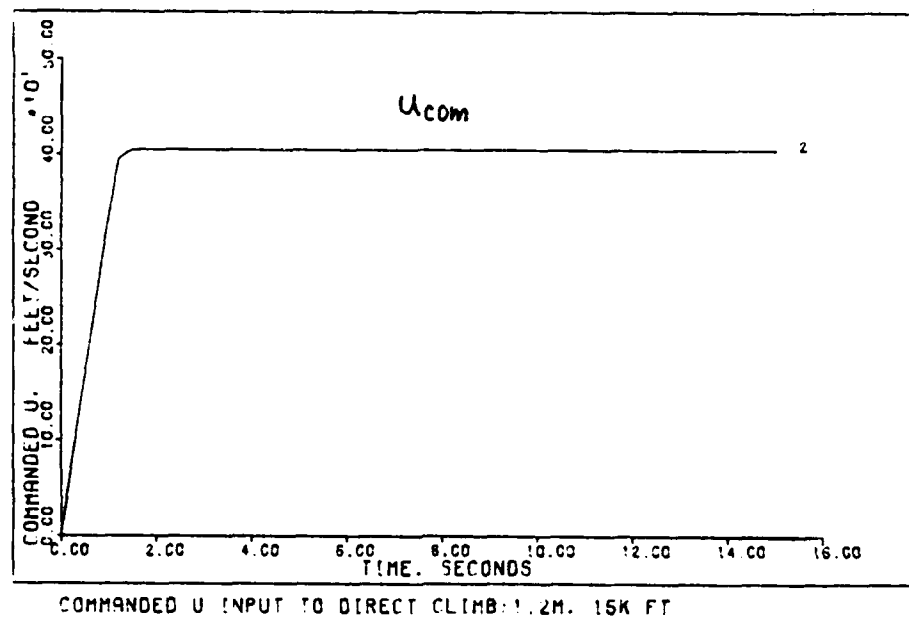
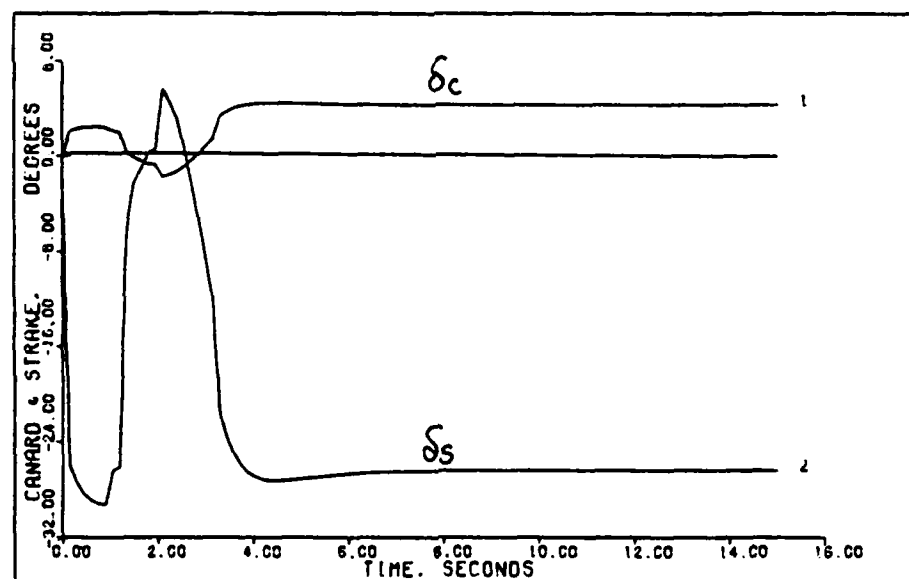
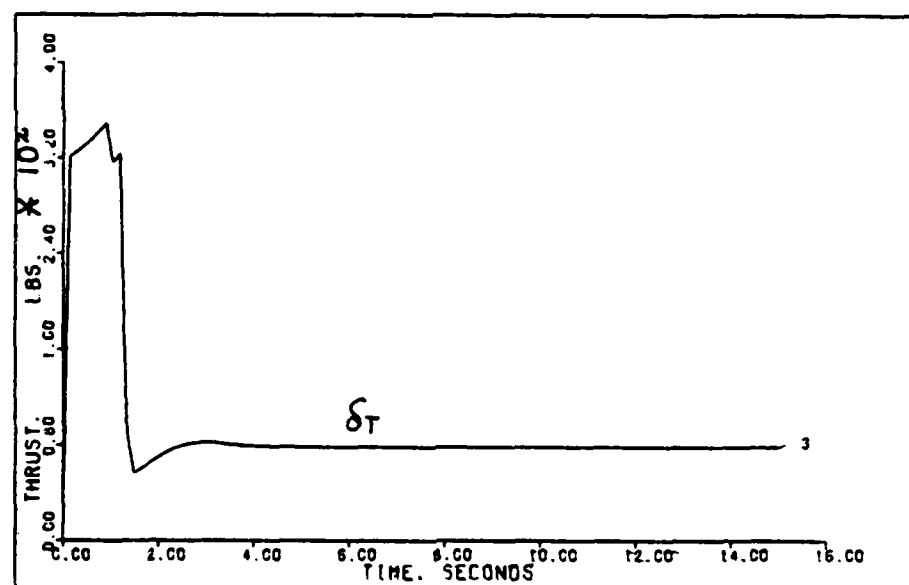


Figure 4-2

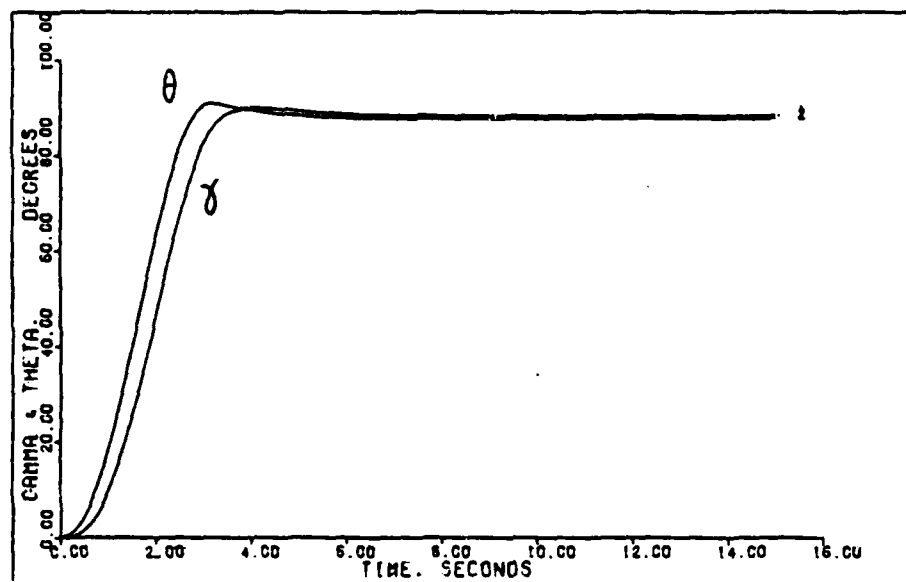


CANARD & STRAKE INPUT TO DIRECT CLIMB: 1.2M, 15K FT



THRUST INPUT TO DIRECT CLIMB: 1.2M, 15K FT

Figure 4-3



GAMMA & THETA FROM DIRECT CLIMB: 1.2M. 15K FT

Figure 4-4

at 1.2 Mach, 15 000 feet to 31 degrees at 0.9 Mach, 50 000 feet.

Maximum allowable deflection rates for the canards and strakes are 100 degrees/second and 30 degrees/second, respectively. Actual canard deflection rates are well within the allowable maximum for all flight conditions. Strake deflection rates, however, greatly exceed the maximum at all flight conditions. For example, the maximum negative and positive strake deflection rates at 1.2 Mach, 15 000 feet, are -173.6 and 131.9 degrees/second. Whenever control input rates are exceeded, the maneuver time must be lengthened and the commanded steady-state value must be decreased, but the controller does not have to be retuned.

Direct lift1, a commanded pitch-rate pulse of only 0.7 seconds duration, has the same controller at each flight condition as direct climb. For this maneuver, the largest commanded inputs are at 1.2 Mach, 15 000 feet; 0.7 Mach, 15 000 feet; 0.9 Mach, sea level; 0.4 Mach, sea level; and 0.9 Mach, 50 000 feet. Transient alpha responses are best minimized at 0.9 Mach, sea level; 1.2 Mach, 15 000 feet; 0.7 Mach, 15 000 feet; 0.4 Mach, sea level; and 0.9 Mach, 50 000 feet. At 1.2 Mach, 15 000 feet, pitch-rate is commanded to a 27 degree/second pulse, while alpha is commanded to zero. Pitch-rate tracks the commanded output excellently, while after a short transient alpha goes to zero (see Figure 4-5). The change in forward velocity is commanded to zero. The u transient is small, with the greatest magnitude a decrease in

u of -0.21 feet/second occurring at 1.2 Mach, 15 000 feet (see Figure 4-6).

Again, the strake is the limiting control input to a greater commanded input. A negligible increase in thrust of 16 pounds is required at 1.2 Mach, 15 000 feet (see Figure 4-7). Again, since alpha is commanded to zero, flight-path should track theta. In the steady-state, gamma, the flight-path angle does indeed equal pitch angle at all flight conditions. The best transient tracking of theta by gamma is provided at 0.9 Mach, sea level; 1.2 Mach, 15 000 feet; 0.7 Mach, 15 000 feet; 0.4 Mach, sea level; and 0.9 Mach, 50 000 feet. A steady-state flight-path angle of 13 degrees is achieved at 1.2 Mach, 15 000 feet (see Figure 4-7).

Unfortunately, allowable control input rates are again exceeded. For example, maximum strake rates are -166 and 167 degrees/second at 1.2 Mach, 15 000 feet. Maximum canard rates are within acceptable limits except at 0.4 Mach, sea level where the maximums are -141 and 143 degrees/second.

Direct lift₂, which is the same maneuver performed with longer maneuver time, permits greater commanded steady-state values. In decreasing order of capability, the greatest commanded inputs are at 1.2 Mach, 15 000 feet; 0.4 Mach, sea level; 0.9 Mach, sea level; 0.7 Mach, 15 000 feet; and 0.9 Mach, 50 000 feet. At 1.2 Mach, 15 000 feet, pitch-rate is commanded to a pulse of 41 degrees/second (see Figure 4-8). Again, excellent tracking is performed of the commanded input (see Figure 4-8). A minimal undershoot of pitch-rate output occurs at the end of the commanded input, but it decays within

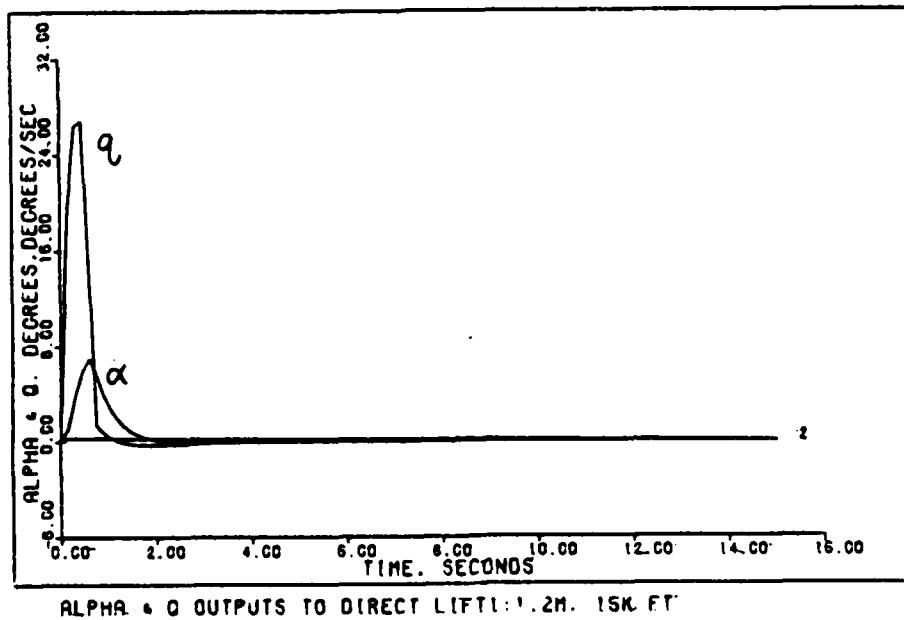
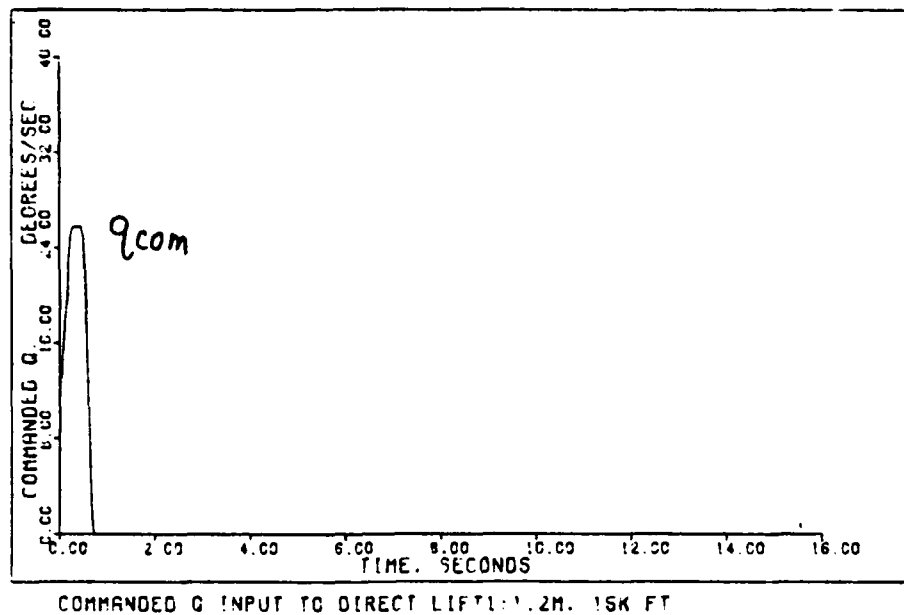
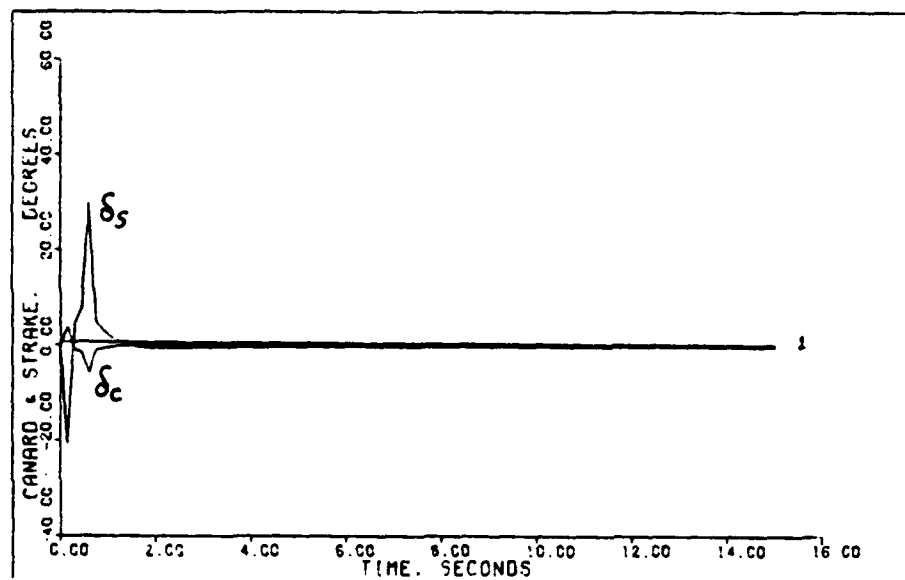
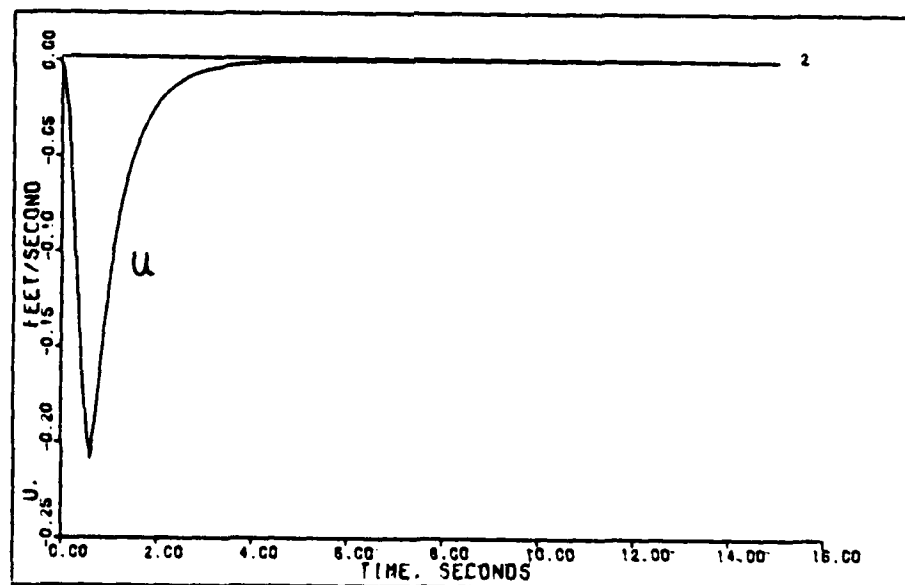


Figure 4-5

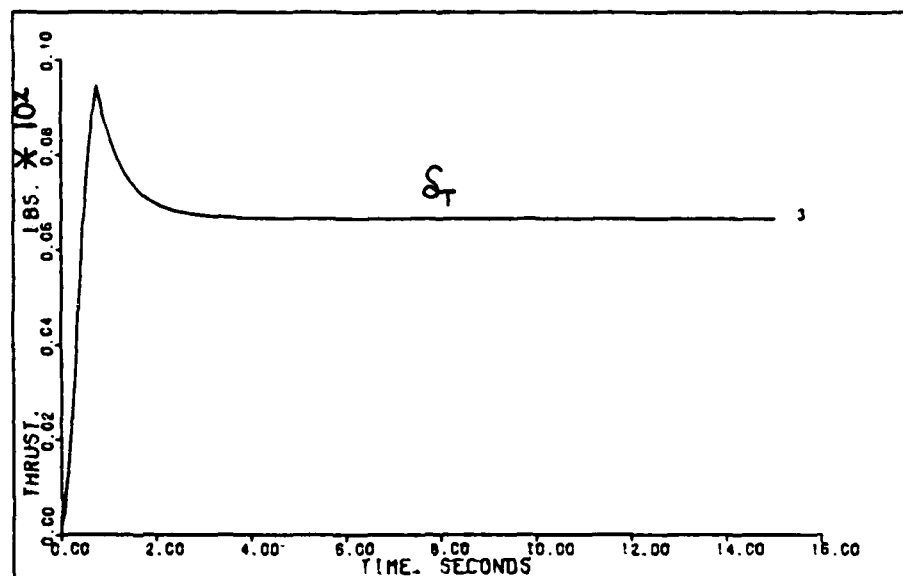


CANARD & STRAKE INPUTS TO DIRECT LIFT: 1.2M. 15K FT

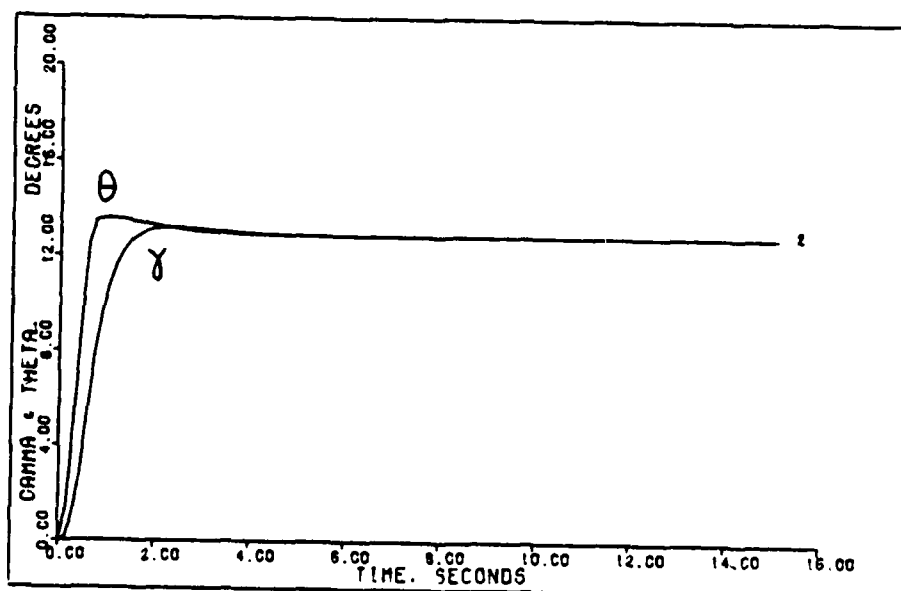


U OUTPUT TO DIRECT LIFT: 1.2M. 15K FT

Figure 4-6



THRUST INPUT TO DIRECT LIFT: 1.2M. 15K FT



GAMMA & THETA FROM DIRECT LIFT: 1.2M. 15K FT

Figure 4-7

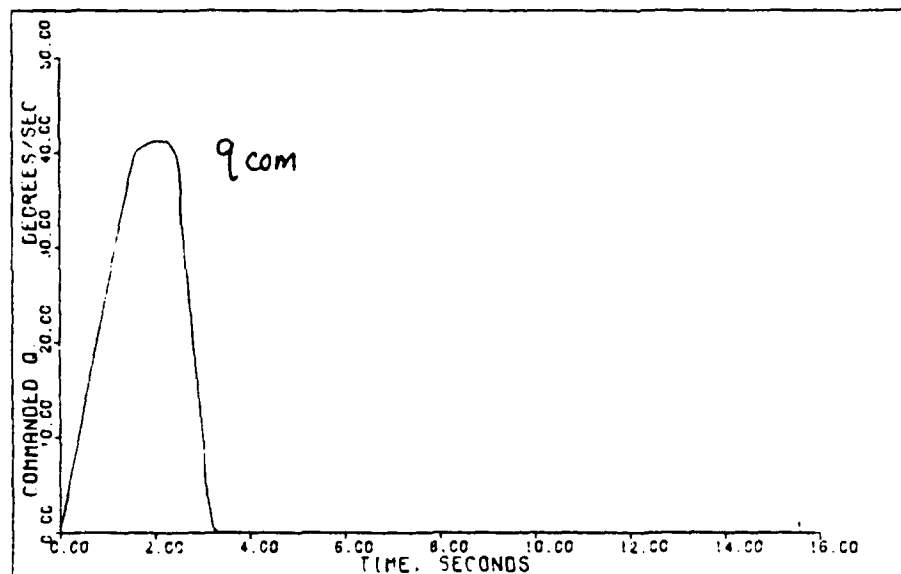
1.5 seconds.

Again, the strakes are the limiting control input. The shape of the control inputs is similar, with a steady-state negative strake deflection required to provide a nose-down pitching moment (see Figure 4-9).

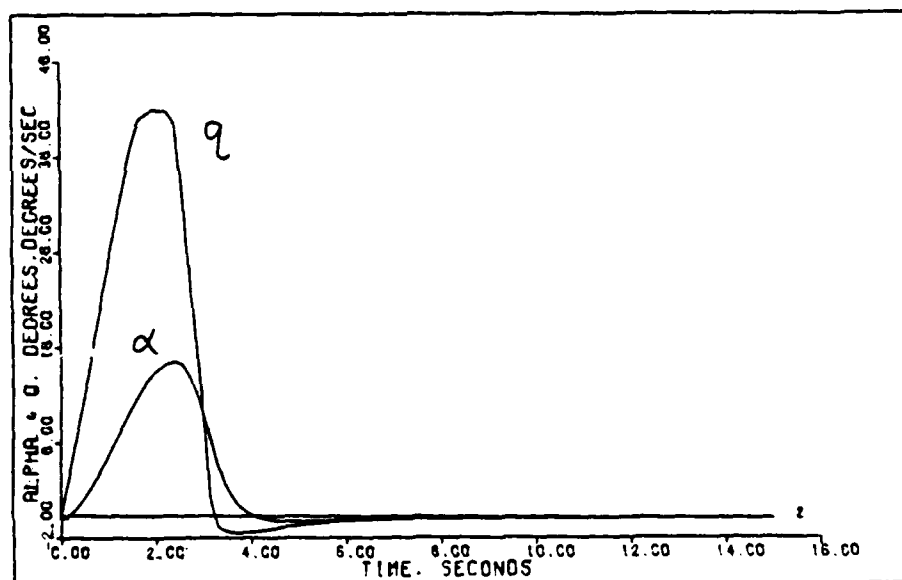
Again, in the steady-state γ equals θ . The best transient tracking of θ by γ occurs at 0.9 Mach, sea level; 1.2 Mach, 15 000 feet; 0.7 Mach, 15 000 feet; 0.4 Mach, sea level; and 0.9 Mach, 50 000 feet. At 1.2 Mach, 15 000 feet a steady-state flight-path angle of 83 degrees is achieved (see Figure 4-10).

Note that an increase in maneuver time, although coupled with an increase in the commanded steady-state value, causes a marked reduction in control input rates. The previously exceeded maximum canard rates decline to -35 and 59 degrees/second at the worst-performing flight condition, 0.4 Mach, sea level. At 1.2 Mach, 15 000 feet, maximum canard rates are -8 and 16 degrees/second. The maximum strake rates are -86 and 41 degrees/second.

Pitch-pointing, the maneuver that commands pitch-rate and angle-of-attack such that flight-path is zero, has a separate controller. The greatest commanded inputs are at 0.4 Mach, sea level; 0.7 Mach, 15 000 feet; 1.2 Mach, 15 000 feet; 0.9 Mach, sea level; and 0.9 Mach, 50 000 feet. The best transient and steady-state tracking of the commanded inputs by the outputs occurs at 0.4 Mach, sea level; 0.9 Mach, 50 000 feet; 0.7 Mach, 15 000 feet; 1.2 Mach, 15 000 feet; and 0.9 Mach, sea level. At 0.4 Mach, sea level, 2.1 degrees of

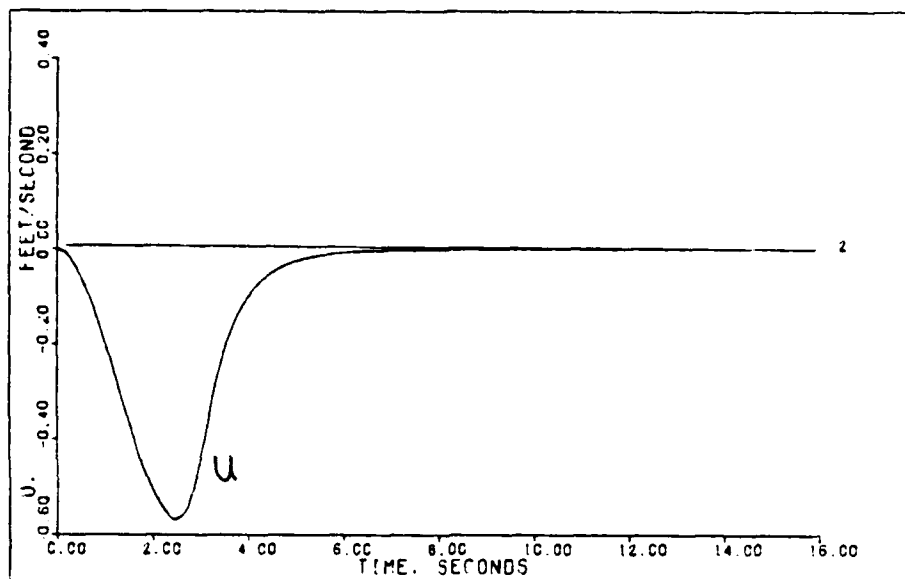


COMMANDED Q INPUT TO DIRECT LIFT 2: 1.2M, 15K FT

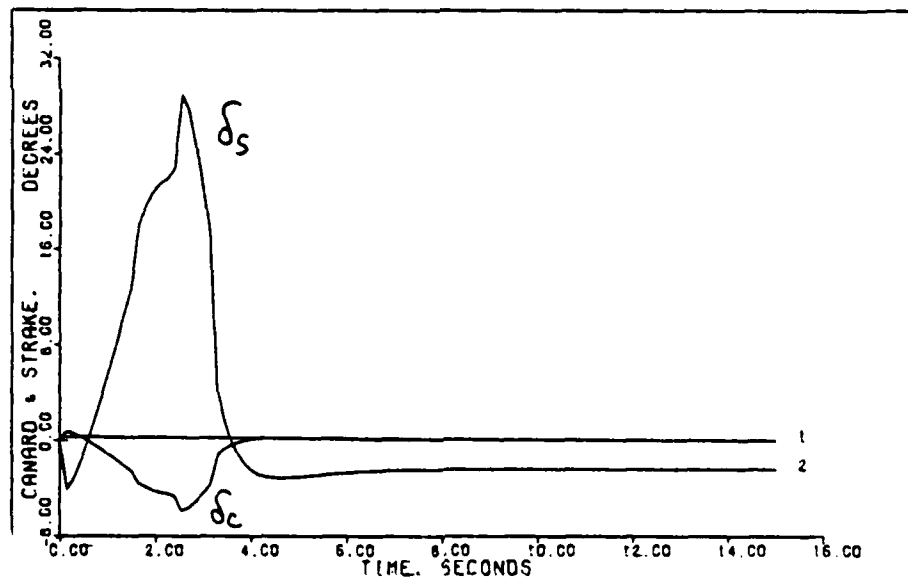


ALPHA & Q OUTPUTS TO DIRECT LIFT 2: 1.2M, 15K FT

Figure 4-8

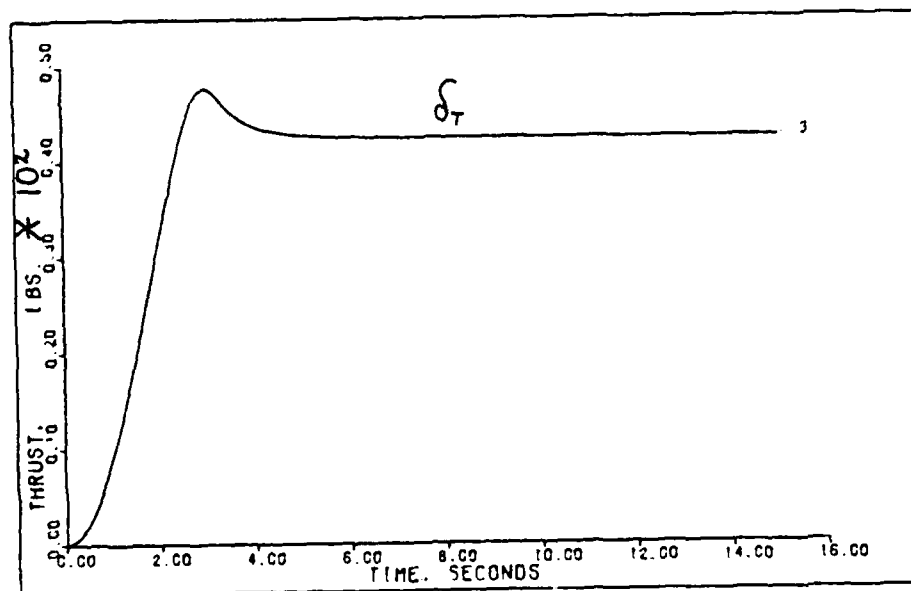


J OUTPUT TO DIRECT LIFT 2: 1.2M. 15K FT

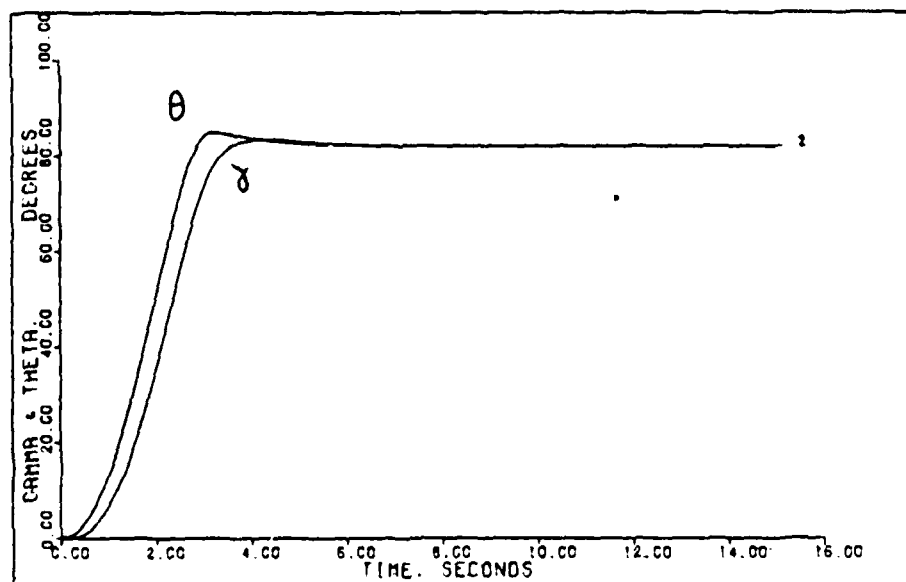


CANARD & STRAKE INPUTS TO DIRECT LIFT 2: 1.2M. 15K FT

Figure 4-9



THRUST INPUT TO DIRECT LIFT2: 1.2M 15K FT



GAMMA & THETA FROM DIRECT LIFT2: 1.2M 15K FT

Figure 4-10

pitch-pointing (the value of α and θ) is possible. At 1.2 Mach, 15 000 feet, the response is degraded to 1.2 degrees of pitch-pointing (see Figure 4-11).

The input responses at the five flight conditions are similar. Again, the strake is the limiting control input. Negative steady-state control values occur in which the canard deflection is approximately half that of the strake deflection (see Figure 4-12). The deflections provide canceling pitching moments about the center of gravity, resulting in a net rotation of the nose about the center of gravity. Since the symmetrical flaperons, and not the strakes, are intended to be the primary lift-vector surfaces, the strakes are a poor match against the canards.

The flight conditions minimizing γ steady-state error are 0.4 Mach, sea level; 0.9 Mach, 50 000 feet; 0.7 Mach, 15 000 feet; 1.2 Mach, 15 000 feet; and 0.9 Mach, sea level. At 1.2 Mach, 15 000 feet, 1.6 degrees of pitch-pointing with a γ steady-state error of .35 degrees is achieved.

Maximum canard rates are well within allowable limits, but the maximum strake rates are again violated. At the best-performing flight condition, 0.4 Mach, sea level, the maximum strake rates are -39 and 27 degrees/second. At 1.2 Mach, 15 000 feet, the maximum canard rates are -18 and 6 degrees/second. The maximum strake rates at this flight condition are -58 and 22 degrees/second.

One controller is used for both vertical translation¹ and vertical translation². The largest commanded α inputs

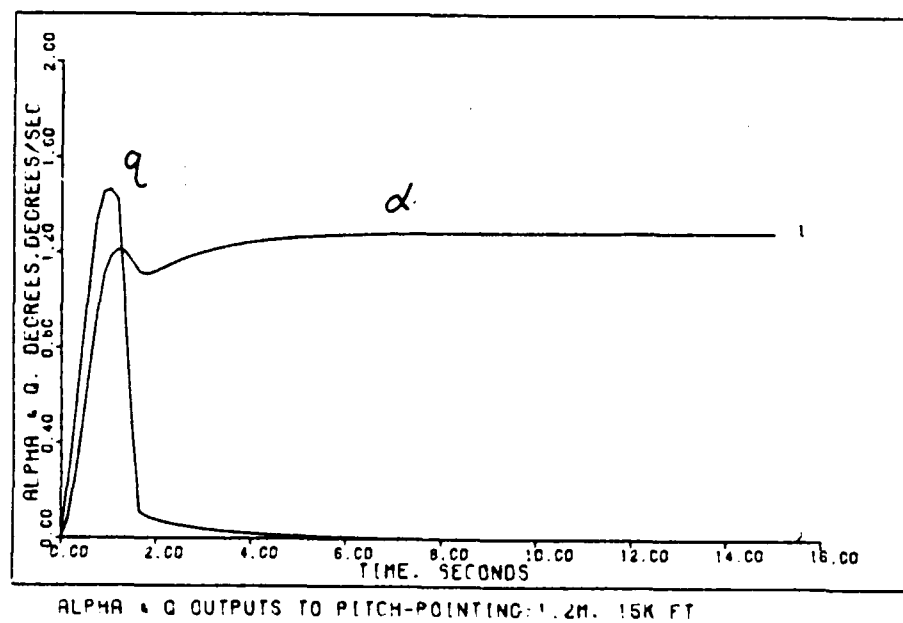
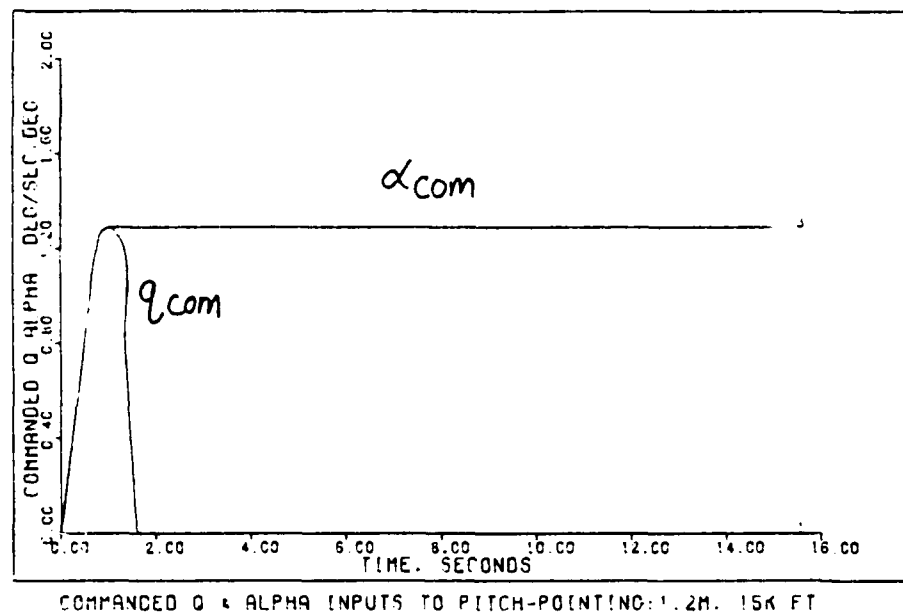
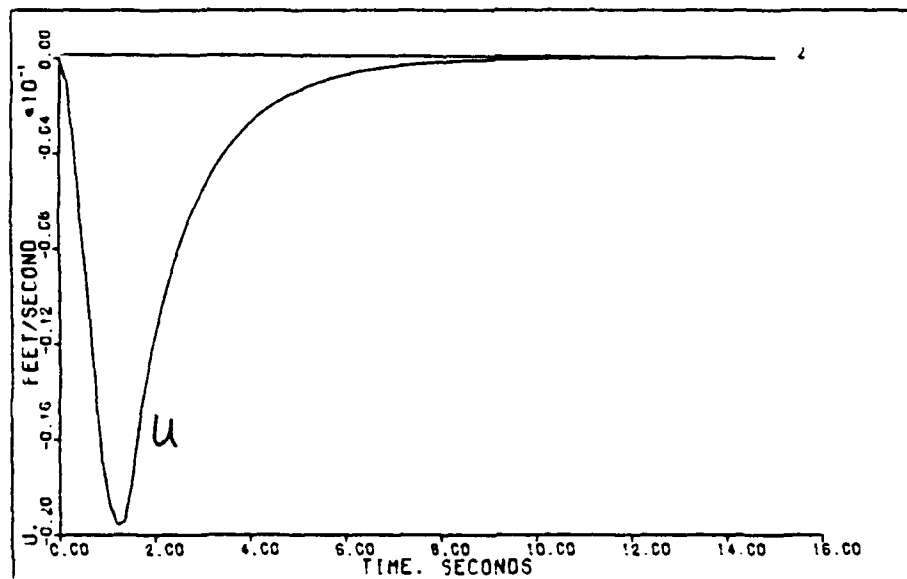
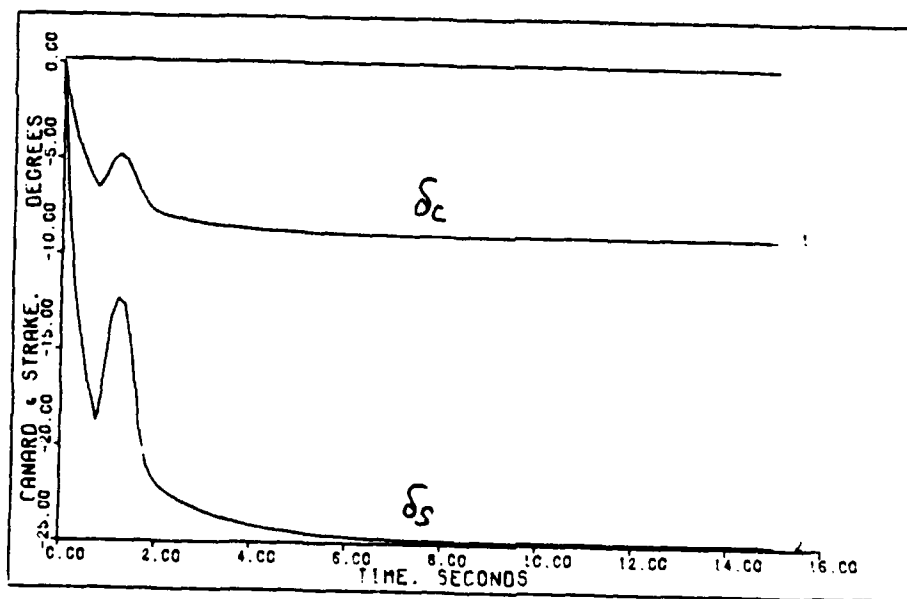


Figure 4-11

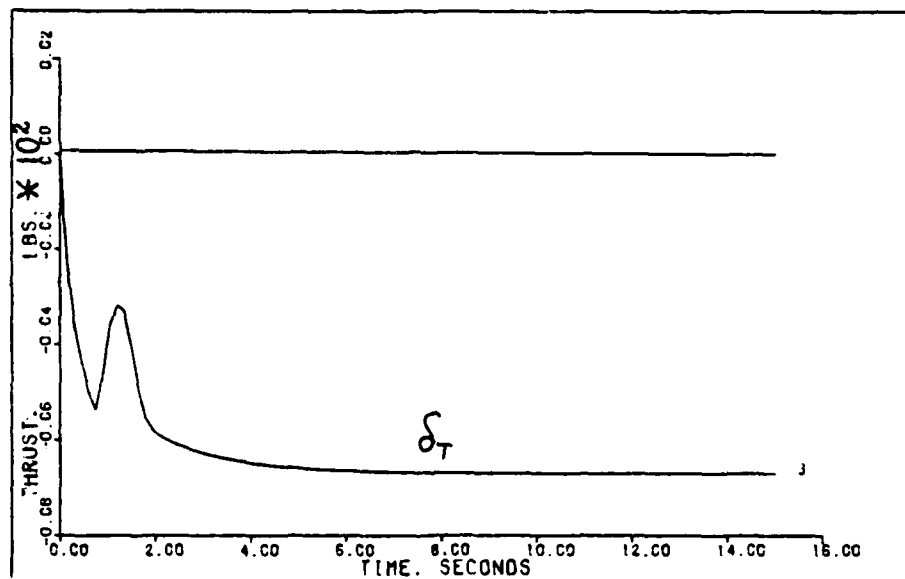


U OUTPUT TO PITCH-POINTING: 1.2M, 15K FT

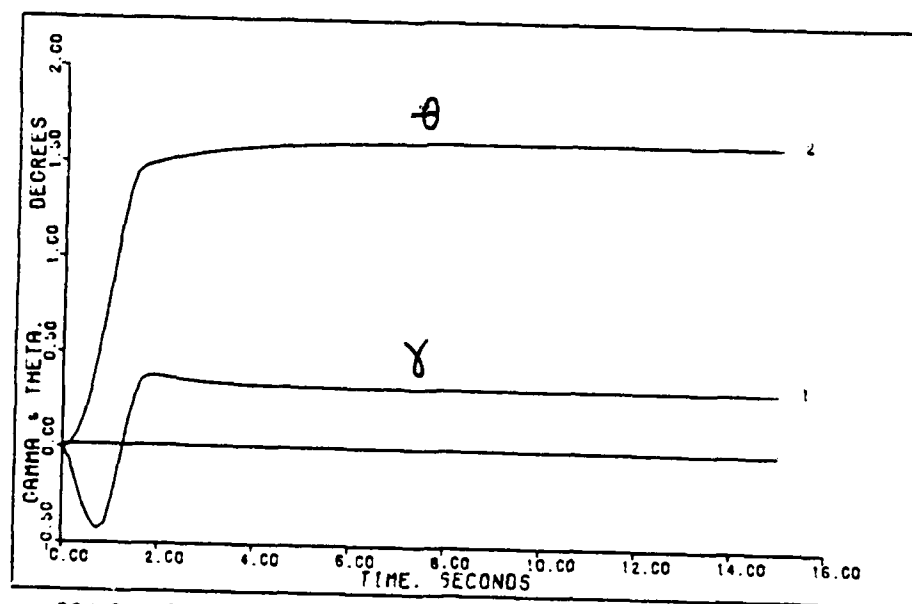


CANARD & STRIKE INPUTS TO PITCH-POINTING: 1.2M, 15K FT

Figure 4-12



THRUST INPUT TO PITCH-POINTING: 1.2M, 15K FT



GAMMA & THETA FROM PITCH-POINTING: 1.2M, 15K FT

Figure 4-13

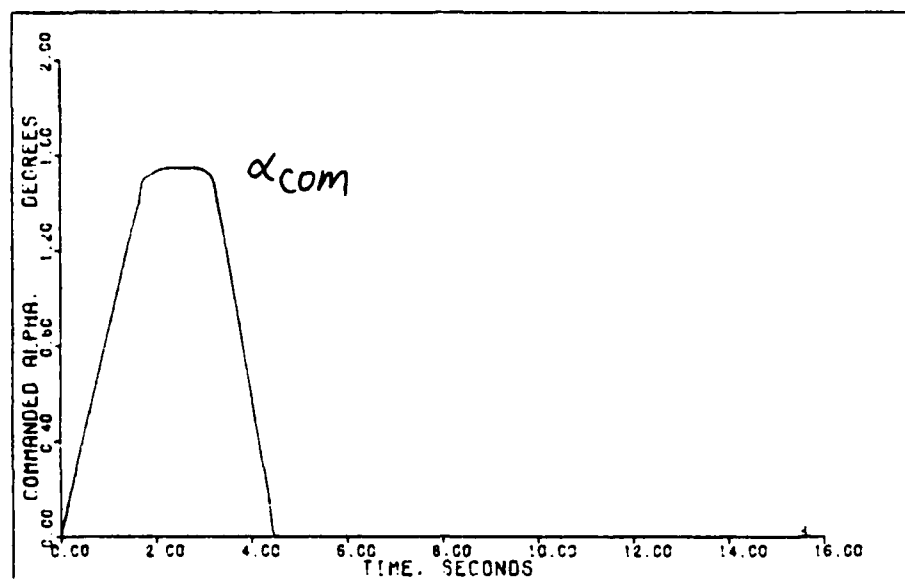
occur at 0.7 Mach, 15 000 feet; 0.4 Mach, sea level; 1.2 Mach, 15 000 feet; 0.9 Mach, sea level; and 0.9 Mach, 50 000 feet. Pitch-rate is commanded to zero, but the resulting positive transient is canceled by an undershoot. In general, the alpha output follows the general shape of the commanded input, although the tracking lags by about 1.6 seconds. At 1.2 Mach, 15 000, alpha is commanded to 1.3 degrees (see Figure 4-14).

The control input shapes are similar at all flight conditions, with the strake hitting the control limit. Thrust control provides excellent u response (see Figure 4-15).

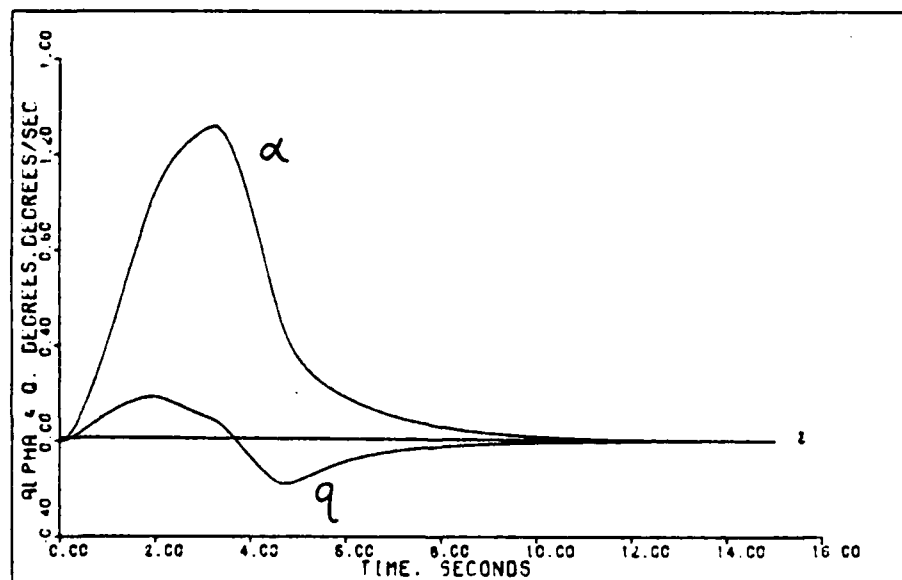
Pitch angle, which should be zero since pitch-rate is commanded to zero, does have a positive transient that eventually decays to zero. At 1.2 Mach, 15 000 feet, the pitch angle transient is .45 degrees, while the resulting flight-path angle is -0.9 degrees (see Figure 4-16). The best transient response is provided by 0.4 Mach, sea level; 0.9 Mach, 50 000 feet; 0.7 Mach, 15 000 feet; 1.2 Mach, 15 000 feet; and 0.9 Mach, sea level.

Maximum canard control input rates are within allowable limits for all flight conditions. Maximum strake control input rates are within allowable limits for all flight conditions but 0.9 Mach, 50 000 feet; -40 and 41 degrees/second. At 1.2 Mach, 15 000 feet, maximum canard rates are -5 and 7 degrees/second. Maximum strake rates are -14 and 18 degrees/second.

In vertical translation², alpha is commanded to a fixed steady-state value. The greatest commanded alpha inputs are

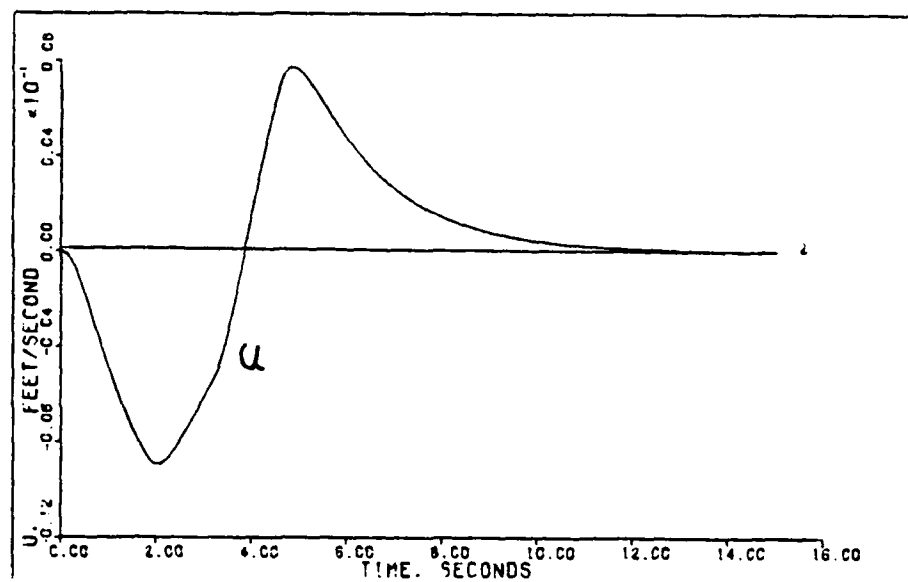


COMMANDED ALPHA INPUT TO VERTICAL TRANSLATION: 1.2M, 15K FT

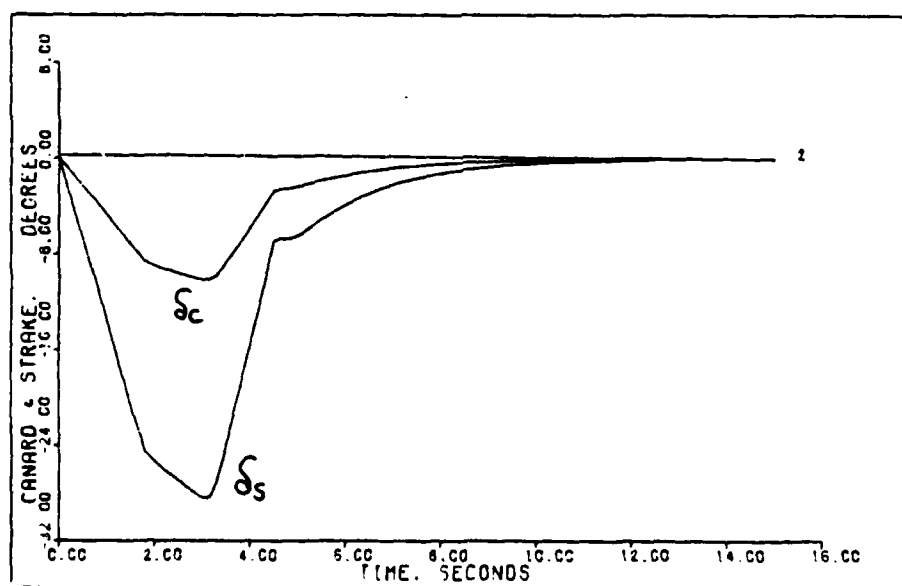


ALPHA & Q OUTPUTS TO VERTICAL TRANSLATION: 1.2M, 15K FT

Figure 4-14

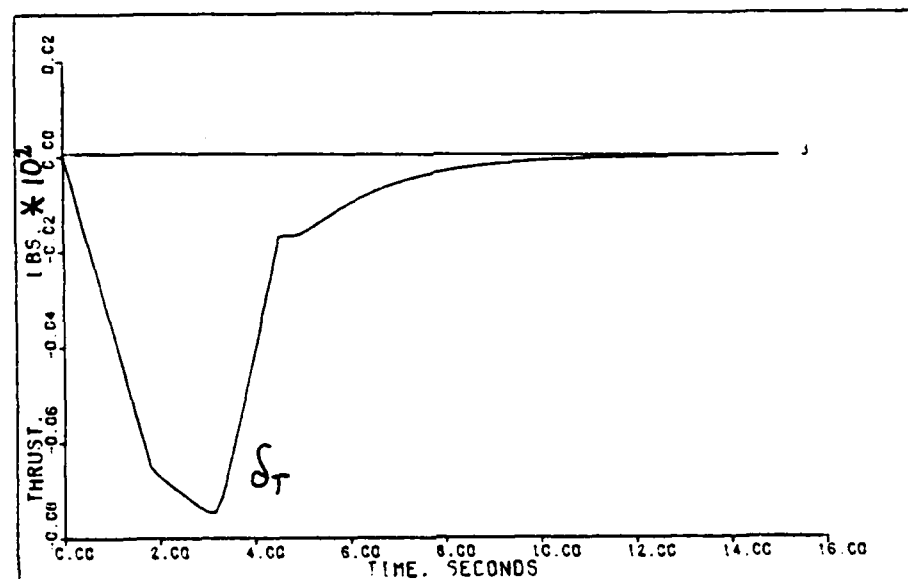


U OUTPUT TO VERTICAL TRANSLATION: 1.2M, 15K FT

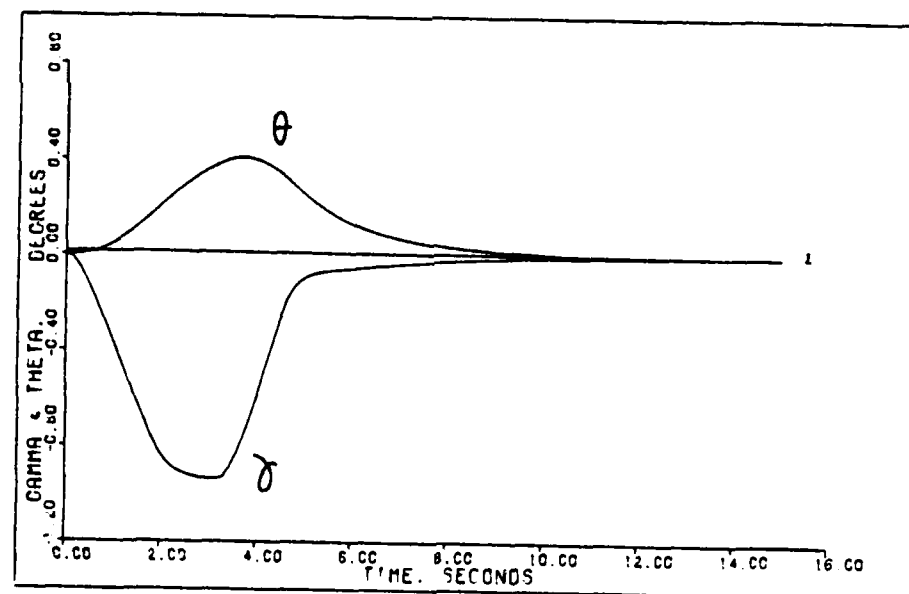


CANARD & STRIKE INPUTS TO VERTICAL TRANSLATION: 1.2M, 15K FT

Figure 4-15



THRUST INPUT TO VERTICAL TRANSLATION: 1.2M, 15K FT



GAMMA & THETA FROM VERTICAL TRANSLATION: 1.2M, 15K FT

Figure 4-16

at 0.7 Mach, 15 000 feet; 0.4 Mach, sea level; 1.2 Mach, 15 000 feet; 0.9 Mach, sea level; and 0.9 Mach, 50 000 feet. The best alpha transient response occurs at 0.9 Mach, 50 000 feet; 0.4 Mach, sea level; 0.7 Mach, 15 000 feet; 1.2 Mach, 15 000 feet; and 0.9 Mach, sea level. A small transient pitch-rate occurs, but this quickly decays (see Figure 4-17).

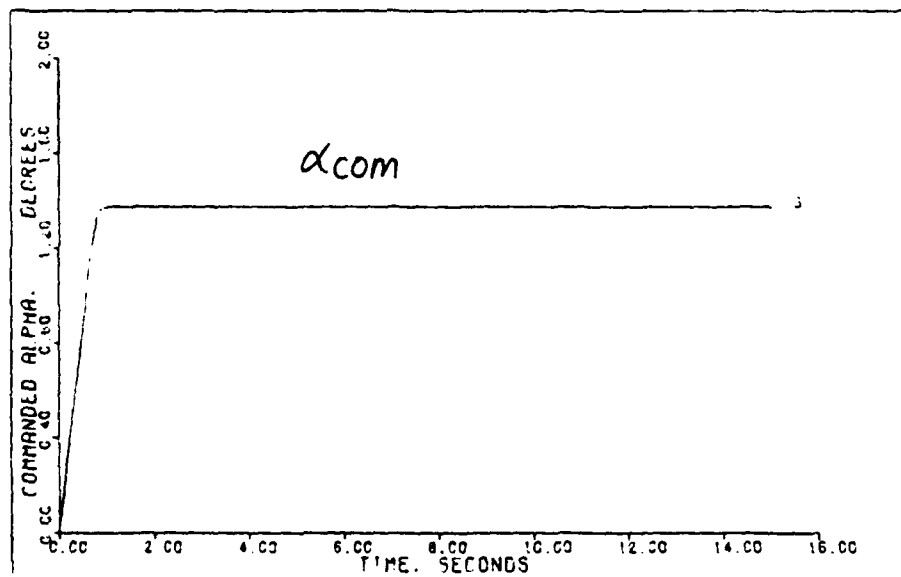
The shape of the control inputs varies somewhat from flight condition to flight condition. At two of the flight conditions the strake transient response reaches the control input limit. At the other flight conditions, however, the steady-state strake response is the limiting factor. At 1.2 Mach, 15 000 feet, the steady-state canard and strake deflections are -9 and -30 degrees, respectively (see Figure 4-18).

Examining the pitch and flight-path angle plots reveals that the minimum theta steady-state errors occur at 0.4 Mach, sea level; 0.9 Mach, 50 000 feet; 0.7 Mach, 15 000 feet; 1.2 Mach, 15 000 feet; and 0.9 Mach, sea level. At 1.2 Mach, 15 000 feet, the steady-state theta and gamma are .5 and -.8 degrees, respectively (see Figure 4-19).

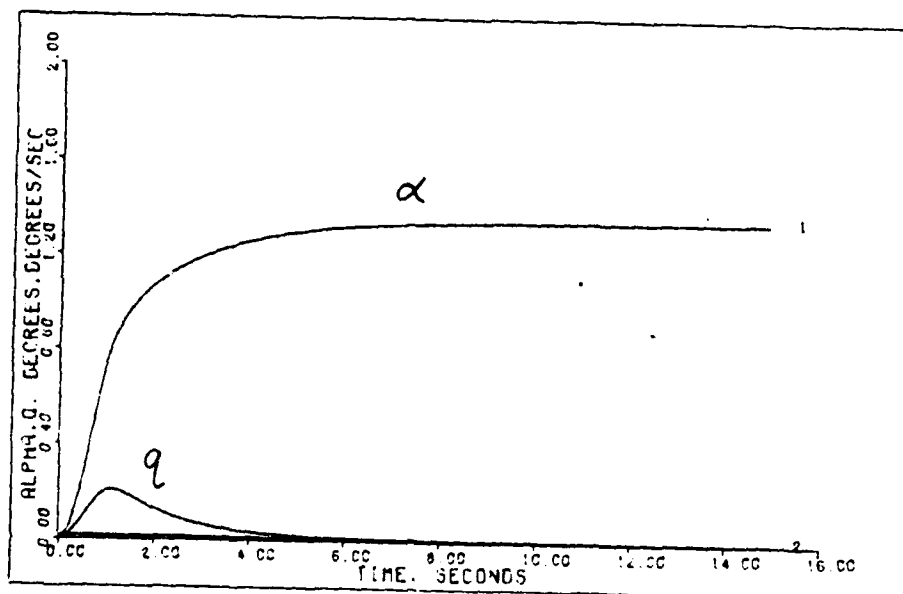
Only maximum strake rates at 0.9 Mach, 50 000 feet exceed the allowable limits for canards and strakes. At 1.2 Mach, 15 000 feet, the maximum canard rates are -9 and 0 degrees/second. The maximum strake rates are -28 and 0 degrees/second.

Summary

This chapter presents the results of a Regular design application to develop longitudinal controllers for the X-29A.



COMMANDED ALPHA INPUT TO VERTICAL TRANSLATION2: 1.2M. 1SK FT



ALPHA & Q OUTPUTS TO VERTICAL TRANSLATION2: 1.2M. 1SK FT

Figure 4-17

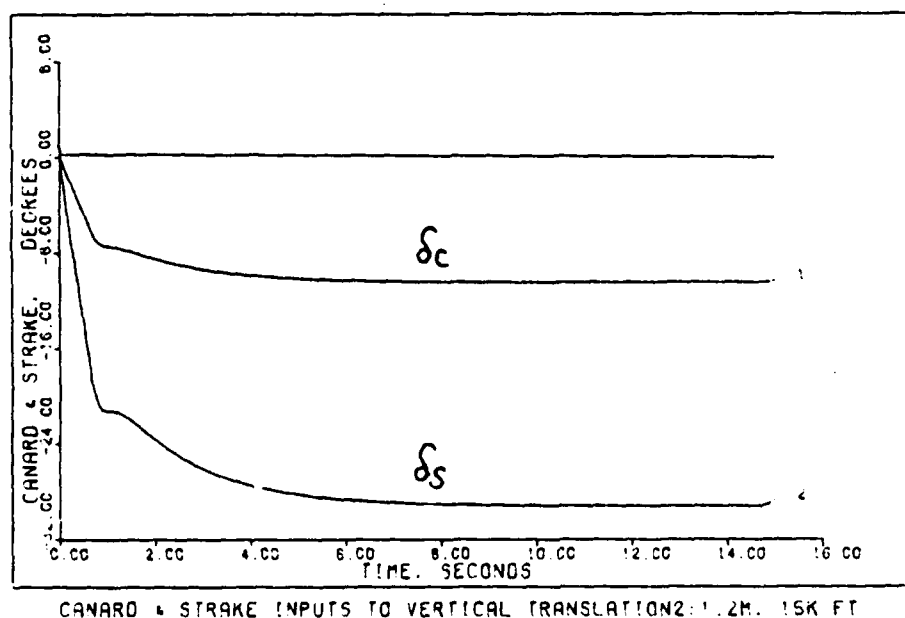
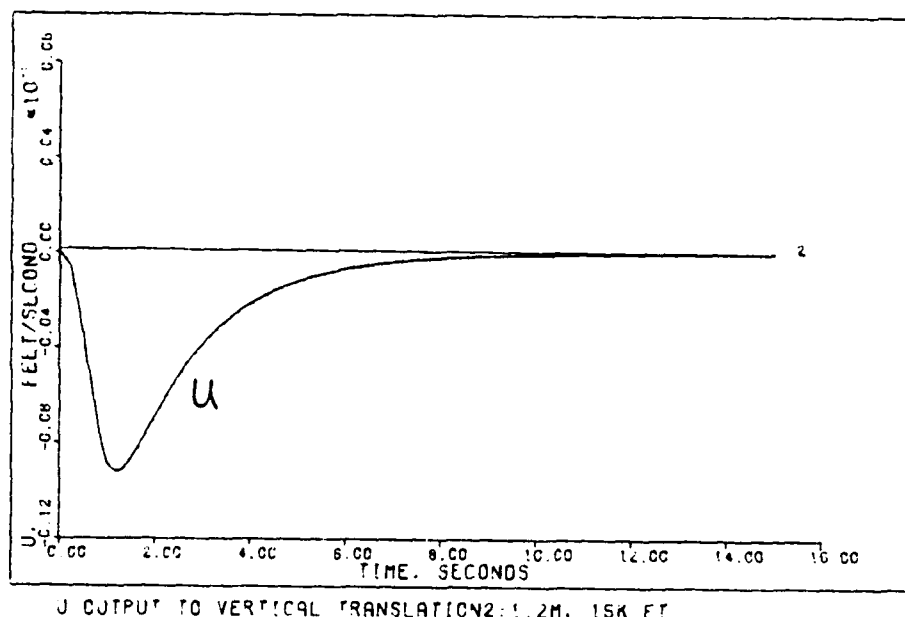


Figure 4-18

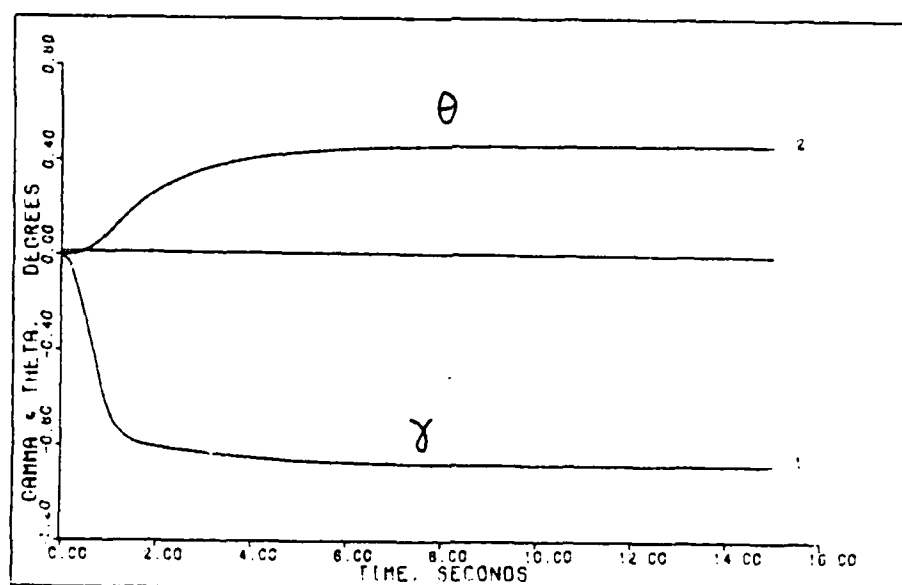
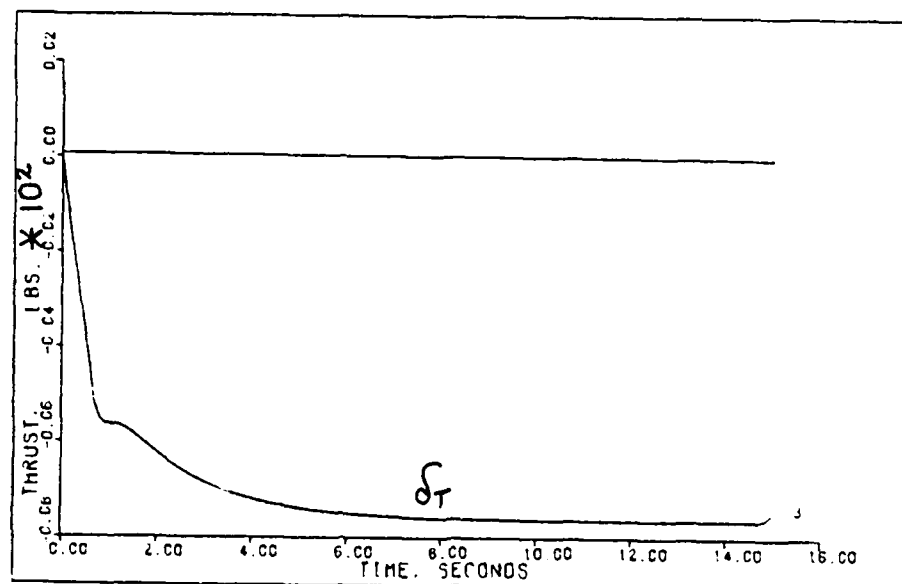


Figure 4-19

A Regular design, which requires that the product CB have full rank, is a minimum phase application. The input and output matrices have full rank, permitting a Regular design. It is stressed that constant output matrices must be used throughout the flight envelope. Otherwise the pilot has to flip a switch to tell the aircraft's flight control system which maneuver he is about to command. It is noted that, with the advent of automatic digital flight control systems, (such as the integrated fire/flight control system) maneuvers are now possible that the pilot would otherwise be incapable of commanding because of his reaction time.

A description is provided of the six longitudinal maneuvers which the aircraft is required to perform. At each flight condition three controllers are designed. One controller for the direct climb, direct lift1, and direct lift2 maneuvers is used with minimal degradation of performance. One controller for pitch-pointing is designed. One controller for vertical translation1 and vertical translation2 is designed. These consolidated controllers are used in the quest for a single robust controller for all maneuvers at all flight conditions. An acceptable alternative would be a single controller at each flight condition with gain-scheduling used between design points.

A general list of assumptions is presented for the development of aircraft equations of motion. A ten step general outline for applying Porter's method is presented. A discussion of design parameters is presented. An outline to

allow the design engineer to immediately start using the interactive CAD program MULTI is given.

Finally, a general discussion of the calcomp plots for all forty maneuvers is provided. Specific details and analysis are furnished at a representative flight condition, 1.2 Mach, 15 000 feet. Comparisons between performance capabilities at different flight conditions for each maneuver are made.

Although allowable control input rates are exceeded for most of the maneuvers, it is shown that only the maximum commanded inputs must be reduced. Retuning of the controllers is not required.

AWD-A140 983

MULTIVARIABLE DIGITAL FLIGHT CONTROL DESIGN OF THE
X-29A(U) AIR FORCE INST OF TECH WRIGHT-PATTERSON AFB OH
SCHOOL OF ENGINEERING R S FELDMANN MAR 84

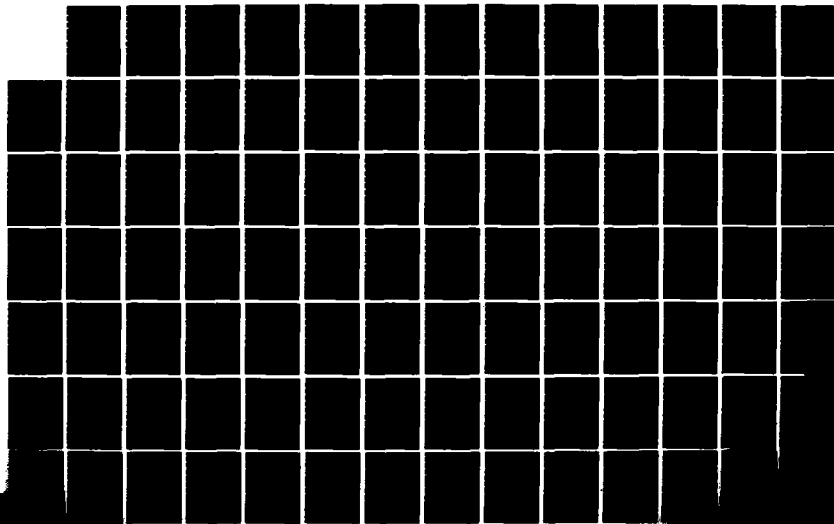
2/4

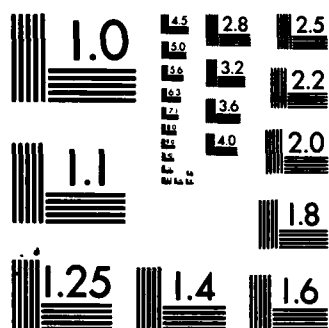
UNCLASSIFIED

AFIT/GE/EE/84M-3

F/G 1/3

NL





MICROCOPY RESOLUTION TEST CHART
NATIONAL BUREAU OF STANDARDS-1963-A

CHAPTER V

LATERAL CONTROLLER DESIGNS

Introduction

This chapter presents the results of the lateral controller designs for the five flight conditions for each of two maneuvers. A sample flight condition, 1.2 Mach, 15 000 feet, is presented. Although each flight condition is discussed, supporting state-space matrices, design parameters, commanded inputs, controller matrices, figures of merit, and plots for the other four flight conditions are included in the appendices.

Since the X-29A demonstrator aircraft's longitudinal and lateral equations of motion are decoupled, separate longitudinal and lateral controllers may be designed. In addition, the controllers may be implemented on separate computer systems, thus increasing processing speed and improving software reliability and maintenance.

Grumman developed a nonlinear simulation computer program for the X-29A. From this program, a simplified reduced-state linearized model at specified flight conditions is used. The linear approximation is valid, but becomes less so the greater the perturbation away from the specified flight condition. The lateral states used are ϕ , roll angle; β , side slip angle; p , angular roll-rate; and r , angular yaw rate.

Differential flaperons and rudder are the lateral control inputs. Note that control-configured vehicle (CCV)

maneuvers are not possible since only two control inputs are available. CCV maneuvers use two control inputs to cancel opposing moments, thus providing a net force in the desired direction. In order to perform lateral CCV maneuvers for the X-29A, vertical stabilizers (canards) would have to be added to cancel the opposing rudder moment about the center of gravity. This, however, would disrupt the smooth airflow beneath the aircraft and increase drag.

Porter's method requires that the number of outputs be equal to the number of inputs. Therefore two states, roll angle and sideslip, are chosen as outputs (see Appendix A for other design approaches). It is of paramount importance that the same output matrix (C) be used. If not, then the pilot has to notify the aircraft in advance which maneuver he intends to perform. In addition, different output matrices require additional sensors to measure the extra outputs. Redundancy requirements mean that additional cost and weight are added to the aircraft, and reliability is reduced.

Description of Maneuvers

As in longitudinal commanded inputs, maximum maneuvers are commanded. The controller is designed to perform two maneuvers, beta-pointing and coordinated turn. The maneuver times and commanded steady-state values vary from flight condition to flight condition.

When an aircraft lands in a crosswind, its initial descent aligns the fuselage of the aircraft parallel with

the centerline on the runway. The wings are straight and level. As the aircraft starts to "flare", the pilot turns the nose of the aircraft into the wind with the rudder, since excessive nonzero roll angle is undesirable. The landing gear of heavier transport aircraft cannot take the strain of landing canted, nose into the wind, but are not as easily blown sideways on the runway. A more agile aircraft, such as the X-29A, must land with its nose into the wind. Beta-pointing is an ideal maneuver for this situation. Sideslip angle, or beta, is defined as the angle between the velocity vector and the nose of the aircraft (in the plane formed by the wings and fuselage). Thus beta-pointing allows the aircraft to continue traveling down the center of the runway while the nose is pointed into the wind. Beta-pointing is also useful for quick minor adjustments in situations, such as flying in formation, where the pilot does not wish to turn. Thus beta-pointing commands roll angle to zero while commanding beta to ramp up and hold its steady-state value.

In a coordinated turn, the aircraft is commanded to a fixed roll angle, while sideslip is commanded to zero. In performing a coordinated turn, it is undesirable to allow sideslip. If sideslip occurs during a turn, the nose drops, and, if left unchecked, causes the aircraft to start spiraling. At all five flight conditions, the aircraft is commanded to a steady-state roll angle of 88.815 degrees while beta is commanded to zero.

Application of Porter's Method

Initially, separate controllers are designed for each maneuver at each flight condition. However, it is discovered that the design parameters used to obtain the controller for a coordinated turn at one flight condition provide excellent results in obtaining controllers for a coordinated turn at other flight conditions. Additionally, it is found that the same controller obtained for a coordinated turn at a specified flight condition can be used for beta-pointing as well. Next, a successful search is made for one controller that will produce excellent tracking for both maneuvers at all flight conditions. Finally, half of the gains in the robust controller are set to zero with only minimal degradation of results.

Since the aircraft model Grumman used for the X-29A is not available, validation of the model is not performed. Data set #3 is used in this thesis (see Appendix A for other design approaches and data sets used).

The outputs selected are two states, roll angle and sideslip angle. The same C matrix is used for both maneuvers at all flight conditions.

The state and output equations for flight condition number three (1.2 Mach at 15 000 feet) are:

$$\dot{\underline{x}} = \begin{bmatrix} \dot{\Phi} \\ \dot{\beta} \\ \dot{P} \\ \dot{R} \end{bmatrix} = \begin{bmatrix} 0 & 0 & 1 & .03777 \\ .0253 & -.4133 & .03774 & -.9993 \\ 0 & -97.95 & -7.959 & 2.658 \\ 0 & 18.68 & -.1450 & -.4644 \end{bmatrix} \begin{bmatrix} \Phi \\ \beta \\ P \\ R \end{bmatrix}$$

$$+ \begin{bmatrix} 0 & 0 \\ -.002243 & .0004275 \\ 1.169 & .2437 \\ .2339 & -.08424 \end{bmatrix} \begin{bmatrix} \delta_F \\ \delta_R \end{bmatrix} \quad (5-1)$$

$$\dot{\underline{x}} = \underline{A}\underline{x} + \underline{B}u$$

$$\underline{y} = \underline{C}\underline{x} = \begin{bmatrix} \phi \\ \beta \end{bmatrix} = \begin{bmatrix} 1 & 0 & 0 & 0 \\ 0 & 1 & 0 & 0 \end{bmatrix} \begin{bmatrix} \phi \\ \beta \\ p \\ R \end{bmatrix} \quad (5-2)$$

Clearly, the product CB is rank deficient, and therefore, an Irregular design is required. Thus the design problem is non-minimum phase (zeros in the right-half plane). A measurement matrix (M) is used to produce a new output:

$$\underline{w} = \underline{y} + \frac{\underline{M}\underline{x}}{1} \quad (5-3)$$

where \underline{x}_1 are the states that the M matrix operates on.

Controllability and observability are checked using the computer program ZERO. The initial results before a measurement matrix is picked are:

1. No decoupling zeros exist. Thus the system is controllable and observable.

2. The number of transmission zeros is equal to the number of states minus the number of outputs. The two transmission zeros are in the stable region (in the open left half Laplace plane).

The addition of a measurement matrix does not move the transmission zeros to the unstable region.

The location of the closed-loop roots are given by equation (4-4). Using the computer-aided-design program TOTAL allows the designer to easily find the roots of $G(s)$.

Since the B matrix does not have n-p zero rows, where n is the number of states and p is the inputs, the B matrix

cannot be transformed to the $\begin{bmatrix} 0 \\ \underline{B} \\ -2 \end{bmatrix}$ form by simply rearranging rows.

However, since the M matrix is only 2x2, it is relatively easy to pick the M elements by trial and error. Thus it is not worth the effort to first transform the B matrix in order to obtain algorithms to pick the elements of the M matrix. A few steps should be followed when selecting

an M matrix when the system is not in $\begin{bmatrix} 0 & \underline{B} \end{bmatrix}^T$ form. First,

write the system such that the first l rows in the plant matrix correspond to derivatives of the states that the designer wishes the M matrix to operate upon. Secondly, initially set all elements to some nonzero value (0.25 is suggested). Then, keeping in mind that at least one element in each column must be nonzero, zero out elements one at a time and examine the effect. The goal is to obtain the sparsest M matrix that provides the best results. It is significant to note that no satisfactory designs with the

system written in $\begin{bmatrix} 0 & \underline{B} \end{bmatrix}^T$ form are obtained in this thesis.

The discussion in the rest of this section pertains to

selecting an M matrix for systems in $\begin{bmatrix} 0 & \underline{B} \\ & \underline{2} \end{bmatrix}^T$ form.

The M matrix must be added so that the matrix \underline{F} has full rank. The new output matrix is:

$$\underline{F} = \begin{bmatrix} \underline{F}_1 & \underline{F}_2 \end{bmatrix} = \begin{bmatrix} \underline{C}_1 + \underline{MA}_{11} & \underline{C}_2 + \underline{MA}_{12} \end{bmatrix} \quad (5-4)$$

$$\text{Where: } \underline{C} = \begin{bmatrix} \underline{C}_1 & \underline{C}_2 \end{bmatrix}$$

Note that C is partitioned such that \underline{C}_2 is p x p, where p is the number of outputs (p must equal m). The matrix M must be chosen so that \underline{F} has full rank. Note that \underline{A}_{12} can be changed by merely rewriting the order of the state equations. In fact, this is necessary before good results are obtained. While merely changing the order of the state equations does not change decoupling or transmission zeros, it does change the selection of the M matrix. The M matrix in turn, changes output decoupling and transmission zeros.

Next, the design parameters are selected by following the procedure given in Chapter IV. Initial attempts did not produce good results, so the order of the state equations was changed. The final order is presented in equation (5-1). One addition is made to the Regular design process for an Irregular design. The M matrix is chosen after ALPHA, EPSILON, and SIGMA elements are selected. The M elements are closely coupled, and to obtain the best results must be chosen simultaneously. For this lateral application only two M elements are required, so selecting the best set of

elements in 2-space is not difficult. However, for applications where the A_{12} matrix (of size $(n-p) \times p$) matrix is large, and the resulting M matrix is not sparse, this can be more difficult. A_{12} is large, for example, when decoupling of the longitudinal and lateral equations of motion does not occur. The following guidelines should be noted when choosing M :

1. M should be as sparse as possible. In addition to minimizing design complexity, fewer measurement gains increase processing speed and improve software reliability.

2. M must be chosen such that $F B_{22}$ has full rank since

the proportional gain matrix is computed as :

$$\underline{K}_0 = (\underline{F} \underline{B}_{22})^{-1} \underline{\Sigma} \quad (5-5)$$

3. The resulting analog transmission zeros (the sampling period is not taken into account) must be in the closed (including the origin) left half Laplace plane. The closed-loop roots approach the transmission zeros as the sampling frequency is increased to infinity. If the analog transmission zeros are in right half plane, it may be possible to keep the closed-loop roots in the stable region by selecting a long enough sample period.

4. Decoupling of outputs in the limit as the sampling frequency goes to infinity is guaranteed only if the product

$\underline{C} \underline{F}_{22}^{-1}$ is a diagonal matrix. Note further that the diagonal

terms must be nonzero, or the matrix is nonsingular.

5. Initially, set the nonzero M elements equal to 0.25. Then change the values by small increments and observe if the response is improved. If M has many nonzero elements, then the elements may be selected one at a time, but superior designs are likely to be missed. In addition, if M elements can be selected to have the same value, then it may be possible to store the reduced number of gains in registers or "cache-memory". Such implementations can greatly improve processing speed.

6. The M elements speed up response and improve tracking as the elements approach zero. Below a certain point, though, increasingly smaller improvements in tracking are achieved at the expense of a degradation in the control input responses. Judgement must be used in choosing the desired tradeoff.

Development of Minimum-Gain Robust Controller

The design parameters in Table 5-1 are obtained by using the computer-aided-design (CAD) program MULTI. Once the design parameters for one maneuver are selected, these parameters should be used as an starting set of parameters for the new maneuver. After obtaining the optimum set of parameters for the new maneuver, the output and control input responses should be compared to the responses obtained when using the initial set of parameters. This is done to try to obtain an individual robust controller, that is, one controller that provides acceptable response for all maneuvers at that flight condition. With this milestone, gain-

scheduling of the individual elements of the K_0 , K_1 , and M elements between flight conditions is possible.

Once this is achieved, the next step is to try to find one robust controller that provides acceptable responses for all maneuvers at all flight conditions. In general, the fewer the gains, the better the design. One robust controller greatly eases the task of software implementation. Even finding one robust gain matrix, K_0 , K_1 , or M is desirable. Individual gain elements may be adjusted to attain this goal. The individual design parameters ALPHA, EPSILON, and SIGMA are not implemented in the digital flight control system. These design parameters are used only to provide a straightforward method of obtaining the best set of gains, K_0 and K_1 .

Since the design method produces a robust M matrix, only the robust K_0 and K_1 matrices have to be determined. Since ALPHA is equal to one, K_0 and K_1 are equal. Thus only one set of robust gains remains to be determined. Using the average of the K elements componentwise, produces good results for every flight condition but one, 0.9 Mach, sea level. It is noticed that componentwise, the K elements at 0.9 Mach, sea level are the smallest of the five flight conditions. Thus the K matrix at 0.9 Mach, sea level, is tried as a universal robust controller. Since the results

appear to be good (see Evaluation of Selected Design Parameters), no further search is made. It is quite possible that better results could be obtained with a trimmed robust controller.

Next, a minimum-gain robust controller is sought. Rather than guessing which gains might be set to zero with minimal degradation of response, it is useful to try to obtain some insight. The rows of the K matrix correspond to the outputs. The columns of the K matrix correspond to the control inputs. The lateral K matrix is thus:

$$\underline{K} = \begin{matrix} & \begin{matrix} \text{flaps} & \text{rudder} \end{matrix} \\ \begin{matrix} \text{phi} \\ \text{beta} \end{matrix} & \begin{bmatrix} * & 0 \\ 0 & * \end{bmatrix} \end{matrix}$$

The elements whose inputs are expected to have minimal effect upon the corresponding outputs are set to zero. The magnitude of the element has nothing to do with its likelihood of acceptable degradation of response when set to zero. For example, the magnitude of the gain corresponding to (phi,rudder) is almost thrice the value of the gain corresponding to (phi,flaps). An interesting sidelight is that the gains corresponding to (phi,flaps) and (beta,rudder) can be set to zero for beta-pointing and coordinated turn, respectively. This is not done for the reasons given below.

It is entirely useless to obtain zero elements unless it is obtained for a robust controller for all maneuvers at all flight conditions. Otherwise, the memory location for the element must still be reserved. The fact the memory loca-

tion sometimes has a zero in it is of no value.

To summarize, a minimum-gain controller requiring a total of only three gains is obtained. Two gains are required for the K matrices corresponding to the elements (phi,flaps) and (beta,rudder). The two gains required for the measurement matrix M have the same value, 0.1, so only one memory location is required. Therefore, since the distinct gains required are few, they may be stored in three registers.

Evaluation of Selected Design Parameters

The design parameters and maximum commanded inputs selected are presented in Table 5-1. The measurement matrix is a (2 x 2) diagonal matrix whose two diagonal elements are chosen to be 0.1 for all lateral controllers. The controller matrices resulting from the selected design parameters are presented in Table 5-2. Figures of merit are provided in Table 5-3. Control input rates are given in Table 5-4. Calcomp plots of outputs, commanded inputs, control inputs, and states are provided in Figures 5-1 to 5-11. Note that only nonzero commanded inputs are plotted. Similar information is provided for the other four flight conditions in Appendices C, D, E, F, G, and H. Since the output matrix is constant and the feedforward matrix is zero, only the plant and input matrices for the other flight conditions are different in Appendix B.

The calcomp plots are organized in the following manner: maneuver; flight condition; outputs, control inputs, and

states; individual robust controllers, full-gain robust controller, and minimum-gain robust controller. The full-gain controller has the letter "U" (for universal) on the time axis label. The minimum-gain robust controller has the letter "Z" (for zeroed out) on the time axis label. No plots at 0.9 Mach, sea level, are given for the full-gain robust controller (U) since the individual robust controller at this flight condition is selected as the full-gain robust controller for all flight conditions.

Beta-pointing

The first lateral maneuver, beta-pointing, is best performed at the flight condition 0.7 Mach, 15 000 feet. A smoothed ramp-up of 15.5 degrees of sideslip is commanded while roll-angle is commanded to zero. The largest commanded inputs (in decreasing order) are achieved at 0.7 Mach, 15 000 feet; 0.9 Mach, sea level; 0.4 Mach, sea level; 0.9 Mach, 50 000 feet; and 1.2 Mach, 15 000 feet. The outputs track the commanded inputs excellently, with no overshoot of the beta output. In fact, the commanded beta input and output are indistinguishable (see Figure 5-1). The roll angle undershoots the zero axis, providing a peak transient roll response from a minimum of -0.10 degrees at 0.4 Mach, sea level to a maximum of -0.8569 degrees at 1.2 Mach, 15 000 feet. The roll response then asymptotically approaches the zero axis, with a maximum roll angle of -0.05 degrees in four seconds.

TABLE 5-1
DESIGN PARAMETERS AND COMMANDED INPUTS
FOR LATERAL CONTROLLERS

Flight Condition - 1.2 Mach, 15 000 feet

Maneuver	Command Vector \underline{v}	ALPHA	EPSILON	SIGMA (Diagonal values)
Beta- Pointing (IRC)				
Beta- Pointing (FGRC)	0,0,0,0 0.8,0.1,16,16			
Beta- Pointing (MGRC)		1.0	1.0	1.0,1.0
Coordina- ted Turn (IRC)				
Coordina- ted Turn (FGRC)	0.8,1.55,16,16 0,0,0,0			
Coordina- ted Turn (MGRC)	0.8,1.5475,16,16 0,0,0,0			

Note: (IRC) - Individual Robust Controller
(FGRC)- Full Gain Robust Controller
(MGRC)- Minimum Gain Robust Controller

Note: The measurement (M) matrix is a (2 x 2) diagonal matrix
with diagonal entries (0.1,0.1) for all lateral controllers

TABLE 5-2

LATERAL CONTROLLER MATRICES

Flight Condition - 1.2 Mach, 15 000 feet

Maneuver	Command Vector \underline{y}	ALPHA	* \underline{K}	
			0	
Beta-Pointing (IRC)	0,0,0,0 0.8,0.1,16,16			
Coordinated Turn (IRC)	.8,1.55,16,16 0,0,0,0		5.887 12.75	-14.52 71.13
Beta-Pointing (FGRC)	0,0,0,0 0.8,0.1,16,16	1.0		
Coordinated Turn (FGRC)	0.8,1.55,16,16 0,0,0,0		3.282 1.384	-8.871 41.67
Beta-Pointing (MGRC)	0,0,0,0 0.8,0.1,16,16		3.282 0	0 41.67
Coordinated Turn (MGRC)	0.8,1.5475,16,16 0,0,0,0			

*Note: $\underline{K}_0 = \text{ALPHA} * \underline{K}_1$

Note: (IRC) - Individual Robust Controller
 (FGRC)- Full Gain Robust Controller
 (MGRC)- Minimum Gain Robust Controller

Note: The measurement (M) matrix is a (2 x 2) diagonal matrix with diagonal entries (0.1,0.1) for all lateral controllers

TABLE 5-3

LATERAL FIGURES OF MERIT

Flight Condition - 1.2 Mach, 15 000 feet

Maneuver	Command Vector \underline{y}	t^*	t^{**}	M^{***}
		s	p	p
Beta-Pointing (IRC)	0,0,0,0 0.8,0.1,16,16	15 1.8	0.9 15	-.0150 .1007
Coordinated Turn (IRC)	.8,1.55,16,16 0,0,0,0	1.05 8.7	1.35 .45	1.5628 -.0013
Beta-Pointing (FGRC)	0,0,0,0 0.8,0.1,16,16	15 2.85	1.05 15	-.0353 .1007
Coordinated Turn (FGRC)	.8,1.55,16,16 0,0,0,0	1.5 12.6	1.2 .3	1.584 -.0088
Beta-Pointing (MGRC)	0,0,0,0 0.8,0.1,16,16	15 2.3	1.05 15	-.0146 .1007
Coordinated Turn (MGRC)	0.8,1.5475,16,16 0,0,0,0	1.05 13.2	1.35 .3	1.5708 -.0110

*Note: settling time in seconds

**Note: peak time in seconds

***Note: peak value (greatest magnitude), angles in radians

Note: commanded inputs are smoothed

Note: commanded inputs in order are - roll angle, and sideslip angle

TABLE 5-4

LATERAL CONTROL INPUT RATES

Flight Condition - 1.2 Mach, 15 000 feet

Maneuver	Command Vector \underline{v}	* $\dot{\delta}_f$	** $\dot{\delta}_r$
Beta-Pointing (IRC)	0,0,0,0 0.8,0.1,16,16	8	37
Coordinated Turn (IRC)	.8,1.55,16,16 0,0,0,0	67	148
Beta-Pointing (FGRC)	0,0,0,0 0.8,0.1,16,16	9	40
Coordinated Turn (FGRC)	.8,1.55,16,16 0,0,0,0	65	157
Beta-Pointing (MGRC)	0,0,0,0 0.8,0.1,16,16	48	13
Coordinated Turn (MGRC)	0.8,1.5475,16,16 0,0,0,0	76	185

*Note: maximum differential flaperon rate in degrees/second

**Note: maximum rudder rate in degrees/second

Note: commanded inputs are smoothed

Note: commanded inputs in order are - roll angle, and side-slip angle

Note: rates presented are the greatest magnitude

The full-gain robust controller does not degrade beta output response, except for minimal transients at the change in slope at 0.9 Mach, 50 000 feet, and 1.2 Mach, 15 000 feet. At 0.9 Mach, 50 000 feet, a transient dip of about 0.4 degrees occurs, while at 1.2 Mach, 15 000 feet the beta response is rounded off slightly (see Figure 5-2). The roll response is degraded by an increase in the transient undershoot. The peak roll undershoot varies from -0.73 degrees at 0.4 Mach, sea level, to -2.02 degrees at 1.2 Mach, 15 000 feet.

The minimum-gain robust controller provides beta output responses that are indistinguishable from the full-gain robust controller. The transient roll response, however, is changed from an undershoot to an oscillation about the zero axis. The oscillations are of approximately equal displacement from the zero axis. The peak roll displacement varies from a minimum of -0.78 degrees at 0.9 Mach, sea level, to a maximum of 1.42 degrees at 0.9 Mach, 50 000 feet. In addition, the minimum-gain robust controller appears to appreciably improve roll angle transient-settling times. The roll angle transient settling-times appear to be approximately one-third of those obtained from the full-gain robust controller. Surprisingly, the roll angle transient settling-times also are approximately one-half of those obtained by the individual robust controllers. Thus, if transient peak and settling time are the criteria used, the

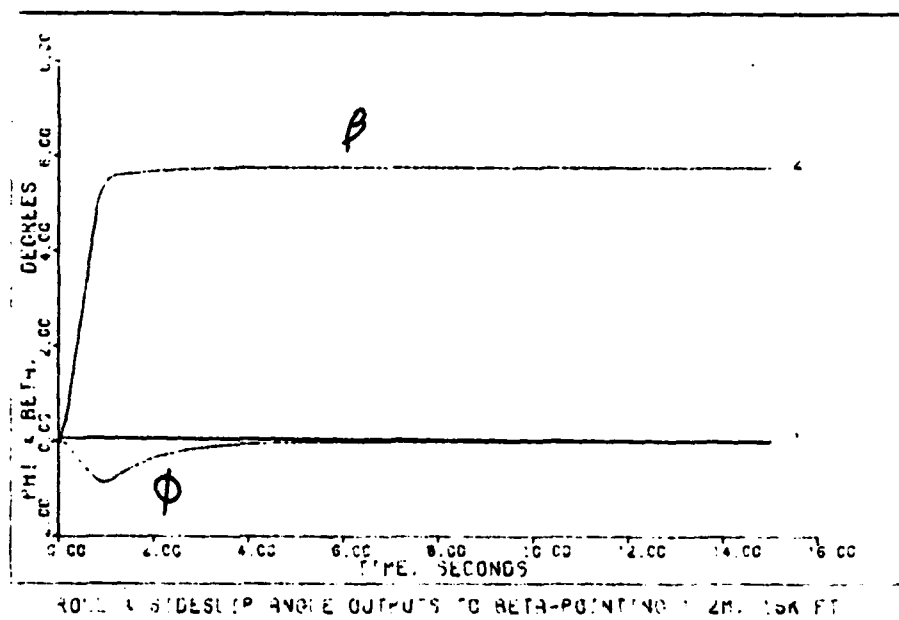
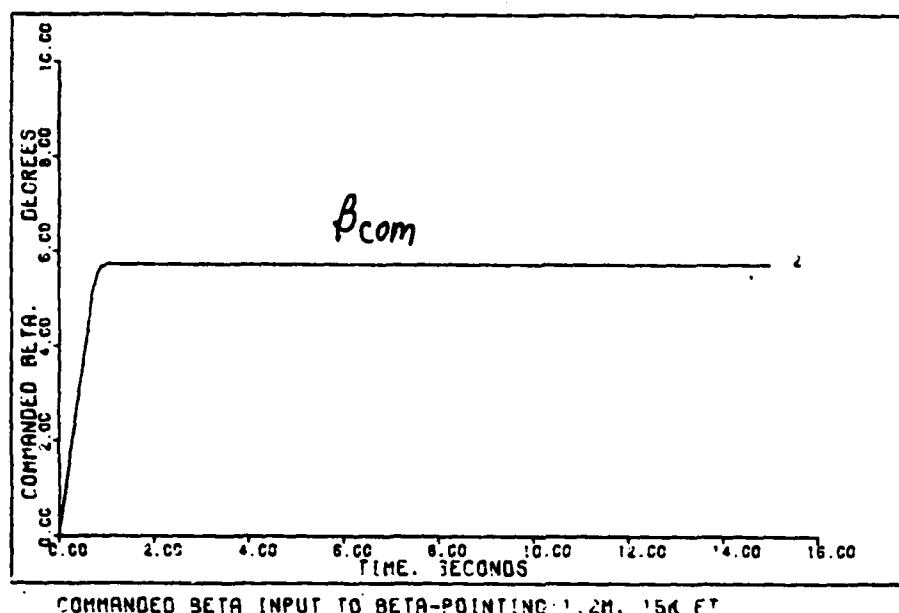


Figure 5-1

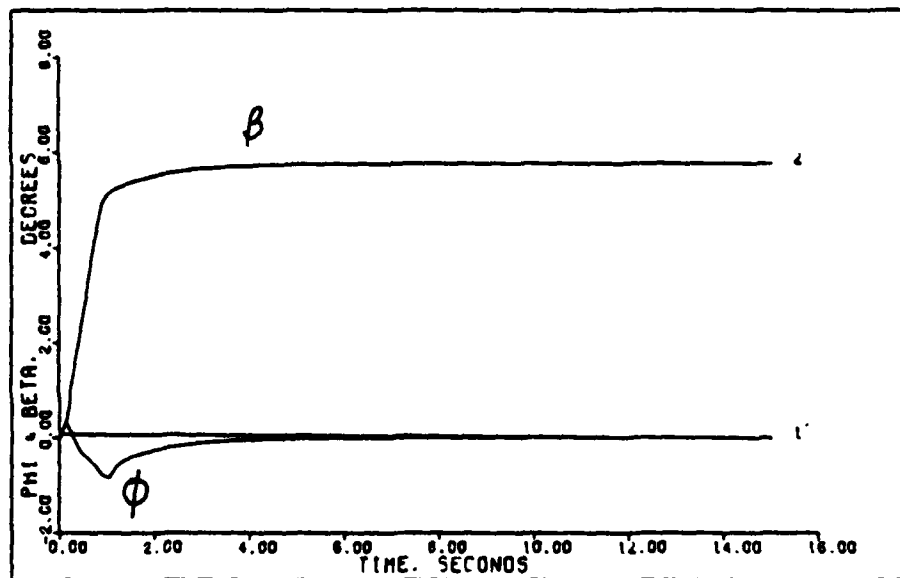
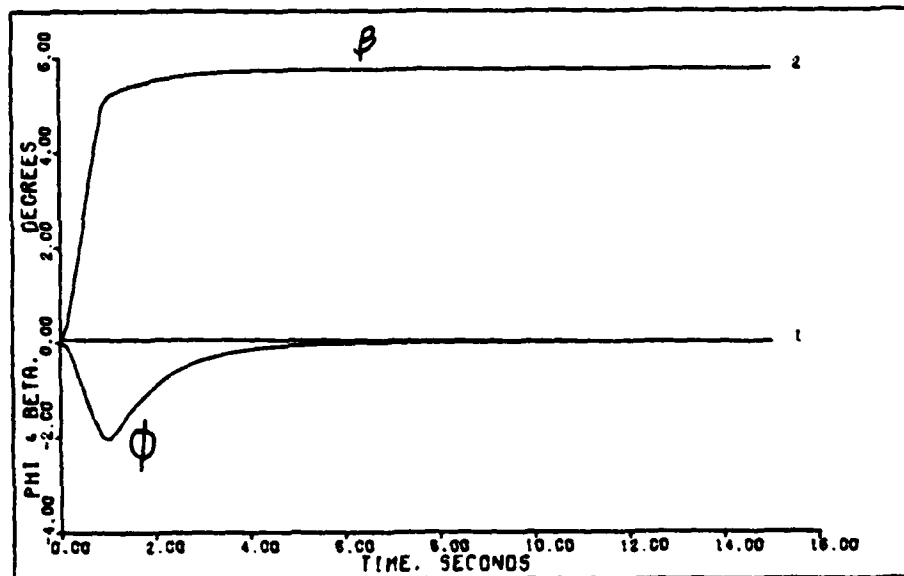


Figure 5-2

minimum-gain robust controller provides superior output response to the full-gain robust controller.

Next, the control input responses are evaluated. An inherent tradeoff exists between output response and control input response. If the designer wishes to improve control input response, the value of the measurement elements can be increased but then tracking of the commanded inputs by the outputs is degraded. The deflection limits of the flaps are -19.5 and 13 degrees. The deflection limits of the rudder are -30 and 30 degrees. The rudder deflection limits an increase in commanded inputs. Although for three of the flight conditions (0.4 Mach, sea level; 0.9 Mach, 50 000 feet; and 0.7 Mach, 15 000 feet) the maximum rudder deflection is less than 30 degrees, no appreciable increase in maximum commanded inputs is possible. The rudder deflections seem to follow differential flaperon deflections with a lag of about 0.1 seconds. Every time a small change in the direction of flap deflection occurs, the rudder deflection changes direction to compensate it. Except for these transient deflections, the rudder follows a ramp-up that provides the sideslip ramp-up. The steady-state flap deflection is approximately two degrees. Note that for the three flight conditions where maximum rudder deflection is less than the maximum, the steady-state roll angle is positive, while full rudder deflection occurs where flap deflection is negative (see Figure 5-3).

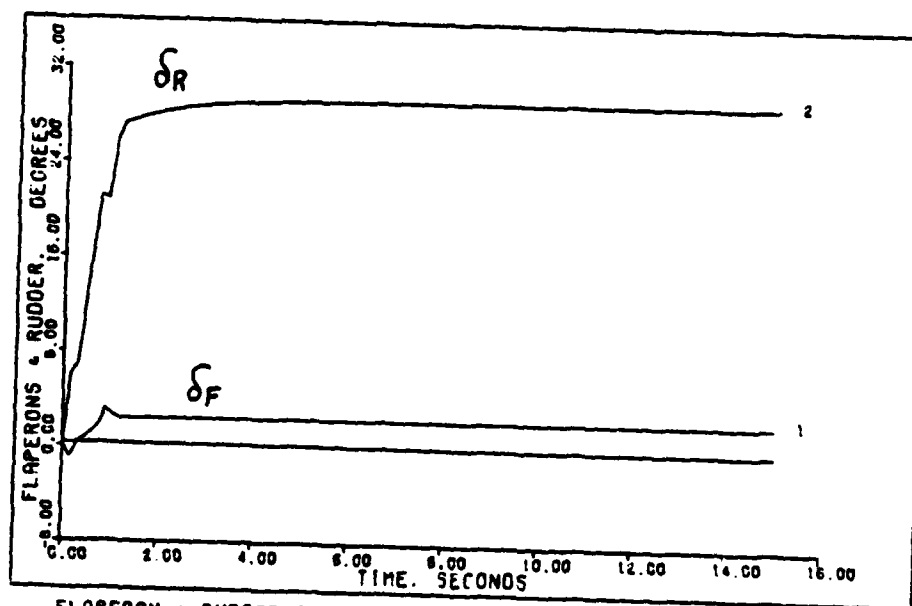
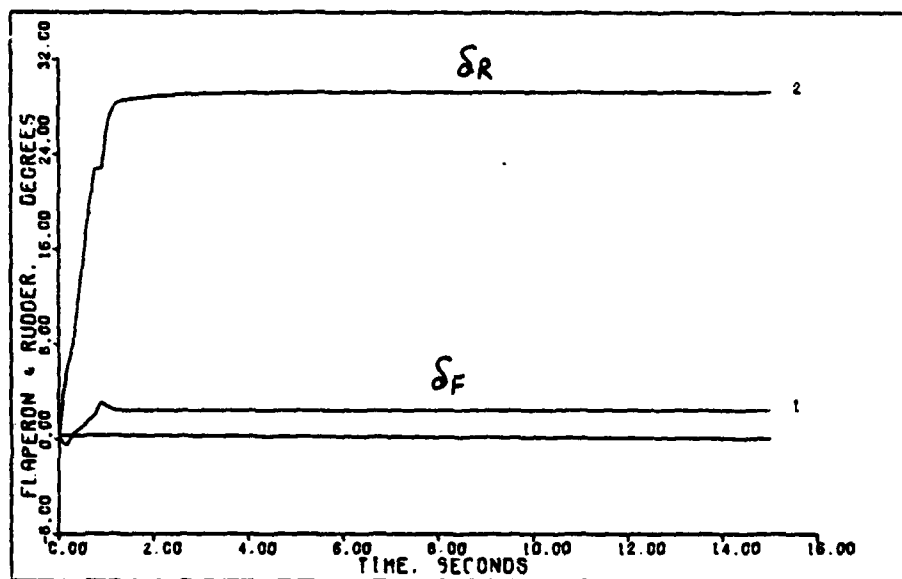
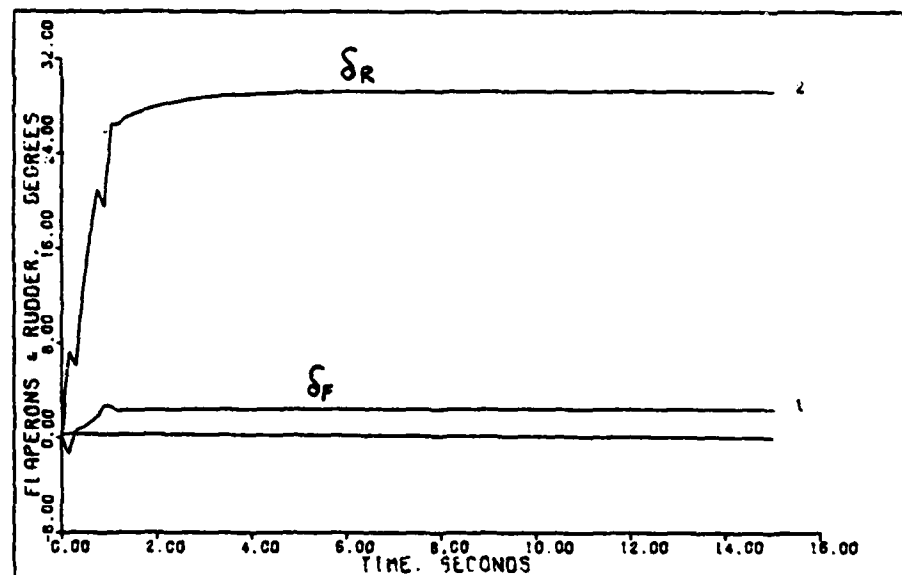
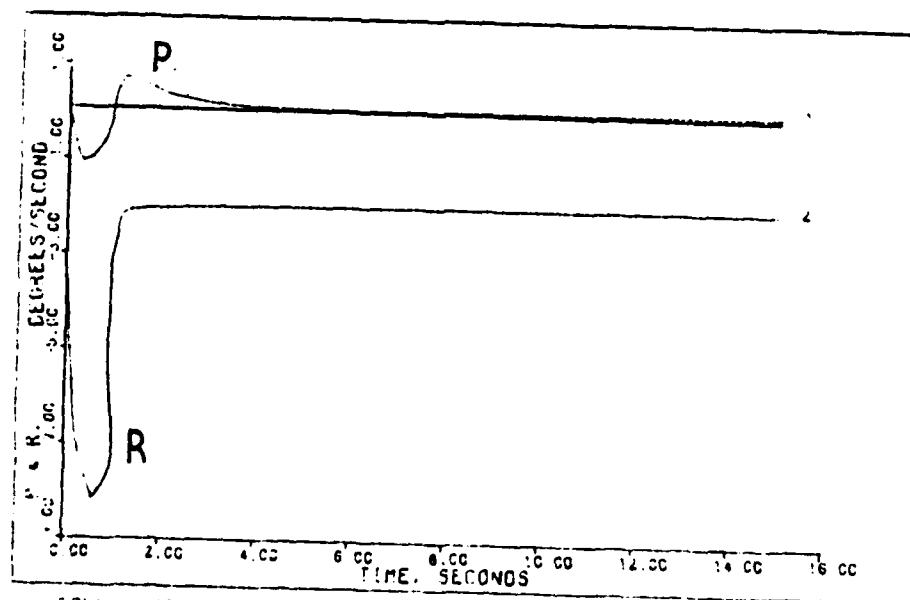


Figure 5-3



FLAPERON & RUDDER INPUTS TO BETA-POINTING: 4:1.2M, 15K FT



ROLL & YAW RATES FROM BETA-POINTING: 4:1.2M, 15K FT

Figure 5-4

The full-gain robust controller degrades the transient rudder response. In addition, the transient flap response is minimally degraded (see Figure 5-3). It is clear that these degradations cause an increase in control input rates.

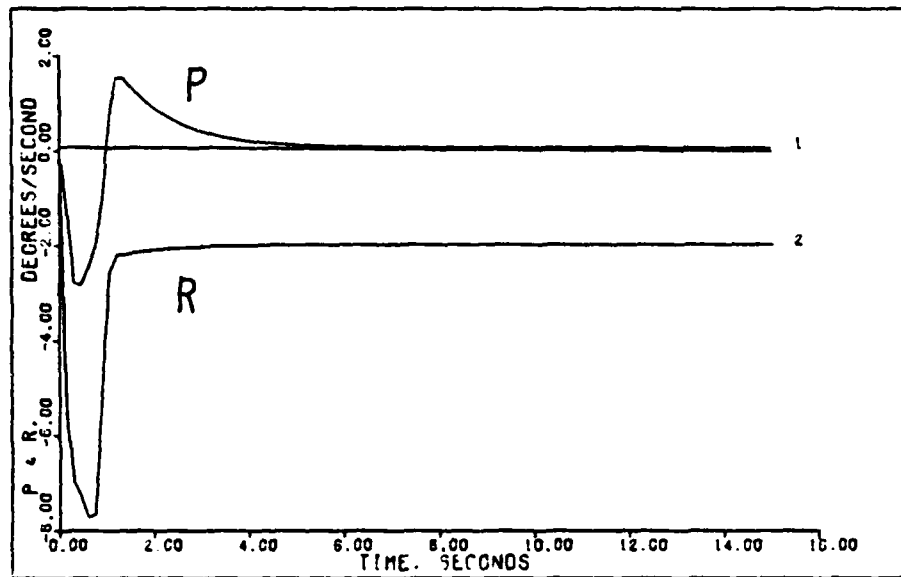
The minimum-gain robust controller slightly degrades the flap input response obtained from the full-gain robust controller (see Figure 5-4). The best measure of this degradation is again the control input rates.

Note that the overall best control input response is obtained from 1.2 Mach, 15 000 feet; 0.9 Mach, sea level; 0.4 Mach, sea level; 0.7 Mach, 15 000 feet; and 0.9 Mach, 50 000 feet.

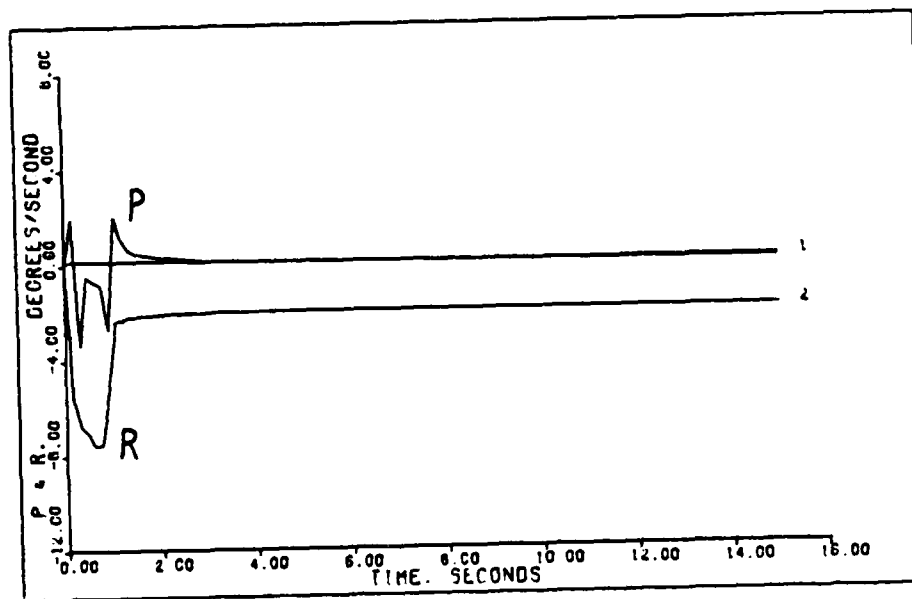
The roll and yaw rate responses have smooth transients (see Figure 5-4). The steady-state roll rate is zero, as expected. Also, as expected, a negative steady-state yaw rate is required to provide the steady-state sideslip. The roll rate has a transient overshoot, while the yaw rate has a transient undershoot.

The full-gain robust controller degrades the yaw rate response only slightly, but causes the transient roll rate to oscillate. In addition the transient roll rate magnitude is approximately doubled, but this is of little consequence because the roll rate is small. Steady-state responses are unaffected (see Figure 5-5).

The minimum-gain robust controller degrades the transient response further (see Figure 5-5). In addition to increasing the magnitude of the roll rate oscillations, oscillations appear in the yaw rate as well. Note, however,



ROLL & YAW RATES FROM BETA-POINTING: U: 1.2M, 15K FT



ROLL & YAW RATES FROM BETA-POINTING: Z: 1.2M, 15K FT

Figure 5-5

that the largest transient roll rate is nine degrees/second at 0.7 Mach, 15 000 feet. The largest transient yaw rate is -22 degrees/second. Settling-times are about the same as for the full-gain robust controller, but are three times those of the individual robust controllers.

Again, degradation varies somewhat with flight condition. The best overall roll and yaw rate responses are provided by 0.9 Mach, sea level; 1.2 Mach, 15 000 feet; 0.7 Mach, 15 000 feet; 0.4 Mach, sea level; and 0.9 Mach, 50 000 feet.

Maximum permissible control input rates are 50 degrees/second for the differential flaperons and 105 degrees/second for the rudder. The maximum negative and positive flap rates for the individual robust controllers are -22 and 23 degrees/second, respectively at 0.9 Mach, 50 000 feet. The maximum negative and positive rudder rates for the individual robust controllers are -83 and 88 degrees/second, respectively, at 0.9 Mach, 50 000 feet. Thus the maneuver beta-pointing with individual robust controllers produces actual control input rates within the allowable limits.

The full-gain robust controller has maximum negative and positive flap rates of -22 and 15 degrees/second, respectively, at 0.9 Mach, 50 000 feet. The maximum negative and positive rudder rates are -87 and 132 degrees/second at 0.7 Mach, 15 000 feet. Thus beta-pointing with the full-gain robust controller requires control input

rates which exceed limits for two flight conditions.

The minimum-gain robust controller has maximum negative and positive flap rates of -32 and 31 degrees/second, respectively, at 0.7 Mach, 15 000 feet. The maximum negative and positive rudder rates are -73 and 134 degrees/second at 0.4 Mach, sea level. Allowable rudder control rates are also exceeded at 0.7 Mach, 15 000 feet.

The maximum flap and rudder rates are increased in three out of four flight conditions (recall that the 0.9 Mach, sea level, individual robust controller is the full-gain robust controller) when comparing the individual robust controllers to the full-gain robust controller. Therefore, it is reasonable to conclude that in general, control input rates are significantly increased when comparing performance between the individual robust controllers and the full-gain robust controller. Practically, the maximum commanded input must be reduced for two flight conditions, 0.4 Mach, sea level, and 0.7 Mach, 15 000 feet. The controllers do not have to be retuned. A reduction in the commanded steady-state value of 10% should be sufficient to bring down the rudder rates to within 105 degrees/second. Alternately, the maneuver time must be lengthened by a small increment in order to reduce the rudder control rates.

Compared to the full-gain robust controller, the minimum-gain robust controller slightly increases flap rates in three of five flight conditions. Since the flap rates are well within the 50 degrees/second limit, this is

of little importance. The rudder rates, however, are slightly reduced (two degrees/second) for four of the five flight conditions. One flight condition has an increase in rudder rates from 40 to 48 degrees/second. Since this is much less than the 105 degrees/second limit, it is not significant. On balance, then, for beta-pointing, minimum-gain robust controller transient response is superior to the full-gain robust controller transient response.

Coordinated turn

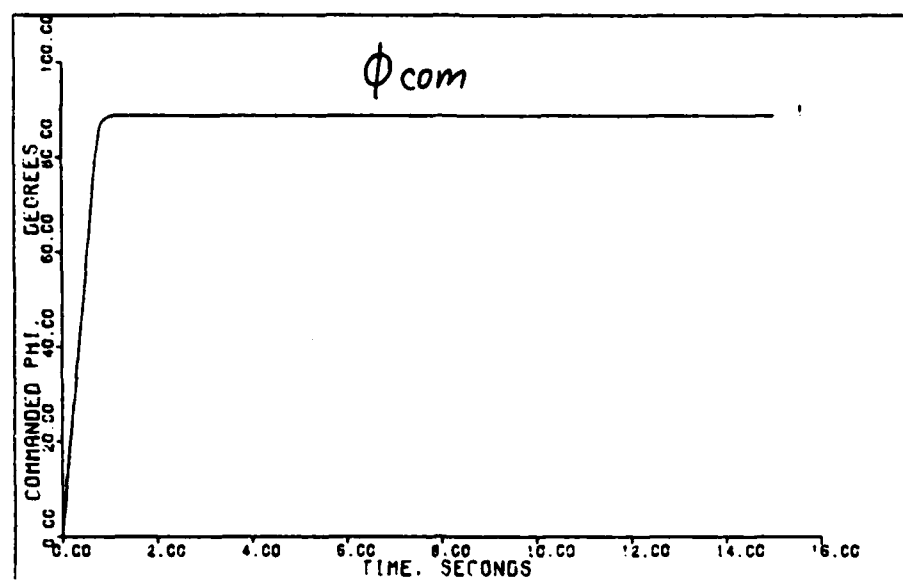
The second lateral maneuver, coordinated turn, has one flight condition, 1.2 Mach, 15 000 feet, where the maximum commanded roll angle input is reduced from 88.815 to 88.672 degrees for the minimum-gain robust controller. This slight degradation is compensated by tracking greater commanded inputs for shorter maneuver times (not presented). The coordinated turn is best performed (in decreasing order) at 0.7 Mach, 15 000 feet; 0.9 Mach, sea level; 1.2 Mach, 15 000 feet; 0.4 Mach, sea level; and 0.9 Mach, 50 000 feet. The first three flight conditions command the roll angle ramp-up to end in 0.8 seconds. The outputs track the commanded inputs excellently, with little overshoot of the roll output. The roll peak transient ranges from a minimum of 0.0000 degrees at 0.7 Mach, 15 000 feet to a maximum of 0.735 degrees at 1.2 Mach, 15 000 feet. In fact, the roll output and commanded input are indistinguishable (see Figure 5-6). The sideslip angle undershoots the zero axis, providing a peak transient sideslip response from a minimum of -.01008 degrees at 0.9 Mach, 50 000 feet to a maximum of

.01301 degrees at 0.7 Mach, 15 000 feet. The greatest steady-state sideslip angle is -.00131 degrees at 0.4 Mach, sea level. No steady-state roll angle error occurs.

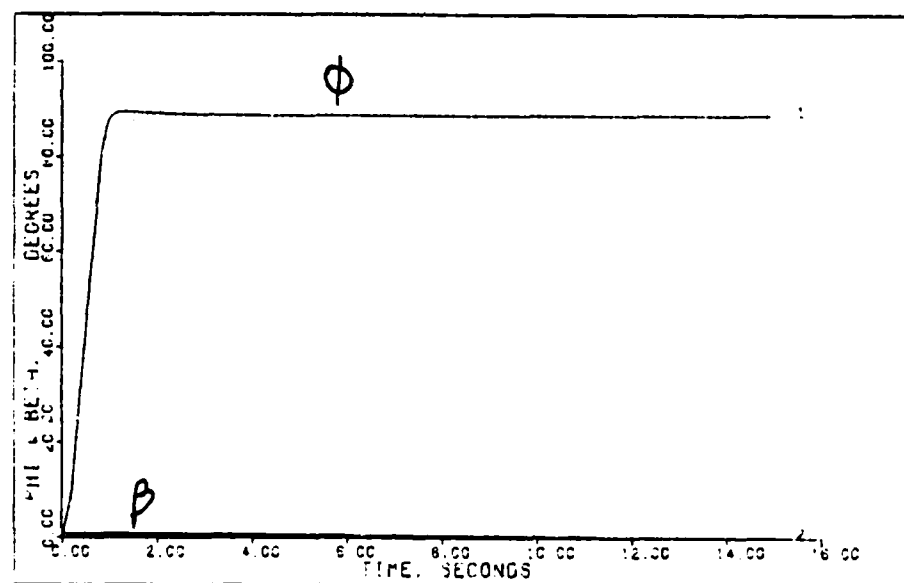
The full-gain robust controller slightly degrades roll output response. Again, the output plots are indistinguishable (see Figure 5-7). The maximum roll peak transient is 1.95 degrees at 1.2 Mach, 15 000 feet. The maximum sideslip peak transient is increased to 0.21180 degrees at 1.2 Mach, 15 000 feet. No steady-state roll angle error occurs.

The minimum-gain robust controller produces roll outputs that improve the roll peak transient (see Figure 5-8). The maximum roll peak transient is 1.337 degrees at 1.2 Mach, 15 000 feet. The maximum sideslip peak transient varies from a minimum of -0.62922 degrees to a maximum of 0.30930 degrees at 1.2 Mach, 15 000 feet. No steady-state roll angle error occurs.

Next, the control input responses are evaluated. An inherent tradeoff exists between output response and control input response. An improvement in control input response can be obtained by increasing the measurement (M) gains, but this degrades output response. The flap deflection limits are -19.5 and 13 degrees. The rudder deflection limits are -30 and 30 degrees. The actual control surface deflections are well within the limits. As expected, a small steady-state rudder deflection of about -0.5 degrees exists. A steady-state flap deflection of about -0.2 degrees also exists (see Figure 5-8).

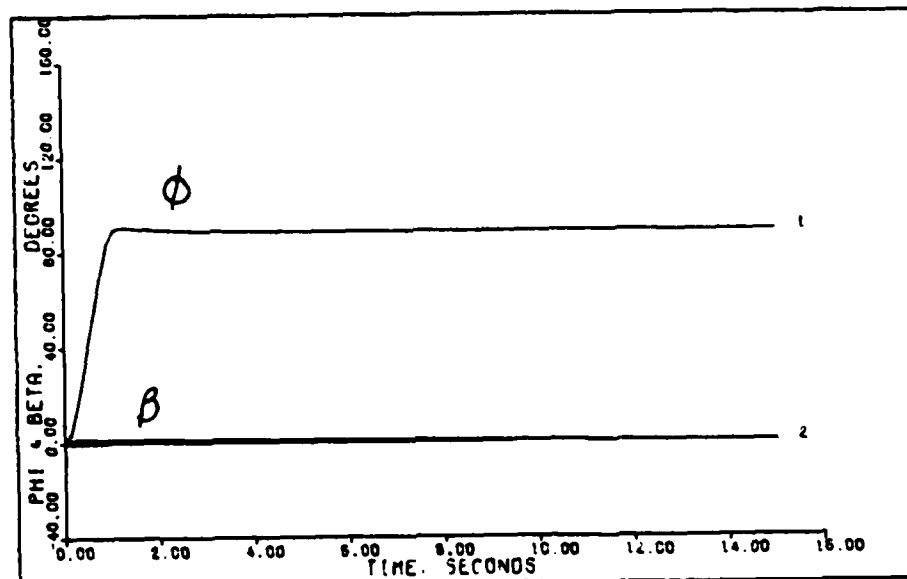


COMMANDED PHI TO COORDINATED TURN: 1.2M, 15K FT

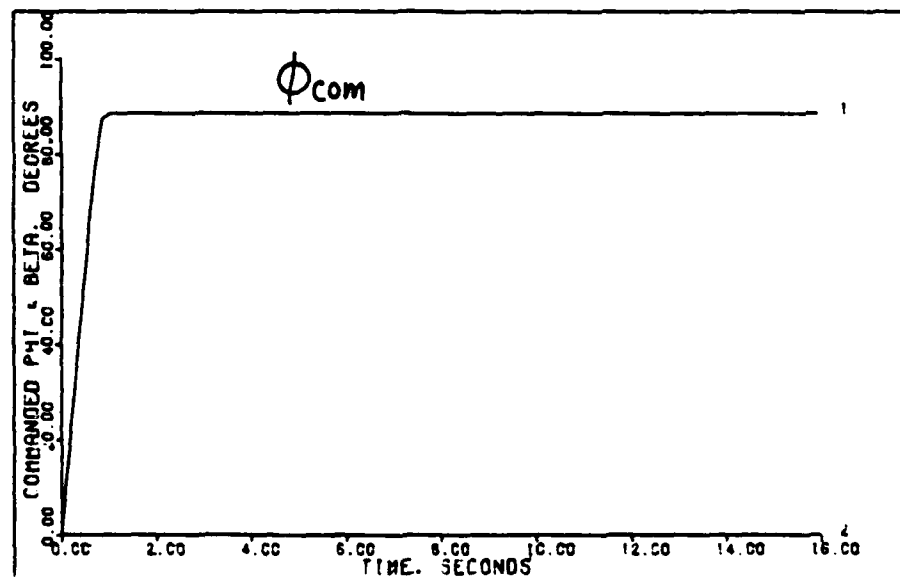


PHI & BETA OUTPUTS TO COORDINATED TURN: 1.2M, 15K FT

Figure 5-6



PHI & BETA OUTPUTS TO COORDINATED TURN: 0.1 2M. 15K FT



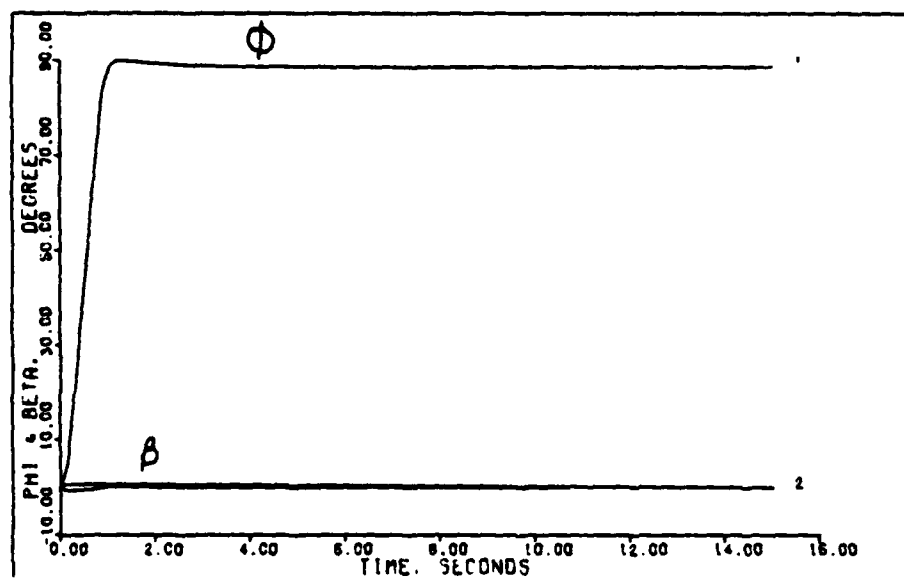
COMMANDED PHI INPUT TO COORDINATED TURN: 0.1 2M. 15K FT

Figure 5-7

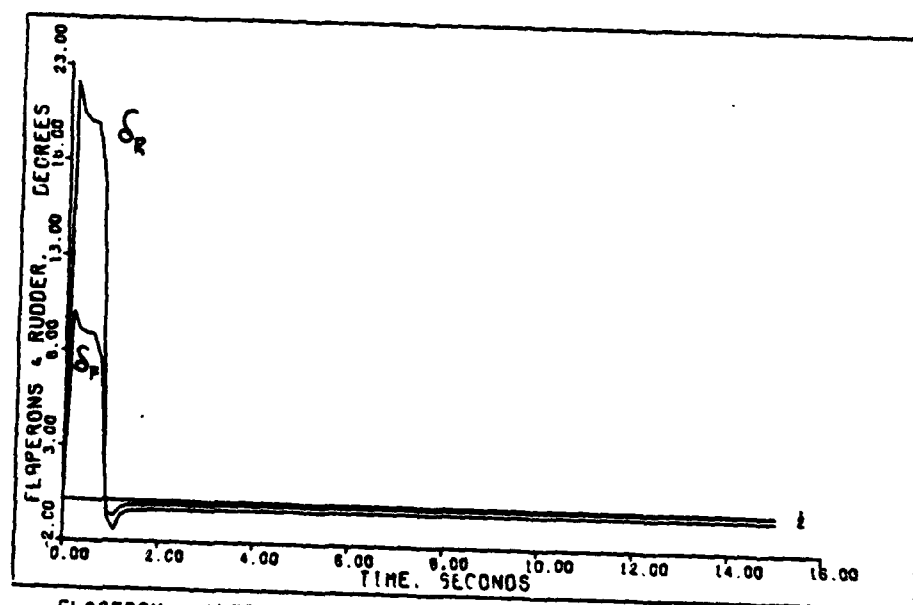
The full-gain robust controller degrades input responses by adding greater transient deflections and oscillations. The flap peak transient deflection increases by about 3.5 degrees, a significant amount. These transient increases degrade the control input rate as well. The transient rudder deflection is approximately doubled. Since, the rudder deflection is small to start with, this is unimportant.

The minimum-gain robust controller improves input responses at 0.4 Mach, sea level, and 0.9 Mach, 50 000 feet by decreasing the number of transient oscillations and by reducing the transient rudder deflections. At 0.7 Mach, 15 000 feet the input response is indistinguishable from that obtained with the full-gain robust controller. The input response obtained at 0.9 Mach, sea level is close to the response obtained from its individual (also full-gain) robust controller. The greatest degradation occurs at 1.2 Mach, 15 000 feet (see Figure 5-9), where the rudder peak transient deflection increases by about 4.5 degrees.

The roll and yaw rate responses are entirely as expected. The roll rate ramps up to a maximum value that varies from a minimum of 37 degrees/second at 0.9 Mach, 50 000 feet, to a maximum of 110 degrees/second at 0.7 Mach, 15 000 feet. After staying at the maximum value, the roll rate ramps-down to a small negative steady-state value (-0.19 degrees/second). After an initial yaw transient peak maximum of 8.03 degrees/second at 0.7 Mach, 15 000 feet, a

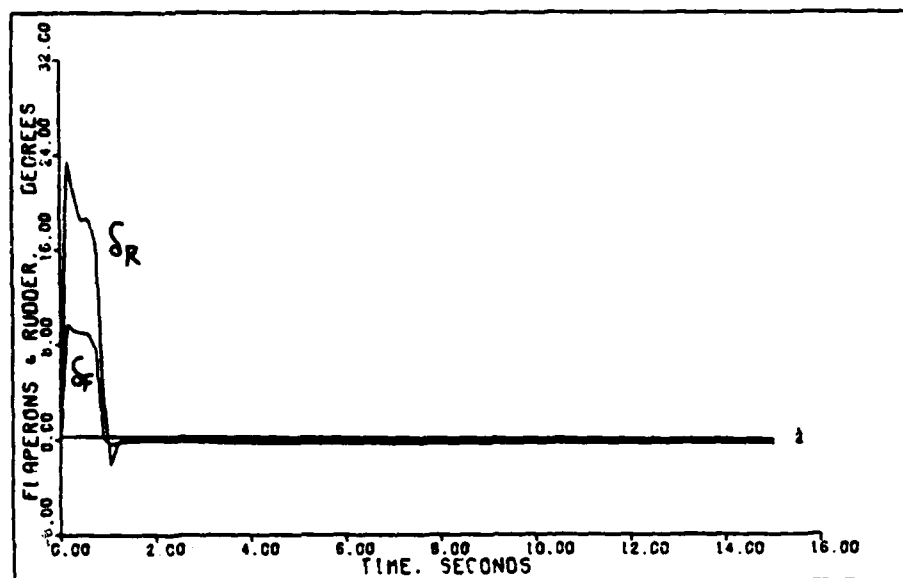


PHI & BETA OUTPUTS TO COORDINATED TURN: 2:1 2M. 15K FT

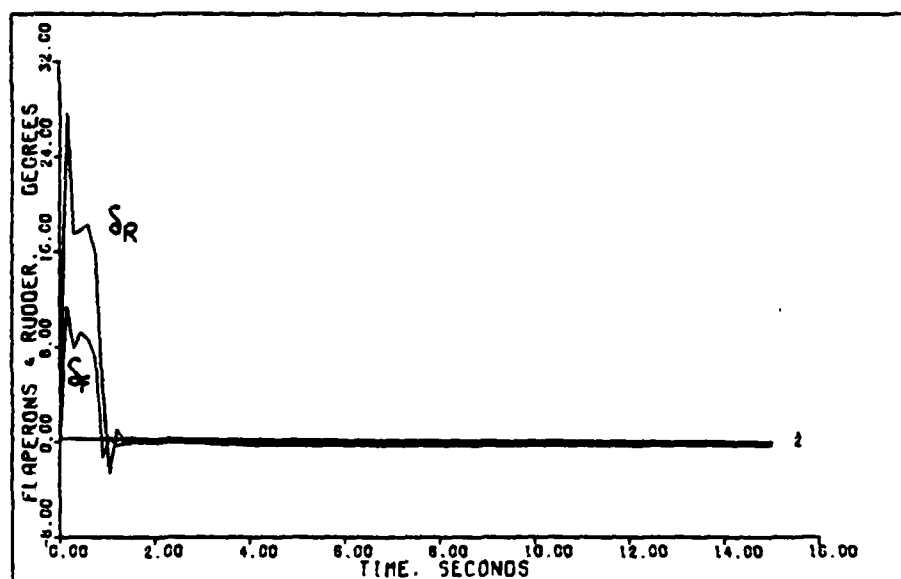


FLAPERON & RUDDER INPUTS TO COORDINATED TURN: 1:2M. 15K FT

Figure 5-8



FLAPERON & RUDDER INPUTS TO COORDINATED TURN: J: 1.2M.15K FT



FLAPERON & RUDDER INPUTS TO COORDINATED TURN: Z: 1.2M.15K FT

Figure 5-9

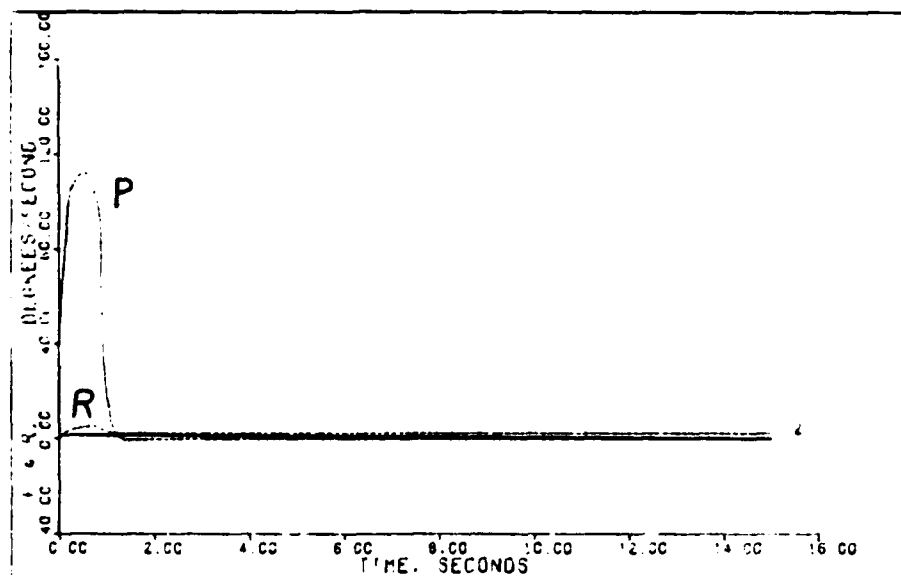
steady-state value of 3.84 degrees/second is established. This is necessary to continue turning the aircraft.

The full-gain robust controller does not degrade the roll rate response. The yaw rate response is not significantly changed. Thus the full-gain robust controller does not degrade the roll or yaw rate responses (see Figure 5-10).

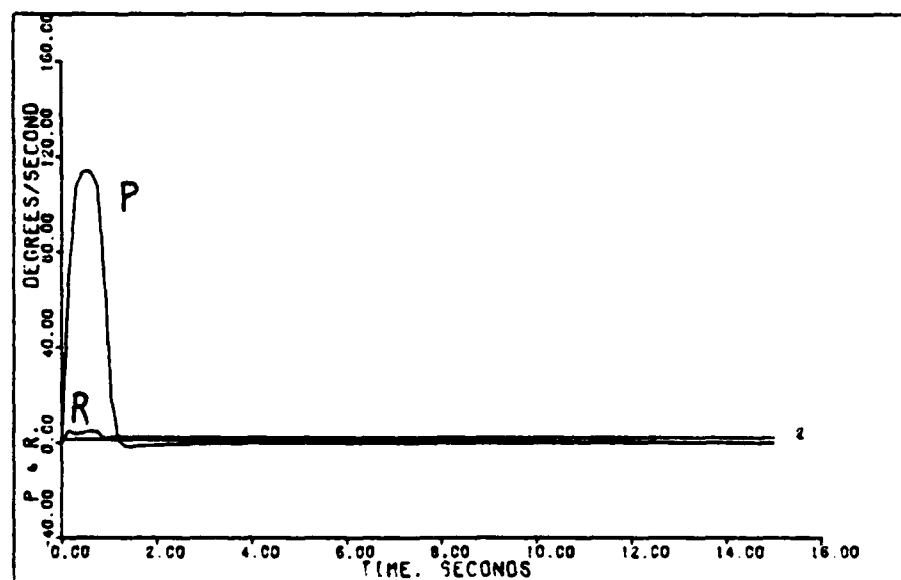
The minimum-gain robust controller also does not degrade the roll or yaw rate response. A small oscillation is introduced into the yaw rate transient, but this is insignificant (see Figure 5-11).

Maximum permissible control input rates are 50 degrees/second for the differential flaperons and 105 degrees/second for the rudder. The maximum negative and positive flap rates for the individual robust controllers are -53 and 67 degrees/second at 1.2 Mach, 15 000 feet. The maximum negative and positive rudder rates for the individual robust controllers are -117 and 148 degrees/second at 1.2 Mach, 15 000 feet. Thus the actual control input rates for a coordinated turn using individual robust controllers exceed the rate limits at one flight condition. Since 88.82 degrees of roll is commanded in 0.8 seconds, the ramp-up time should be lengthened to 0.9 seconds to reduce the actual rates to remain within limits.

The full-gain robust controller has maximum negative and positive flap rates of -49 and 65 degrees/second at 1.2 Mach, 15 000 feet. The maximum negative and positive rudder

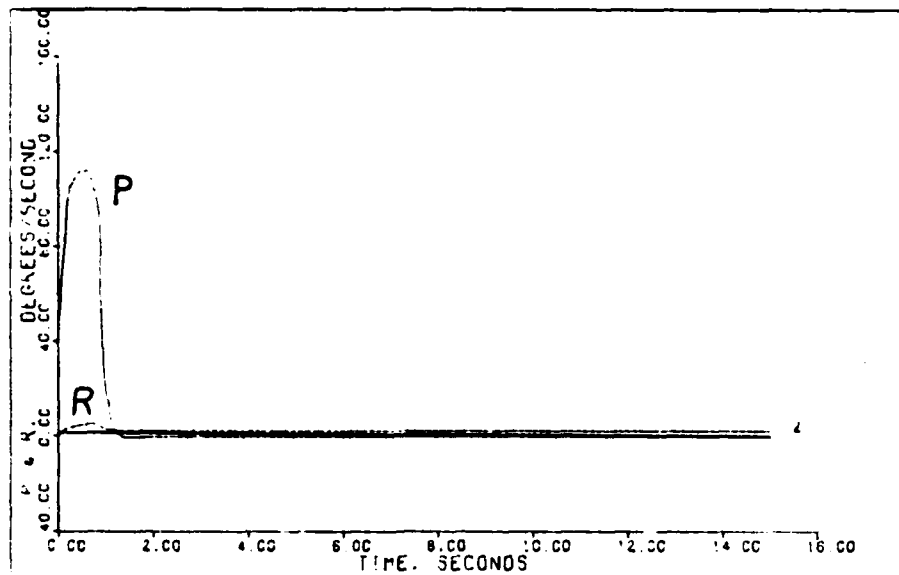


ROLL & YAW RATES FROM COORDINATED TURN: 1.2M, 15K FT

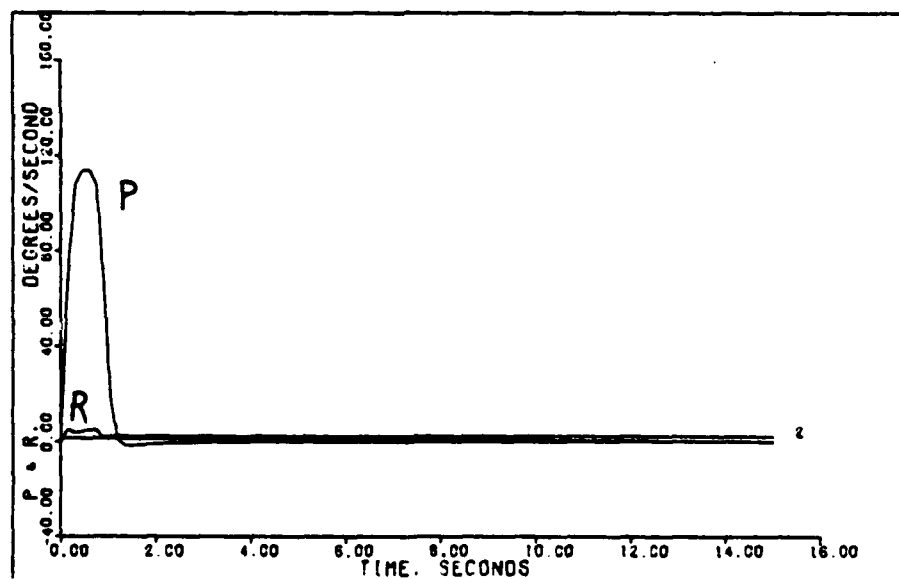


ROLL & YAW RATES FROM COORDINATED TURN: 1.2M, 15K FT

Figure 5-10



ROLL & YAW RATES FROM COORDINATED TURN: 1.2M, 15K FT



ROLL & YAW RATES FROM COORDINATED TURN: 1.2M, 15K FT

Figure 5-10

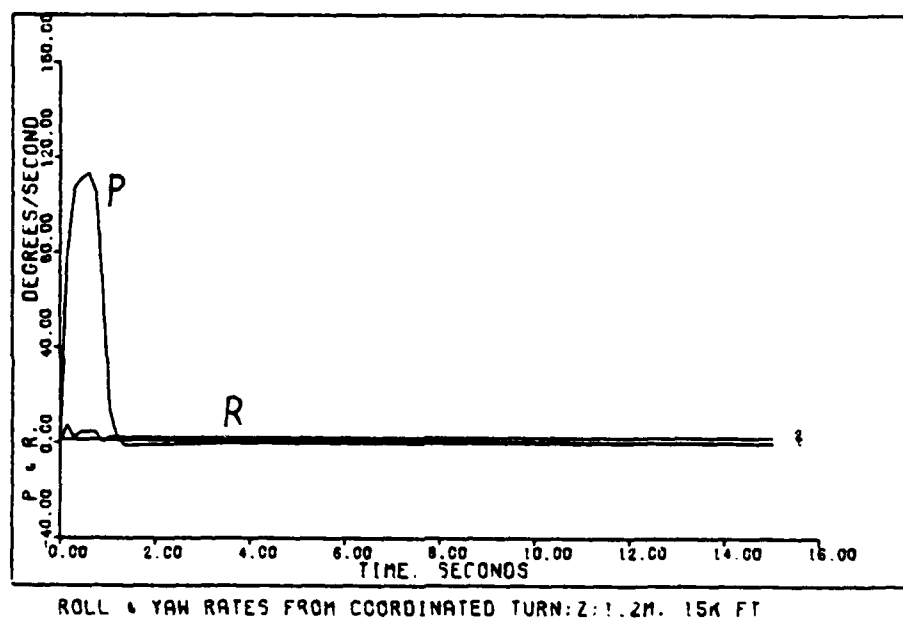


Figure 5-11

rates are -82 and 157 degrees/second at 1.2 Mach, 15 000 feet. While the flap rates are slightly reduced, the rudder rates are increased. Thus the full-gain robust controller provides a slight control input rate degradation.

The minimum-gain robust controller has maximum negative and positive flap rates of -57 and 76 degrees/second at 1.2 Mach, 15 000 feet. The maximum negative and positive rudder rates are -75 and 185 degrees/second at 1.2 Mach, 15 000 feet. Surprisingly, this is the only flight condition to exceed the rudder rate limits. Other flight conditions have much lower rates, with minimum negative and positive rudder rates of -3 and 2 degrees/second at 0.4 Mach, sea level. The controller does not have to be retuned, only the maximum commanded input value must be reduced. Except for the significant degradation of rates at 1.2 Mach, 15 000 feet, the minimum-gain controller improves or does not degrade rates compared with the full-gain controller.

Summary

Since the X-29A demonstrator aircraft's longitudinal and lateral equations of motion are decoupled, separate longitudinal and lateral controllers may be designed. In addition, the controllers may be implemented on separate computers, thus increasing processing speed and improving software reliability and maintenance.

The outputs selected are two states, roll angle and

sideslip angle. The same output (C) matrix is used for both maneuvers at all flight conditions.

As in longitudinal commanded inputs, maximum maneuvers are commanded. The controller is designed to perform two maneuvers, beta-pointing and coordinated turn. The maneuver times and commanded steady-state values vary from flight condition to flight condition.

In a coordinated turn, the aircraft is commanded to a fixed roll angle, while sideslip is commanded to zero. In performing a coordinated turn, it is undesirable to allow sideslip. If sideslip occurs during the turn, the nose drops, and must be corrected to avoid having the aircraft spiral. At all five flight conditions, the aircraft is commanded to a steady-state roll angle of 88.815 degrees while beta is commanded to zero.

Initially, separate controllers are designed for each maneuver at each flight condition. However, it is discovered that the design parameters used to obtain the controller for a coordinated turn at one flight condition provide excellent results in obtaining controllers for a coordinated turn at the other flight conditions. Additionally, it is found that the same controller obtained for a coordinated turn can be used for beta-pointing at the same flight condition. Next, a successful search is made for one controller that produces excellent tracking for both maneuvers at all flight conditions. Finally, half of the gains in the robust controller are set to zero with only minimal degradation of results. Thus a digital minimum-gain

controller requiring only three distinct gains is achieved.

Since the product CB is rank deficient, an Irregular design is required. Thus the design problem is non-minimum phase (zeros in the right-half Laplace plane) (Ref 3:7). An M matrix, or measurement matrix, is used to provide measurements of the derivatives of the states to augment the outputs.

The M elements are closely coupled and must be chosen simultaneously to obtain superior designs. For this lateral application only two M elements are required, and selecting the best set of elements in 2-space is not difficult. However, this becomes more difficult for applications where the A matrix (of size $(n-p) \times p$, where n =number of states
12

and p =number of outputs) is large, and the resulting M matrix is not sparse. A is large, for example, when de-
12

coupling of the longitudinal and lateral equations of motion does not occur.

Decreasing the measurement gains speeds up response and improves output tracking of the commanded inputs. Below a certain point, though, increasingly smaller improvements in tracking are obtained at the expense of degradation of control inputs.

Since the design method produces a robust M matrix, only the robust K_0 and K_1 have to be determined. Since ALPHA is selected equal to one, K_0 and K_1 are equal. Thus only one

set of robust gains must be determined. It is found that the controller which has the smallest component gains, 0.9 Mach, sea level, produces excellent results as a universal robust controller at all flight conditions.

Next, a minimum-gain robust controller is found. The elements whose inputs are expected to have minimal effect upon the corresponding outputs are set to zero. The magnitude of the element has nothing to do with its likelihood of acceptable degradation of response when set to zero. Thus the elements corresponding to rudder affecting roll and differential flaps affecting sideslip are set to zero.

Thus a minimum-gain controller requiring a total of only three gains is obtained. Two gains are required for the K matrices corresponding to the elements (ϕ , flaps) and (β , rudder). The two gains required for the measurement matrix in M have the same value, 0.1, so only one memory location is required. Therefore, since only three distinct gains are required, they may be stored in registers.

The individual robust controllers produce excellent tracking of commanded inputs by outputs. The full-gain robust controller minimally degrades tracking by increasing the transients at two flight conditions. The settling times are lengthened by about 50%. The peak times for three of the four flight conditions (the full-gain robust controller is the individual robust controller at 0.9 Mach, sea level) are the same. The minimum-gain robust controller reduces this transient peak degradation by more than 50% at 1.2

Mach, 15 000 feet. The peak and settling times are slightly degraded further for most flight conditions. In addition, the plots reveal that transient settling times are markedly improved. The transient settling times are half that of the individual robust controllers and one third of those from the full-gain robust controllers.

The control inputs are degraded by the full-gain robust controller but less by the minimum-gain robust controller. It is clear that this causes an increase in control input rates.

For beta-pointing, the individual robust controllers produce actual control rates within allowable limits. Unfortunately, for beta-pointing, the full-gain robust controller produces a degradation of control input rates. This requires that the maximum commanded steady-state input be reduced at two flight conditions. A reduction of no more than 10% of the commanded steady-state value should be sufficient to reduce the rudder rates to within the limit of 105 degrees/second. Alternately, the maneuver time must be slightly increased. It is important to note that the controller does not have to be retuned. The minimum-gain robust controller ameliorates the degradation of rudder rates slightly.

On balance the minimum-gain robust controller provides superior transient response to that obtained from the full-gain robust controller. Clearly, since the degradation is slight, a minimum-gain robust controller offers advantages

of implementation that outweigh the degradation.

The second lateral maneuver, coordinated turn, commands a roll angle of 88.8 degrees at all flight conditions. For the individual robust controllers, the greatest transient sideslip is 0.013 degrees. The full-gain robust controller degrades the transient by increasing the peak transient to 0.21 degrees. The minimum-gain robust controller increases the magnitude of the peak sideslip transient to 0.63 degrees. In general, transient roll overshoot is small for the individual robust controller (maximum 0.735 degrees), full-gain robust controller (1.95 degrees), and minimum-gain robust controller (1.337 degrees).

The full-gain robust controller degrades input responses by adding greater transient deflections and oscillations. The minimum-gain robust controller improves input responses.

The actual control input rates for a coordinated turn using individual robust controllers exceed the rate limits at one flight condition. This can be remedied by increasing the maneuver ramp-up time from 0.8 seconds to 0.9 seconds. The full and minimum gain robust controllers degrade the rudder rates but these can also be reduced to acceptable limits by increasing the ramp-up time or decreasing the roll angle.

The transient peak times are reduced by about 15% by the full-gain robust controller. This is balanced by about a 15% increase in settling times. The minimum-gain robust controller produces transient peak times equal to those of the individual robust controllers but the settling times are

lengthened by about 20%.

In general, very slight degradation occurs when comparing the performance of minimum and full gain robust controllers to the individual robust controllers. Also, the difference in performance between the full and minimum gain robust controllers is minimal. Clearly, the reduction in performance is not enough to warrant using individual robust controllers at each flight condition. The superior implementation advantages of a digital flight controller requiring only three gains are considerable.

An error was found in MULTI that affected Irregular designs not in $\begin{bmatrix} 0 \\ \frac{B}{2} \end{bmatrix}$ form. The "bug" significantly in-

creased the transient and steady-state errors obtained. Subsequent computer simulations with the corrected program show marked improvement over the excellent results presented here.

CHAPTER VI

CONCLUSIONS and RECOMMENDATIONS

General Comments

Porter's method offers the advantage that the analog theoretical equations have straightforward equivalent digital equations with no loss of generality. As yet, the location of the transmission zeros gives no a priori information as to the actual performance of the system. Only general statements about performance in the limit as the sampling frequency goes to infinity can be made.

Whenever the system model represents a Regular system, the designer has the option of using an Irregular design approach instead. A Regular design often gives better performance in the theoretical limit because the closed-loop poles corresponding to the transmission zeros become unobservable. However, heuristically it seems that Irregular designs offer better actual performance. In addition to the advantage in the theoretical limit, the Regular design has the advantage of requiring fewer gains.

Porter's method offers a quick, fairly straightforward design. Once the designer is familiar with the aircraft and Porter's method, many approaches can be tried in a short time period. Furthermore, once good results at a particular flight condition are obtained, the same design parameters can often be used as good initial values for other flight

conditions. For example, one set of lateral design parameters produced individual robust controllers at all five flight conditions.

The design techniques currently implemented in MULTI do not allow the designer to have fewer outputs than inputs. For a control-configured-vehicle (CCV) with many control surfaces and hence outputs, it may be difficult to determine what each commanded input should be (see Appendix A).

Another limitation of Porter's method that should be noted is the requirement that the number of outputs be less than the number of states when using an Irregular design. MULTI does allow the user to have as many outputs as states

when the system is not in $\begin{bmatrix} 0 & \underline{B}^T \\ & 2 \end{bmatrix}$ form. This is a possible error and should be examined (see Appendix A).

Also, MULTI does not currently have the capability to model the effects of noise upon outputs. Consider that the measured value of an output is equal to the actual value of the output added to some noise, whose statistics are unknown (see Figure 6-1):

$$\underline{Y} = \underline{C}x + \underline{v} \quad (6-1)$$

where \underline{Y} are the outputs, \underline{C} is the output matrix, x are the states, and \underline{v} is the noise. As the sampling period approaches zero, the gain which is equal to the sampling frequency approaches infinity. For high-gain systems, the noise is increased as well. Thus the noise can saturate the sensors. As sample periods decrease with the improvement of digital flight control systems, the noise saturation problem

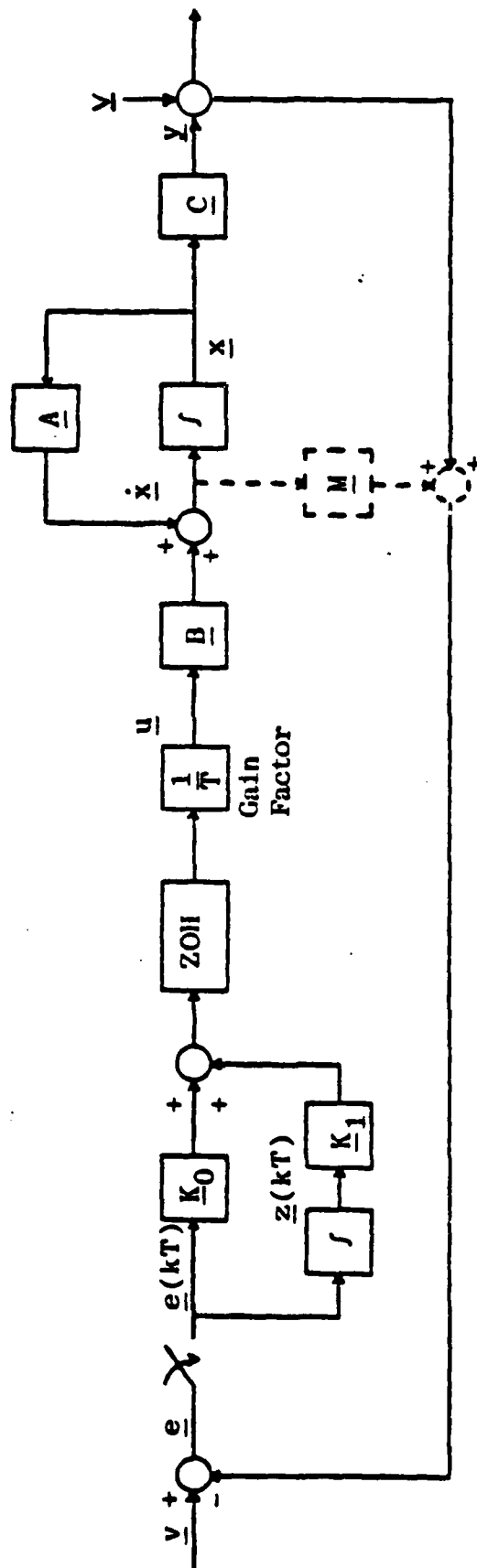


Figure 6-1 System Block Diagram - Discrete Design
With Sensor Noise

becomes even worse. An inherent tradeoff exists for conditionally stable systems. As sampling frequencies increase to obtain better precision, attention must be paid to stability concerns. Fortunately, it would not be difficult to modify MULTI to accept a stochastic model.

An assumption of white Gaussian noise can be made for v . In general, sensors do produce noise that exhibits the characteristics of whiteness and normality. Since Gaussian random variables are completely determined by their first two moments, only the mean and covariance must be determined. It is not unreasonable to expect that the noise might have a bias level and be time-correlated when the sensors are first turned on. Whiteness refers to the property that the noises are not time-correlated; the assumption of small perturbations in steady level flight is consistent with whiteness.

Since sensors can be corrected for biases, a zero mean assumption of the sensor noises is a good one. To simplify the analysis, assume that the non-diagonal terms of the covariance matrix are zero. This is equivalent to independence of sensor noises from one another. In order to determine the diagonal values of the covariance matrix, a determination or assumption must be made as to the quality of the sensors used. In fact, a sensitivity analysis of the quality of sensors required can be made. If very noisy sensors do not degrade stability and tracking, then cheaper sensors for the digital flight control system may be used.

By the central limit theorem, a Gaussian random variable

can be well-modeled by the sum of random variables of uniform distribution, which are easy to generate. Random number generators could be used to generate the random variables. This white Gaussian noise should then be added to the newly generated states returned from the subroutine ODE (Ordinary Differential Equations). This sum, the output of the noisy sensor, is then fed back to the summer and differenced with the commanded input.

This is only correct, though, for the assumption of a perfect truth model for the actual system. In addition to modeling sensor noise, uncertainties in the state equation can be modeled as well (see Figure 6-2):

$$\dot{\underline{x}} = \underline{A}\underline{x} + \underline{B}u + \underline{G}w \quad (6-2)$$

where \underline{x} are the states, \underline{A} is the plant matrix, \underline{B} is the input matrix, u are the inputs, \underline{G} is the noise-input matrix, and w are white Gaussian noises. Assuming that the driving noises in different state equations are independent, then the covariance of w is a diagonal matrix. Information on wind gusts must then be obtained to determine the covariance of w . Since wind gusts are not time-correlated, whiteness is assured. In addition, w and v are assumed to be independent. This, however, may not be an adequate model since it is expected that wind gusts also increase the sensor noise. Sensitivity analysis of w and v can then be performed to determine under what conditions significant degradation of the performance of digital flight control system occurs.

After the new states are generated by ODE, and multi-

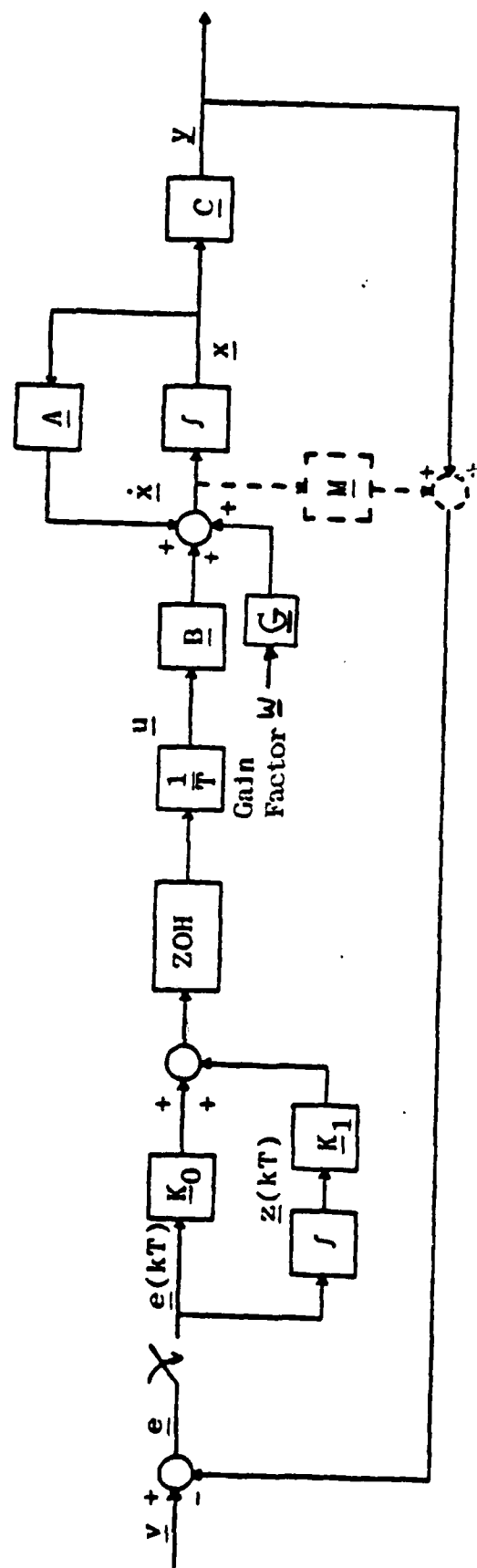


Figure 6-2 System Block Diagram - Discrete Design
With State Noise

plied by the plant matrix A , the noise is added and the sum fed back (see Figure 6-2).

Note that acceleration outputs often require a feedforward (D) matrix. However, the state equations can be rewritten to imbed the D matrix into the output (C) matrix. Since Porter's method was not developed for systems with a D matrix, it is not clear whether good designs under these conditions can consistently be achieved. If the output is the derivative of one of the states, then a transmission zero is present at the origin in the Laplace domain (equivalently, is situated on the unit circle in the z domain for the discrete case), indicating conditional stability (as the sampling period approaches zero for the discrete case). This poses some serious limitations since the measurement of angles is difficult. The pilot actually commands rates with the control stick and feels accelerations with his body.

Conclusions

After an introduction and description of the X-29A, a set of fifteen longitudinal controllers is developed for six maneuvers at five flight conditions. Next, Porter's method is applied to the lateral state-space equations. First, individual lateral robust controllers are developed for each flight condition. Next, a single full-gain lateral robust controller which achieves good performance at all flight conditions is chosen. Finally, a minimum-gain lateral robust controller is developed.

The straightforwardness of Porter's method is due

primarily to the structure of decoupling of the outputs in the limit as the sampling frequency goes to infinity for Regular systems and for Irregular systems with a $C F_{2 \times 2}$ diagonal matrix. Actual decoupling is reasonably good not only for the above-mentioned systems but also for Irregular systems where the $C F_{2 \times 2}^{-1}$ matrix is only diagonally dominant.

As the order of the system increases, the possibility of intercoupling increases as $(p-1)!$, where p is the number of outputs (assuming the restriction that the number of outputs, p , must equal the number of inputs, m). Clearly, such design methods can be extremely complex.

The X-29A demonstrator aircraft integrates several different advanced technologies of aircraft design. In Chapter III forward-swept wings, close-coupled canards, strake-flaps, variable camber, fly-by-wire, and relaxed static stability are discussed. Although knowledge of the aircraft design is not needed to apply Porter's method, insight into how the aircraft "should" behave can be helpful.

Chapter IV presents the results of a Regular design application to develop longitudinal controllers for the X-29A. It is stressed that the output matrix (C) must be the same for all maneuvers throughout the flight envelope. The Regular design, which requires that the product CB be non-singular, is also a minimum phase application (transmission zeros in the left-half Laplace plane). If it is non-minimum

phase, then the system is conditionally stable. Since the closed-loop poles are driven to the transmission zeros as the sampling frequency is increased, there is a lower bound on the sampling period.

A description of the six longitudinal maneuvers designed for is provided. At each flight condition three controllers are designed. One controller for the direct climb, direct lift1, and direct lift2 maneuvers is used with minimal degradation of performance. One controller for pitch-pointing is designed. One controller for vertical translation1 and vertical translation2 is designed. These consolidated controllers are used in the quest for a single robust controller for all maneuvers at all flight conditions. An acceptable, less desirable alternative to a robust controller would be a single controller at each flight condition with gain-scheduling used between design points.

A ten step general outline for applying Porter's method is presented. A discussion of design parameters follows. An outline to allow the design engineer to immediately start using the interactive CAD program MULTI is given.

When the allowable control input rates are exceeded as occurred for some of the longitudinal maneuvers, the maximum commanded inputs must be reduced or the maneuver time must be lengthened. Retuning of the controllers is not required.

Since the X-29A demonstrator aircraft's longitudinal and lateral equations of motion are decoupled, separate longitudinal and lateral controllers may be designed. In

addition, the controllers may be implemented on separate computers, thus increasing processing speed and improving software reliability and maintenance.

As in longitudinal commanded inputs, maximum lateral maneuvers are commanded. Two maneuvers, beta-pointing and coordinated turn, are designed for. The maneuver times and commanded steady-state values vary from flight condition to flight condition.

Initially, separate lateral controllers are designed for each maneuver at each flight condition. However, it is discovered that the design parameters used to obtain the controller for a coordinated turn at one flight condition provide excellent results in obtaining controllers for a coordinated turn at the other flight conditions. Additionally, it is found that the same controller obtained for a coordinated turn can be used for beta-pointing at the same flight condition. Next, a successful search is made for one controller that will produce excellent tracking for both maneuvers at all flight conditions. Finally, half of the gains in the robust controller are set to zero with only minimal degradation of results. Thus a digital minimum-gain controller requiring only three distinct gains is achieved.

Since the product CB is rank deficient, an Irregular design is required. Thus the design problem is non-minimum phase (zeros in the right-half Laplace plane). An M matrix, or measurement matrix, is used to provide measurements of the derivatives of specified states in order to form a new output matrix. The M elements are closely coupled, and must

be chosen simultaneously to obtain superior designs. The choice of which states are fed back is determined by the order in which the state equations are written. Changing the order changes the A_{12} matrix; the measurement matrix (M) operates on A_{12} . More specifically, the first (n-p) derivatives of the states are operated on by M.

It is found that the controller which has the smallest component gains, 0.9 Mach, sea level, produces excellent results as a universal robust controller. Next, a minimum-gain robust controller is found by setting to zero those elements whose inputs are expected to have minimal effect upon the corresponding outputs.

The individual robust controllers produce excellent tracking of commanded inputs by outputs. For beta-pointing, the control inputs are degraded by the full-gain robust controller but less by the minimum-gain robust controller. It is clear that this causes an increase in control input rates. In order to restrain the control input rates the maximum commanded steady-state inputs must be reduced at two flight conditions. Alternately, the maneuver time must be slightly increased. It is important to note that again, the controller does not need to be retuned.

On balance the minimum-gain robust controller provides superior transient response to that obtained from the full-gain robust controller. Clearly, since the degradation is slight, a minimum-gain robust controller offers advantages

of implementation that outweigh the degradation.

For the coordinated turn, slight degradation occurs when comparing the performance of minimum and full gain robust controllers to the individual robust controllers. Also, the difference in performance between the full and minimum gain robust controllers is minimal. Clearly, the reduction in performance is not enough to warrant using individual robust controllers at each flight condition. The superior implementation advantages of a digital flight controller requiring only three gains are considerable. Indirect control of rates and accelerations is possible but unsatisfying.

Recommendations

First, suggestions for improvements in MULTI's capabilities and enhancements are provided. Next, a series of design algorithms that significantly reduce the trial-and-error required with Porter's method are presented. Finally, suggestions for the direction of future digital flight control designs for the X-29A are given.

Suggestions for improvements

MULTI, as it is presently constituted, is not written with structured programming. In addition to adding substantial enhancement of MULTI's capabilities, this year's group of theses have achieved an order of magnitude reduction in the central processing units (CPUs) required to run a simulation. Future improvements to MULTI should include "timing runs" in order to discover what part of the code is used most often. This code should then be rewritten

to reflect maximum computational efficiency. In addition, "blending", or the use of assembly language to speed up the parts of the code used most often should be considered. These improvements in efficiency would permit the additional CPU time required for the addition of algorithms to eliminate the trial-and-error presently necessary. To increase maintainability, comment statements should be added to MULTI. At present, MULTI is not well documented.

The capability to command a series of maneuvers should be added to MULTI. This capability allows the determination of the number of flight condition design points required to adequately design for the entire flight envelope. For example, after the direct climb maneuver at 1.2 Mach, 15 000 feet, the aircraft has changed its flight condition to 1.6 Mach, 21 000 feet. The simulation parameters at the end of the simulation run are then used as the starting parameters for a new maneuver. The results are then compared with those obtained by using linearized state-space matrices at 1.6 Mach, 21 000 feet that are provided by Grumman's nonlinear simulation program. If the difference in simulations is slight, then the assumption of small perturbations is not violated. If the difference is great, then perhaps another intermediate flight condition between 1.2 Mach, 15 000 feet and 1.6 Mach, 21 000 feet should be used.

After a robust controller(s) is attained, a dynamic range analysis of the controller and measurement matrices should be performed. If the initial heuristic objective of

obtaining controller gains with magnitudes from 0.001 to 1000 is achieved, then the implementation of the software can be done in single precision. This increases processing speed and addresses the problem of finite wordlength implementations.

Enough applications of Porter's method have been made that an analysis of digital transmission zeros should be made. Perhaps some insight into heuristically determined good values of transmission zeros would assist the designer in choosing the measurement matrix in Irregular designs. This is analogous to choosing the closed-loop eigenvalues of the system. A priori information might also help in the selection of design parameters and controller gains.

In addition, perhaps an analog to the frequency-domain Neil-Smith analysis of handling qualities can be made with transmission zeros and closed-loop poles.

The program ZERO should be rewritten and incorporated into MULTI. This would enable one of proposed algorithms to accept only a measurement matrix that moved the transmission zeros into the unconditionally stable region (within the unit circle in the z -domain).

Since MULTI already calculates the control input rates, it would not be difficult to add rate limiting to MULTI simulations. Assuming that the commanded maneuver is reasonable, this would prevent the designer from pursuing designs that require excessive aircraft hinge moments.

A major improvement to Porter's method would be to allow the number of control inputs to be greater than the outputs.

If another independent control input, such as the symmetrical flaperons on the X-29A, is added, MULTI requires that another output be added. It is possible to "fool" the design method by commanding flight path angle when pitch rate (and thus pitch angle) and angle-of-attack is already commanded, but this can complicate the design. Adding unneeded outputs increases the number of sigma elements and for Irregular designs increases the order of the measurement matrix.

A simple, useful addition would be the addition of a parsing routine to allow the user to interactively enter several commands on one input line at once.

Design algorithms

The following is a series of algorithms that mimic the design procedure. These algorithms, if implemented in MULTI, would permit a significant reduction in the trial-and-error presently required. Each option stops when one of two conditions is met. If the performance specifications are met, then MULTI returns the answer. If, however, the specification is not met the designer has the option of using the best answer obtained, or giving MULTI more CPU time. If the user does not specify how much computer time should be used in selecting an option, then a default value is used.

An implicit assumption in these algorithms is that the model of small linear perturbations is accurate. Since the system is linear, the designer can determine the direction

from the initial value that a design parameter must be adjusted to provide better performance. For example, if increasing the value of ALPHA causes a degradation in performance, then increasing ALPHA further will only make matters worse. Many good designs are possible for the set of unspecified design parameters. However, for a single design parameter there is a single best value (for values already assigned to other design parameters). Thus, part of the design problem is: in what order should the design parameters be chosen? Note that the order in which the design parameters are chosen will limit the amount of further tuning that is possible. In practice, the designer will retune each parameter until significant additional improvements in performance are unobtainable.

It is unknown if a single design superior to others exists, or how to find such a design. More likely, many good designs exist that each exhibit superior qualities in some respects and deficiencies in others. Also, diminishing marginal returns force the designer to decide at what point additional design effort is worth the improvement in performance.

It is suggested that the following proposed options have a prefix of two.

Option 211- This option selects the initial values of ALPHA, EPSILON, and SIGMA based upon the algorithm presented in Chapter IV (see suggested design procedure for using MULTI, step 3).

Option 212- Given a range of values for ALPHA and

EPSILON, find the best set of ALPHA and EPSILON (e.g. ALPHA between zero and 1.5, EPSILON between zero and four). This option, used in the retuning phase of design, solves the problem in 2-space. Note that the other design parameters are held constant. Thus, no more than four simulations must be run to determine the direction that (ALPHA, EPSILON) must be varied.

Option 213- (For Irregular designs) Regenerate the state-space model in an equivalent form, with the rows in different order. This allows a different set of states to be fed back, a different A_{12} matrix, and hence a different M (measurement) matrix. The designer would input the initial state order. Then he would specify which states (up to maximum of $n-p$, where n is the number of states and p is the number of outputs) he wanted fed back.

Option 214- (For Irregular designs) Given that the states to be fed back are already selected, find all acceptable M matrices. Note that the actual gains are not found, just the location of the nonzero elements. The default is to list the sparsest M matrix.

Note that $F B_2$ must have full rank. Since B_2 must have full rank (or the control inputs are redundant) this requirement can probably be met by choosing F_2 to have full rank. It is possible, though, for F_2 and B_2 to have full rank, and yet their product could be rank deficient. Thus

the nonzero M elements should be chosen such that F_2 has nonzero entries along either, but not both, diagonals (this ensures decoupling in the limit). If a diagonal F_2 matrix is not possible, then M is chosen to have the fewest elements. This can be done in following manner:

1. Set each M element to an initial value between zero and one such that no M element in the same column has the same value.
2. Set one M element to zero.
3. Form F_2 .
4. Try to invert F_2 .
5. If successful, keep that element set to zero. If not, reset the M element to its initial value.
6. Repeat steps 2-5 until all M elements have been tried.

Option 215- (For Irregular designs) Given that the states to be fed back are already selected, print the transformation (T) matrix that changes the B matrix into $\begin{bmatrix} 0 \\ \frac{B}{2} \end{bmatrix}$ form. This allows the designer to pick the M elements using existing algorithms.

Option 216- (For Irregular designs) Given a selected M matrix, find the best values of the M matrix. This is done as follows:

1. Set all nonzero M elements to their initial

values selected in Option 214.

2. Next, find the solution in N-space, where N is the number of nonzero M elements. This is done by an exhaustive search in which each element is increased and decreased simultaneously with the other elements and the best improvement in performance determined. Note that each iteration will require 2^N simulations to be run. Where N is large, MULTI may be run in batch or the M elements can be selected one row at a time.

It is reasonable to assume that the design which best tracks (as determined by the figures of merit) the maximum commanded input will also best track a less demanding maneuver. The less demanding maneuver commands a fraction of the maximum steady-state value. In addition, the length of the maneuver is reduced. In this thesis all maneuvers and simulation times are 16 seconds long. A maneuver that is only three seconds, for example, reduces the amount of CPU time required to evaluate each design.

Option 217- For a given set of TREND(I), TPEND(I), and TZERO(I), determine find the maximum VSS(I). TREND(I), TPEND(I), TZERO(I), and VSS(I) are values used in Option 22 in MULTI to ramp up a commanded value to a steady-state value and then ramp it back to zero. TREND(I) is the time the ramp ends (steady-state is reached). TPEND(I) is the time the input leaves steady-state. TZERO(I) is the time the input returns to zero. This option finds the maximum commanded maneuver within control input limit and rate restrictions.

Option 218- For a final set of individual robust controllers with a constant output (C) matrix, find a universal robust controller of best performance. This is done as follows:

1. First try the controller with the most gains of minimum magnitude. If the performance is within specified limits, stop. Otherwise proceed to step 2.

2. Next try individual robust controllers at each flight condition. After selecting the individual robust controller with the best performance, check to see if the performance is acceptable. If acceptable, stop. If not, proceed to step 3.

3. Form a composite robust controller composed of the lowest gains, component-wise, from each of the individual robust controllers. If performance is acceptable, stop. If not, abandon the search for a universal robust controller.

Option 219- For a given universal robust controller, find a minimum-gain robust controller. For given performance specifications, determine which controller gains can be set to zero. This is done by setting the controller elements to zero one at a time and determining if the performance specifications are met.

Option 221- This option is used to obtain a measure of the robustness of the controller matrices. This is done as follows:

1. Set the commanded steady-state value for a given

maneuver to one-half its maximum value.

2. Vary controller gains one at a time until control input limits are reached or performance degrades unacceptably. This gives an indication of how robust each gain is in the design.

3. Next, vary the controller gains in sets, but only up to half the gain variation found in step 2. This gives an overall robustness measure.

Option 222- For a given set of performance specifications, determine how much sensor noise can be tolerated by varying the mean and variance (assume white Gaussian noise). This gives an indication of how good the sensors must be.

Option 223- For a given set of performance specifications, determine how much uncertainty in the states can be tolerated (such as that caused by wind gusts). Again, vary the mean and variance (assume white Gaussian noise).

Note that Option 28 can be used to set performance specifications. Also, MULTI must be modified to enable it to simultaneously store all controller and measurement matrices from each flight condition. In addition, MULTI must be modified to simultaneously store all maneuvers. Note that the search for a universal robust controller, search for a minimum-gain robust controller, and tests for robustness must be repeated for each maneuver.

Future designs for the X-29A

In general, it is better to command rates and

accelerations than angles. The pilot commands rates with the control stick and can feel accelerations. Angles do not have such a physical interpretation. In addition, angles are often difficult to measure. For Irregular designs where the derivative of a state is fed back, noise can be a serious difficulty. Some angles, such as angle-of-attack and sideslip, are very difficult to measure, hence their derivatives are noisy. It is with these considerations in mind that the following suggestions are made.

Two longitudinal controllers should be designed for the X-29A. One would provide minimum drag by incorporating variable camber. This controller would have only two independent control inputs and thus would command two outputs. The first independent control input, thrust, would permit control of u , change in forward velocity. The second independent control input would consist of the canards, symmetrical flaperons, and strake tied together. In practice, Grumman's present design feeds a signal from the canards to the symmetrical flaperons and then the strake deflection is determined by a computer "table look-up" of the symmetrical flaperons' deflection. This design models the airflow. The second output chosen could be either q , pitch rate, which is the output chosen for Grumman's analog backup design, or N_z .

A second flight control system, which would be activated by the pilot's control stick, is required for maximum maneuverability. This design would treat the canards,

symmetrical flaperons, and strakes as independent control inputs. Since four independent control inputs are available, four outputs must be commanded. Since a reduced-order state-space model of four states is used, all four states could be commanded (see Appendix A). The addition of pitch angle to the outputs is done only to meet a requirement of Porter's method, that is, the number of independent control inputs must equal the number of outputs. Since a primary-lift control surface, symmetrical flaperons, is being added to the aircraft model, a substantial increase in performance over the results presented in this thesis is expected.

For the lateral mode, an Irregular design using p , roll rate, and r , yaw rate, should be made (see Appendix A). In addition, an Irregular design with N and p as outputs y should also be attempted. In both cases, high priority should be place on not choosing the derivative of sideslip as one of the states to be fed back.

The results of this thesis may be useful in determining the values to which p and r should be commanded for the first design. For the second lateral design attempt, for beta-pointing, N should be commanded as a pulse while p y should be commanded to zero. For a coordinated turn N y should be commanded to zero while p is commanded as a pulse.

BIBLIOGRAPHY

1. Barfield, F. Multivariable Control Law Development For The AFTI/F-16. Master Thesis, Air Force Institute of Technology, Wright-Patterson AFB OH, December 1982.
2. Simmers, J. Multivariable Digital Flight Control Design For The FPCC Aircraft. Master Thesis, Air Force Institute of Technology, Wright-Patterson AFB OH, December 1983.
3. Porter, B. Design of High-Performance Tracking Systems. USAME/DC/120/81. Air Force Flight Dynamics Laboratory, Wright-Patterson AFB OH, November 1981.
4. DeMeis, R. "Forward-Swept Wings Add Supersonic Zip" High Technology, January/February, 1982. Volume II.
5. Spacht, G. Forward Swept Wing Demonstrator Technology Integration And Evaluation Study. Grumman Aerospace Corporation, Bethpage, NY, December 1980. AFWAL-TR-80-3145, Volume I.
6. Bauschliker, J. Design of a Complete Multivariable Digital Flight Control System. Master Thesis, Air Force Institute of Technology, Wright-Patterson AFB OH, December 1982.
7. Blakelock, J. Automatic Control of Aircraft and Missiles. New York: John Wiley & Sons, Inc., 1965.
8. Mayhew, B. Digital Control Laws for the UH-60A Black Hawk Helicopter. Unpublished Master Thesis, Air Force Institute of Technology, Wright-Patterson AFB OH, March 1984.
9. Lewis, T. High Gain Error Actuated Flight Control for Continuous Linear Multivariable Plants. Master Thesis, Air Force Institute of Technology, Wright-Patterson AFB OH, December 1982.

10. Porter, B. and Bradshaw, A. "Design of Linear Multivariable Continuous-Time Tracking Systems Incorporating High-Gain Error-Actuated Controllers", International Journal of Systems Science, Vol. 10, No. 4: pp. 461-469 (1979).
11. Ridgely, B., and D'Azzo, J. Lecture materials distributed in EE 7.08, Advanced Multivariable Control Workshop on Singular Decomposition Methods. School of Engineering, Air Force Institute of Technology. Wright-Patterson AFB OH, 1983.
12. D'Azzo, J., Professor of Electrical Engineering. Lecture materials distributed in EE 7.08, Advanced Multivariable Control. School of Engineering, Air Force Institute of Technology. Wright-Patterson AFB OH, 1983.
13. Ridgely, B., Banda, S., and D'Azzo, J. "Decoupling of High-Gain Multivariable Tracking Systems", AIAA 21st Aerospace Sciences Conference, Reno, Nevada, January 1983, AIAA Paper No. 83-0280.
14. Pulcini, Jeffrey, "Constructing Benchmarks that Measure Up", Computer Design, Vol. 22, No. 11, p. 162, October, 1983.

Appendix A

Other Design Approaches

This appendix outlines some design approaches that were tried and found to be unsatisfactory. First, a discussion of longitudinal design approaches is presented. Next, a discussion of lateral design approaches is given. Lastly, a comparison in performance between two different models of the X-29A is made. The results of the first model, "data set2", are not given. This thesis presents only the results obtained using "data set3" supplied by Grumman Aerospace Corporation. For a list of future suggested designs, see Recommendations in Chapter VI.

Longitudinal Designs

The first longitudinal design attempt was applied to a 4 x 4 system model. That is, four control inputs and four outputs were incorporated into the model. The control inputs available were horizontal canard, flaperons, strakes, and thrust. The outputs chosen were pitch rate, change in forward velocity, angle-of-attack, and normal acceleration. This is the same as the model chosen for this thesis, except that one additional control input (flaperons) and output (normal acceleration) were added.

The acceleration output added a D (feedforward) matrix to the system model. Consequently, an Irregular design was required. Although no decoupling zeros were present, the program ZERO output one transmission zero in the right-half Laplace domain. That was an error in the program ZERO,

since the number of transmission zeros should be equal to the number of states minus the number of outputs. Since the reduced-order state-space model uses only four states (pitch angle, pitch rate, change in total velocity, and angle-of-attack), the number of transmission zeros should have been zero.

If the system model is not in $\begin{bmatrix} \text{zero} & B \\ & 2 \end{bmatrix}^{-1}$ form, then the measurement (M) matrix must be chosen by guessing, subject to the constraint that the resulting product FB matrix must have full rank. Note that since the number of states is equal to the number of outputs, Porter's method collapses for an Irregular design applied to a system in $\begin{bmatrix} \text{zero} & B \\ & 2 \end{bmatrix}^{-1}$ form. Porter's method would require the M matrix to have dimension 4 x 0. MULTI, however, did allow design attempts to be made (maybe because the system was not in $\begin{bmatrix} \text{zero} & B \\ & 2 \end{bmatrix}^{-1}$ form). Results were poor.

The second approach tried was to imbed first order actuators into the system to accomplish two objectives: first, to transform the system into $\begin{bmatrix} \text{zero} & B \\ & 2 \end{bmatrix}^{-1}$ form; and second, to increase the number of states to eight while keeping the number of outputs constant at four. Although algorithms were now available for picking the location of nonzero elements in the M matrix, the algorithms did not assist in picking the value of the nonzero elements. Since

the M matrix was now a nonsparse 4 x 4 matrix, the assumption of linear behavior requires that 2^s simulations (where s is the number of nonzero elements in the M matrix) be performed in order to determine in what direction each element must be changed (increased or decreased) in order to improve performance in the best possible manner. Since $s > 8$, guessing the value of the M elements was all that could be practically accomplished. Although a stable system could be achieved, the most modest maneuver would cause increasing oscillations in the control inputs.

Next, a pseudo-short-period approximation was made to the system. The term "pseudo" is used because the short-period roots were on the real axis. The short-period approximation, which assumed that the derivative of the change in forward velocity is zero, also allowed the removal of the theta state. Thus an Irregular design was applied to a 5 x 5 system with three control inputs and outputs. The states were pitch rate, angle-of-attack, canard deflection, strake deflection, and flaperon deflection. The control inputs were the canard actuator, strake actuator, and flaperon actuator. The outputs were pitch rate, angle-of-attack, and normal acceleration. Unfortunately, for the same reasons as given before, results were unacceptable because of growing oscillations in the control inputs.

Lateral Designs

Regular designs were achieved for the following flight conditions (the others were not attempted): 0.4 Mach, sea

level; 0.9 Mach, 50 000 feet; and 1.2 Mach, 15 000 feet. The outputs were roll rate and yaw rate. These outputs were chosen because rates are easier to measure than angles. Unfortunately, the best designs achieved could not remove a large transient roll angle (e. g., -4 degrees at 0.9 Mach, 50 000 feet) in the beta-pointing maneuver. Similarly, a large transient sideslip angle occurred in the coordinated turn (e. g., 4 degrees at 0.4 Mach, sea level with roll angle indirectly commanded to 90 degrees).

Data set2

Data set2 was designed for at three flight conditions: 0.4 Mach, sea level; 0.9 Mach, 50 000 feet; and 1.2 Mach, 15 000 feet. For most maneuvers, the maximum commanded input for data set2 was 40% greater than the maximum commanded input achieved for data set3. This applies for both longitudinal and lateral maneuvers. Data set3 was used in this thesis because it was judged by Grumman to be a better model of the X-29A demonstrator aircraft.

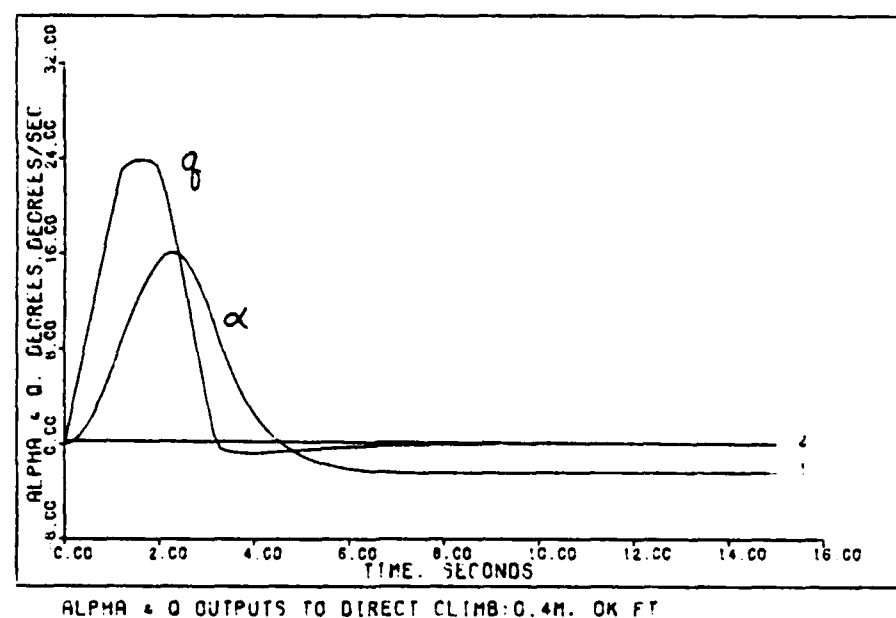
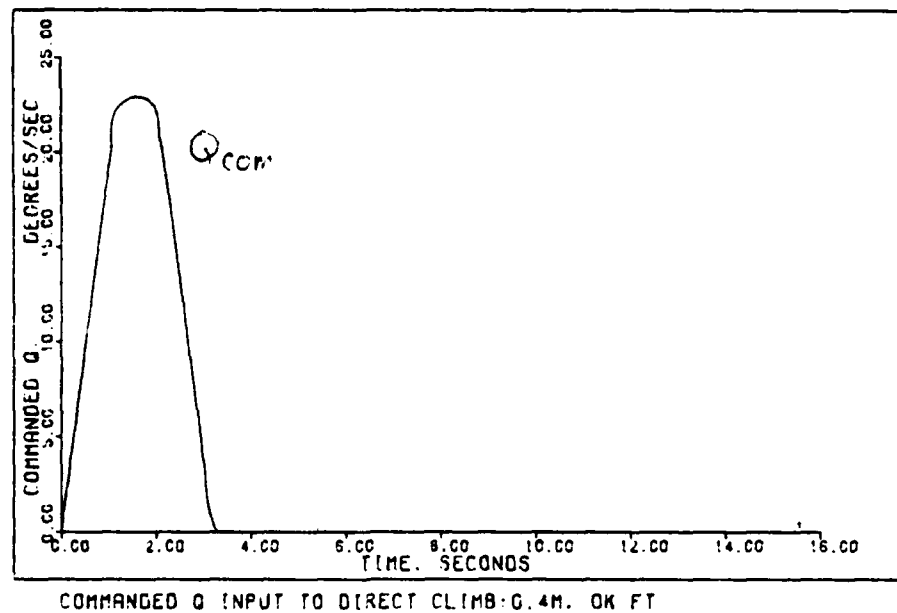
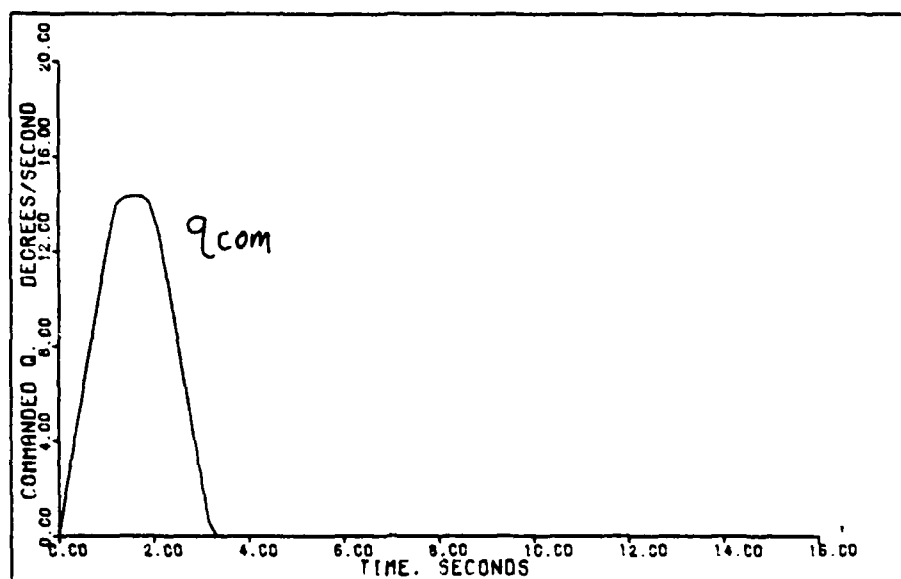
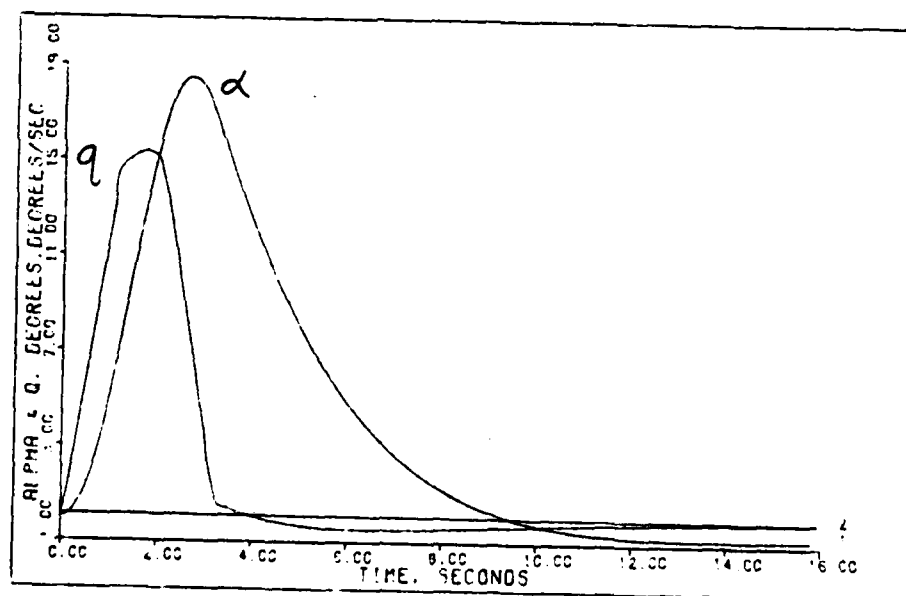


FIGURE B - 1

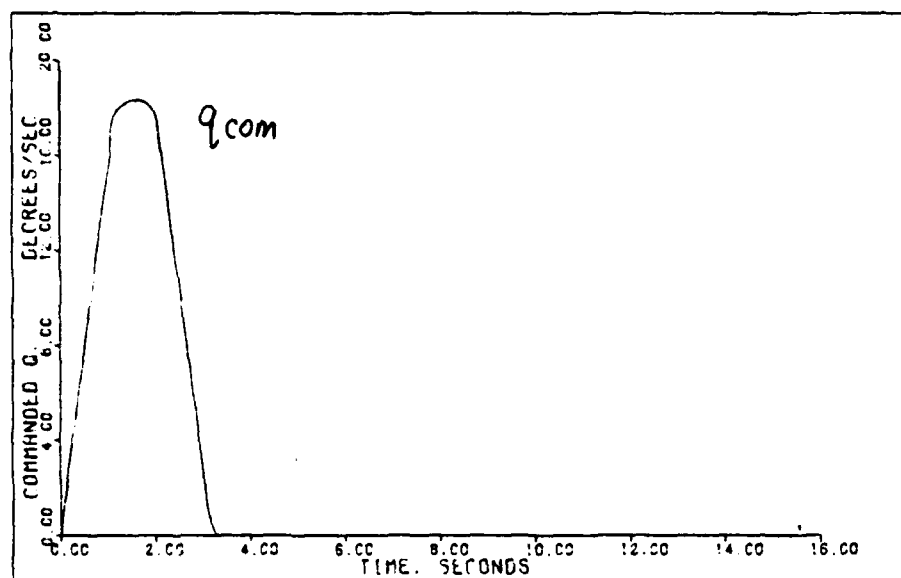


COMMANDED Q INPUT TO DIRECT CLIMB: 0.9M, 50K FT

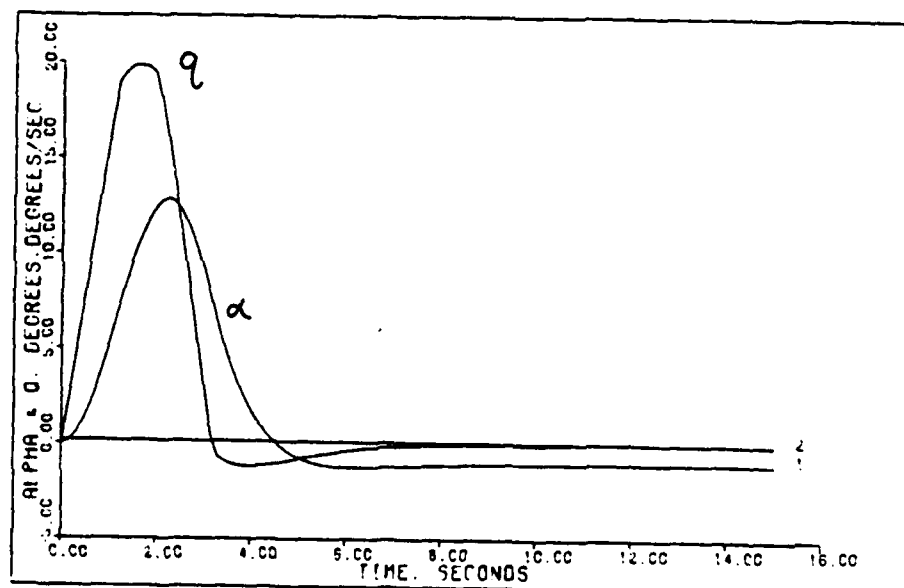


ALPHA & Q OUTPUTS TO DIRECT CLIMB: 0.9M, 50K FT

FIGURE B - 2

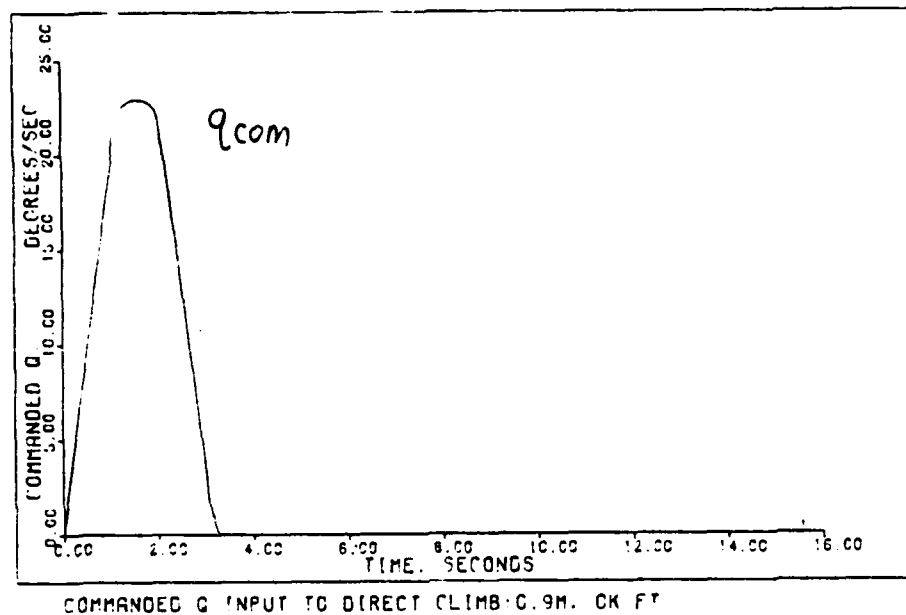


COMMANDED Q INPUT TO DIRECT CLIMB: 0.7M, 15K FT

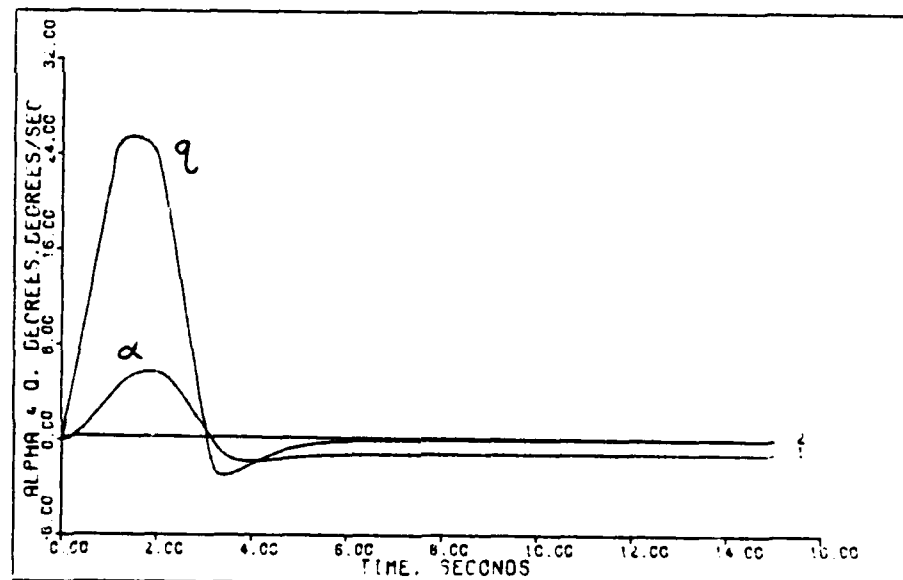


ALPHA & Q OUTPUTS TO DIRECT CLIMB: 0.7M, 15K FT

FIGURE B - 3



COMMANDED Q INPUT TO DIRECT CLIMB: 0.9M. CK FT



ALPHA & Q OUTPUTS TO DIRECT CLIMB: 0.9M. CK FT

FIGURE B - 4

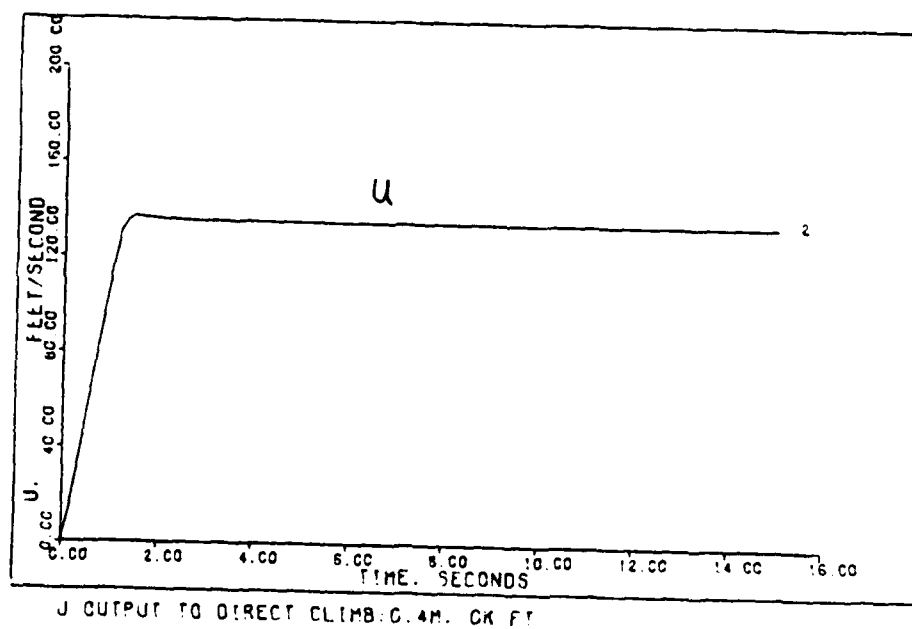
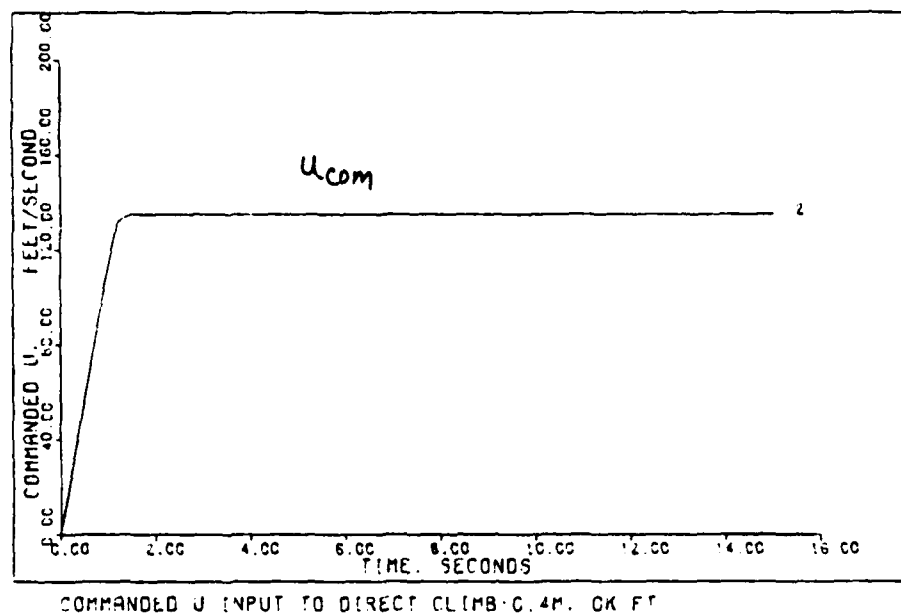


FIGURE B - 5

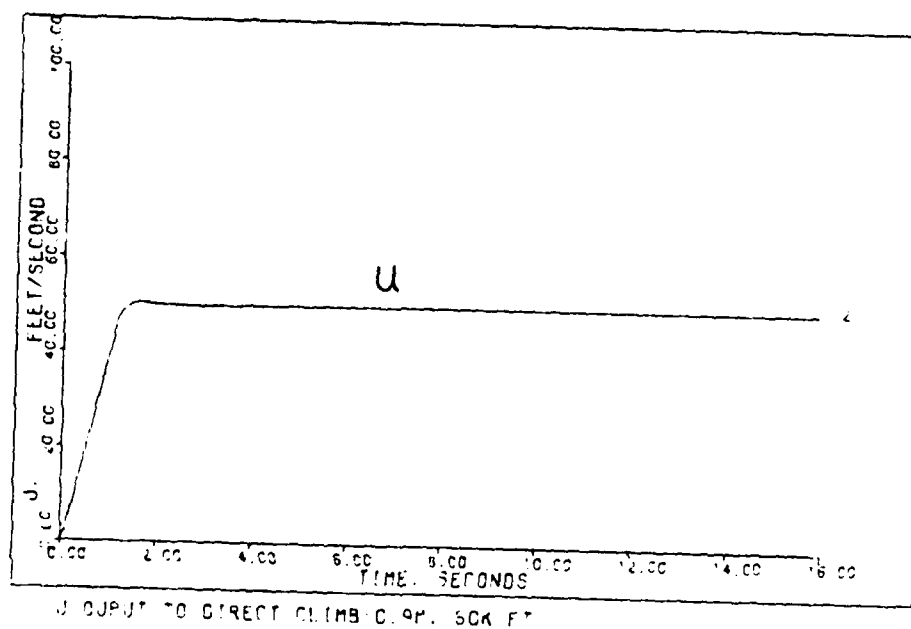
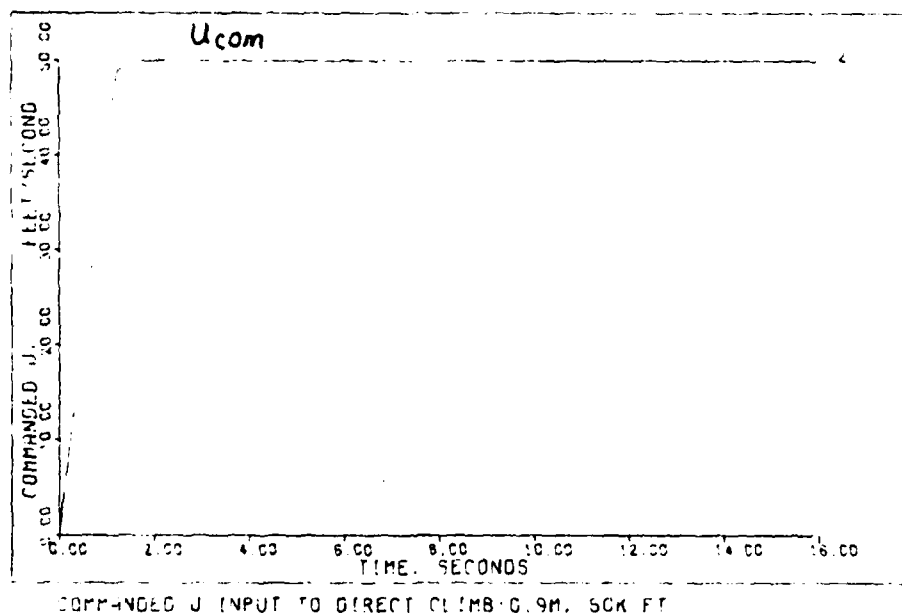


FIGURE B - 6

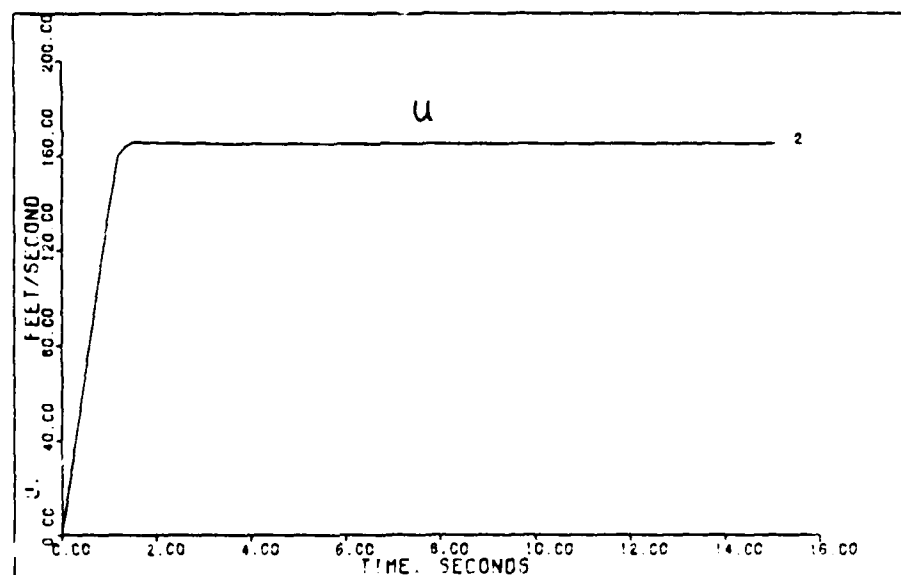
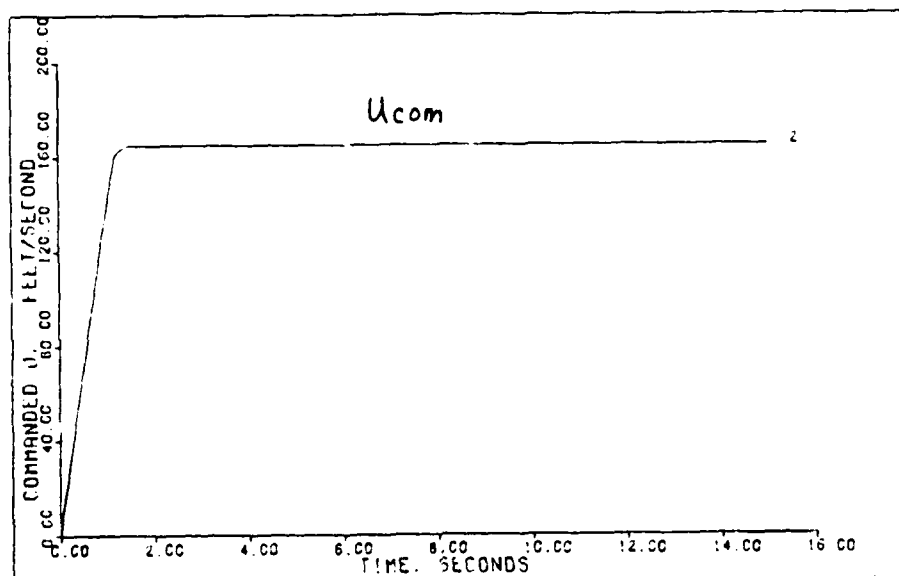
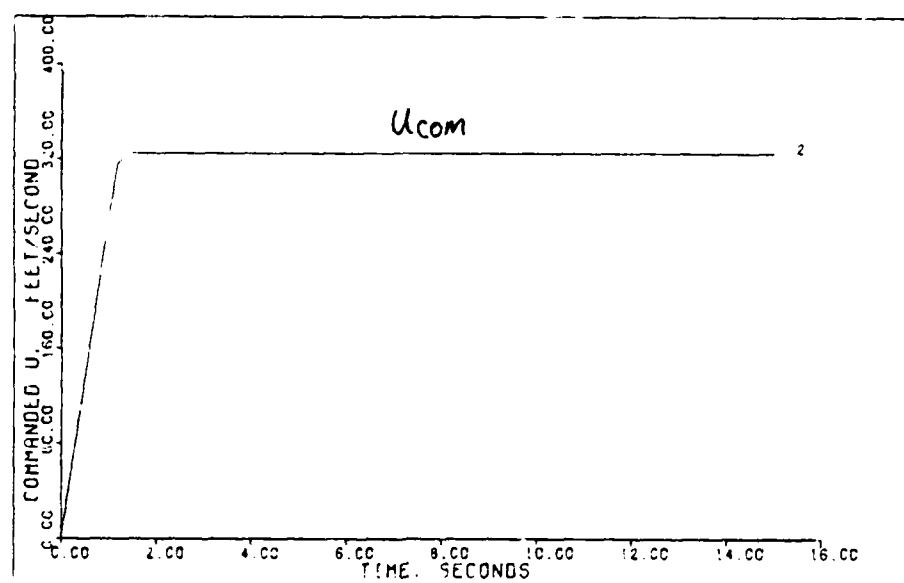
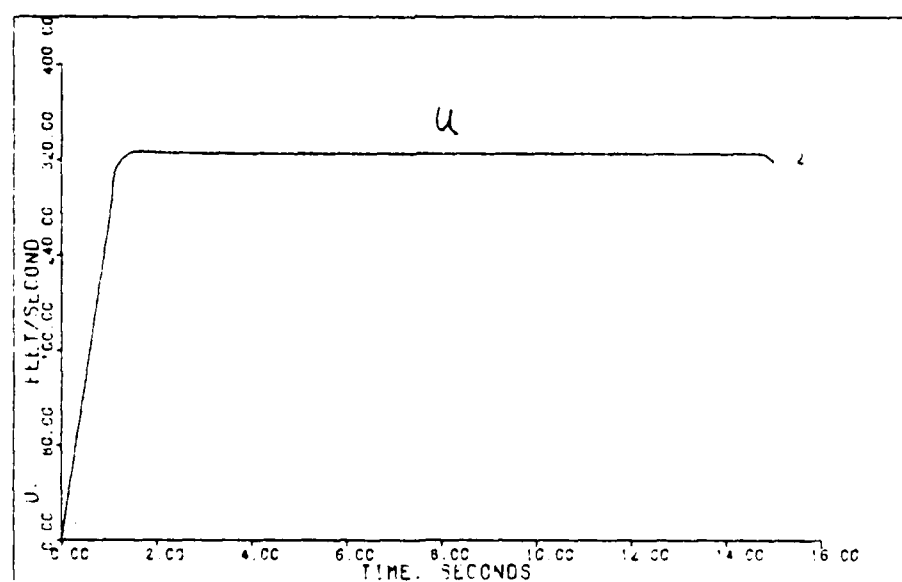


FIGURE B - 7

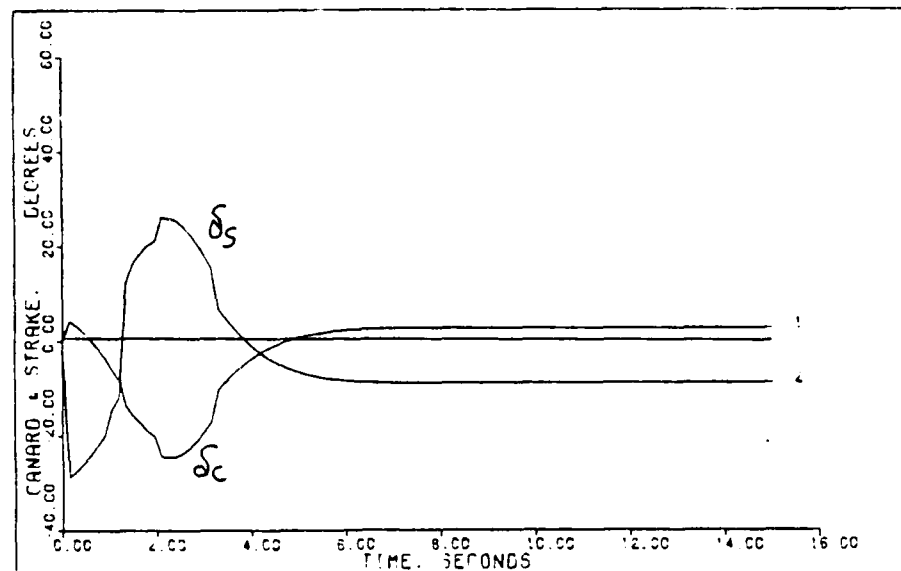


COMMANDED U INPUT TO DIRECT CLIMB: 0.9M. OK FT

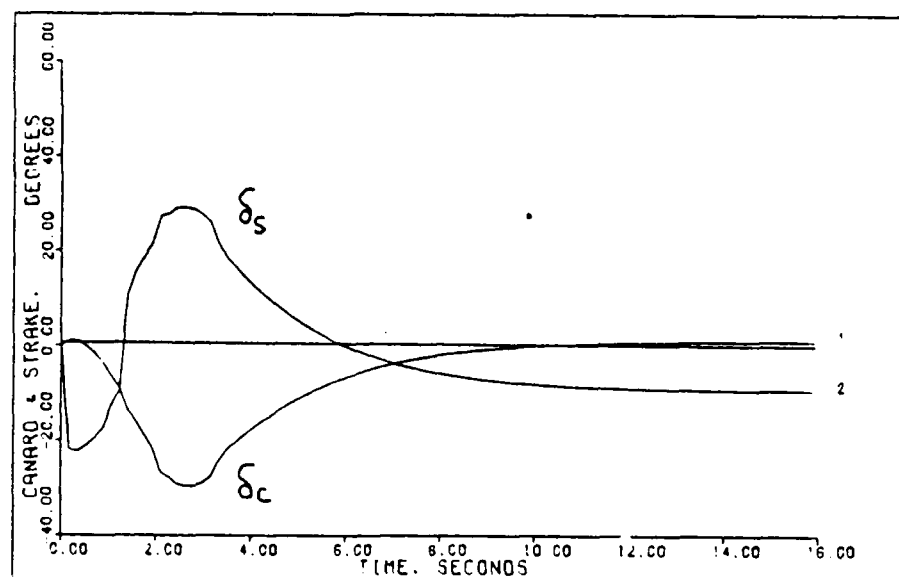


U OUTPUT TO DIRECT CLIMB: 0.9M. OK FT

FIGURE B - 8



CANARD & STRAKE INPUTS TO DIRECT CLIMB C. 1M. 0K FT



CANARD & STRAKE INPUTS TO DIRECT CLIMB C. 9M. 50K FT

FIGURE B - 9

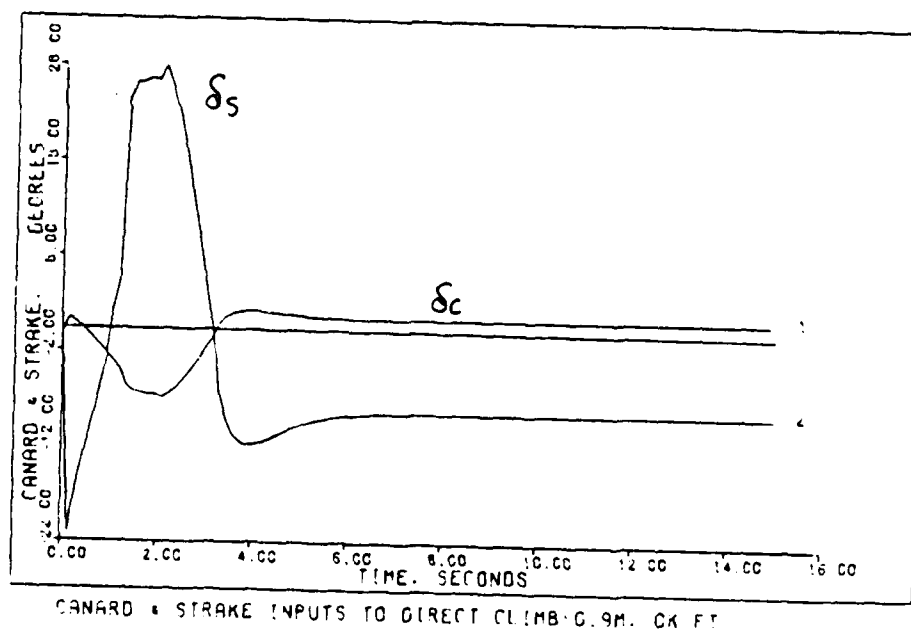
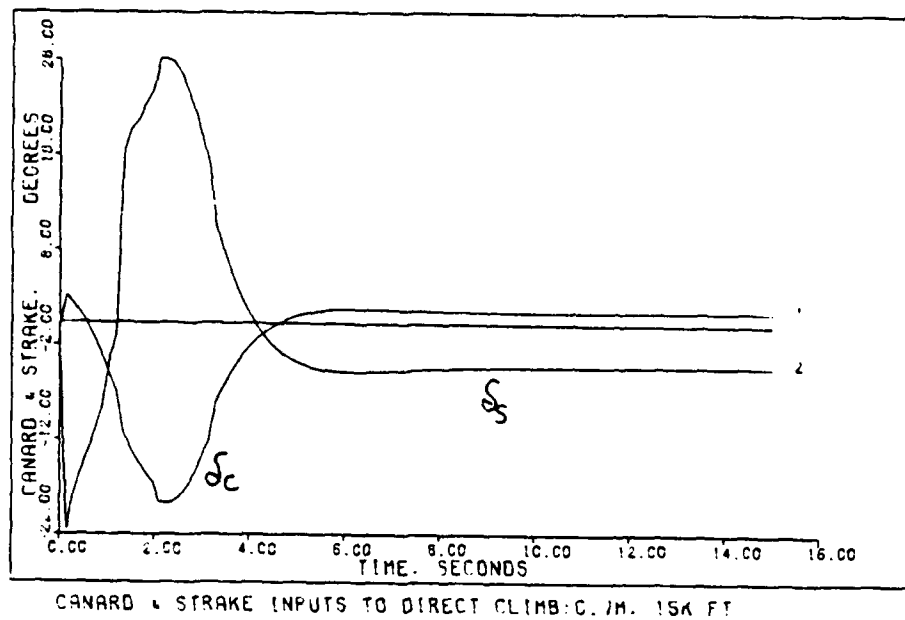


FIGURE B - 10

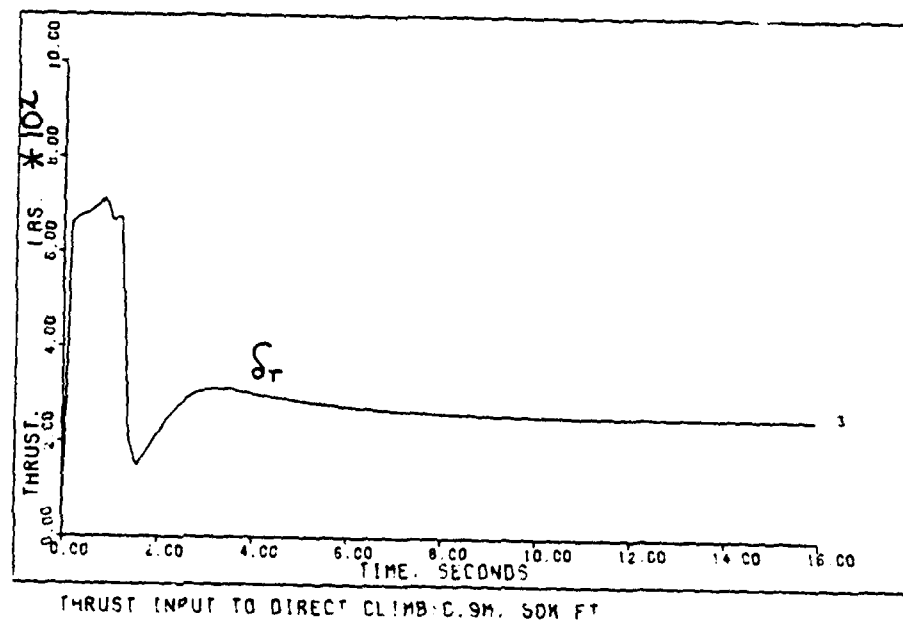
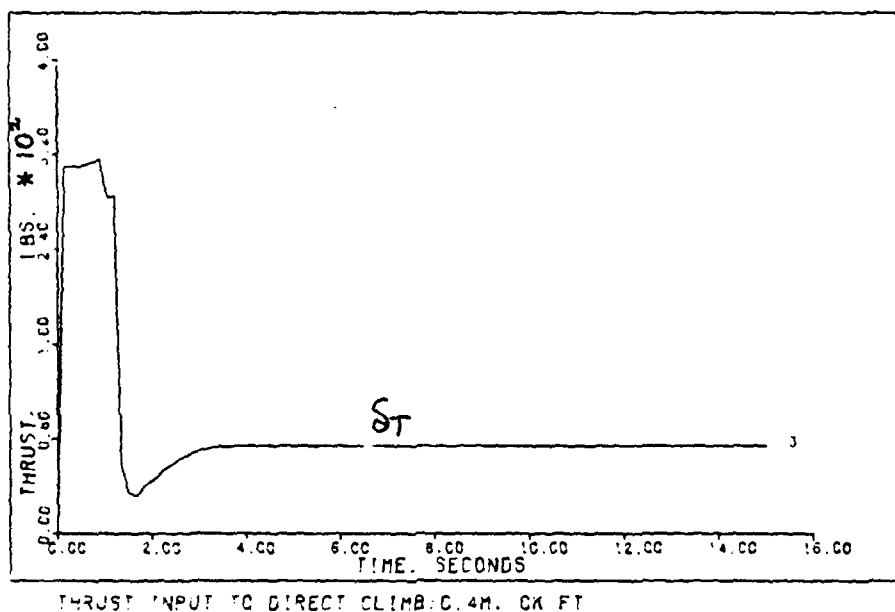


FIGURE B - 11

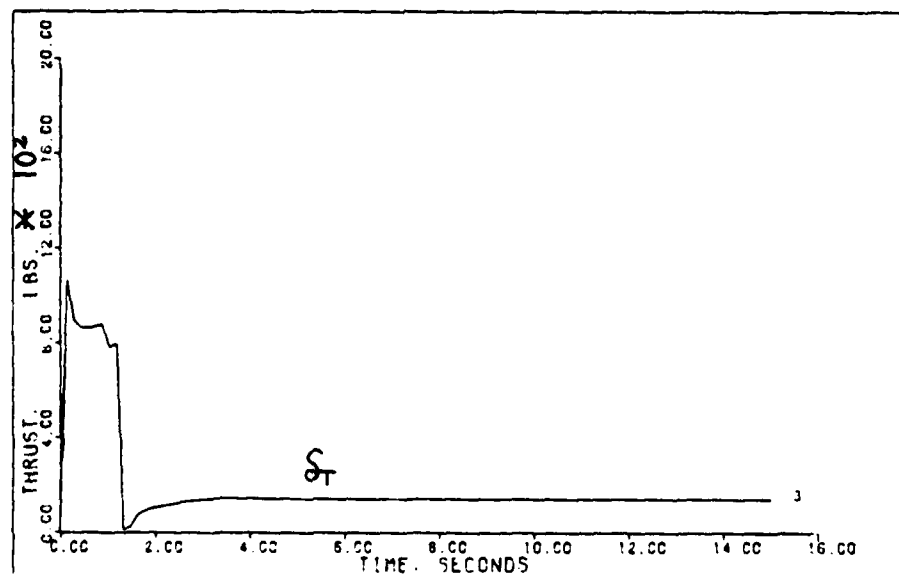
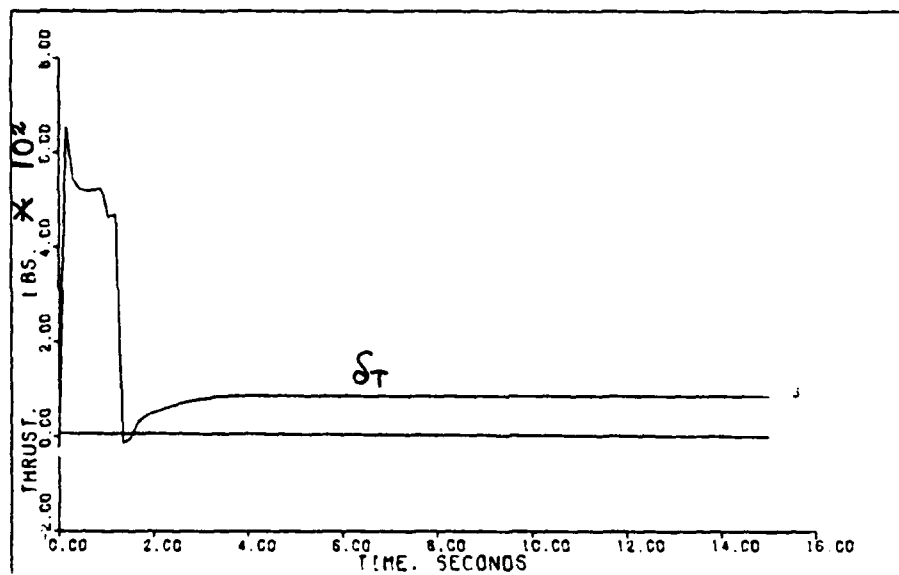
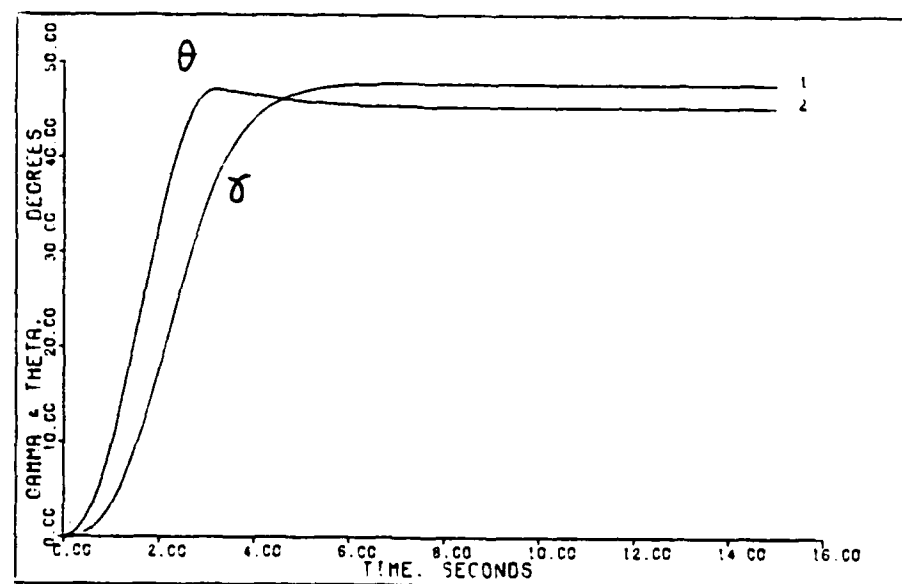
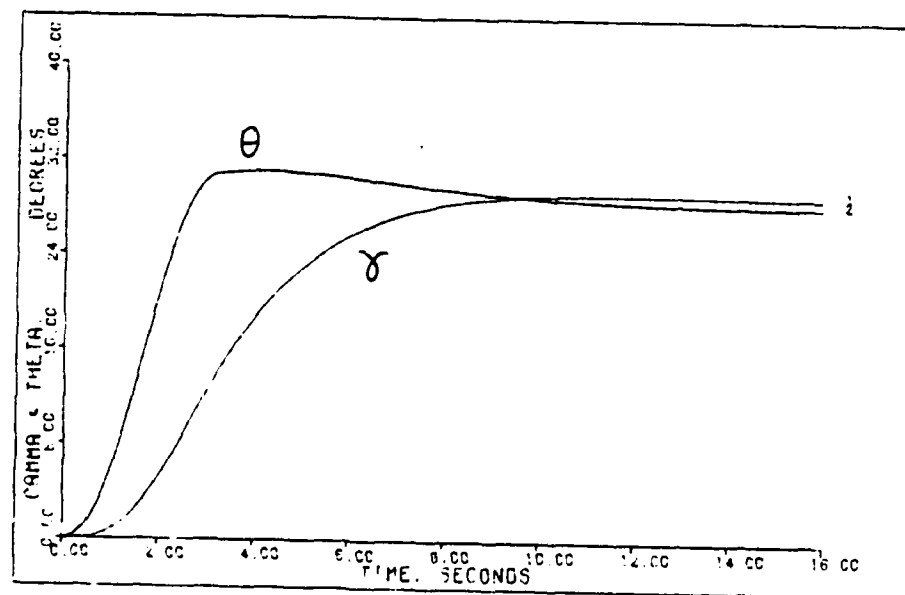


FIGURE B - 12

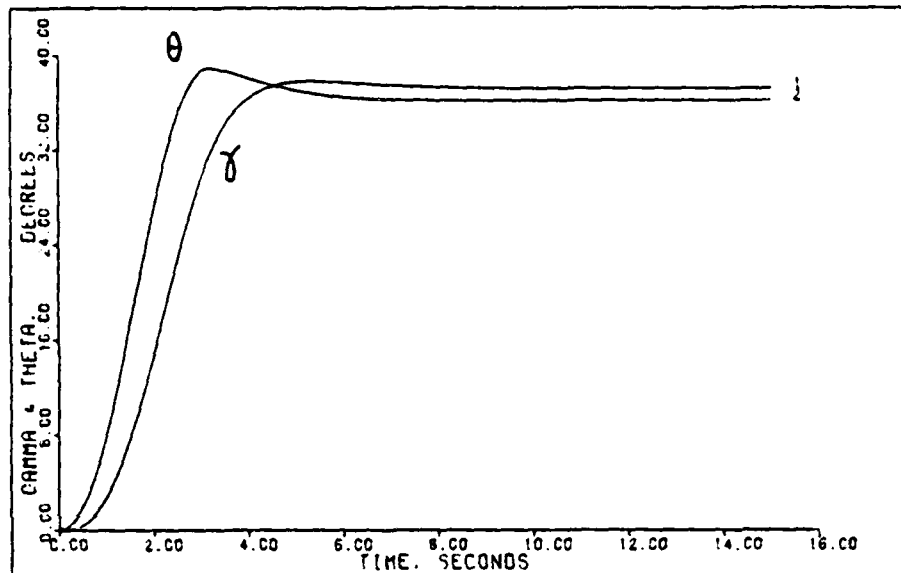


GAMMA & THETA FROM DIRECT CLIMB: 0.4M, 50K FT

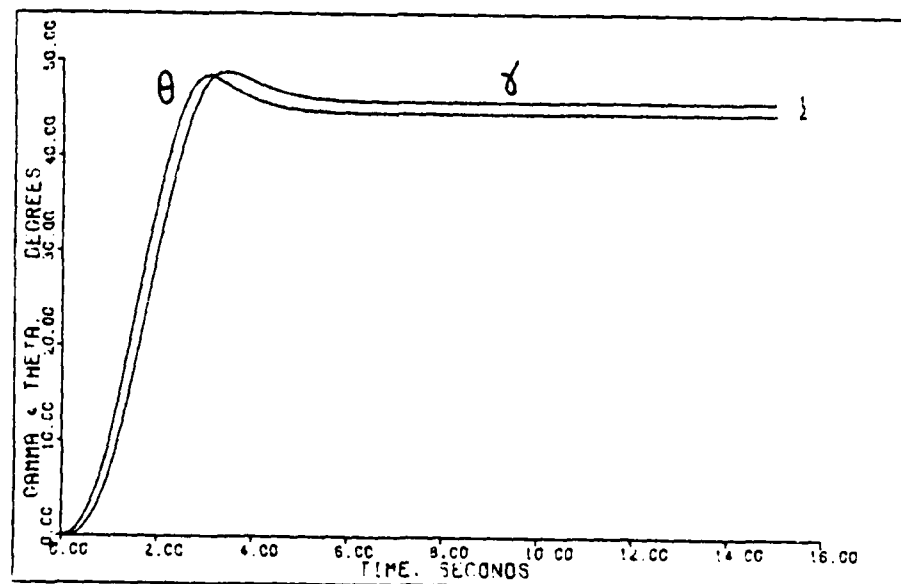


GAMMA & THETA FROM DIRECT CLIMB: 0.9M, 50K FT

FIGURE B - 13

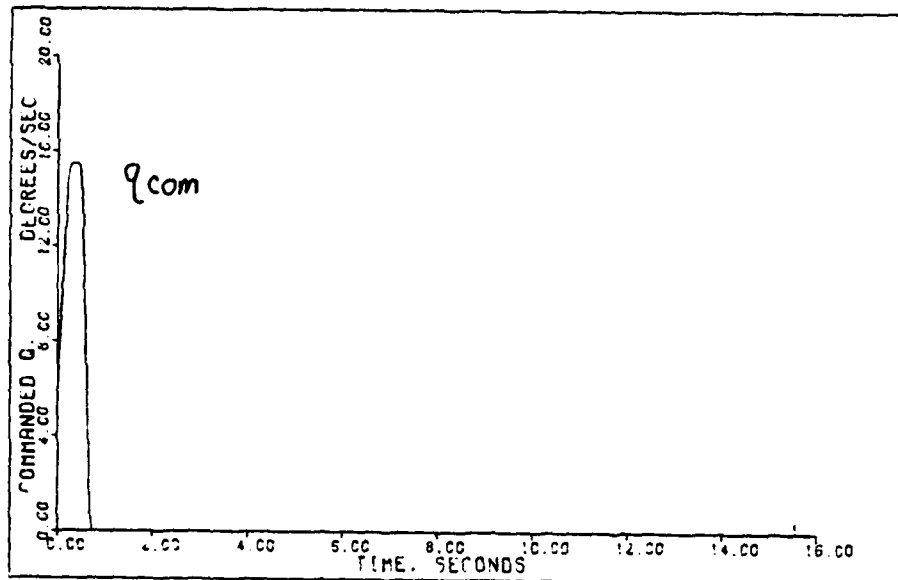


GAMMA & THETA FROM DIRECT CLIMB: 15K FT

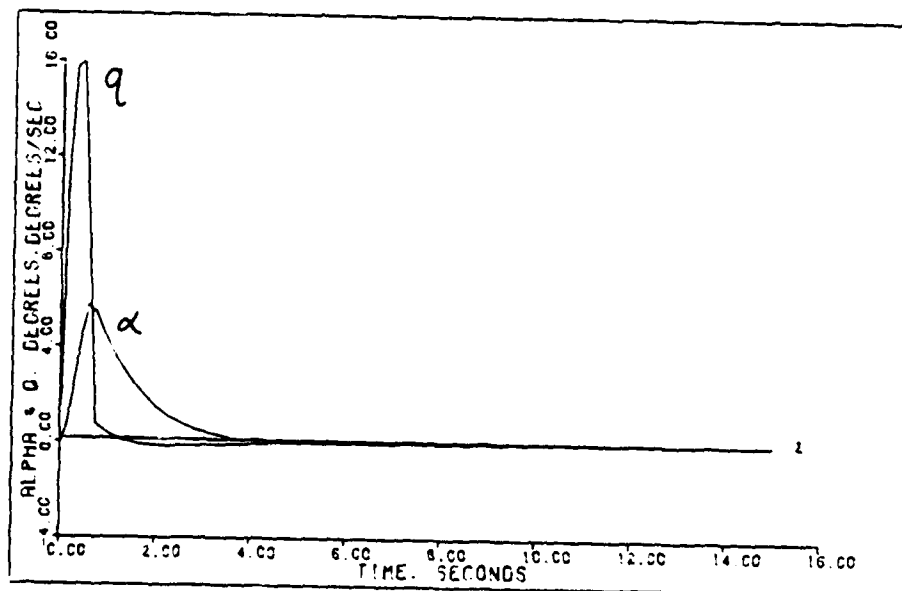


GAMMA & THETA FROM DIRECT CLIMB: 9M, 0K FT

FIGURE B - 14

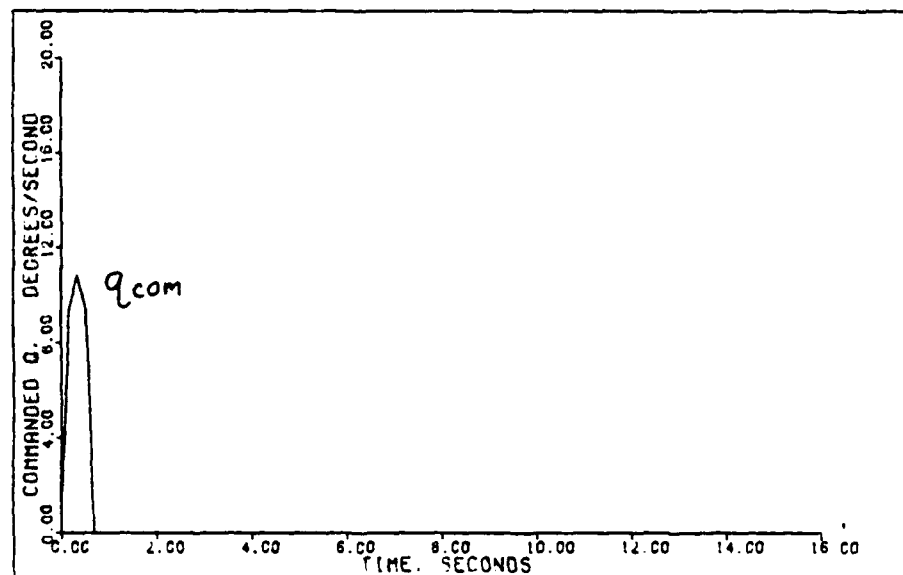


COMMANDED Q INPUT TO DIRECT LIFT: 0.4M. CK FT

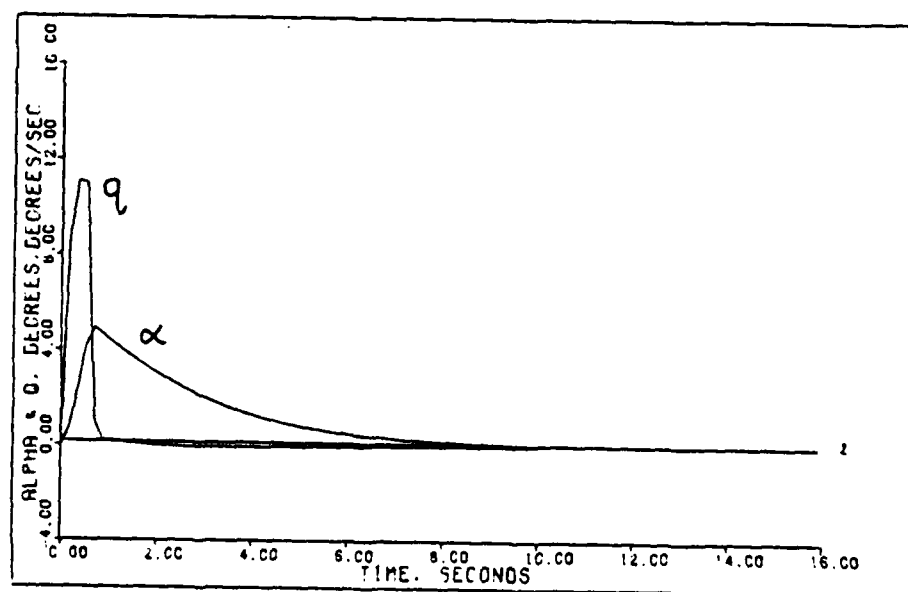


ALPHA & Q OUTPUTS TO DIRECT LIFT: 0.4M. CK FT

FIGURE B - 15

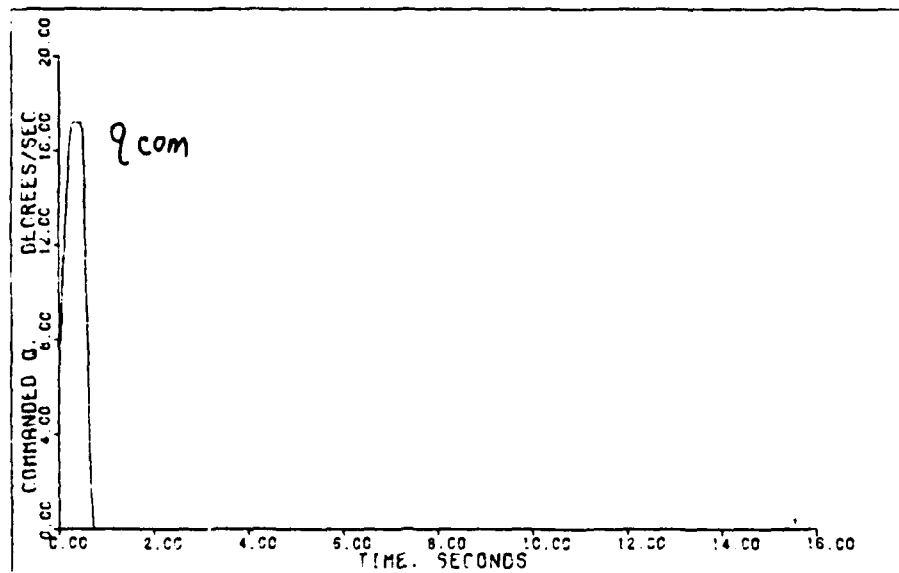


COMMANDED Q INPUT TO DIRECT LIFT: 0.9M. 50K FT

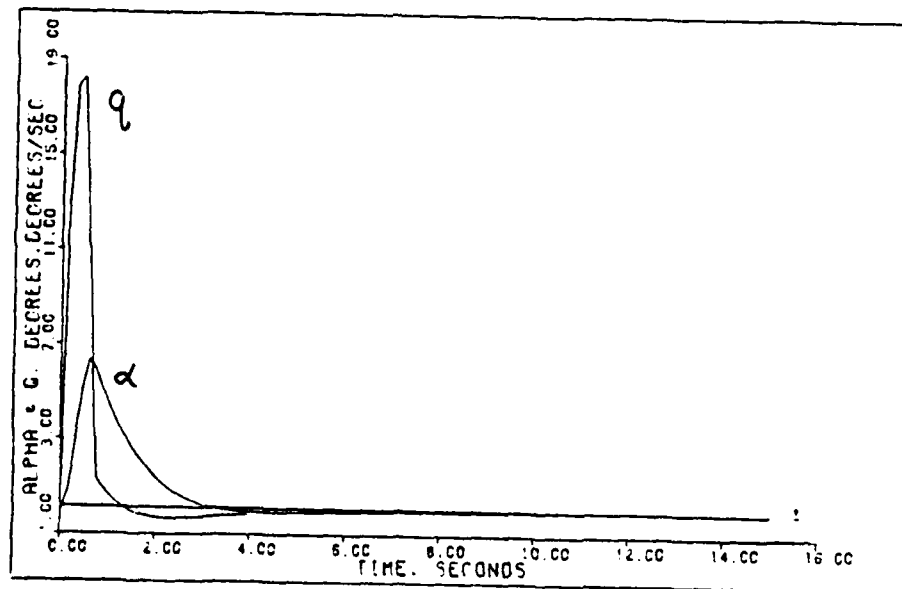


ALPHA & Q OUTPUTS TO DIRECT LIFT: 0.9M. 50K FT

FIGURE B - 16



COMMANDED Q INPUT TO DIRECT LIFT: 0.7M, 15K FT



ALPHA & Q OUTPUTS TO DIRECT LIFT: 0.7M, 15K FT

FIGURE B - 17

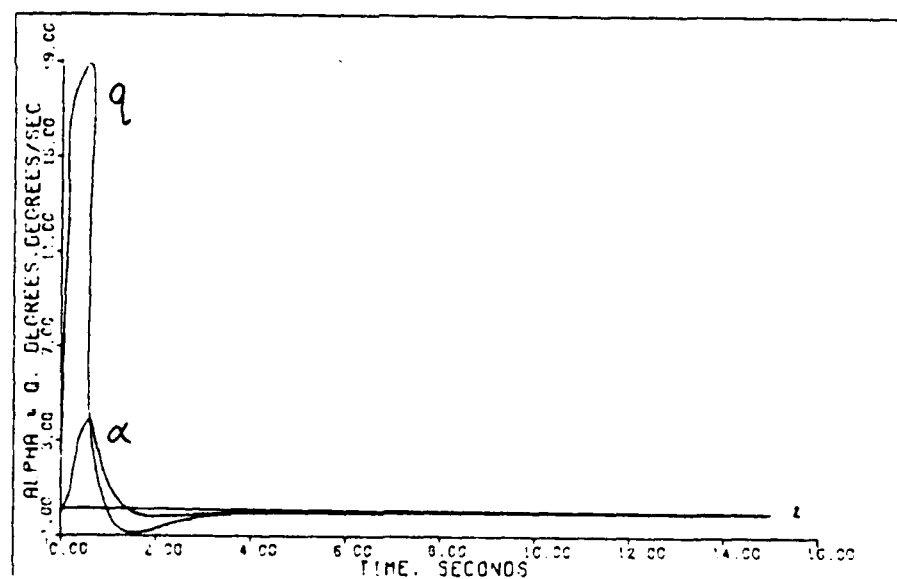
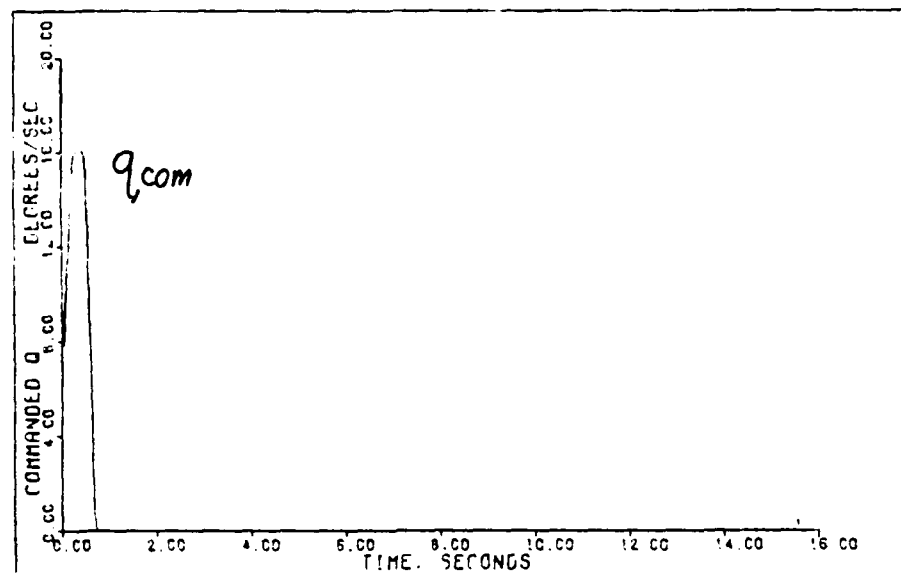
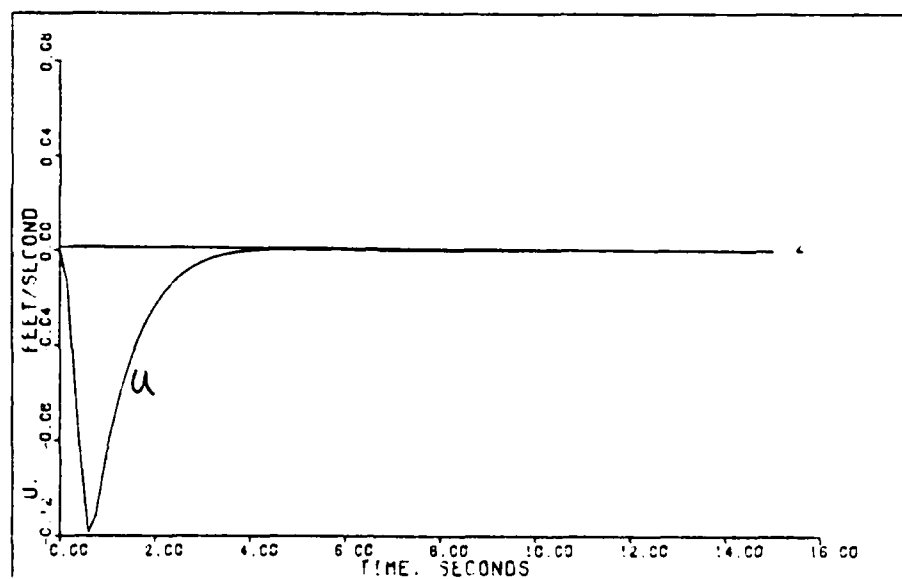
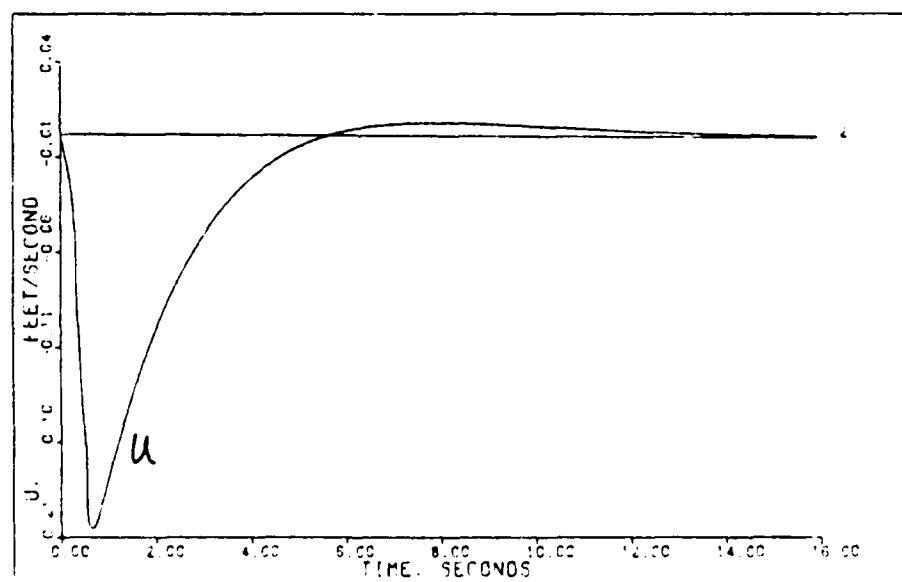


FIGURE B - 18

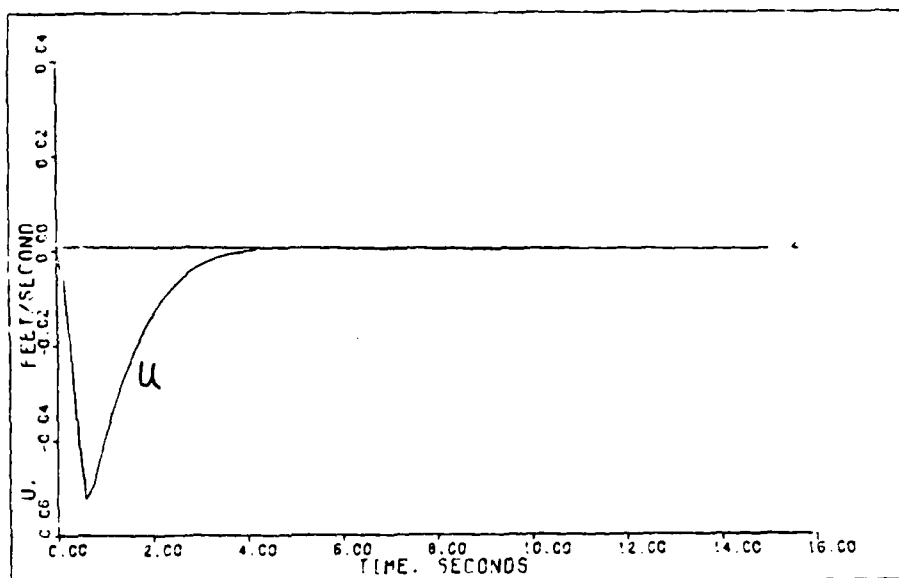


U OUTPUT TO DIRECT LIFT: 0.4M GK FT

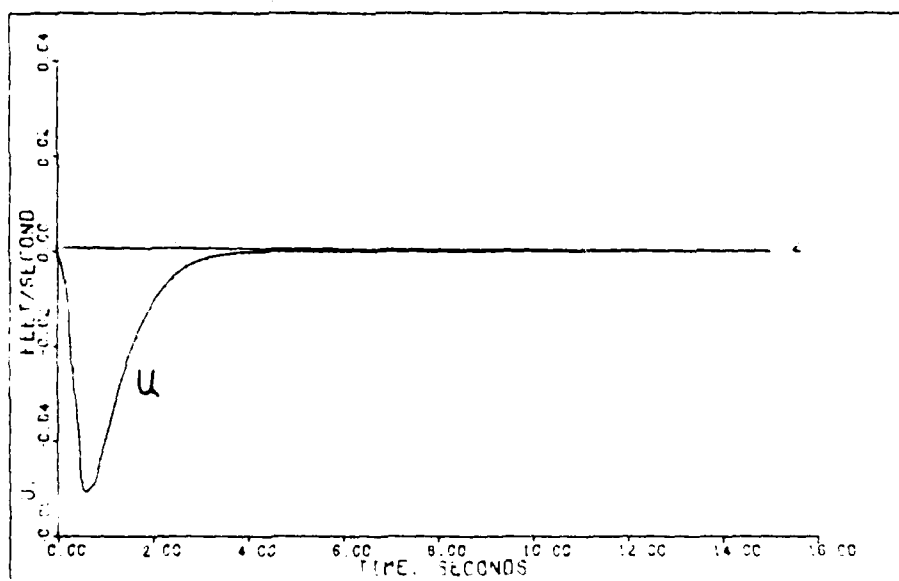


U OUTPUT TO DIRECT LIFT: 0.9M SKK FT

FIGURE B - 19

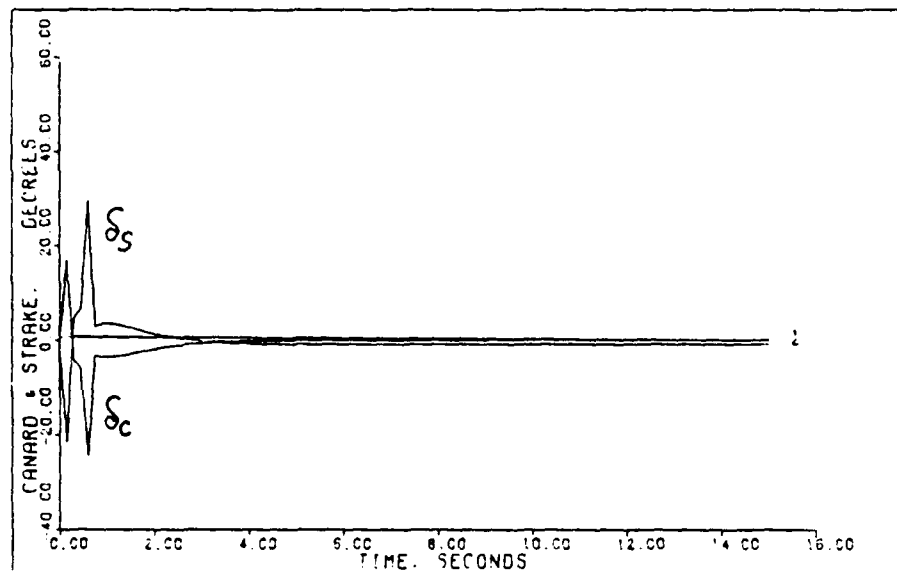


J OUTPUT TO DIRECT LIFT 15K FT

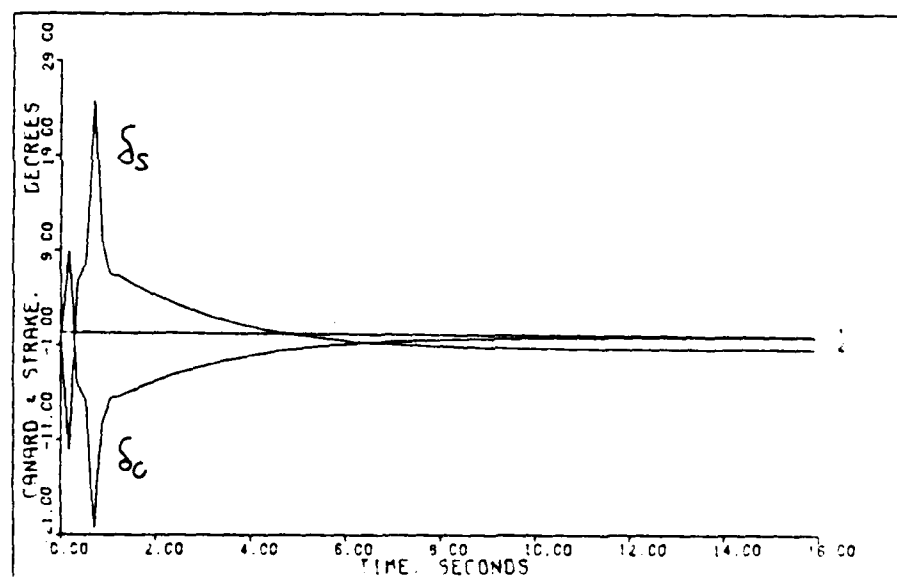


J OUTPUT TO DIRECT LIFT 15K FT

FIGURE B - 20

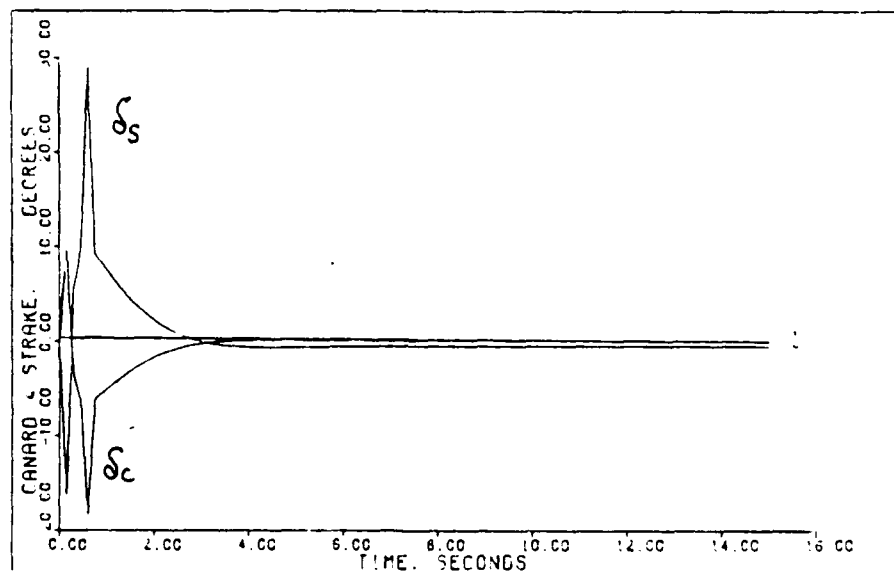


CANARD & STRAKE INPUTS TO DIRECT LIFT: 0.4M, 0K FT

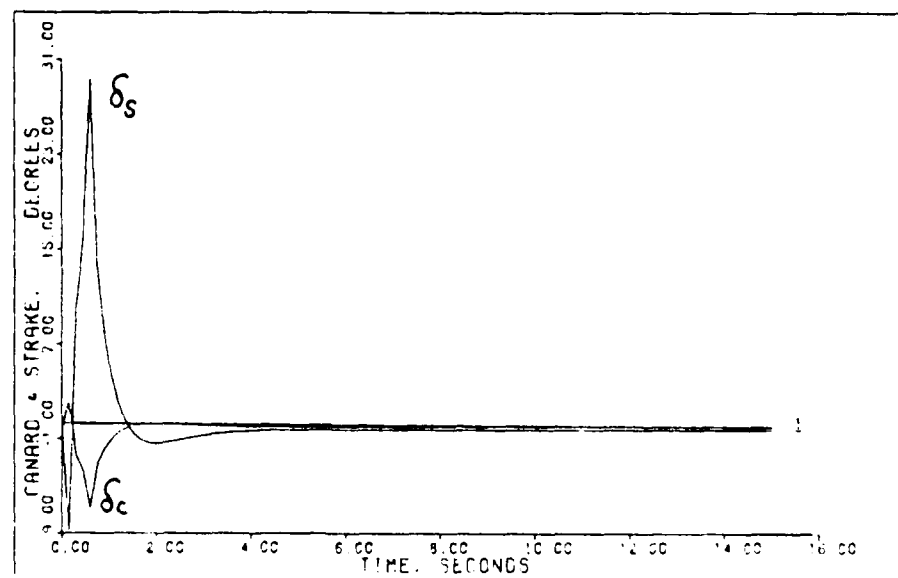


CANARD & STRAKE INPUTS TO DIRECT LIFT: 0.9M, 50K FT

FIGURE B - 21



CANARD & STRAKE INPUTS TO DIRECT LIFTING 15K FT



CANARD & STRAKE INPUTS TO DIRECT LIFTING 9M. 0K FT

FIGURE B - 22

AD-A140 983

MULTIVARIABLE DIGITAL FLIGHT CONTROL DESIGN OF THE
X-29A(U) AIR FORCE INST OF TECH WRIGHT-PATTERSON AFB OH
SCHOOL OF ENGINEERING R S FELDMANN MAR 84

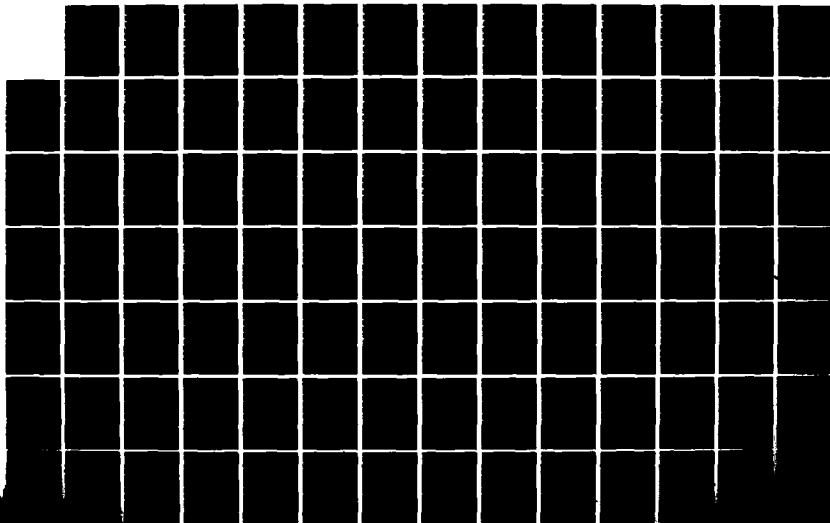
374

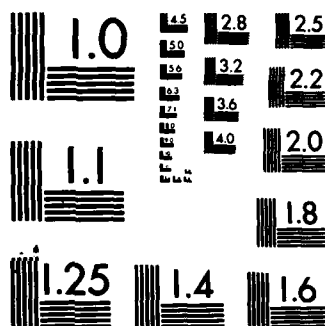
UNCLASSIFIED

AFIT/GE/EE/84M-3

F/G 1/3

NL





MICROCOPY RESOLUTION TEST CHART
NATIONAL BUREAU OF STANDARDS-1963-A

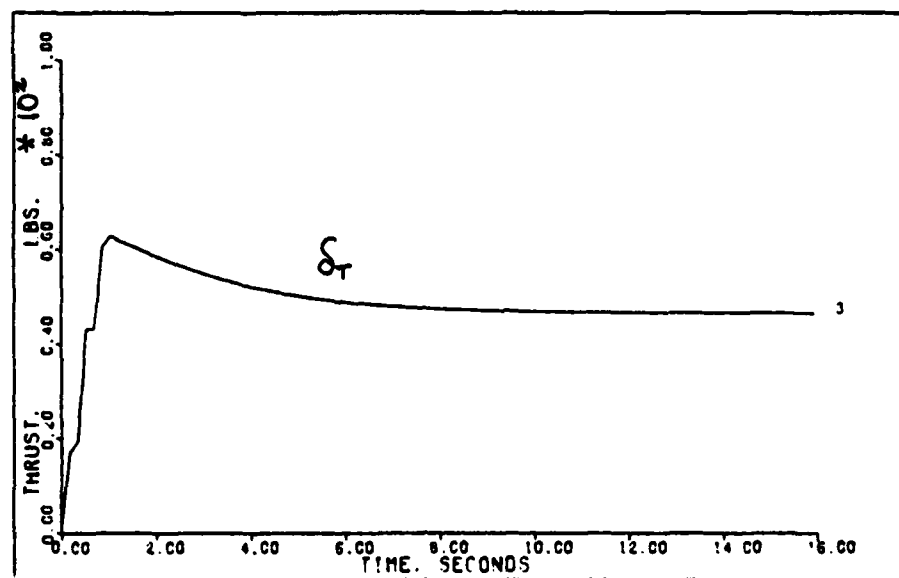
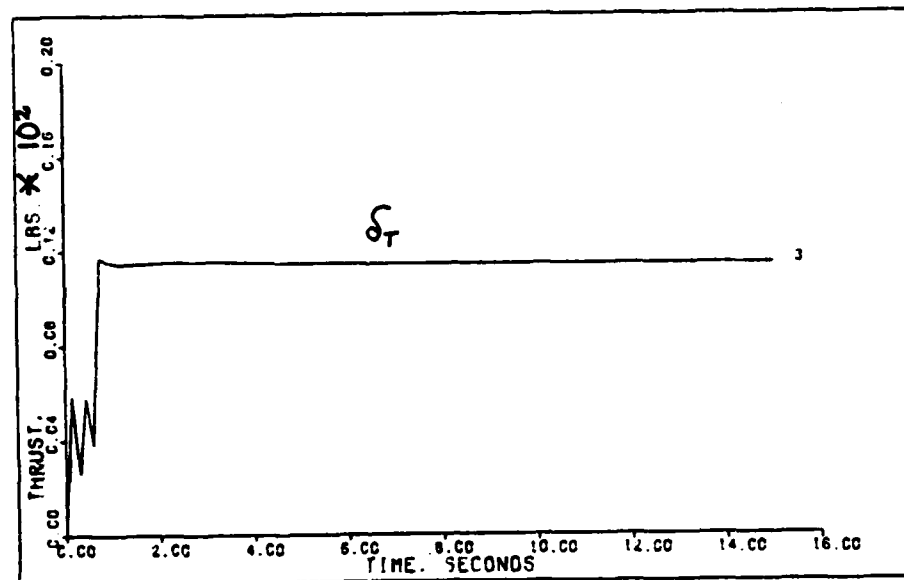


FIGURE B - 23

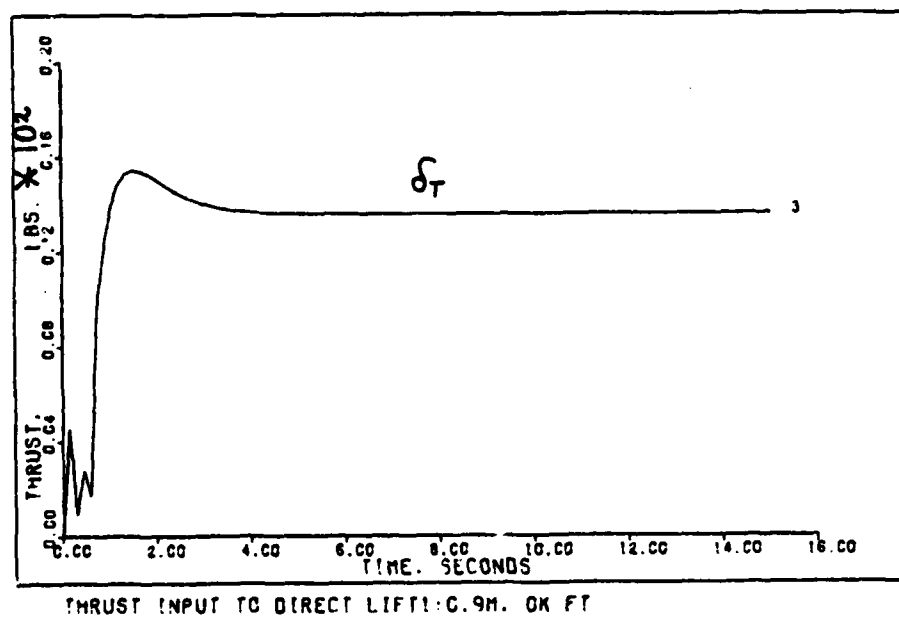
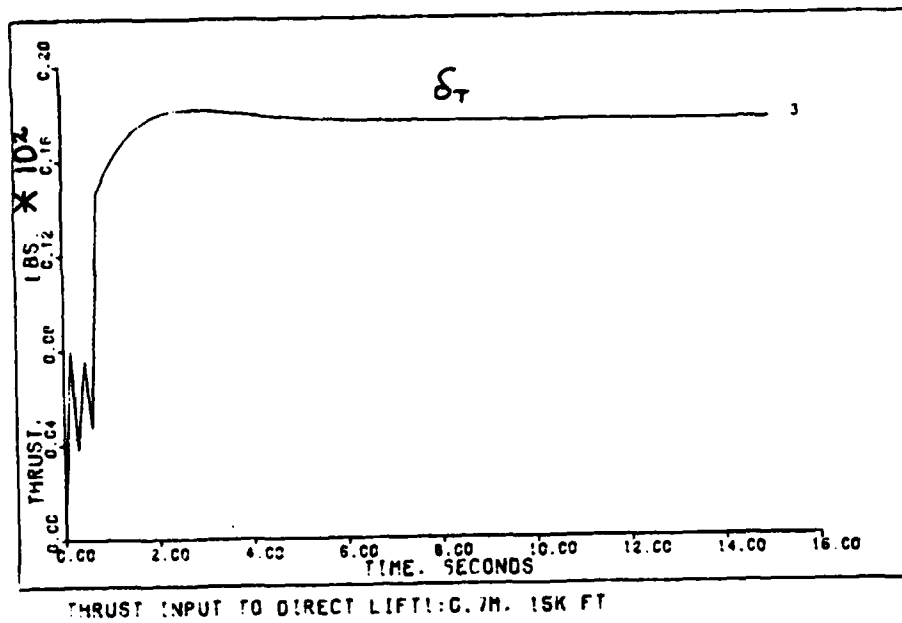
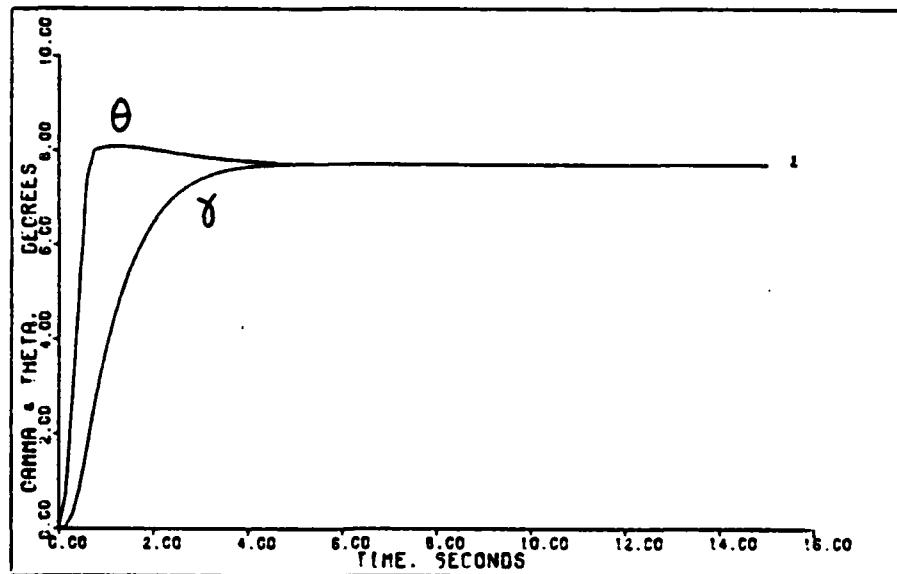
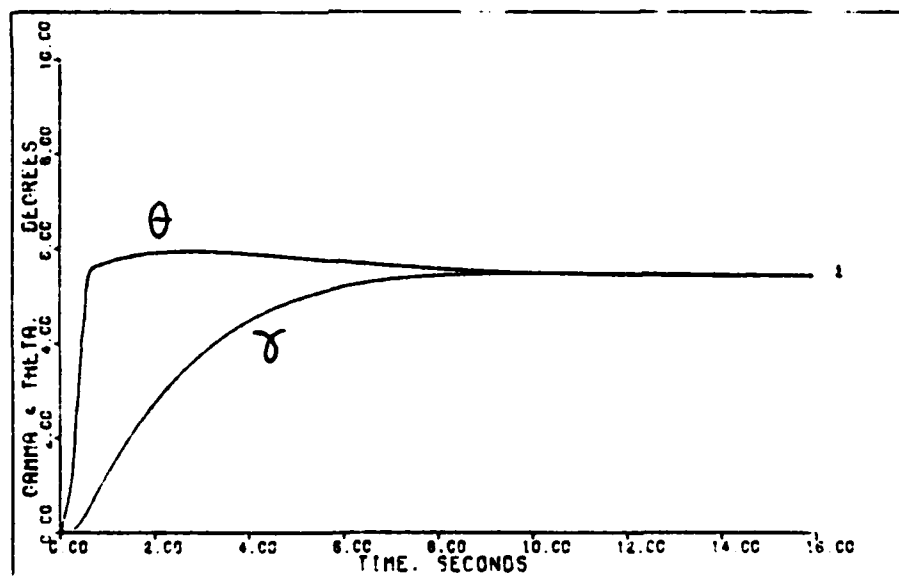


FIGURE B - 24

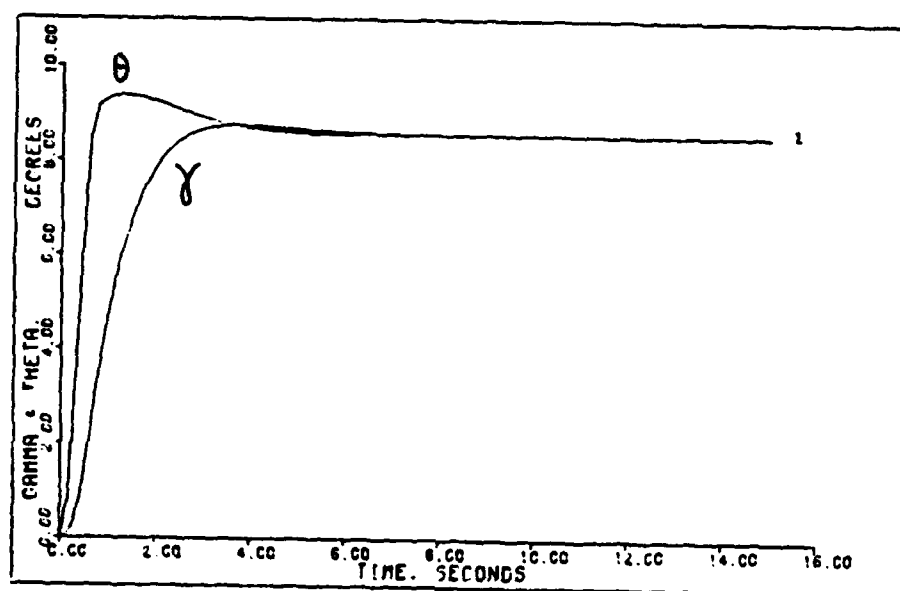


GAMMA & THETA FROM DIRECT LIFT: 0.4M. OK FT

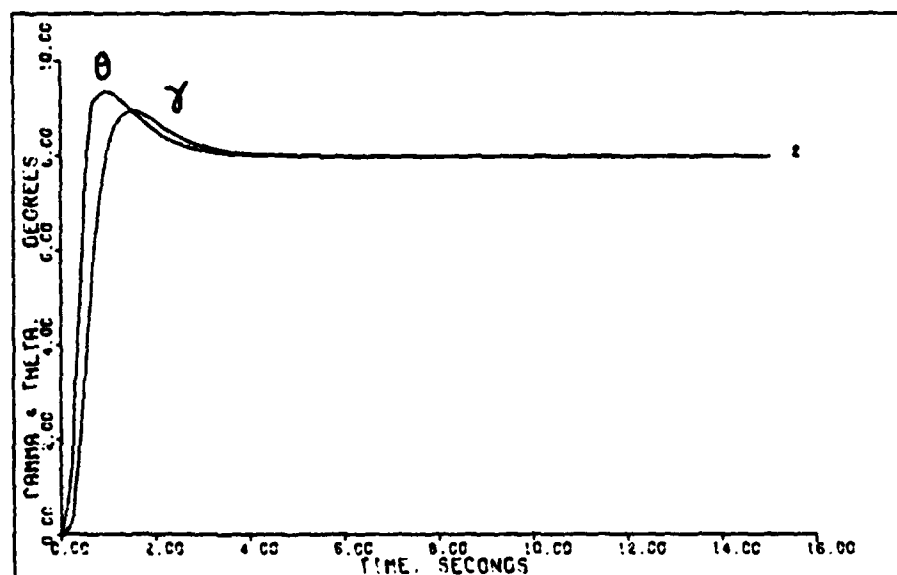


GAMMA & THETA FROM DIRECT LIFT: 0.9M. 50K FT

FIGURE B - 25

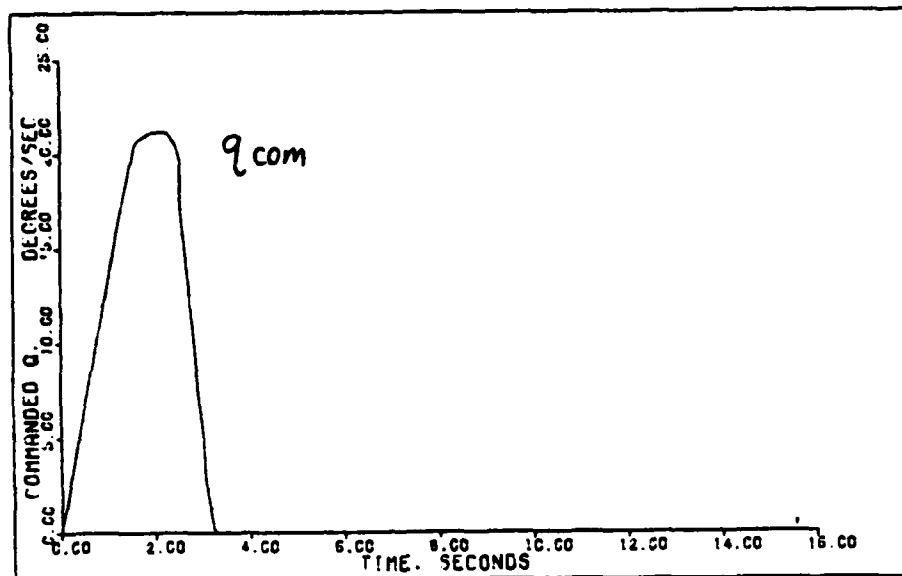


GAMMA & THETA FROM DIRECT LIFT: G. 7M. 154 FT

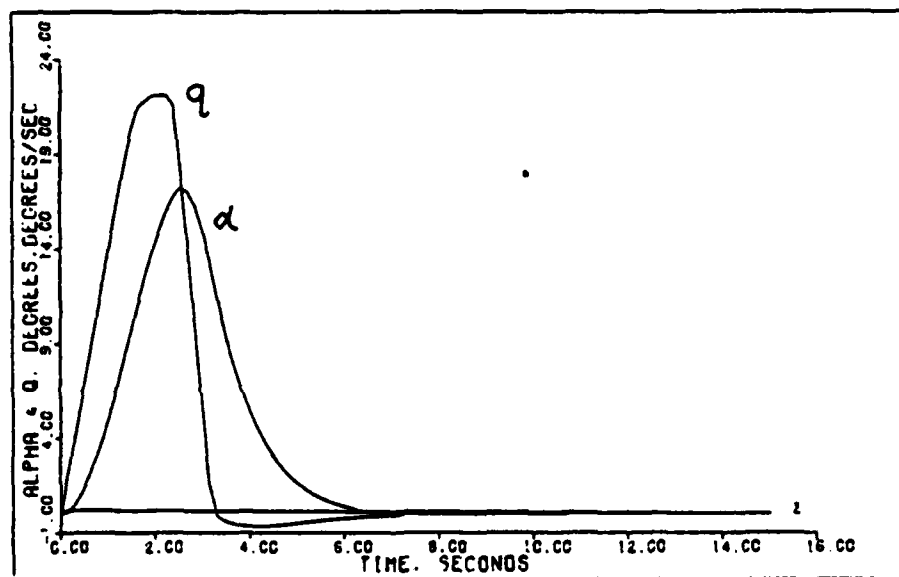


GAMMA & THETA FROM DIRECT LIFT: G. 9M. 0K FT

FIGURE B - 26

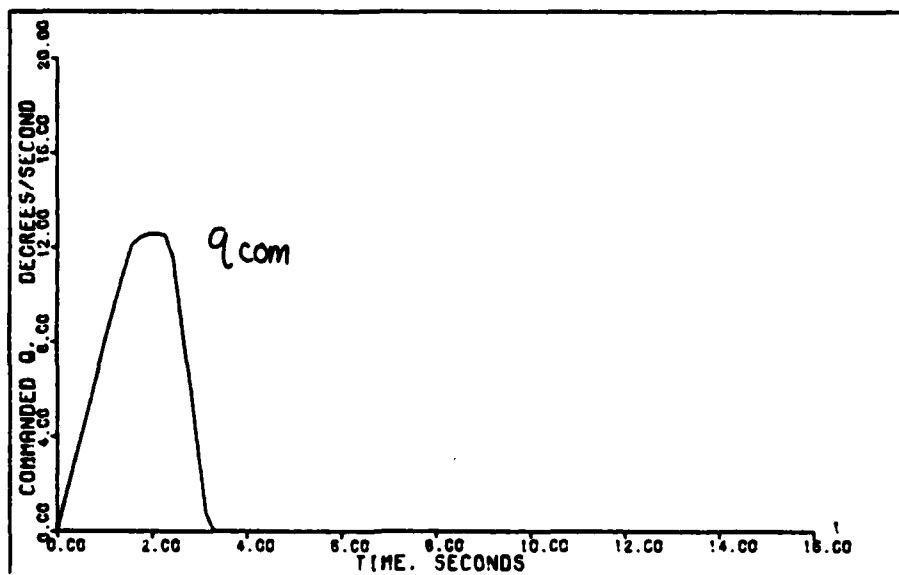


COMMANDED Q INPUT TO DIRECT LIFT2: G. 4H. CK FT

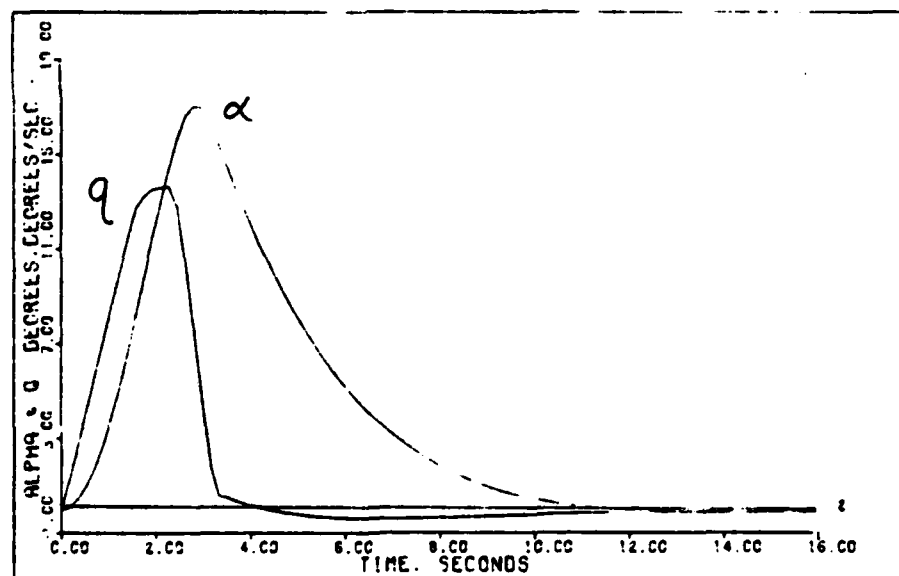


ALPHA & Q OUTPUTS TO DIRECT LIFT2: G. 4H. CK FT

FIGURE B - 27



COMMANDED Q INPUT TO DIRECT LIFT2:0.9M, 50K FT



ALPHA & Q OUTPUTS TO DIRECT LIFT2:0.9M, 50K FT

FIGURE B - 28

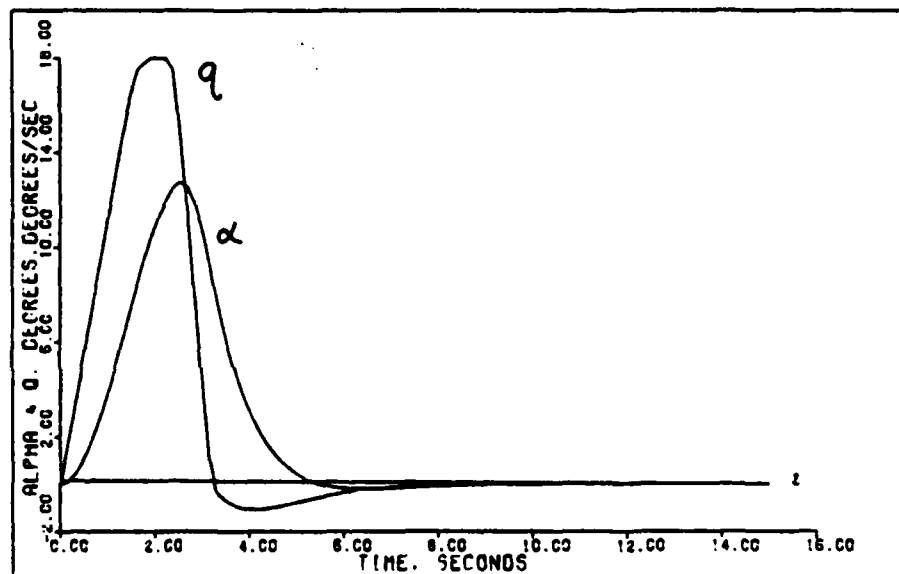
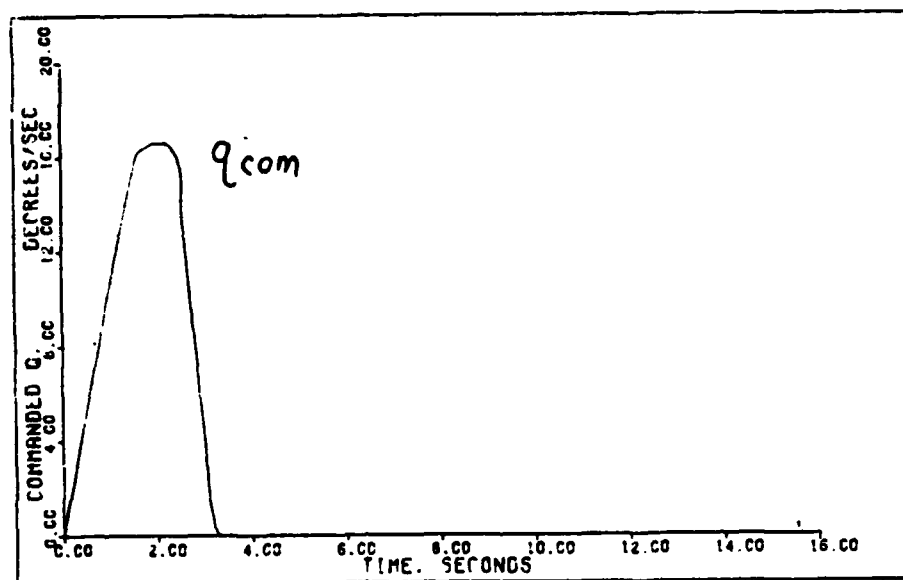
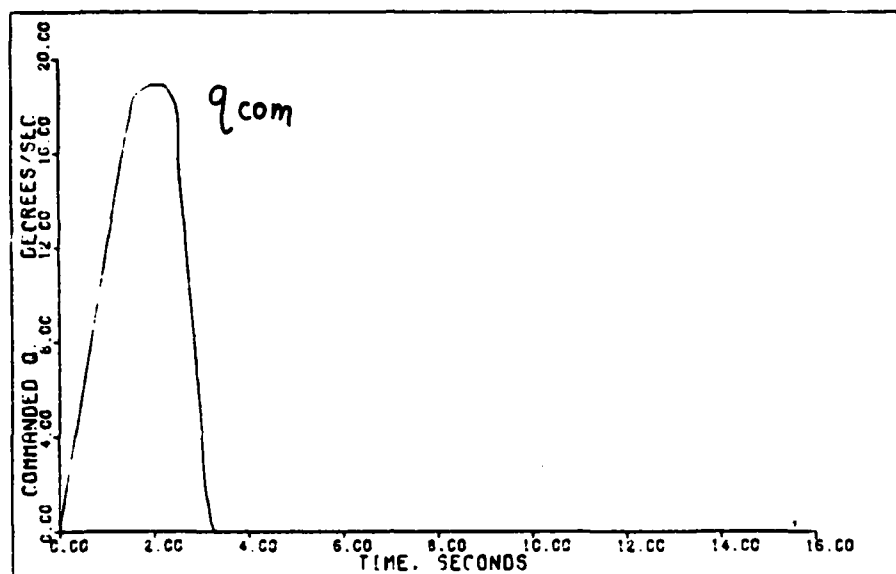
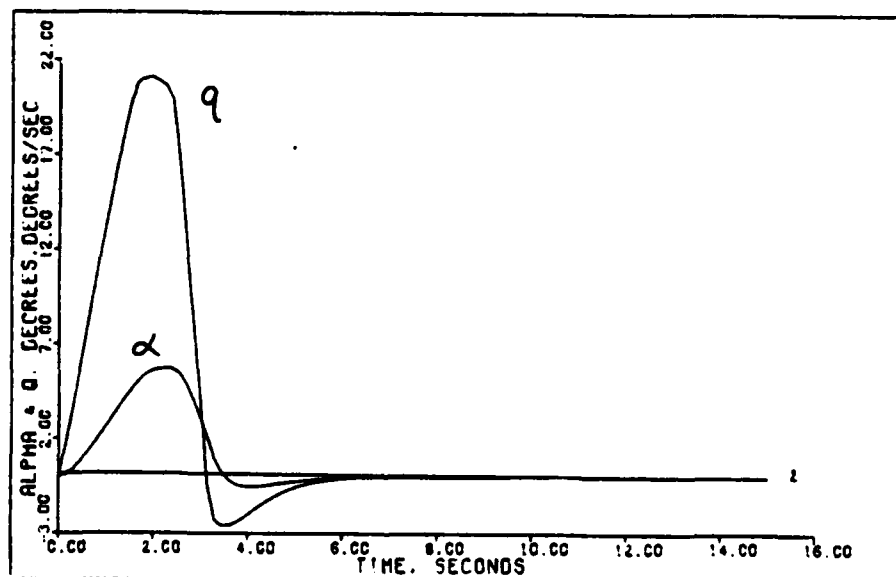


FIGURE B - 29

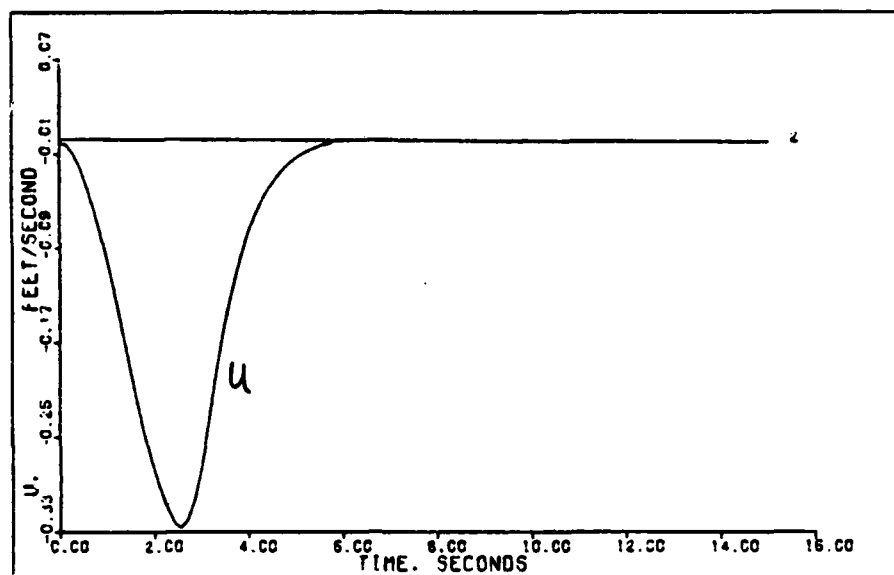


COMMANDED Q INPUT TO DIRECT LIFT 2:G.9M. OK FT

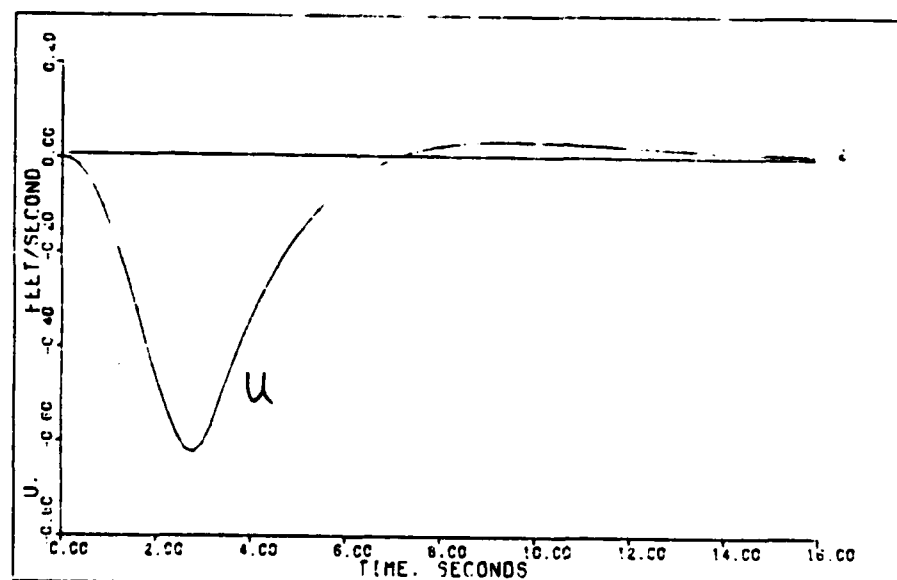


ALPHA & Q OUTPUTS TO DIRECT LIFT 2:G.9M. OK FT

FIGURE B - 30

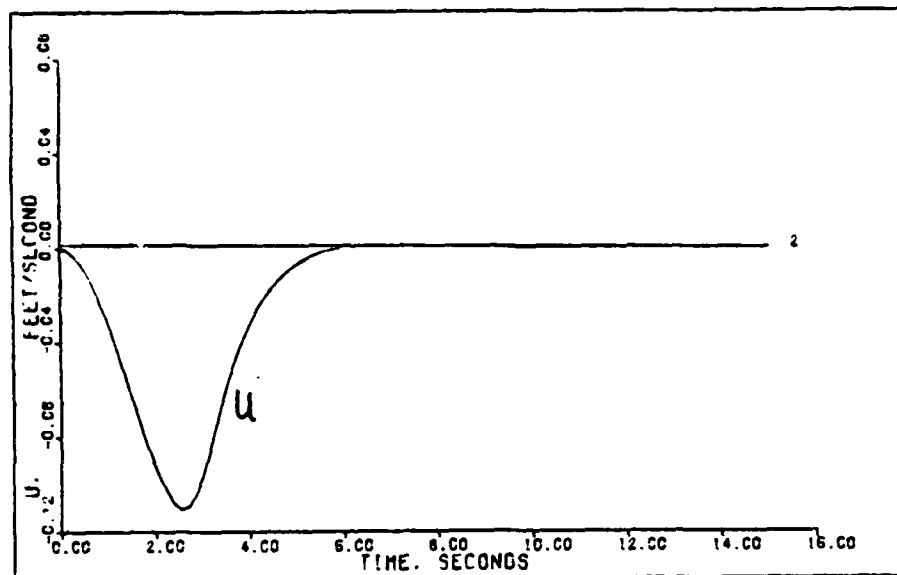


U OUTPUT TO DIRECT LIFT 2-0.4M. OK FT

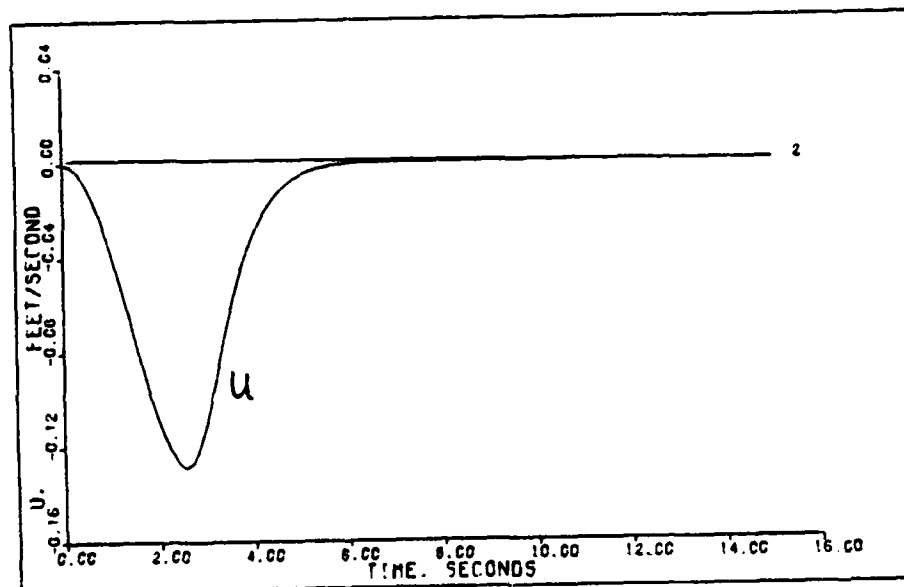


U OUTPUT TO DIRECT LIFT 2-0.9M. 5CK FT

FIGURE B - 31



U OUTPUT TO DIRECT LIFT 2:0.7M. 15K FT



U OUTPUT TO DIRECT LIFT 2:0.9M. 0K FT

FIGURE B - 32

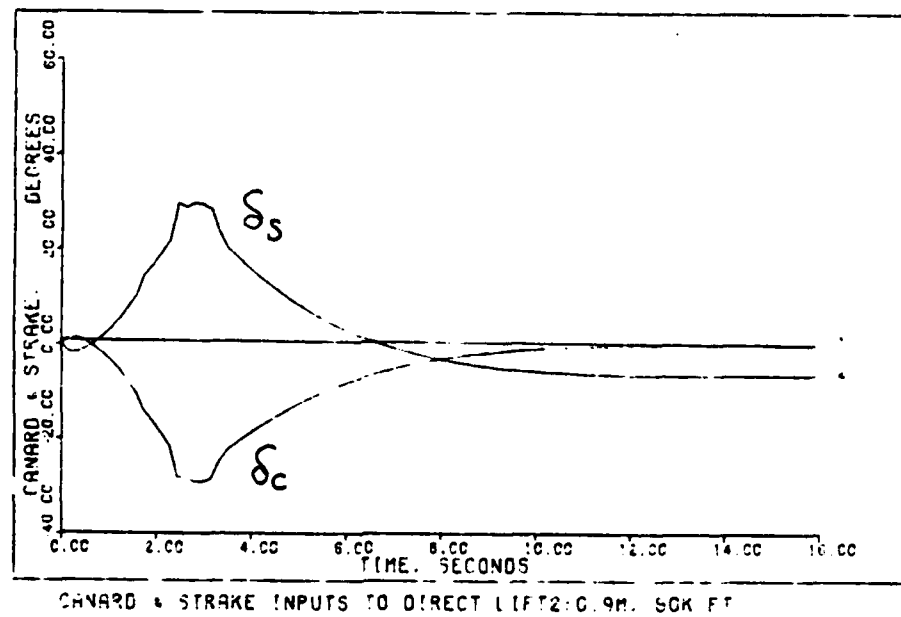
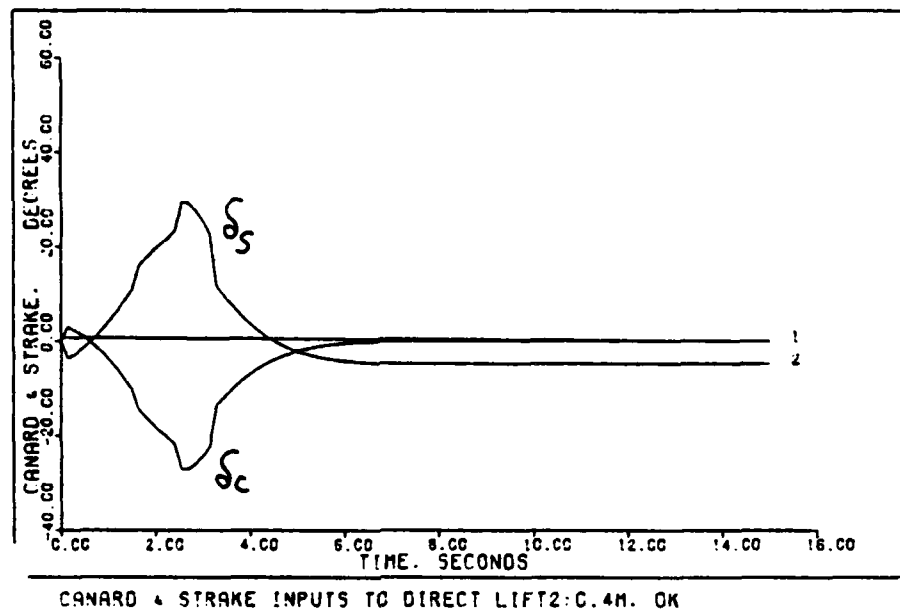


FIGURE B - 33

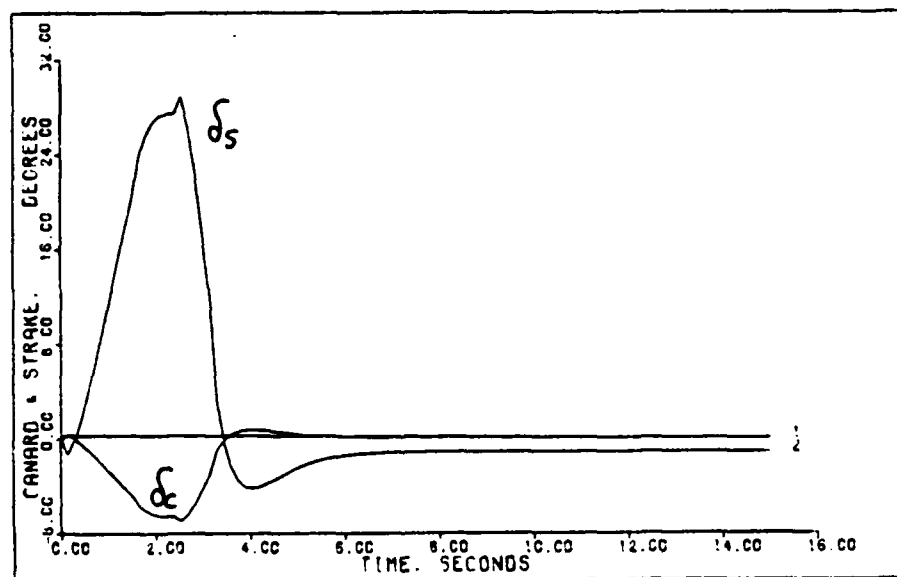
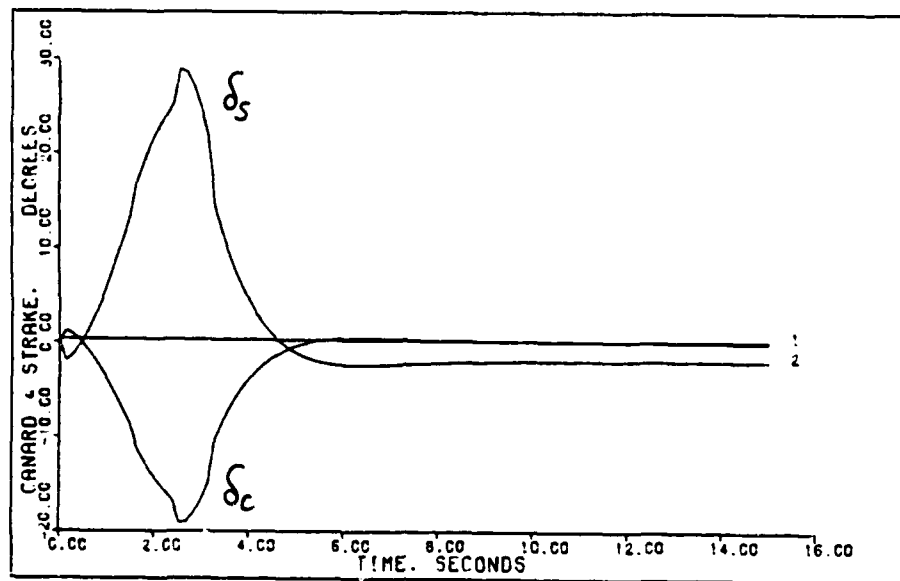
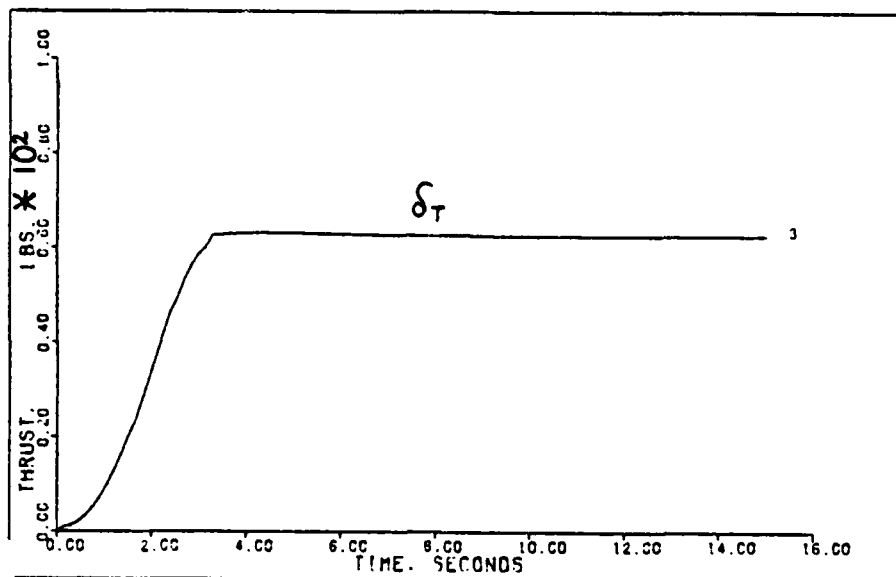
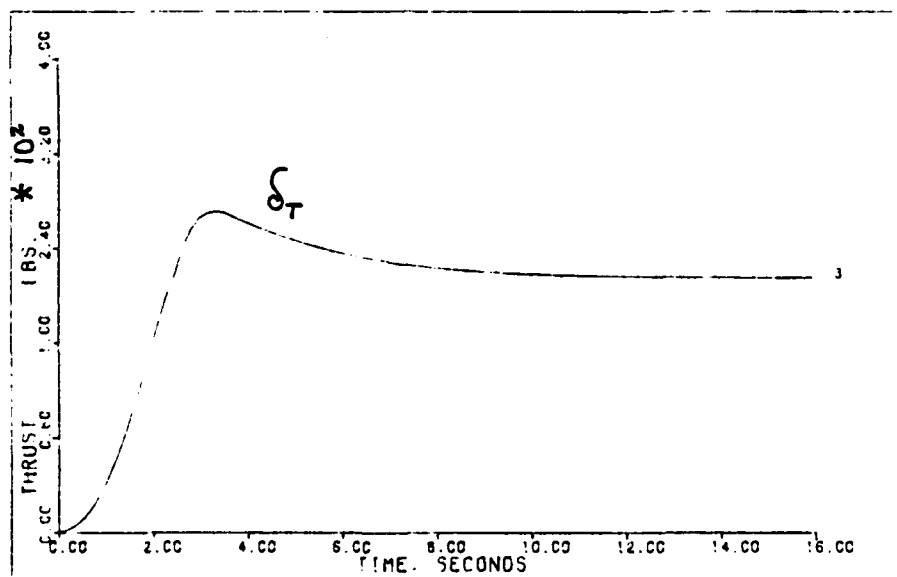


FIGURE B - 34



THRUST INPUT TO DIRECT LIFT 2:0.4M. OK FT



THRUST INPUT TO DIRECT LIFT 2:0.9M. 50K FT

FIGURE B - 35

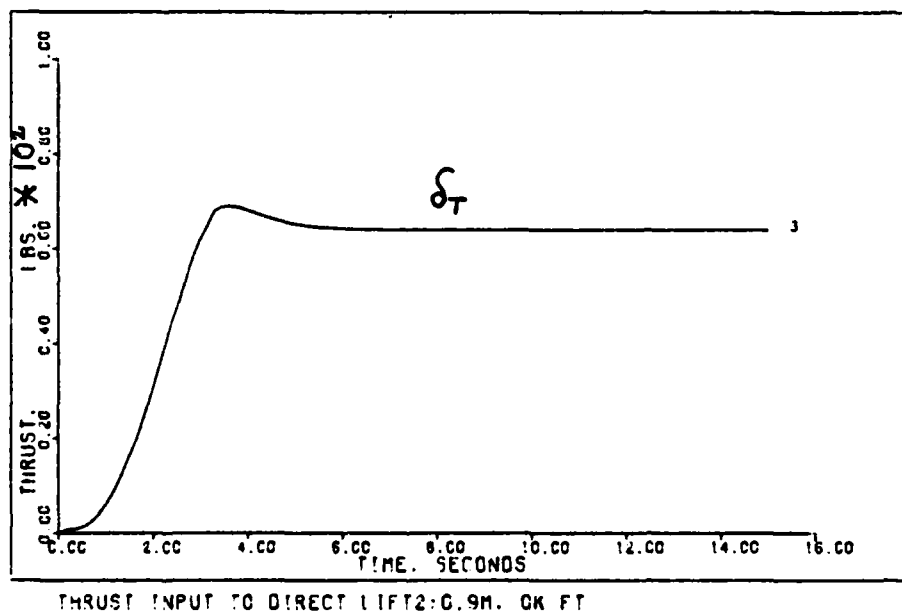
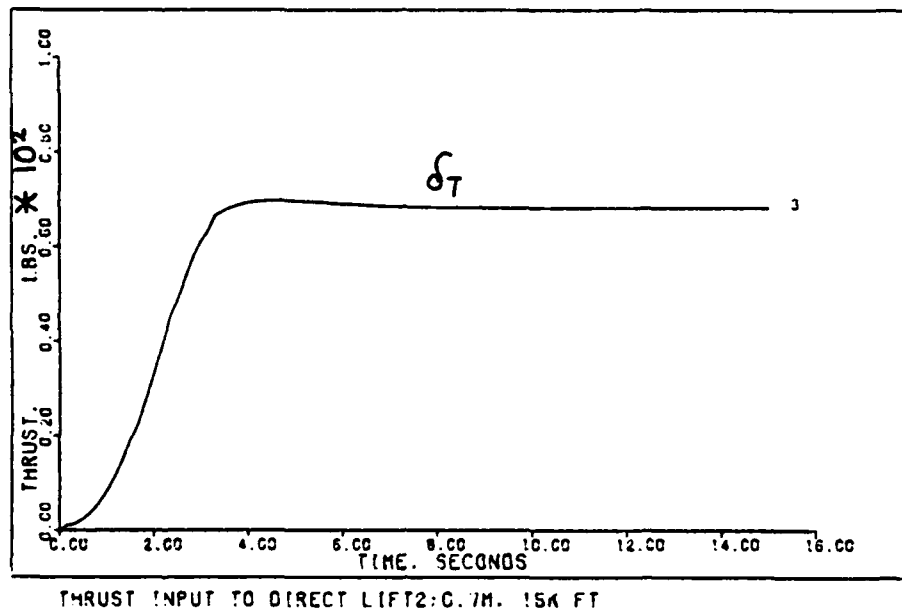
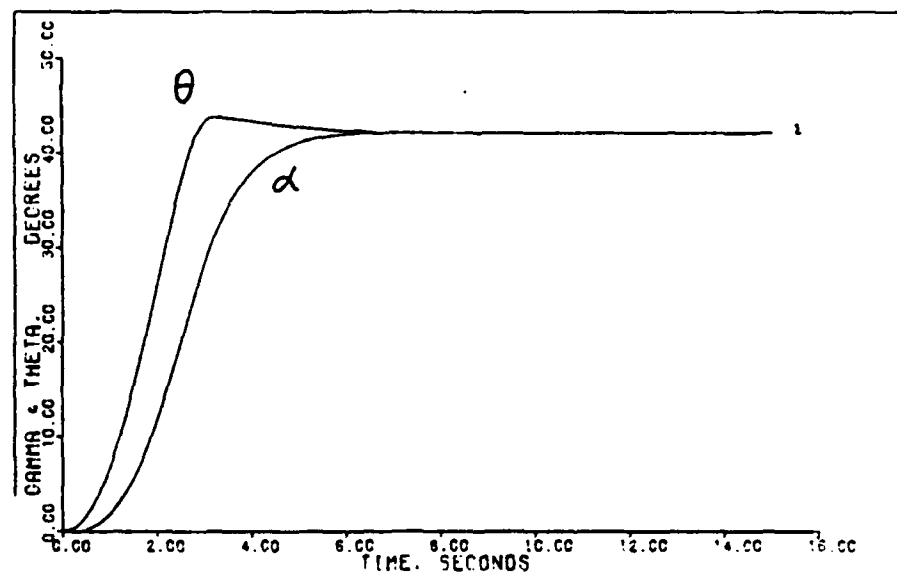
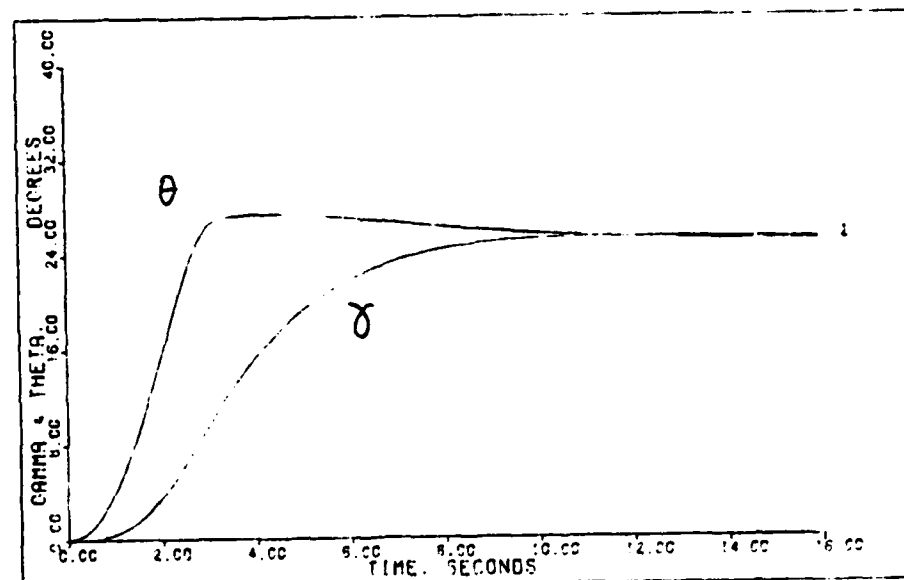


FIGURE B - 36

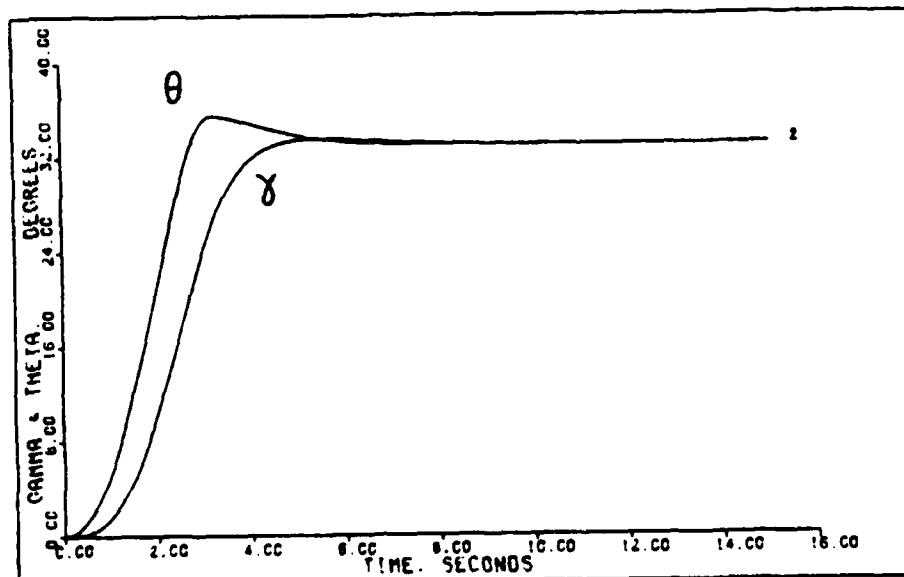


GAMMA & THETA FROM DIRECT LIFT 2.04M. OK FT

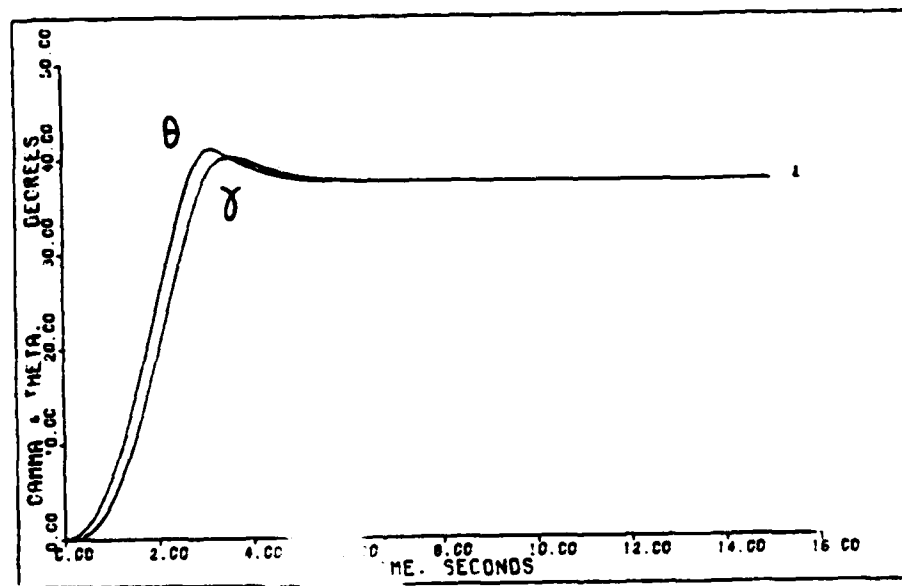


GAMMA & THETA FROM DIRECT LIFT 2.09M. 50K FT

FIGURE B - 37

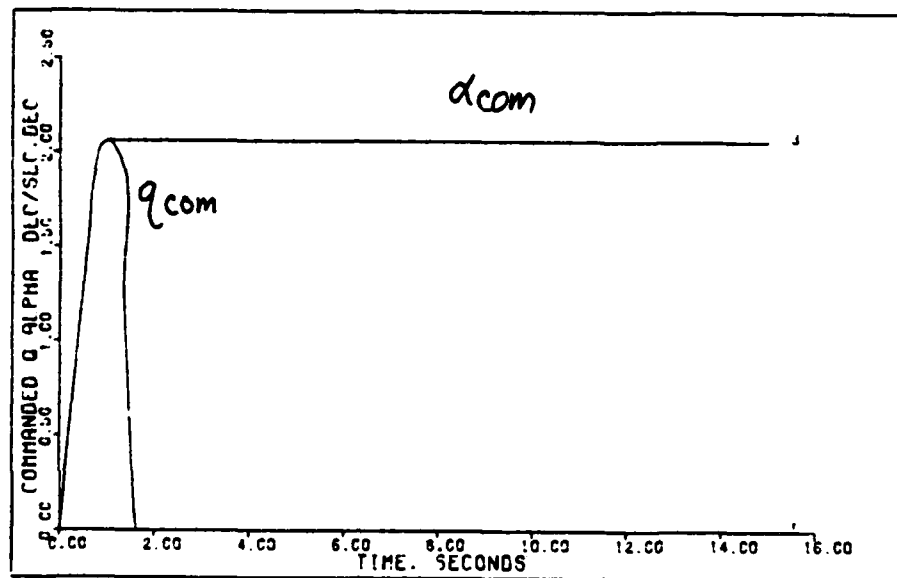


GAMMA & THETA FROM DIRECT LIFT 2:0.7M, 15K FT

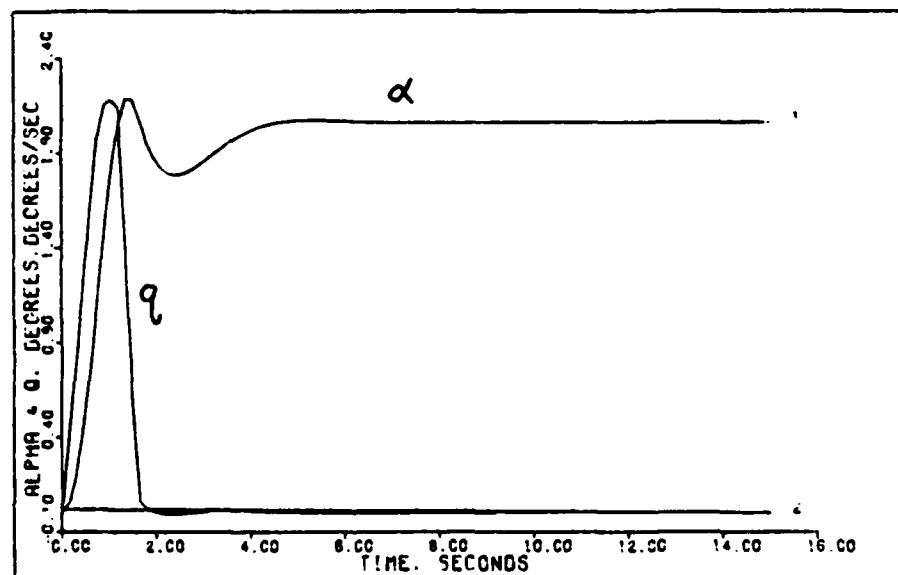


GAMMA & THETA FROM DIRECT LIFT 2:0.9M, 0K FT

FIGURE B - 38

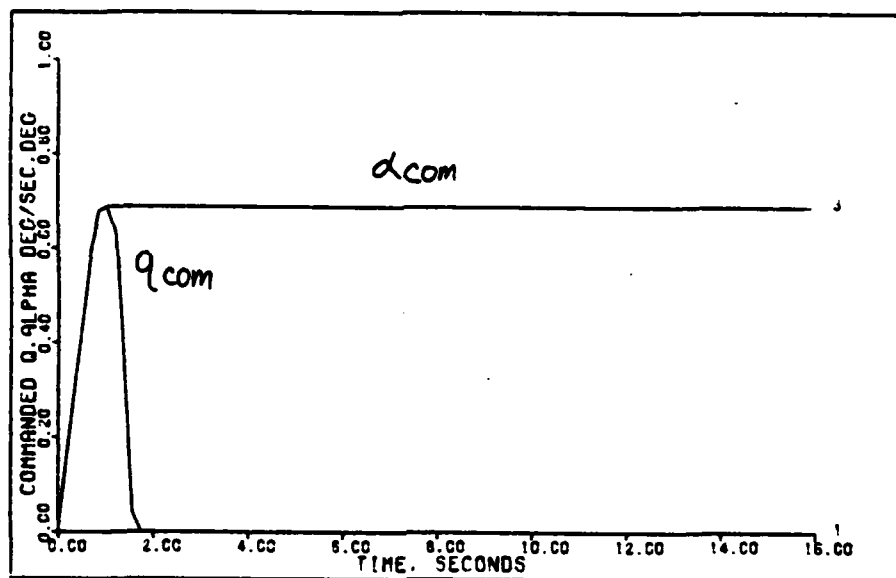


COMMANDED Q & ALPHA INPUTS TO PITCH-POINTING G.4M. CK FT

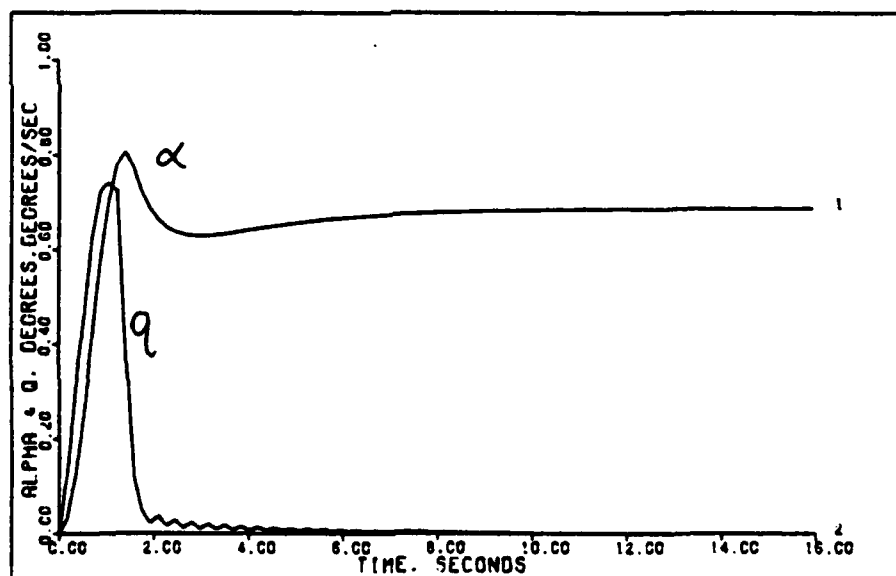


ALPHA & Q OUTPUTS TO PITCH-POINTING G.4M. CK FT

FIGURE B - 39

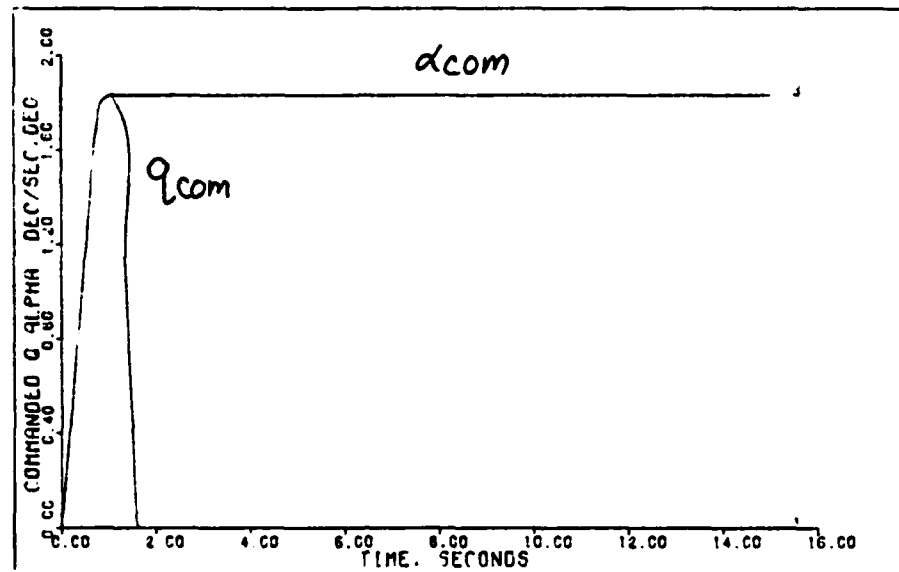


COMMANDED Q & ALPHA INPUTS TO PITCH-POINTING: 0.9M. 50K FT

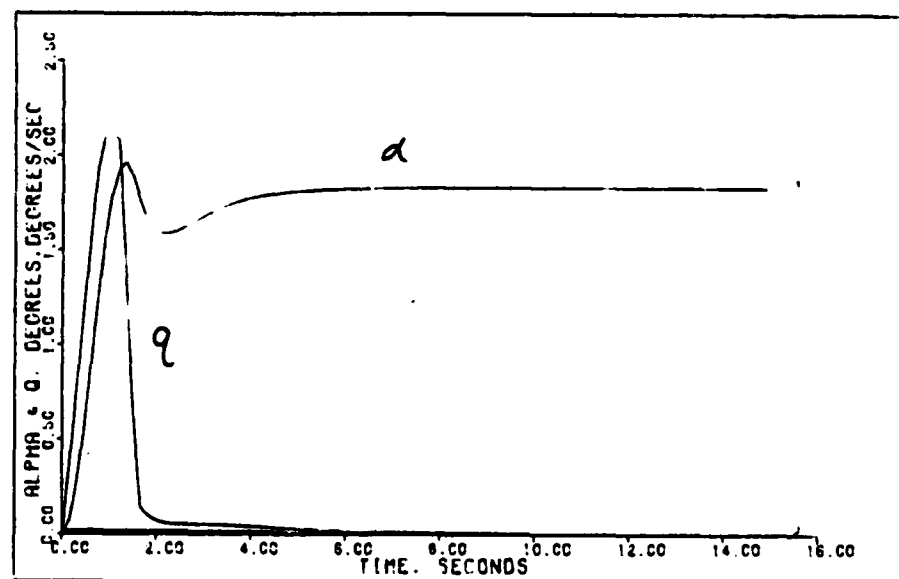


ALPHA & Q OUTPUTS TO PITCH-POINTING: 0.9M. 50K FT

FIGURE B - 40



COMMANDED Q & ALPHA INPUTS TO PITCH-POINTING C.M. 1SK FT



ALPHA & Q OUTPUTS TO PITCH-POINTING C.M. 1SK FT

FIGURE B - 41

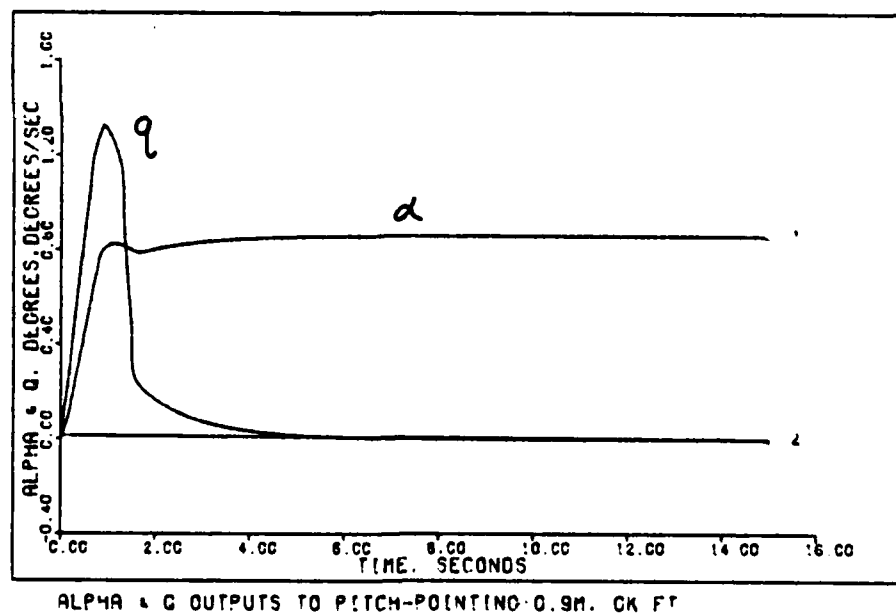
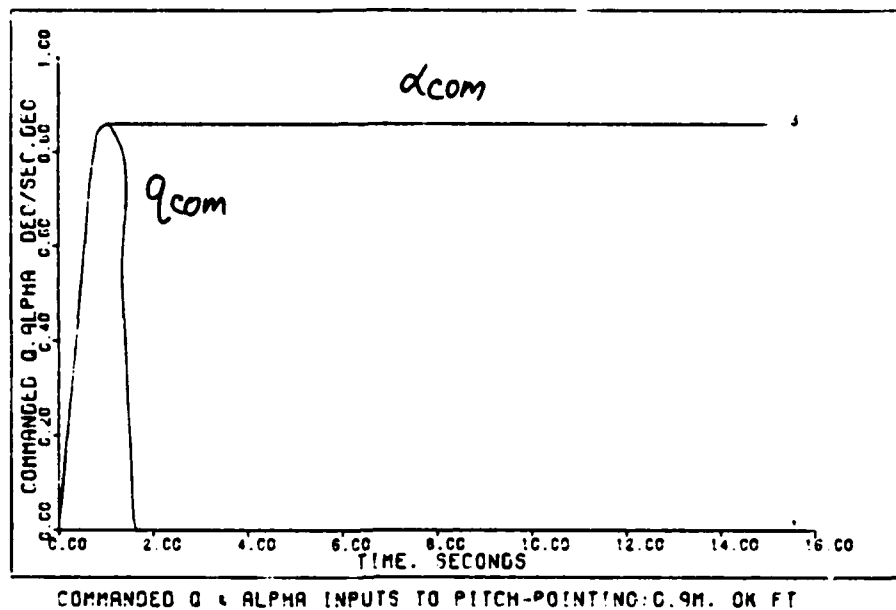
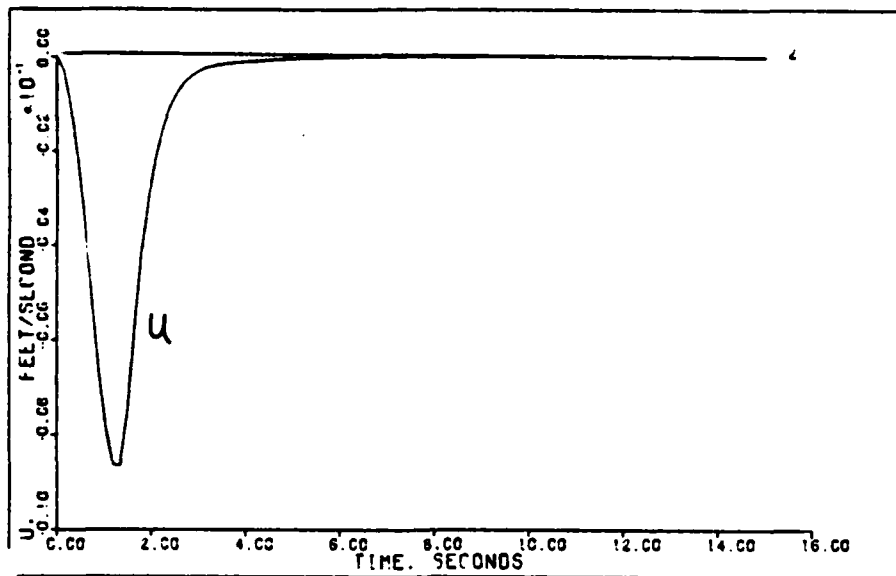
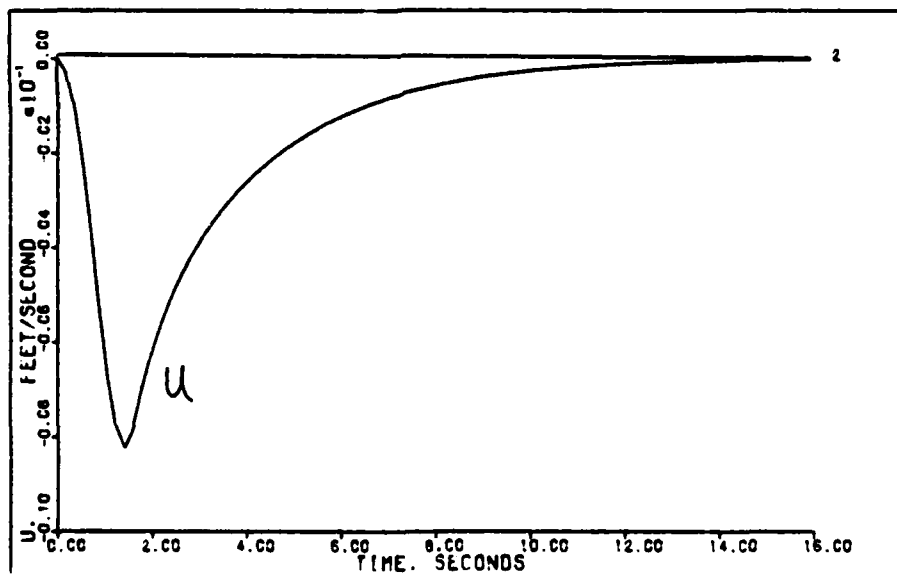


FIGURE B - 42

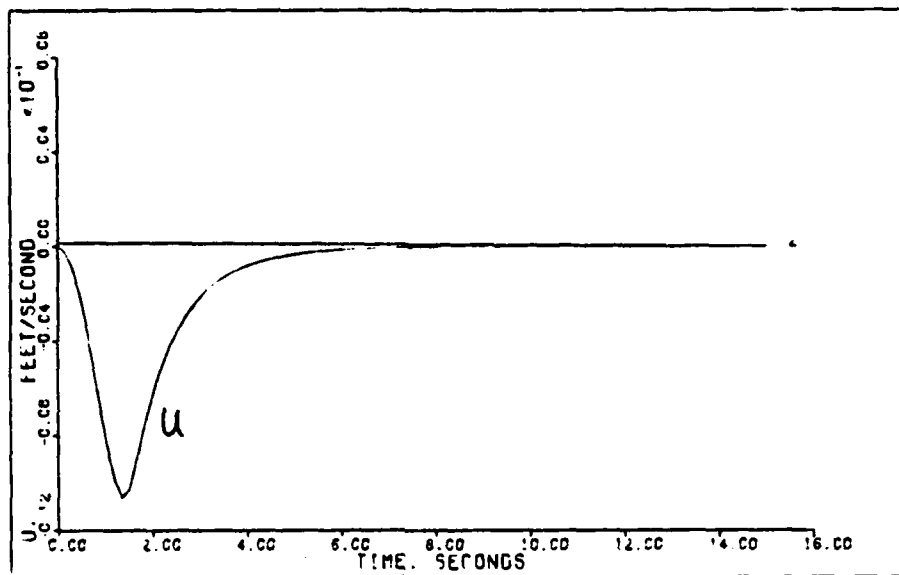


U OUTPUT TO PITCH-POINTING: 0.4M. 0K FT

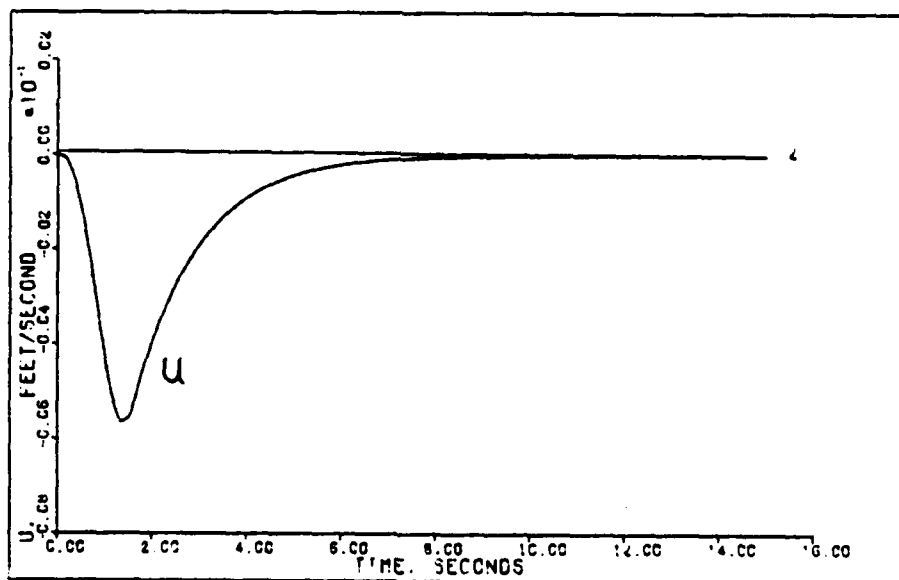


U OUTPUT TO PITCH-POINTING: 0.9M. 50K FT

FIGURE B - 43

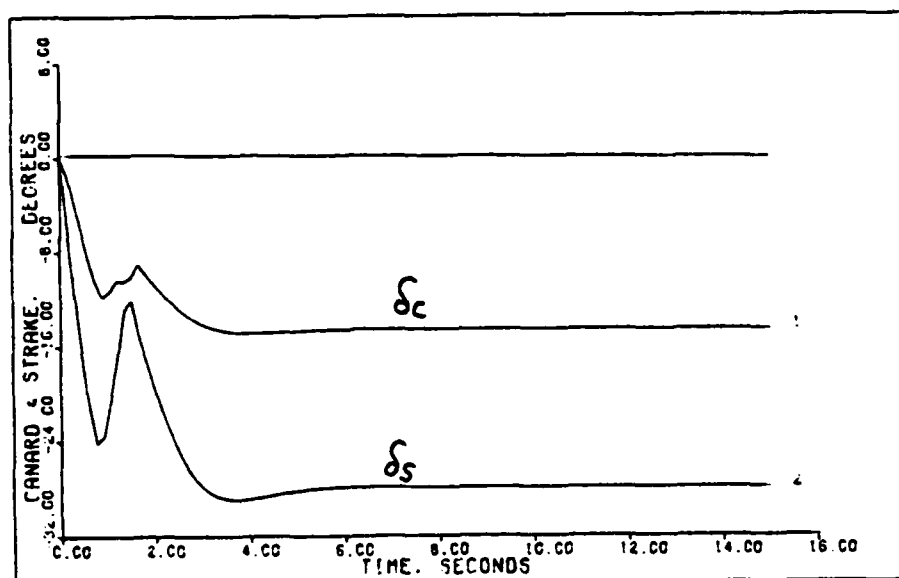


J OUTPUT TO PITCH-POINTING: 0.7M, 15K FT

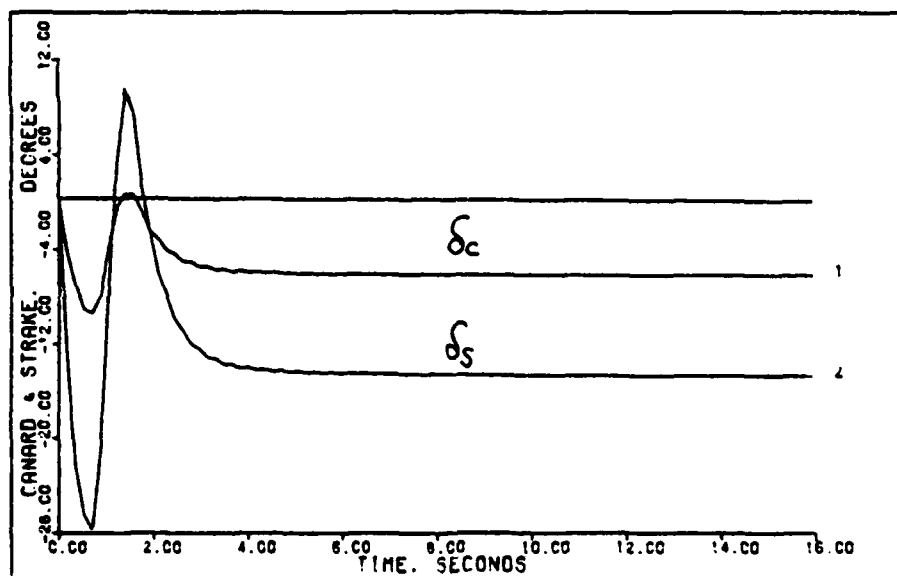


J OUTPUT TO PITCH-POINTING: 0.9M, 0K FT

FIGURE B - 44

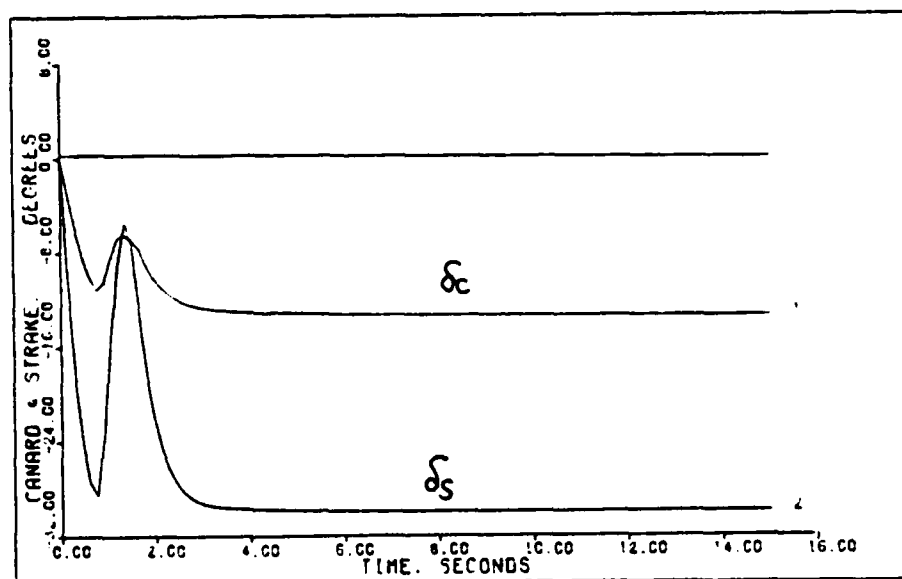


CANARD & STRAKE INPUTS TO PITCH-POINTING: G.4M, 0K FT

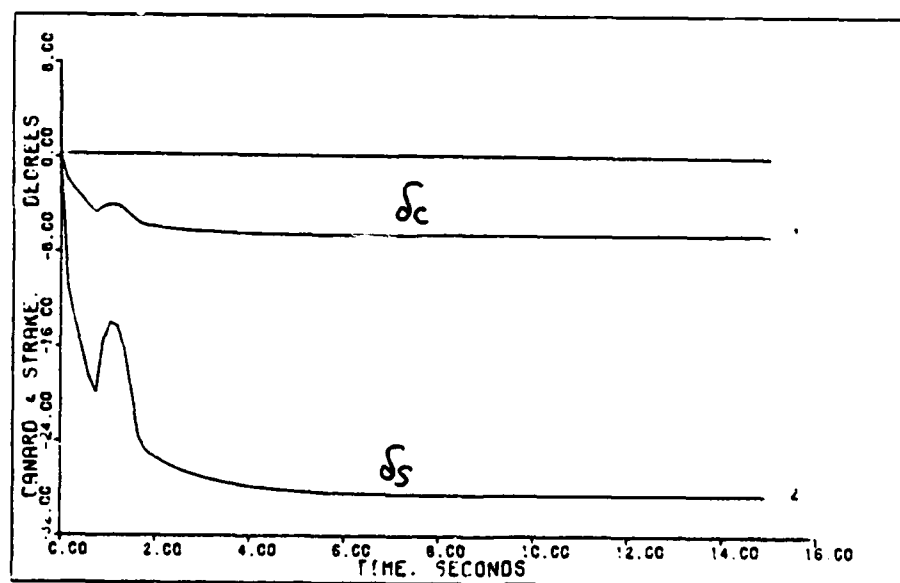


CANARD & STRAKE INPUTS TO PITCH-POINTING: G.9M, 50K FT

FIGURE B - 45

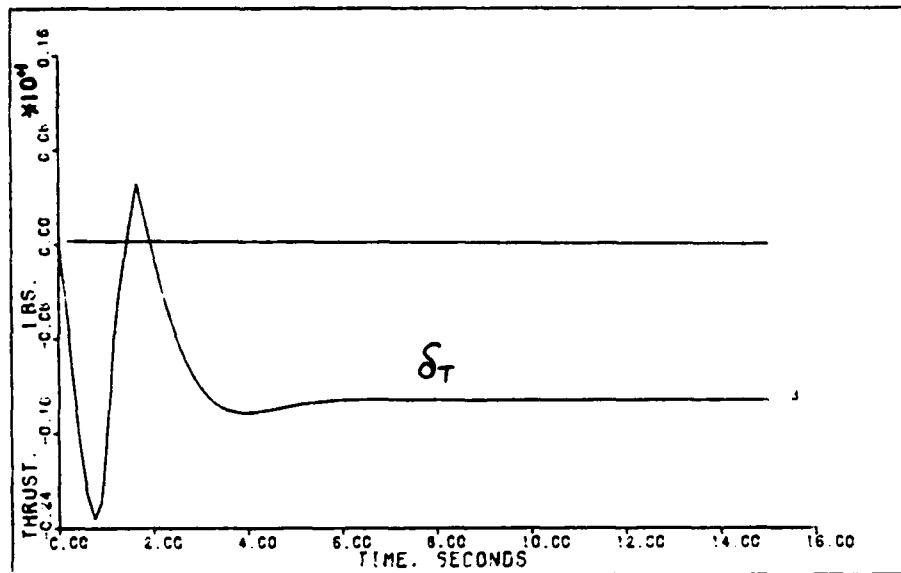


CANARD & STRAKE INPUTS TO PITCH-POINTING-G. 1M. 15K FT

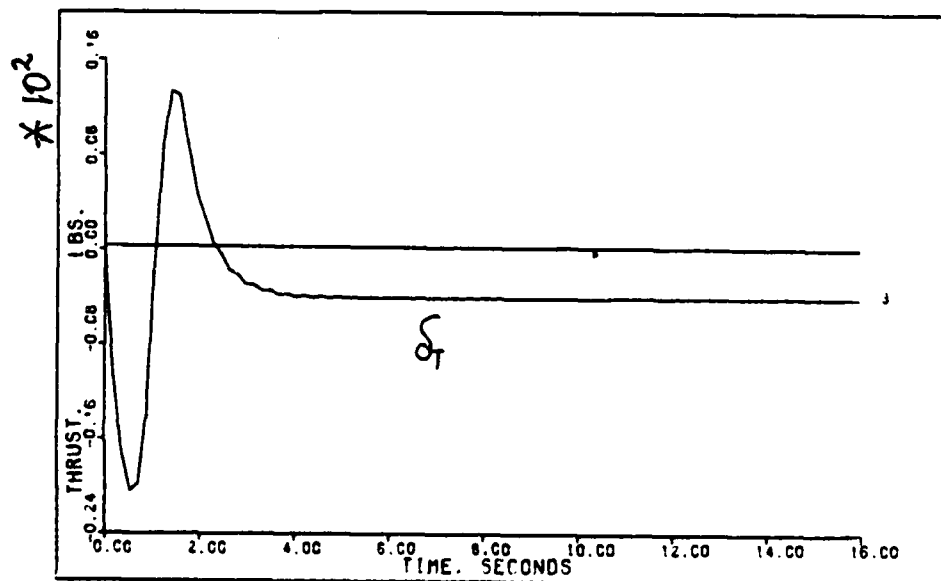


CANARD & STRAKE INPUTS TO PITCH-POINTING-G. 9M. 0K FT

FIGURE B - 46



THRUST INPUT TO PITCH-POINTING: 0.4M. CK FT



THRUST INPUT TO PITCH-POINTING: 0.9M. 50K FT

FIGURE B - 47

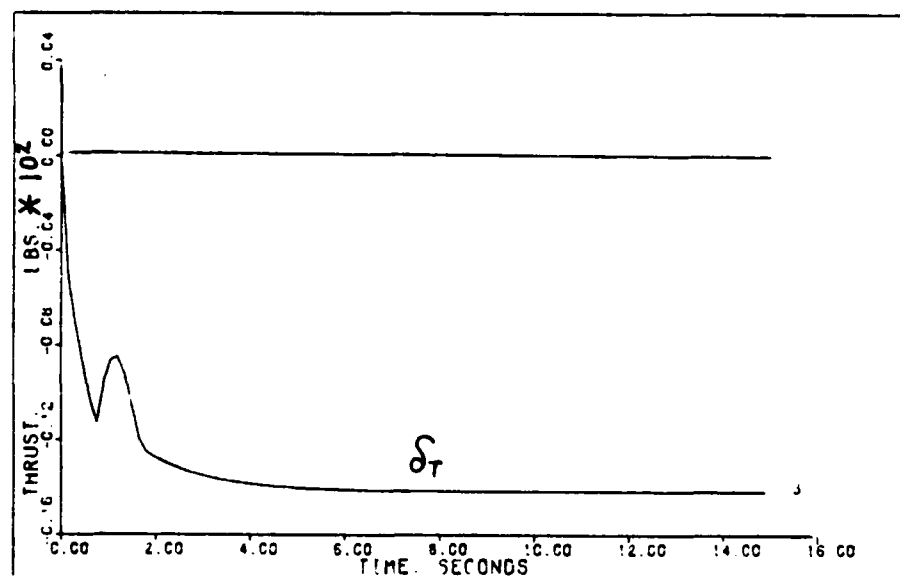
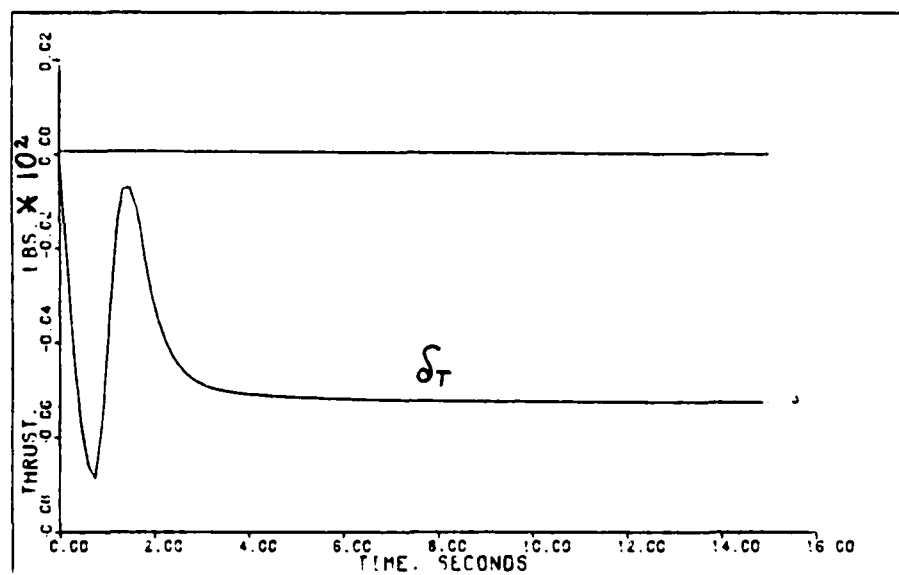
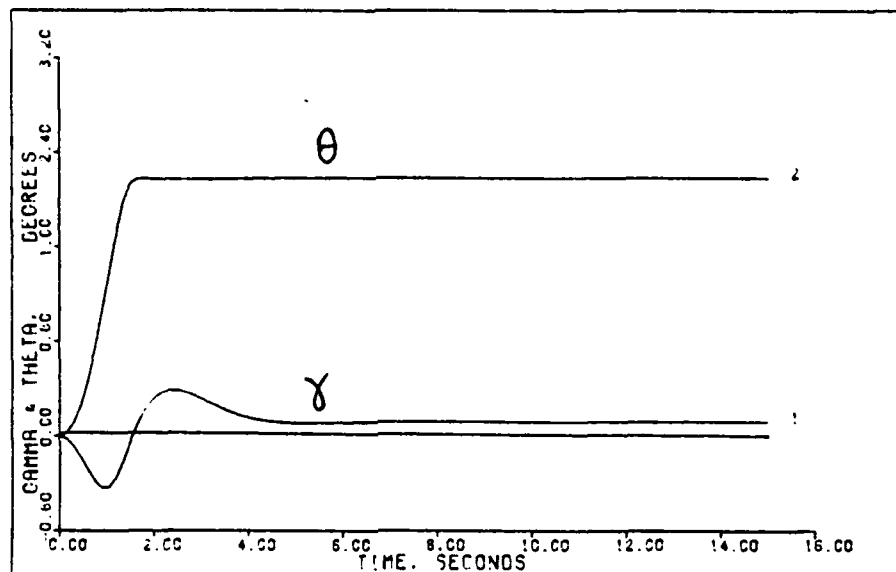
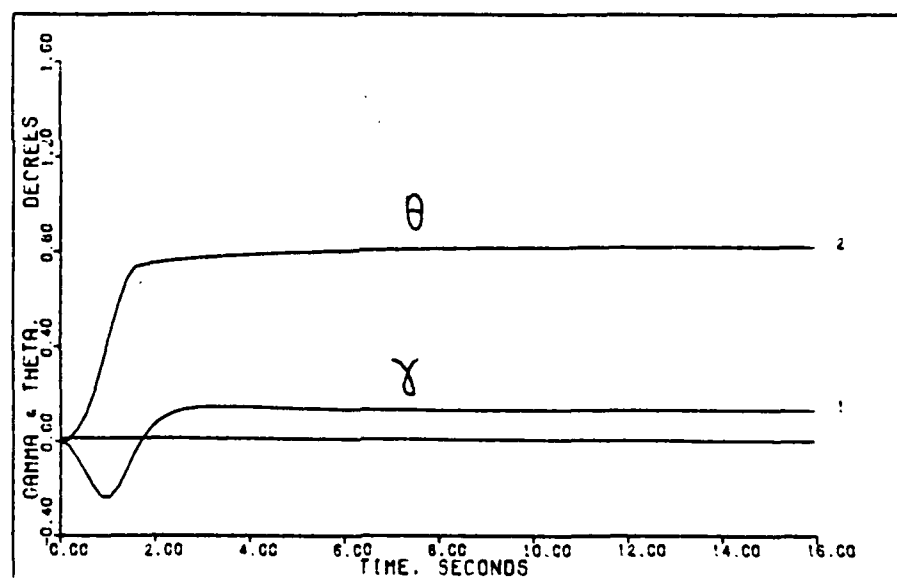


FIGURE B - 48



GAMMA & THETA FROM PITCH-POINTING: 0.14M, 0K FT



GAMMA & THETA FROM PITCH-POINTING: 0.9M, 50K FT

FIGURE B - 49

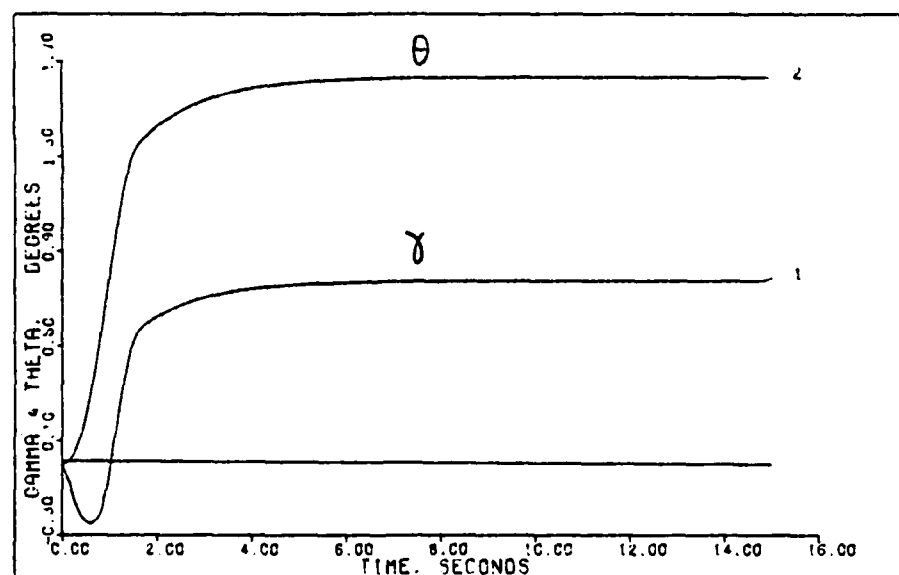
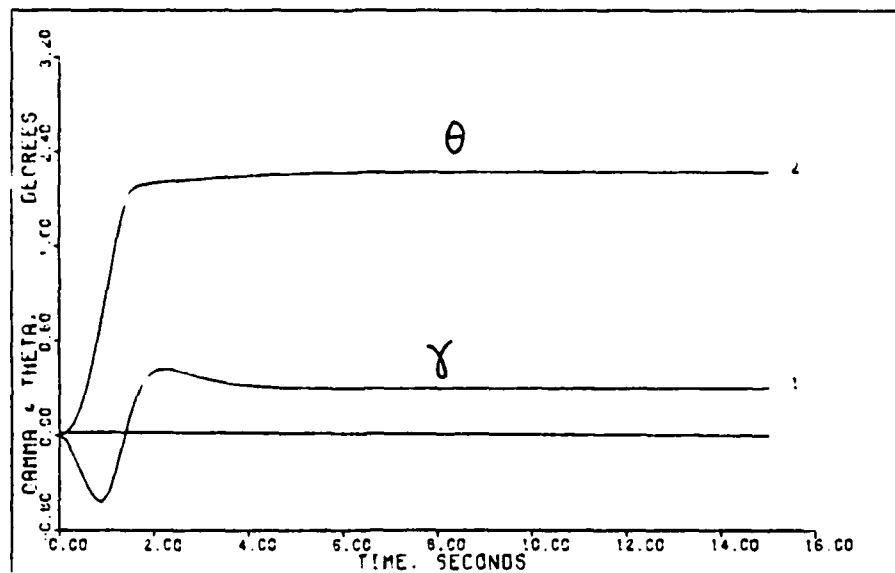
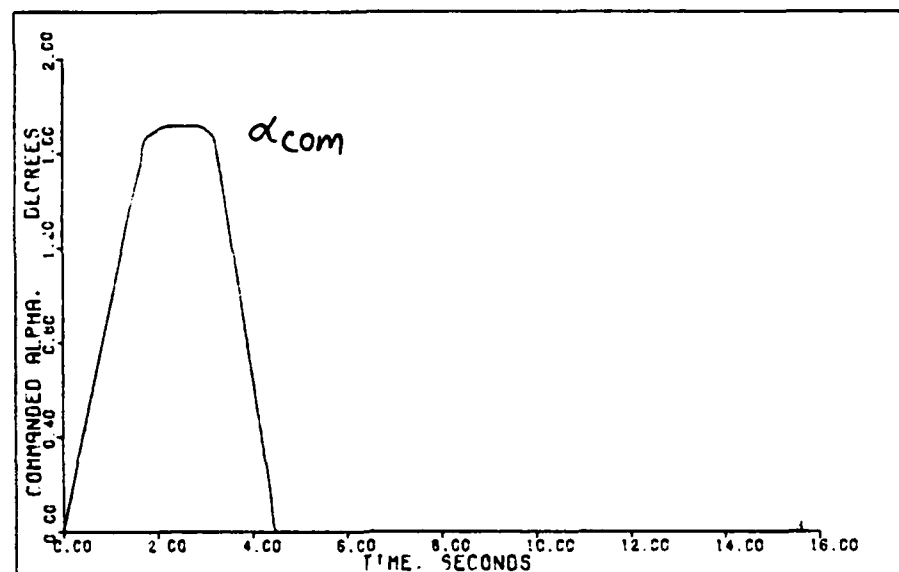
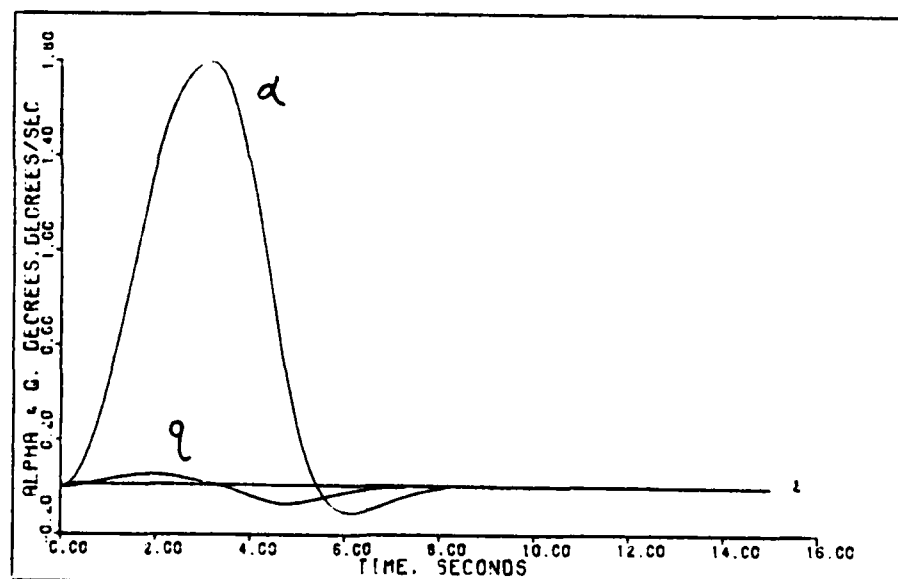


FIGURE B - 50

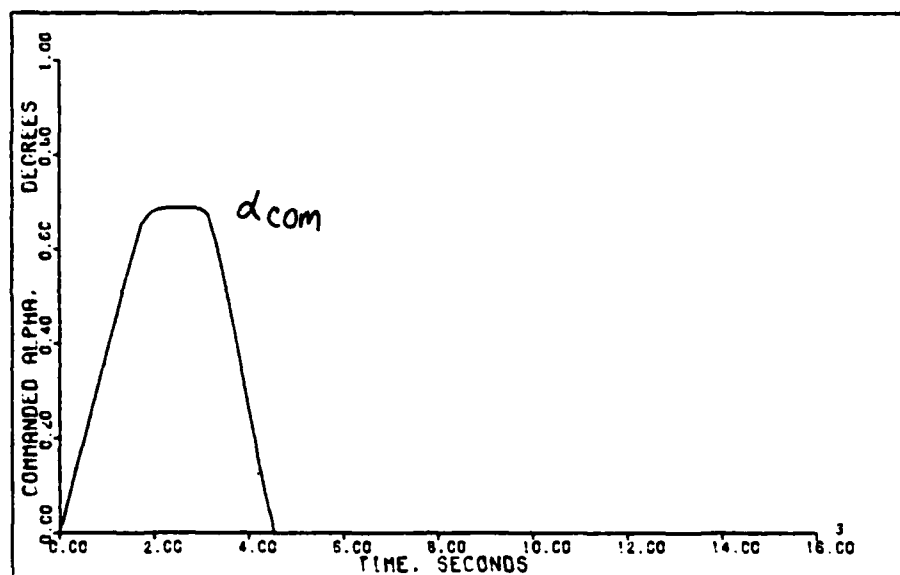


COMMANDED ALPHA INPUT TO VERTICAL TRANSLATION: C. 4M. OK FT

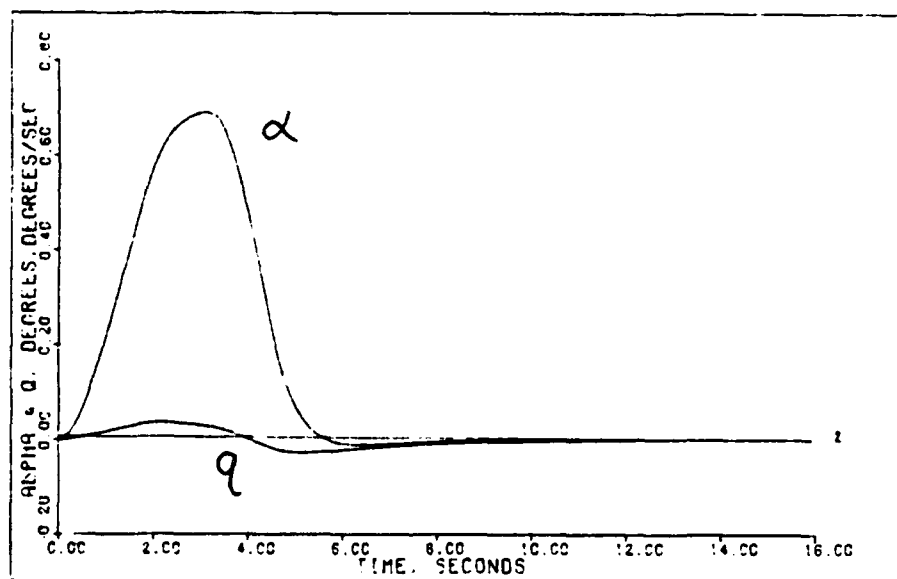


ALPHA & Q OUTPUTS TO VERTICAL TRANSLATION: C. 4M. OK FT

FIGURE B - 51

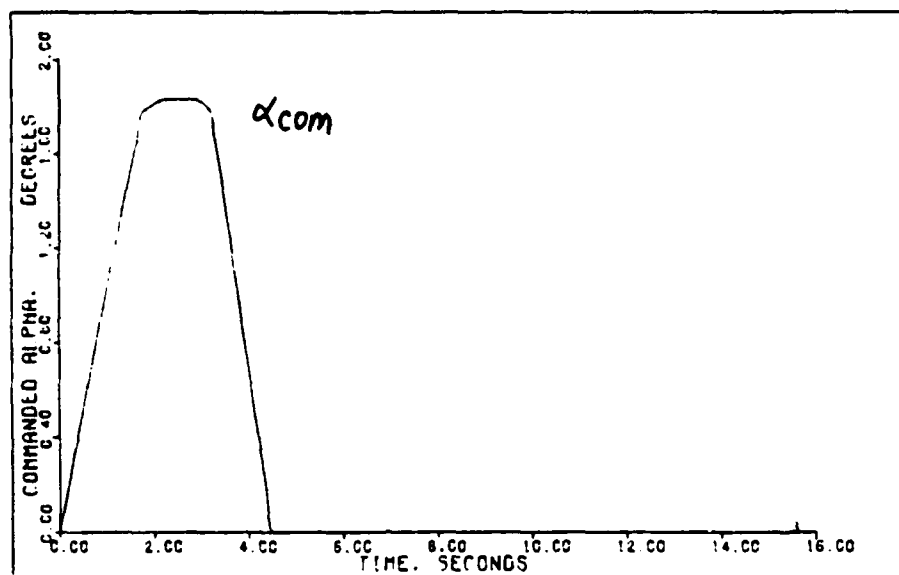


COMMANDED ALPHA INPUT TO VERTICAL TRANSLATION: 9M.50K FT

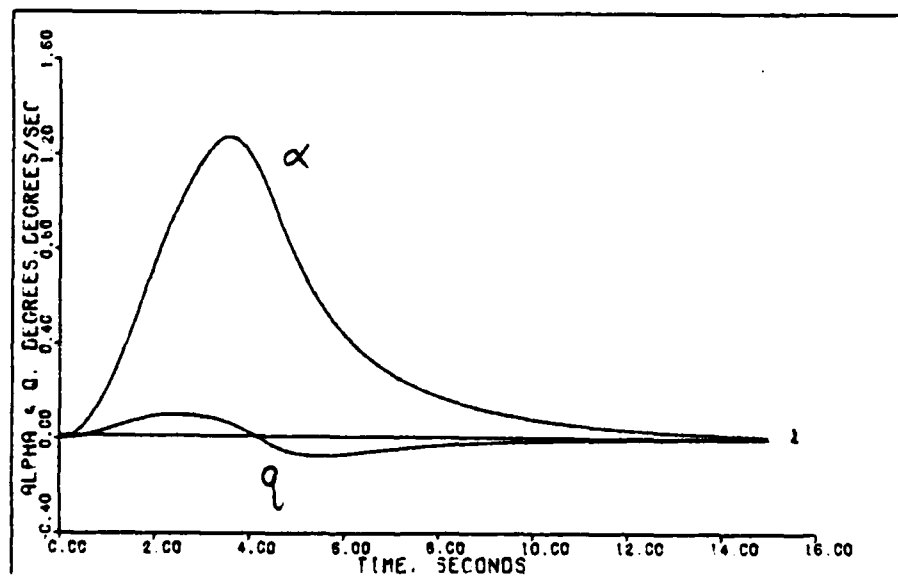


ALPHA & Q OUTPUTS TO VERTICAL TRANSLATION: 0.9M. 50K FT

FIGURE B - 52

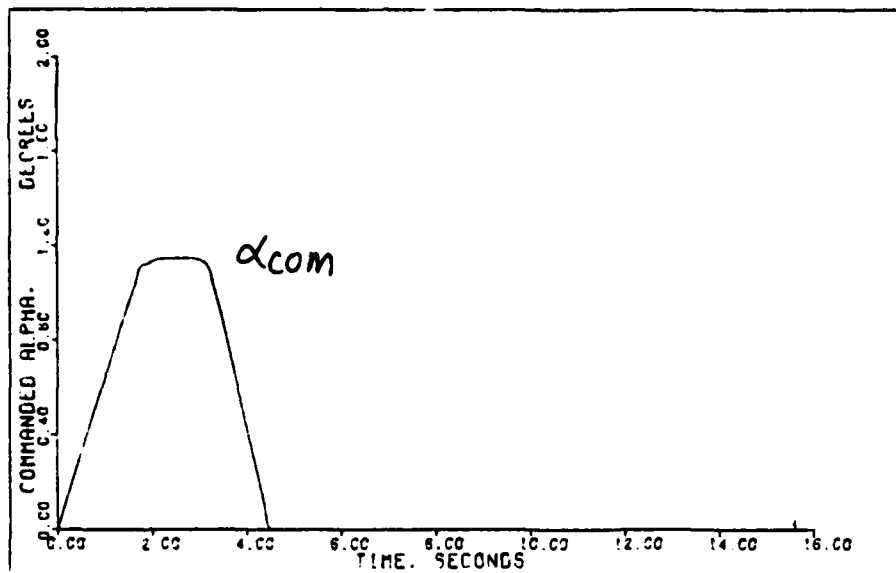


COMMANDED ALPHA INPUT TO VERTICAL TRANSLATION: G. 7M. 15K FT

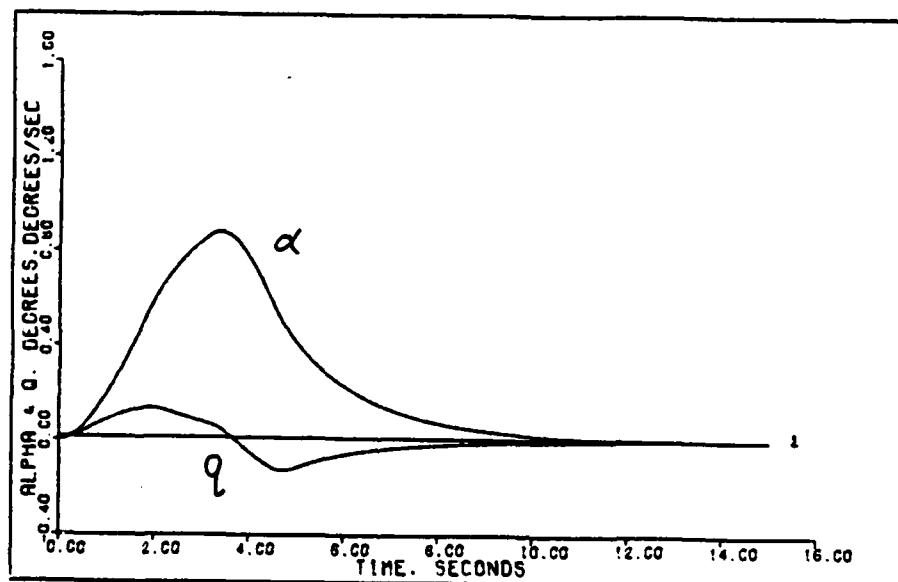


ALPHA & Q OUTPUTS TO VERTICAL TRANSLATION: G. 7M. 15K FT

FIGURE B - 53

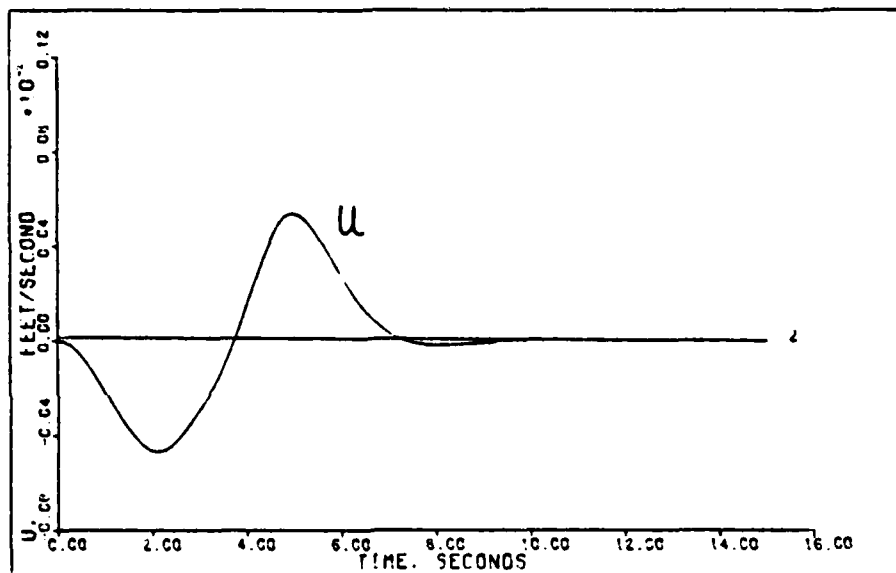


COMMANDED ALPHA INPUT TO VERTICAL TRANSLATION: 0.9M. OK FT

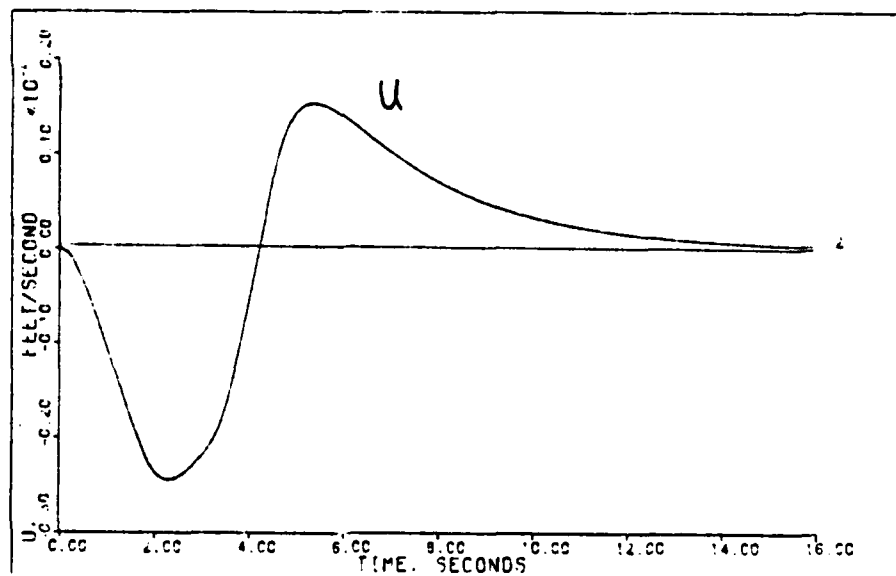


ALPHA & Q OUTPUTS TO VERTICAL TRANSLATION: 0.9M. OK FT

FIGURE B - 54



U OUTPUT TO VERTICAL TRANSLATION: 0.4M. OK FT



U OUTPUT TO VERTICAL TRANSLATION: 0.9M. 50K FT

FIGURE B - 55

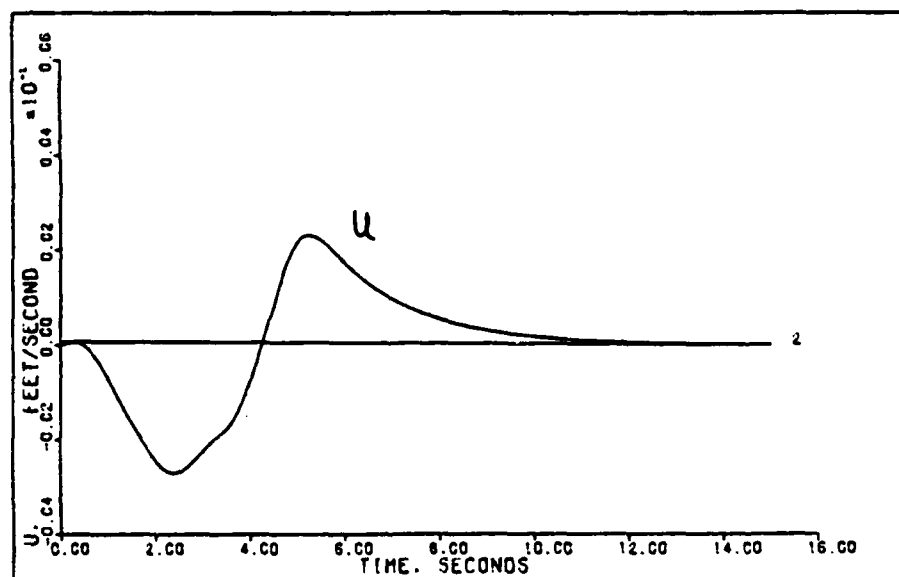
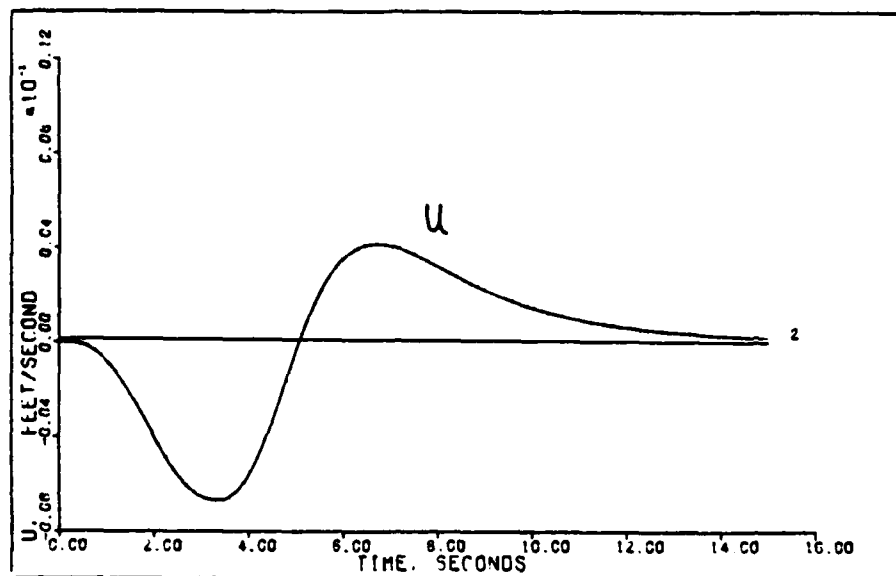


FIGURE B - 56

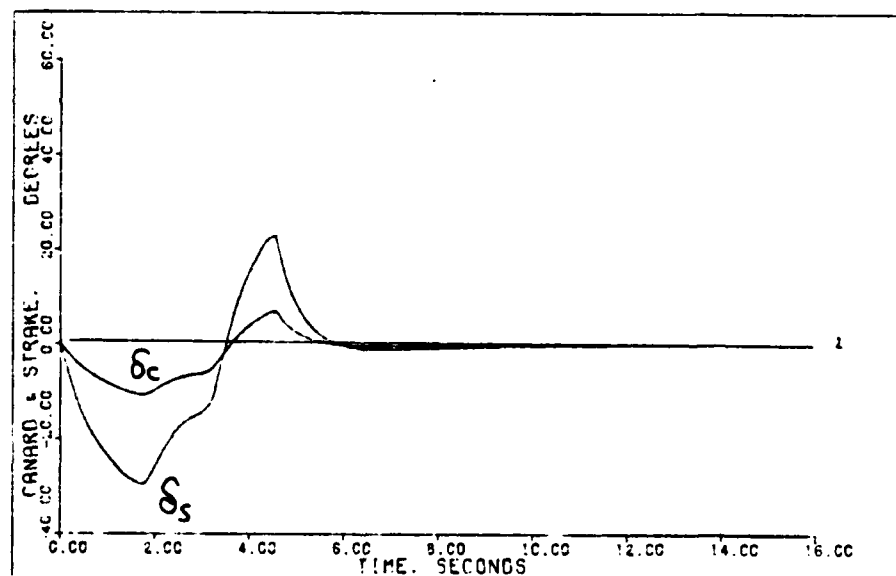
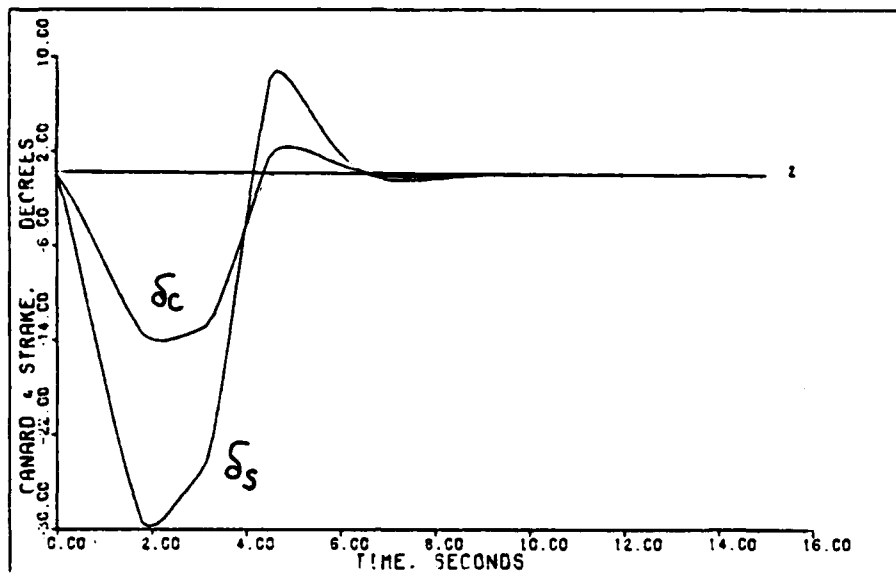


FIGURE B - 57

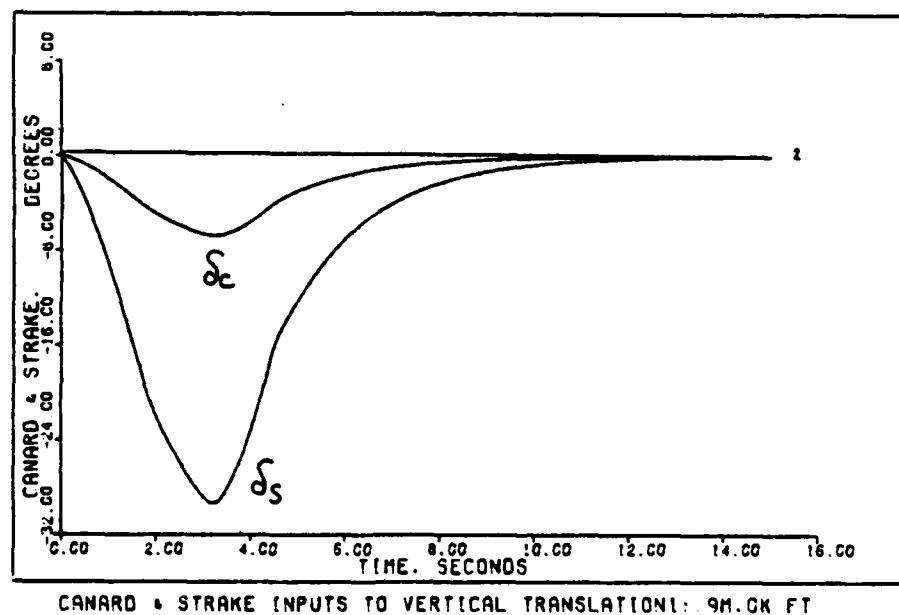
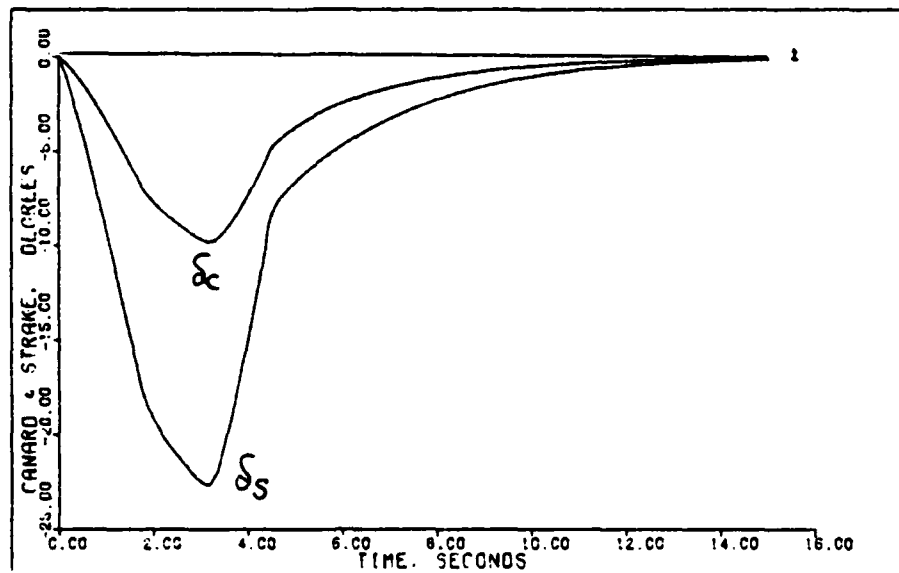


FIGURE B - 58

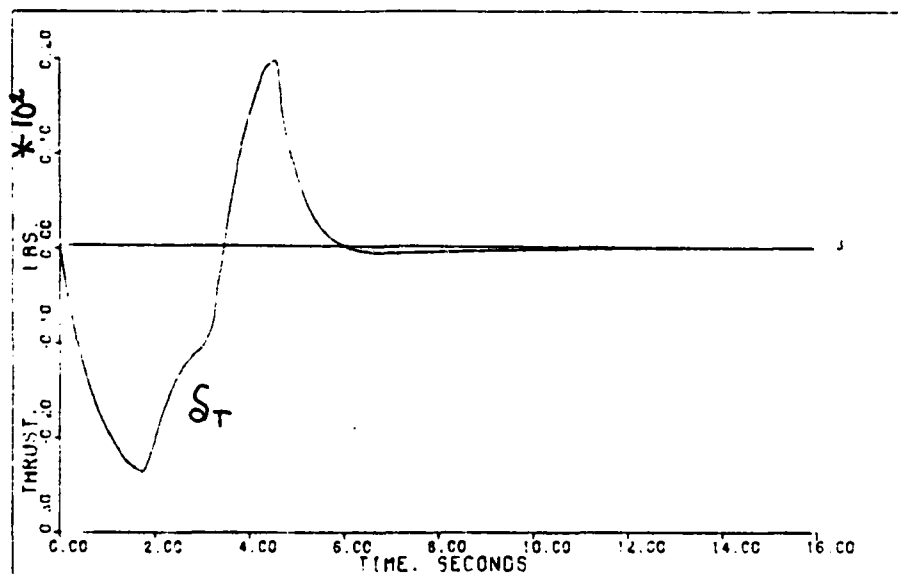
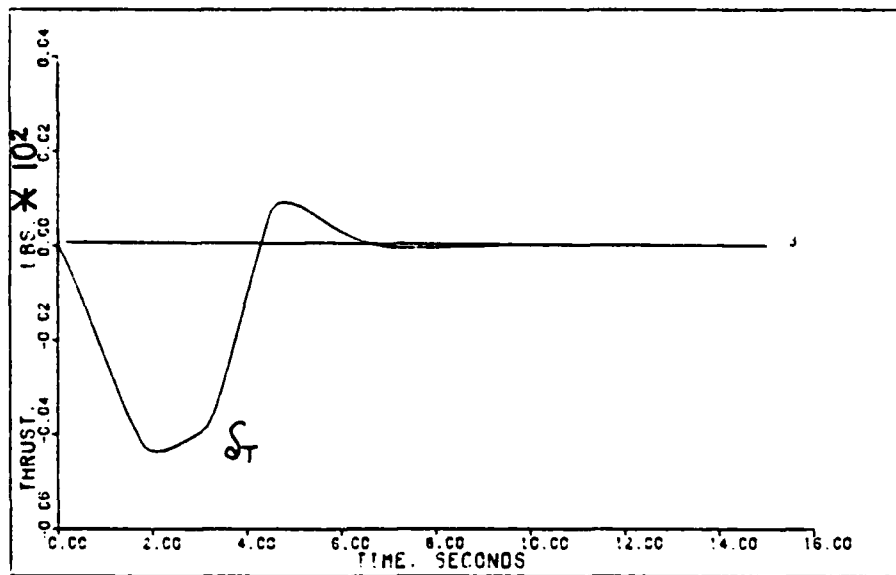


FIGURE B - 59

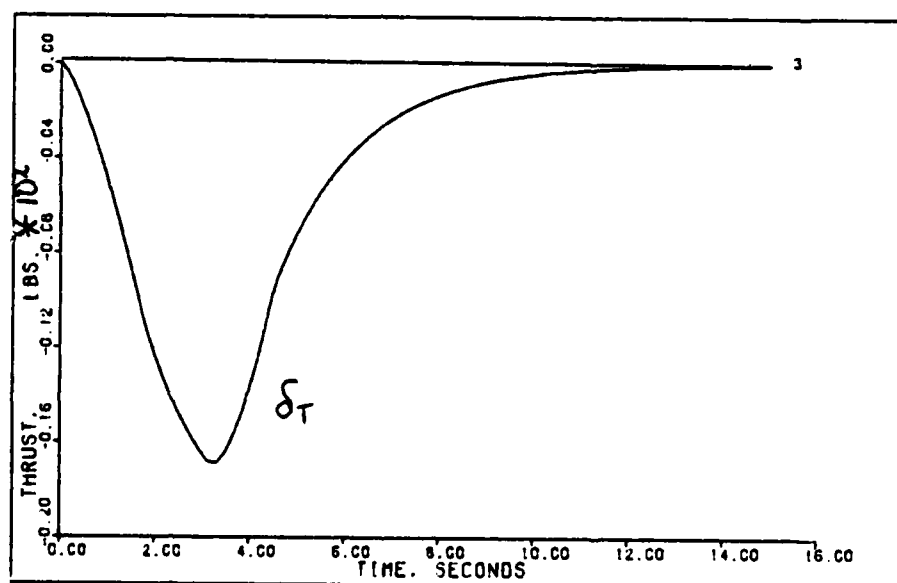
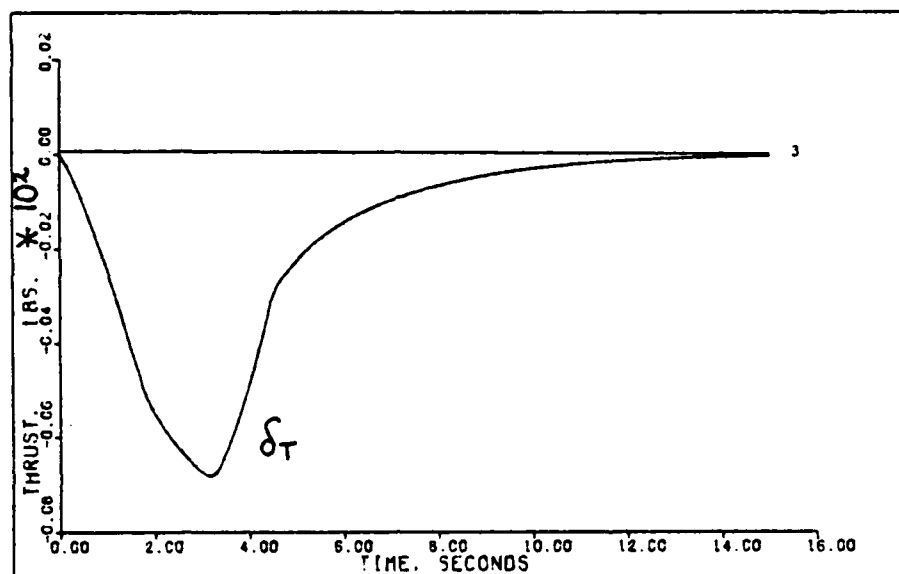
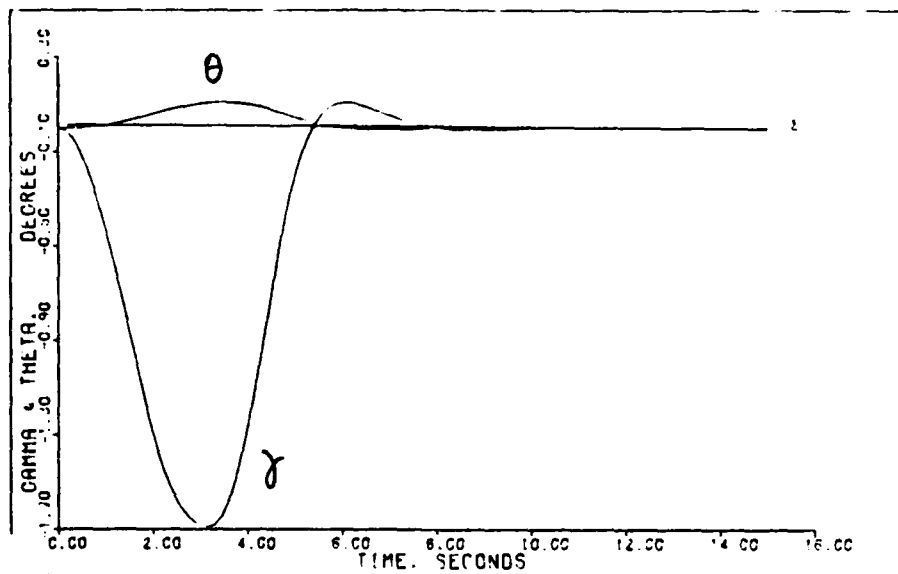
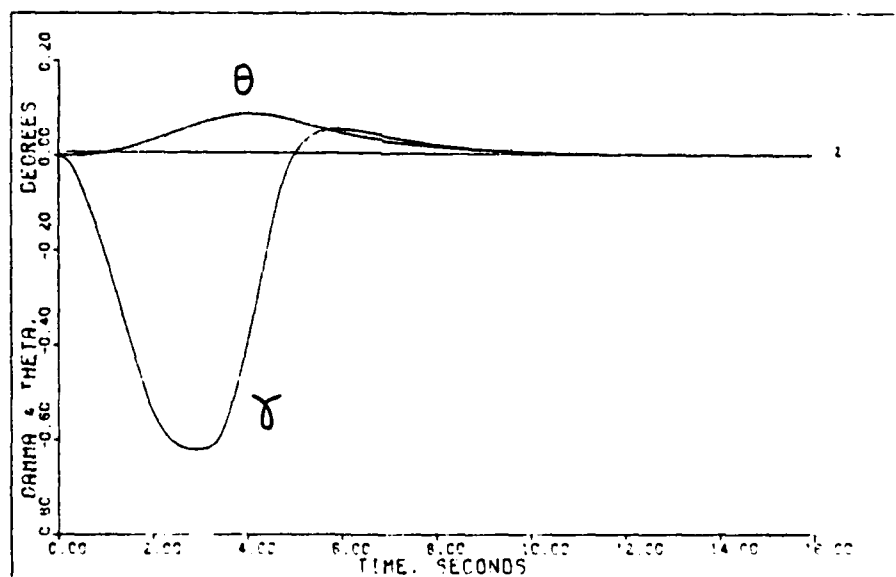


FIGURE B - 60

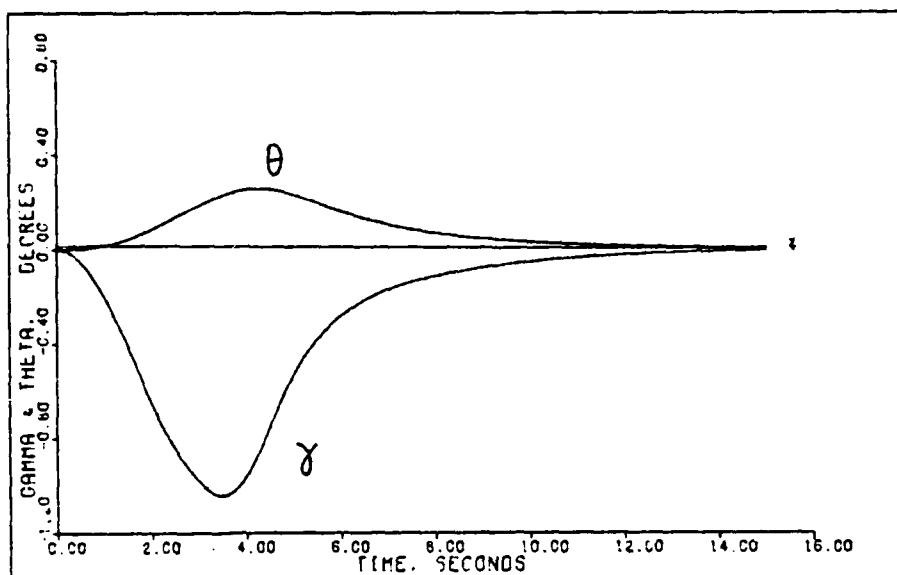


GAMMA & THETA FROM VERTICAL TRANSLATION: 0.4M. OK FT

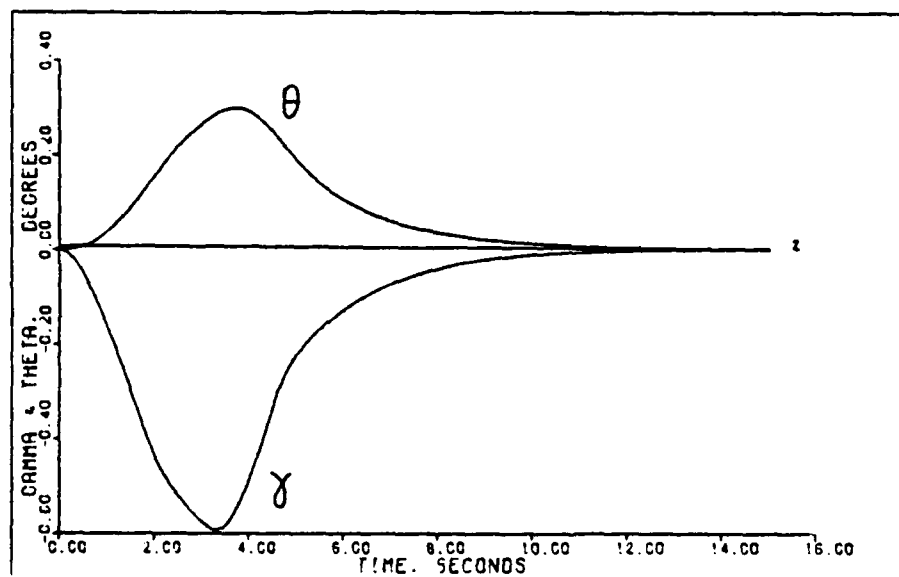


GAMMA & THETA FROM VERTICAL TRANSLATION: 0.9M. 5CK FT

FIGURE B - 61

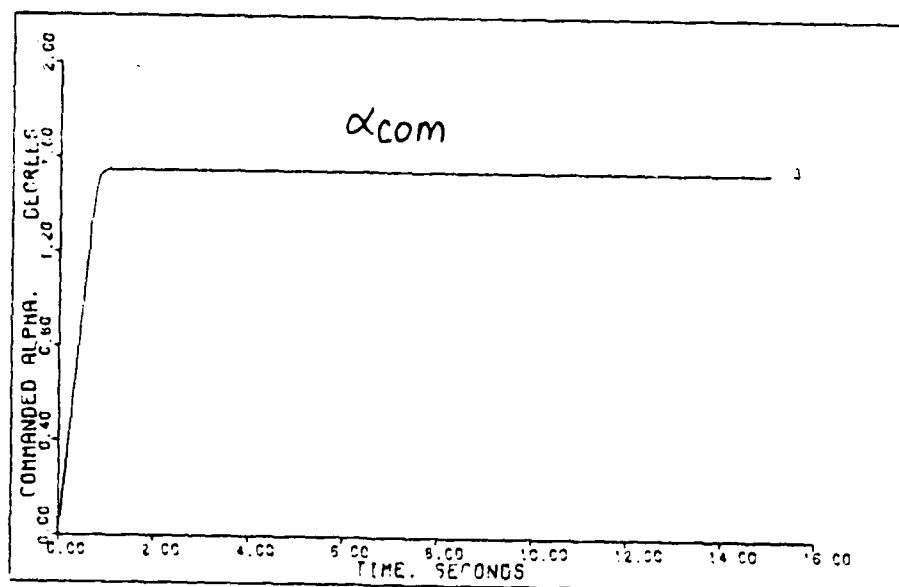


GAMMA & THETA FROM VERTICAL TRANSLATION: 0.7M. 1SK FT

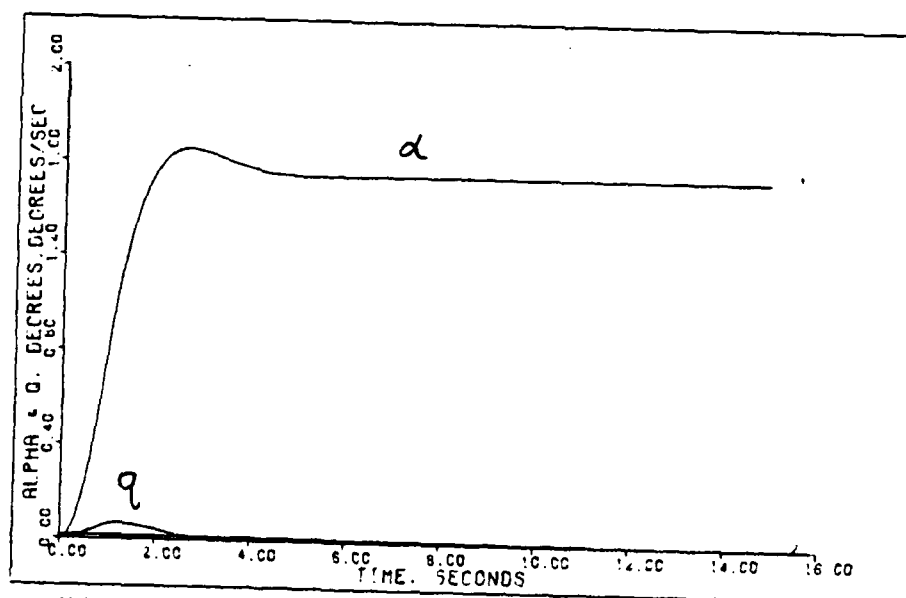


GAMMA & THETA FROM VERTICAL TRANSLATION: 0.9M. 0K FT

FIGURE B - 62

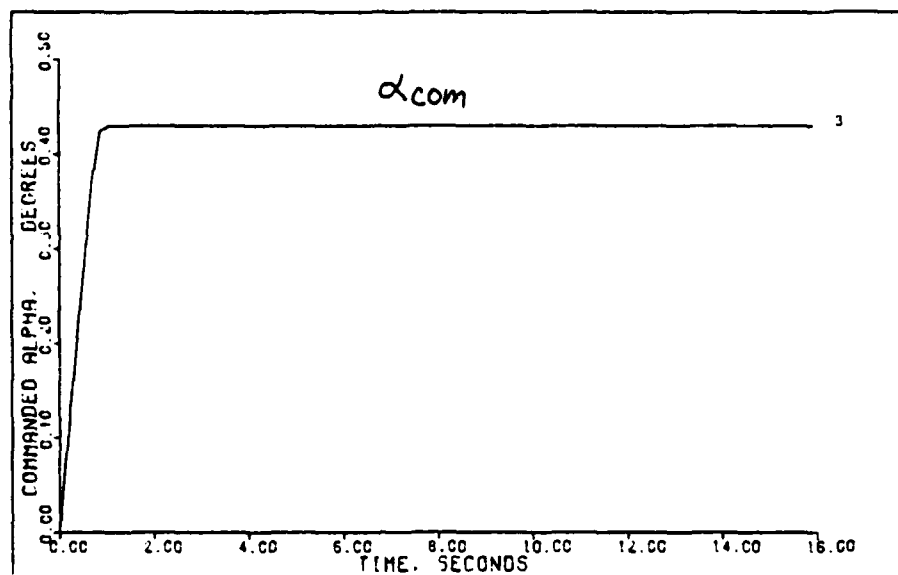


COMMANDED ALPHA INPUT TO VERTICAL TRANSLATION2: 0.4M. OK FT

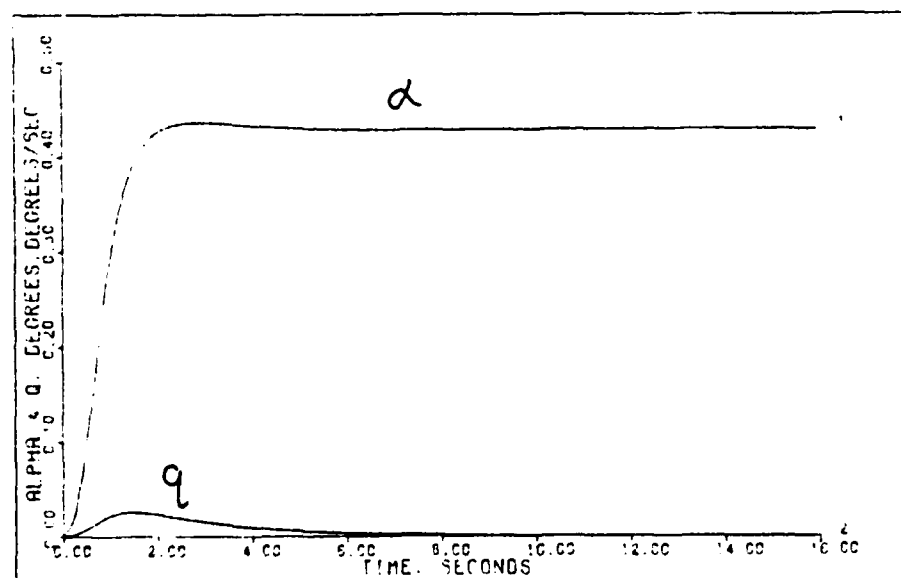


ALPHA & Q OUTPUTS TO VERTICAL TRANSLATION2: 4M. OK FT

FIGURE B - 63

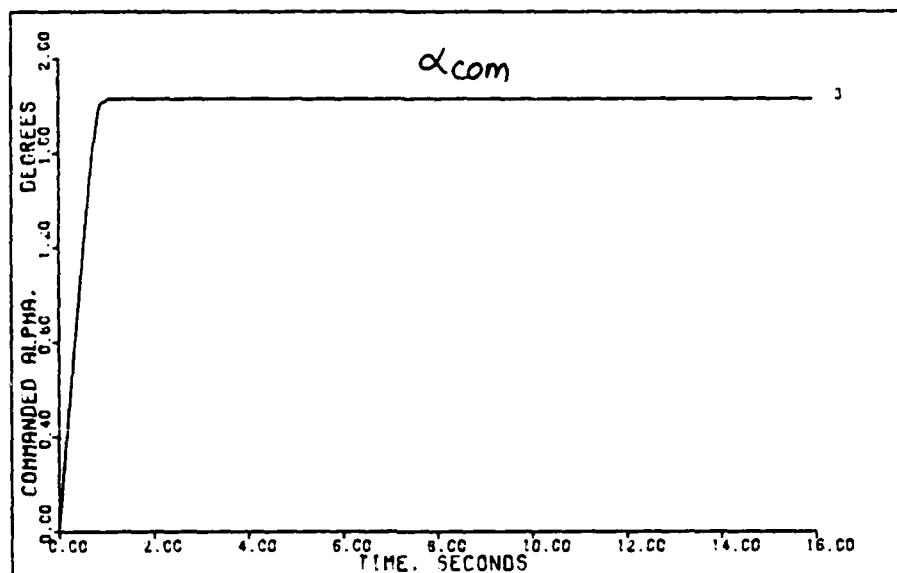


COMMANDED ALPHA INPUT TO VERTICAL TRANSLATION2: C.9M. 50K FT

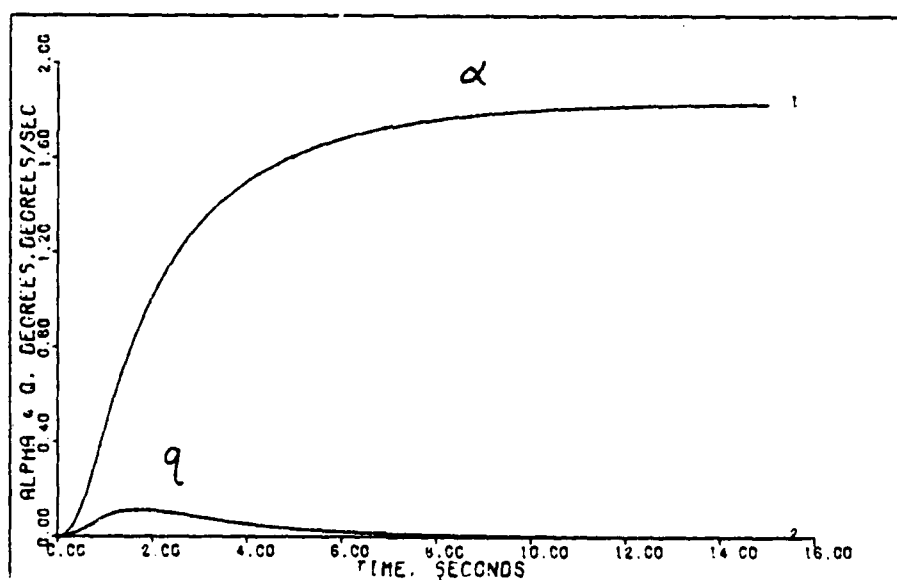


ALPHA & Q OUTPUTS TO VERTICAL TRANSLATION2: C.9M. 50K FT

FIGURE B - 64

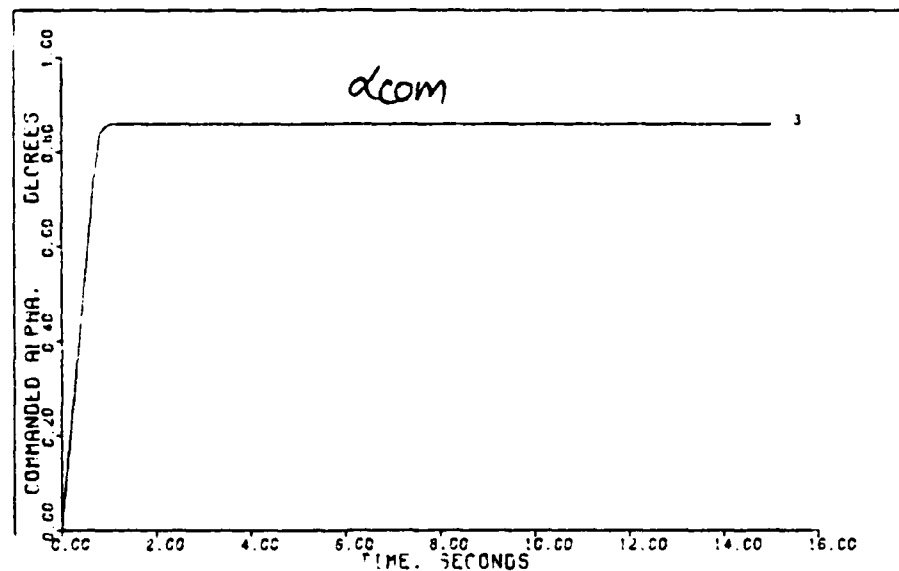


COMMANDED ALPHA INPUT TO VERTICAL TRANSLATION2: G. 7M. 15K FT

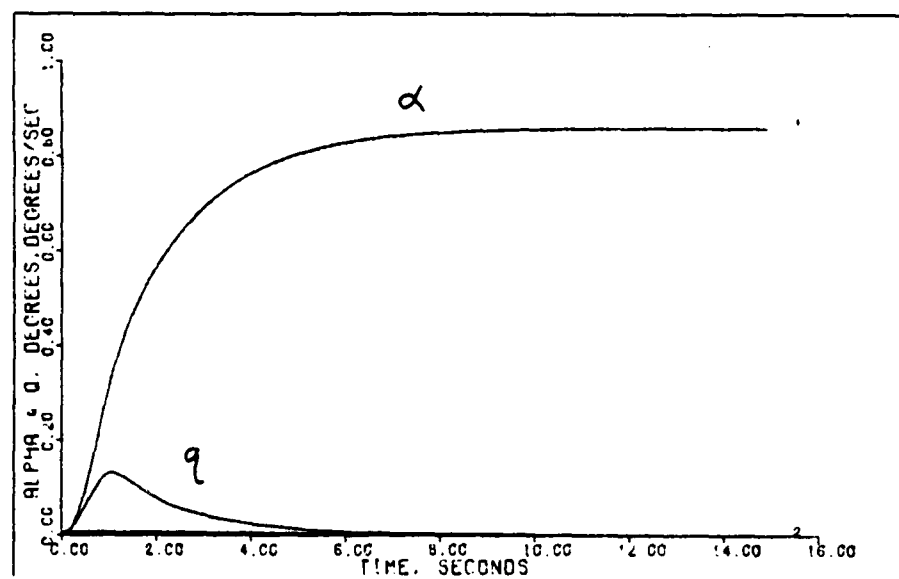


ALPHA & Q OUTPUTS TO VERTICAL TRANSLATION2: G. 7M. 15K FT

FIGURE B - 65

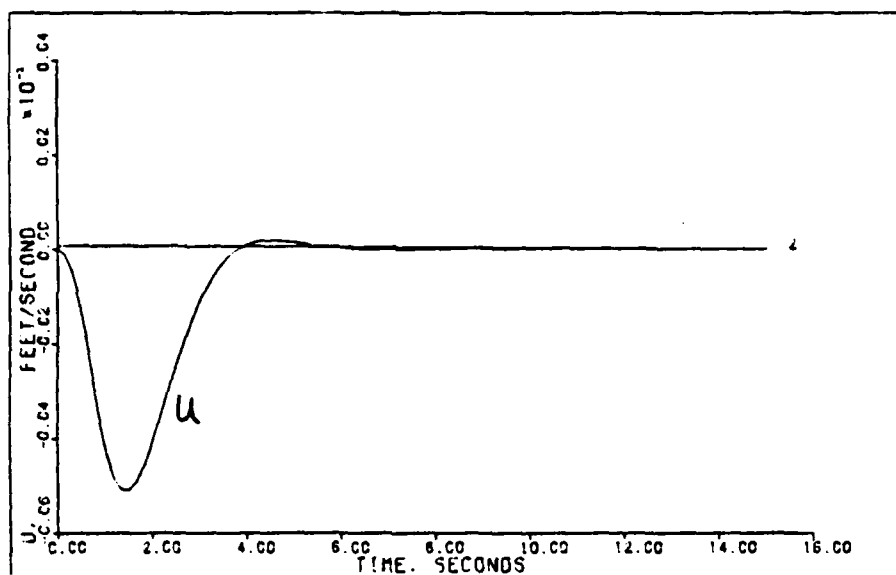


COMMANDED ALPHA INPUT TO VERTICAL TRANSLATION 2 C. 9M. GK FT

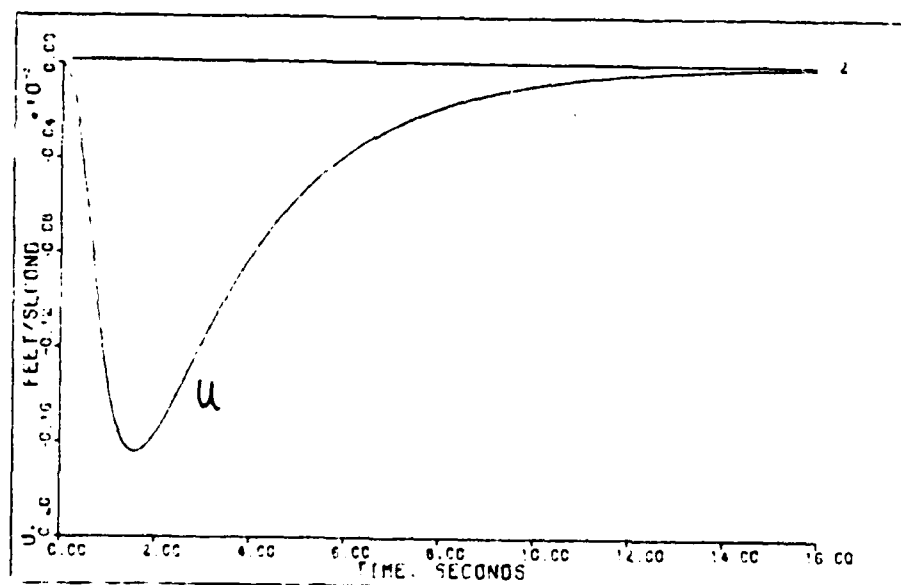


ALPHA & Q OUTPUTS TO VERTICAL TRANSLATION 2 C. 9M. GK FT

FIGURE B - 66



U OUTPUT TO VERTICAL TRANSLATION 2.0.4M. OK FT



J OUTPUT TO VERTICAL TRANSLATION 2.0.9M. 50K FT

FIGURE B - 67

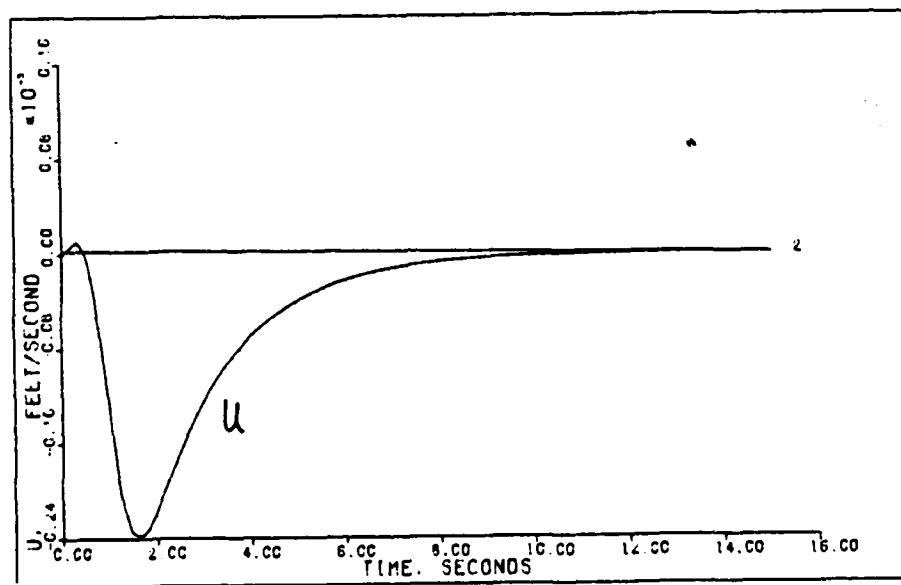
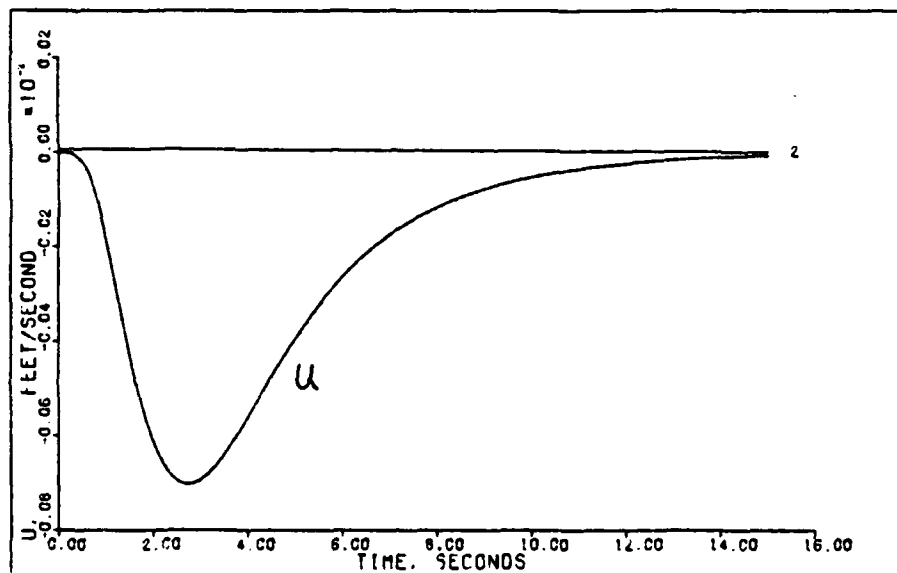
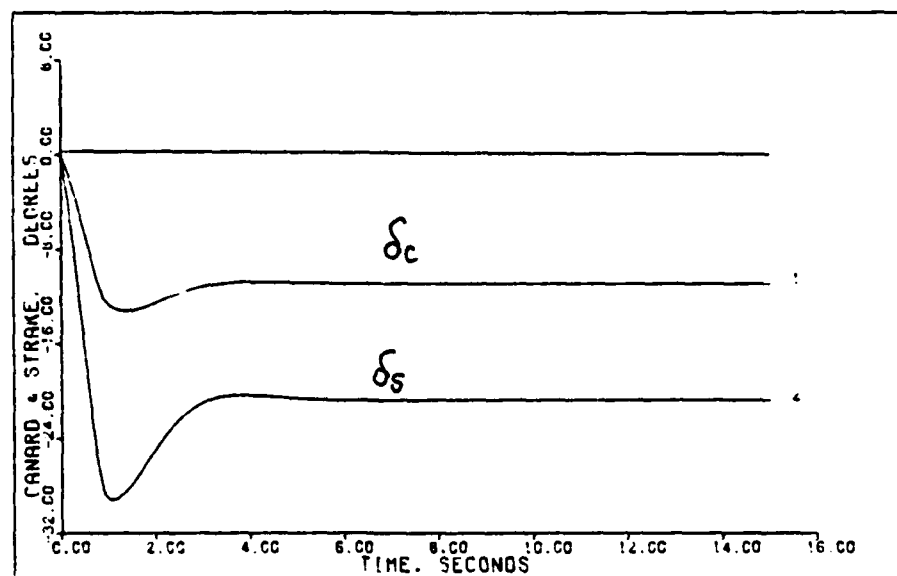
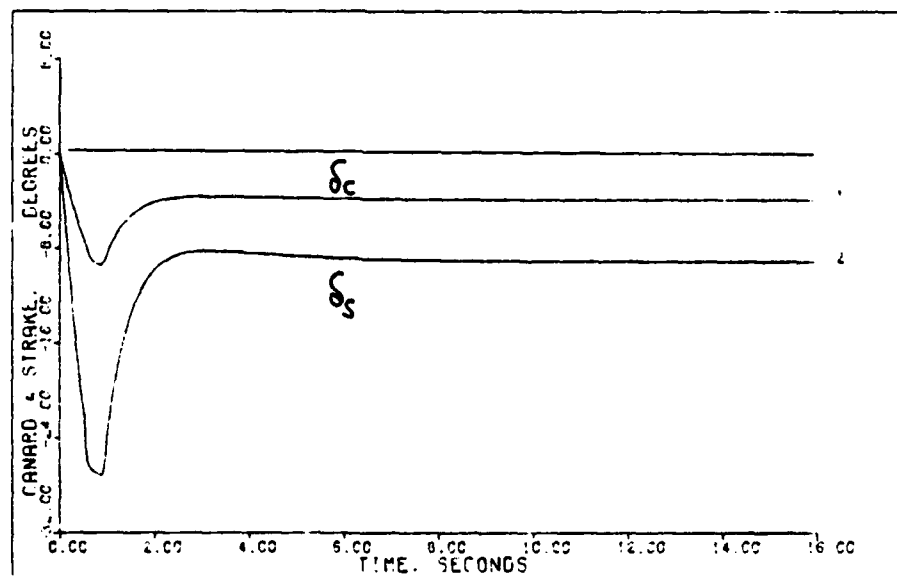


FIGURE B - 68

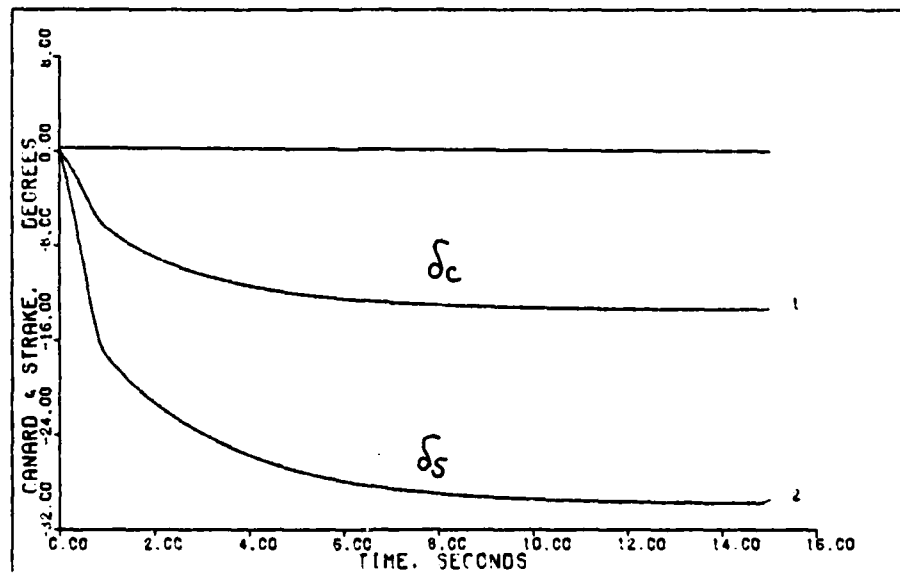


CANARD & STRAKE INPUTS TO VERTICAL TRANSLATION 0.4M. OK FT

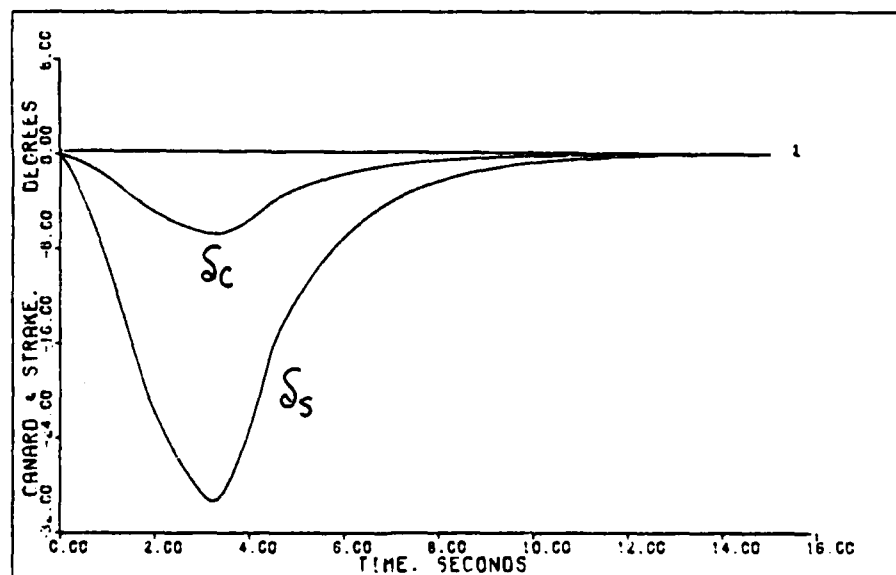


CANARD & STRAKE INPUTS TO VERTICAL TRANSLATION 0.5M. OK FT

FIGURE B - 69

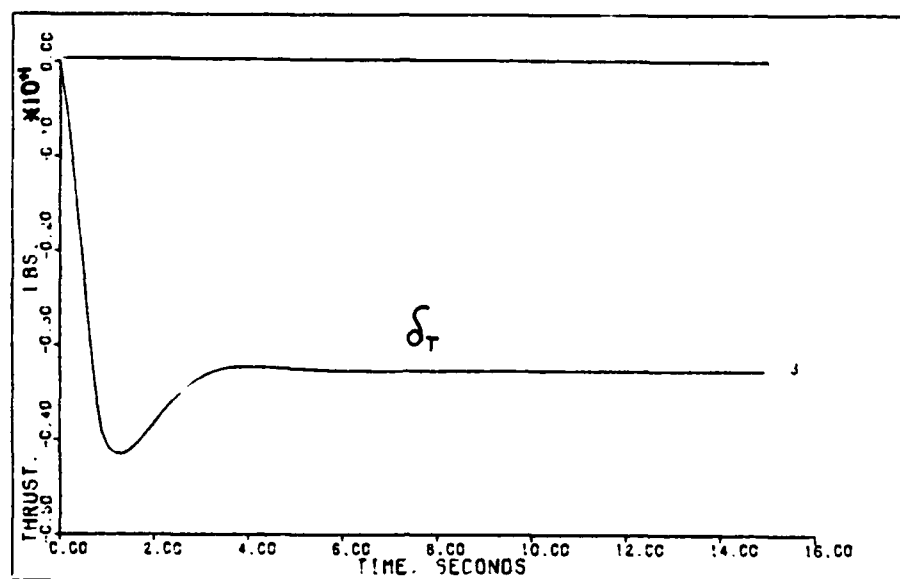


CANARD & STRAKE INPUTS TO VERTICAL TRANSLATION2: 7M. 15K FT

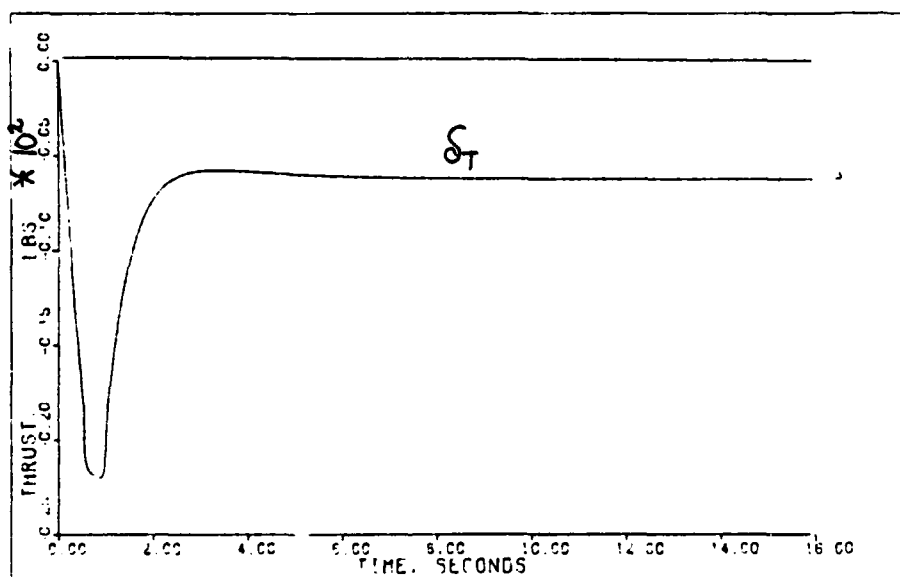


CANARD & STRAKE INPUTS TO VERTICAL TRANSLATION2: 9M. 0K FT

FIGURE B - 70



THRUST INPUT TO VERTICAL TRANSLATION 0.4M. CK FT



THRUST INPUT TO VERTICAL TRANSLATION 0.9M. 5CK FT

FIGURE B - 71

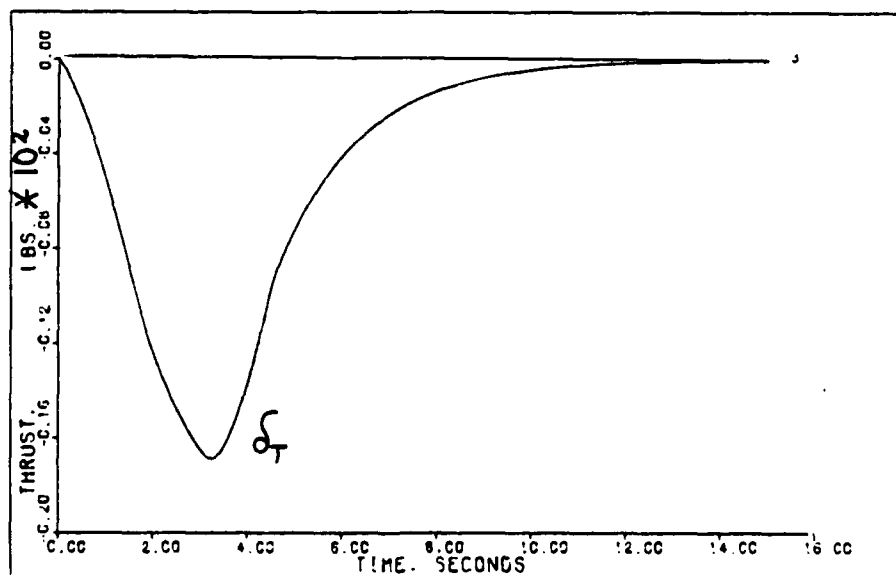
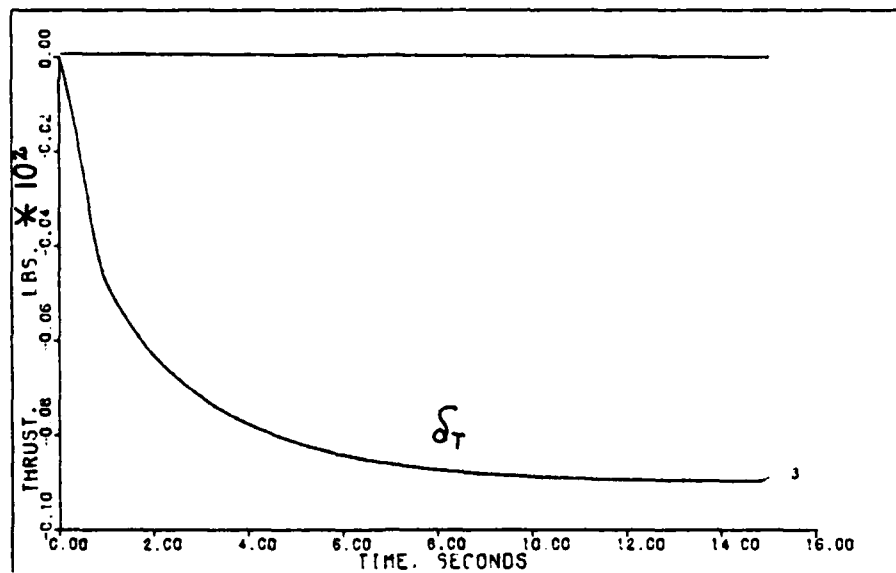
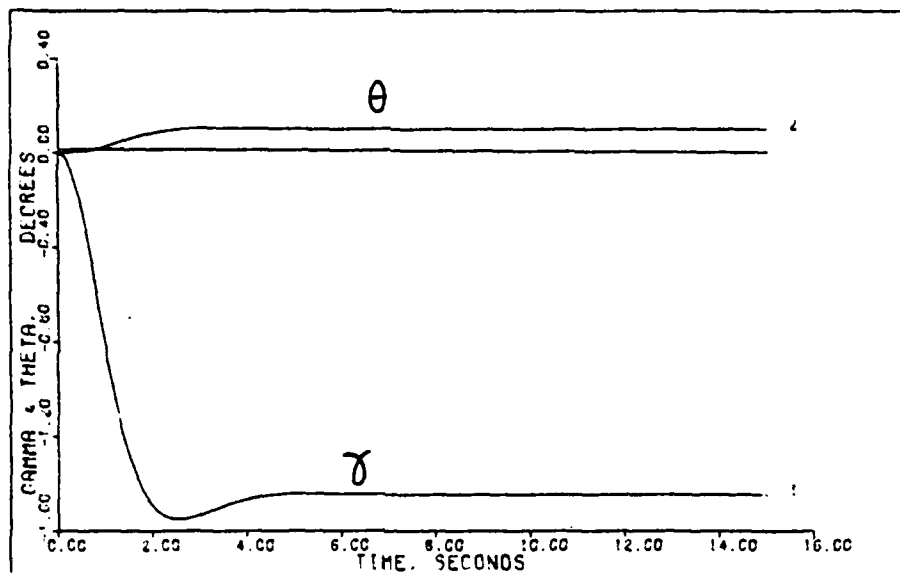
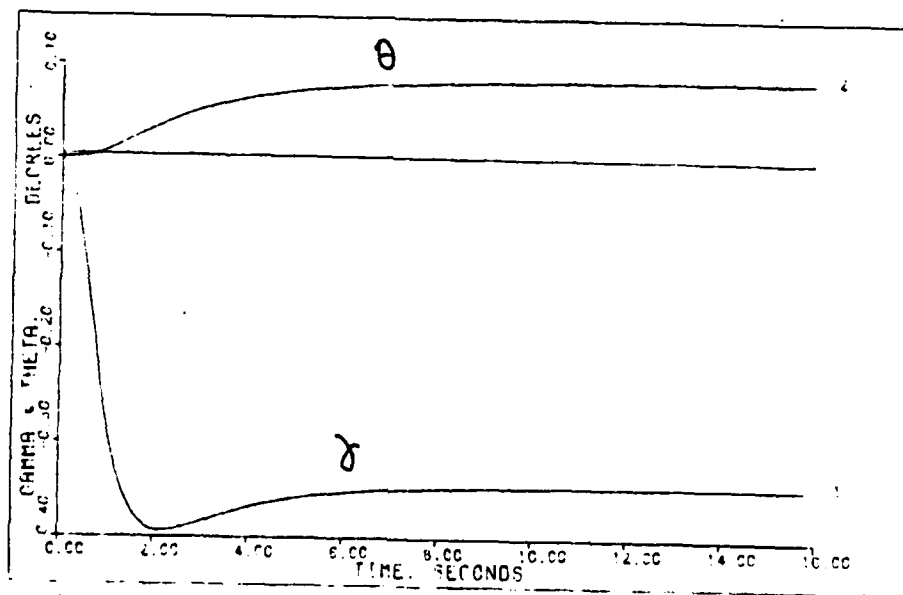


FIGURE B - 72

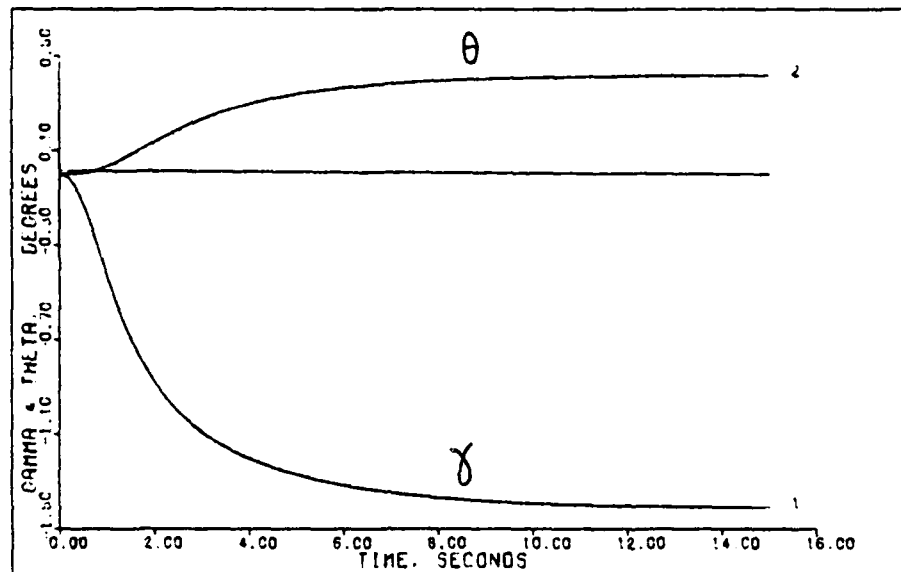


GAMMA & THETA FROM VERTICAL TRANSLATION 2:0.4M. OK FT

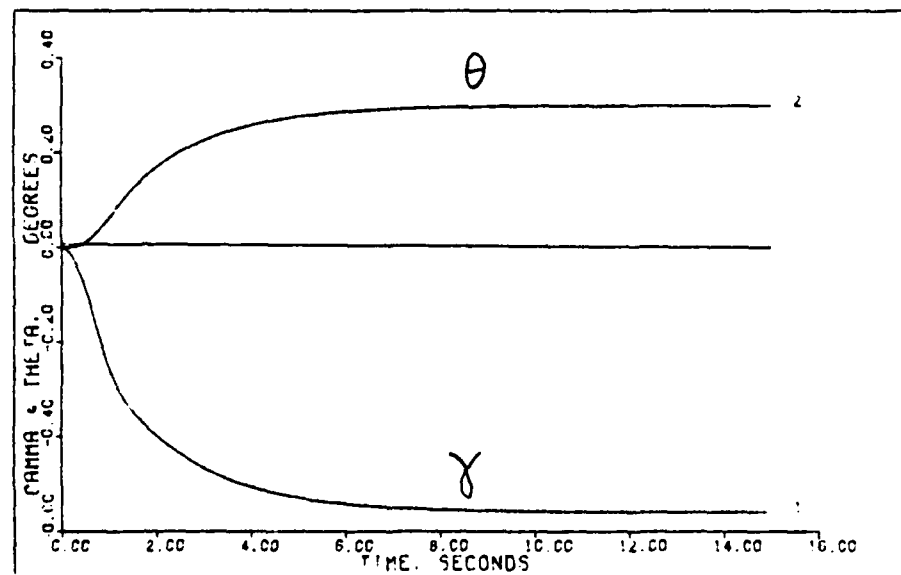


GAMMA & THETA FROM VERTICAL TRANSLATION 2:0.9M. 50K FT

FIGURE B - 73

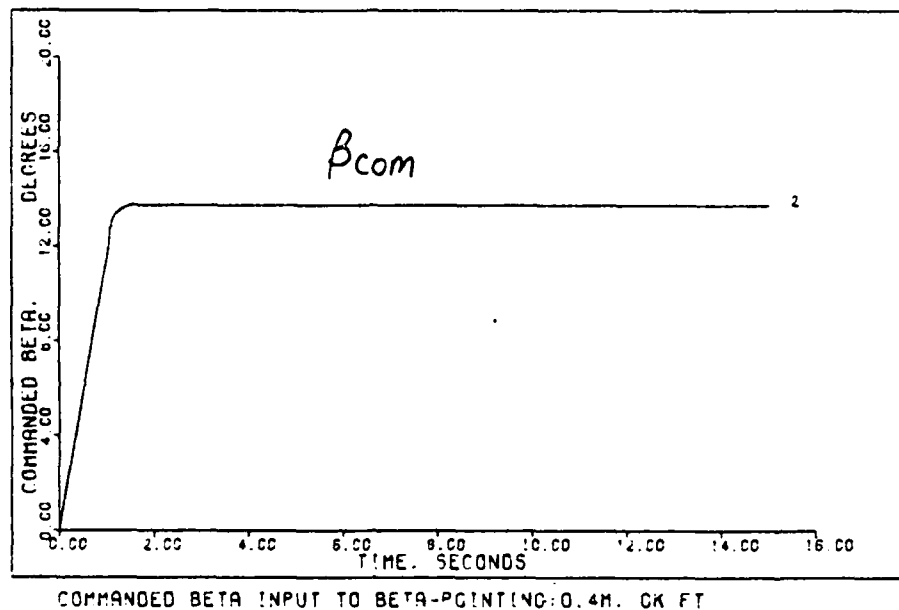


GAMMA & THETA FROM VERTICAL TRANSLATION 2:0.7M. 1SK FT

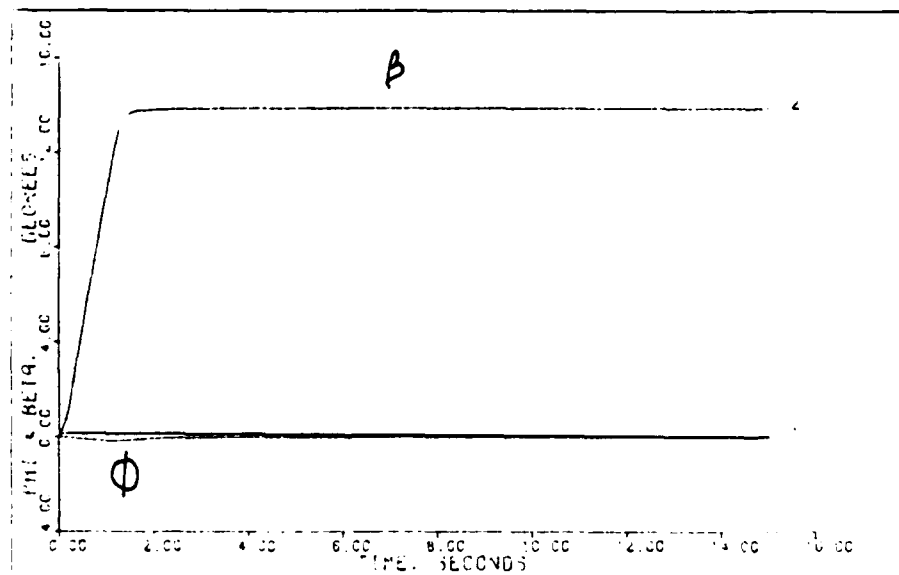


GAMMA & THETA FROM VERTICAL TRANSLATION 2:0.9M. 0K FT

FIGURE B - 74

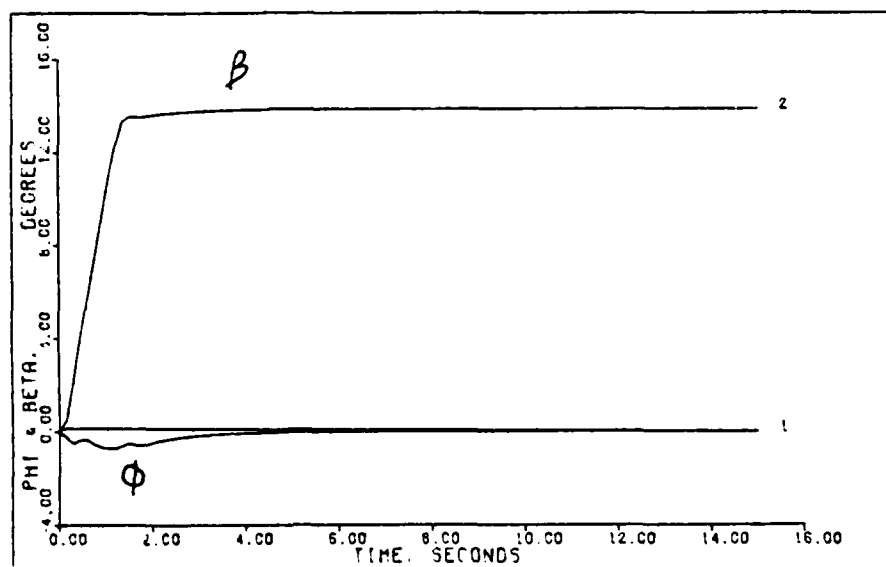


COMMANDED BETA INPUT TO BETA-POINTING: 0.4M. OK FT

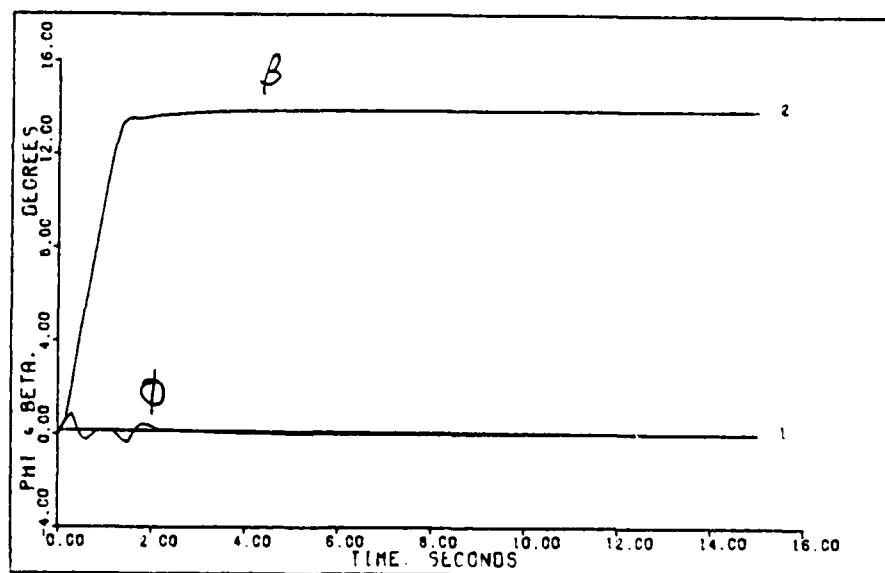


RO - SIDERIP ANDRE OUTPUTS TO BETA-POINTING: 0.4M. OK FT

FIGURE C - 1



PHI & BETA OUTPUTS TO BETA-POINTING: J.C. 4M. OK FT



PHI & BETA OUTPUTS TO BETA-POINTING: Z.C. 4M. OK FT

FIGURE C - 2

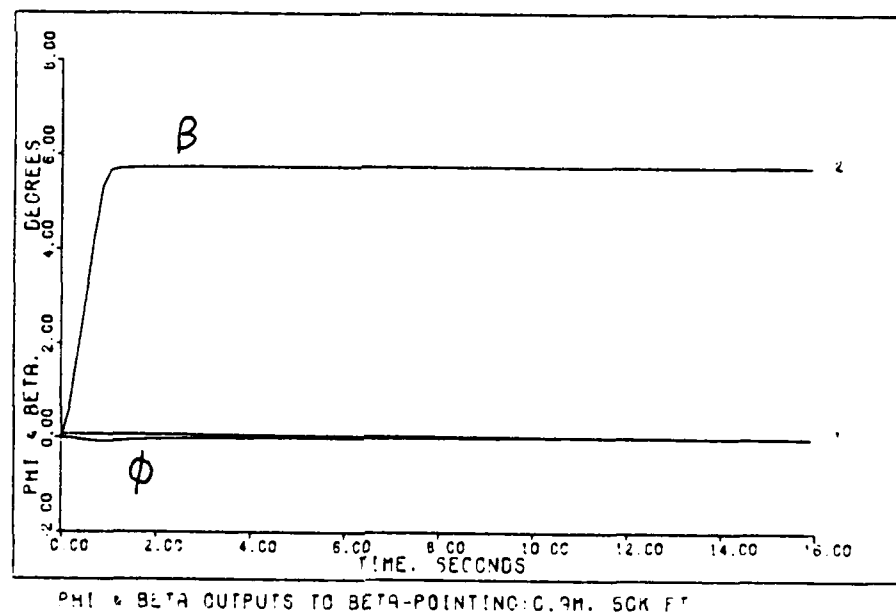
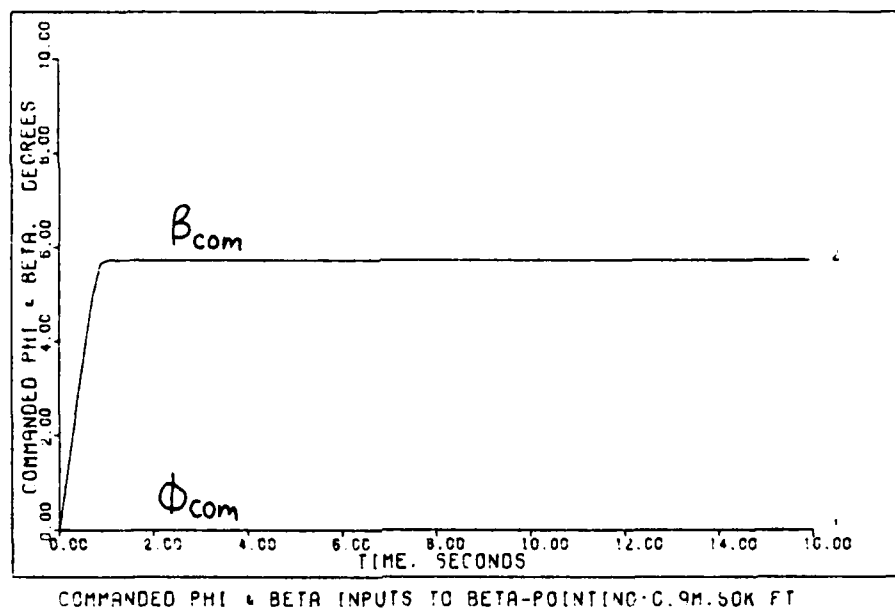
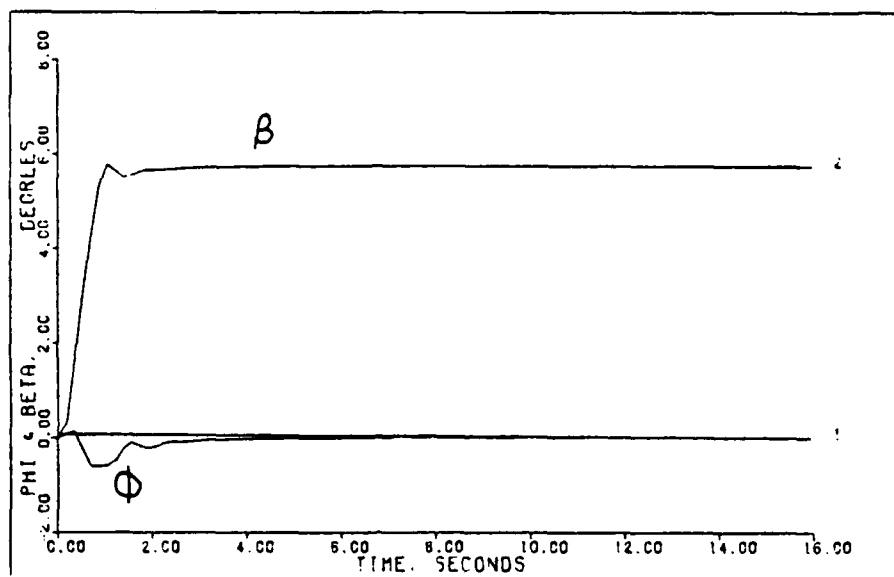
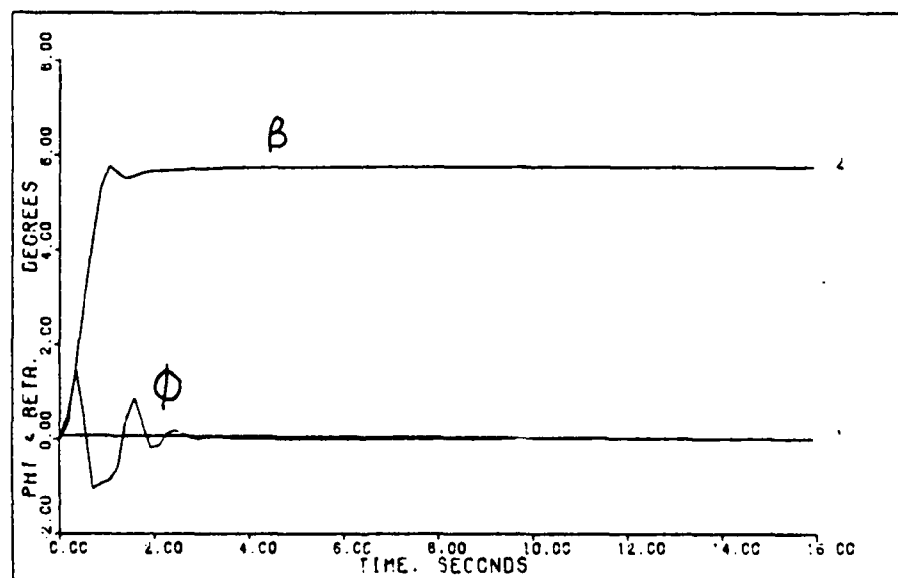


FIGURE C - 3

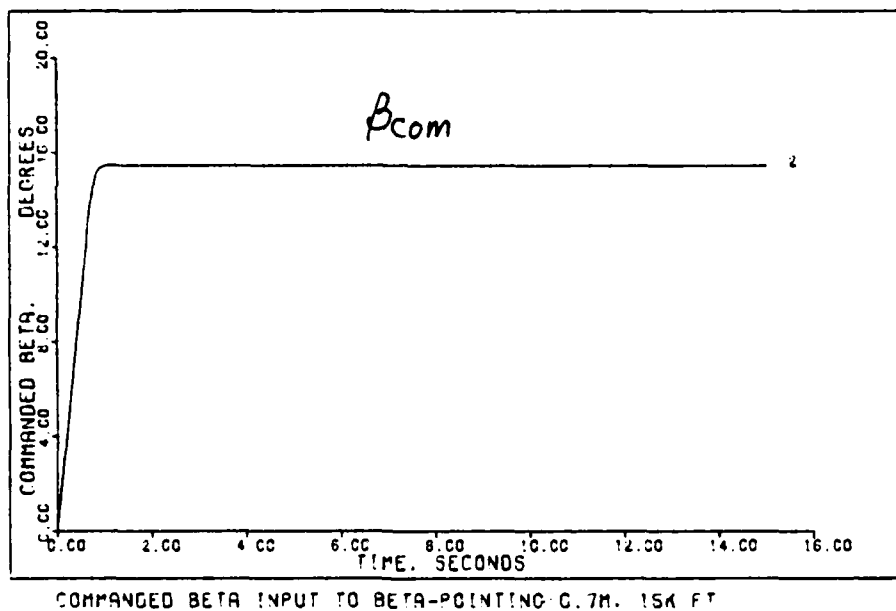


PHI & BETA OUTPUTS TO BETA-POINTING: J-C. 9M. 50K FT

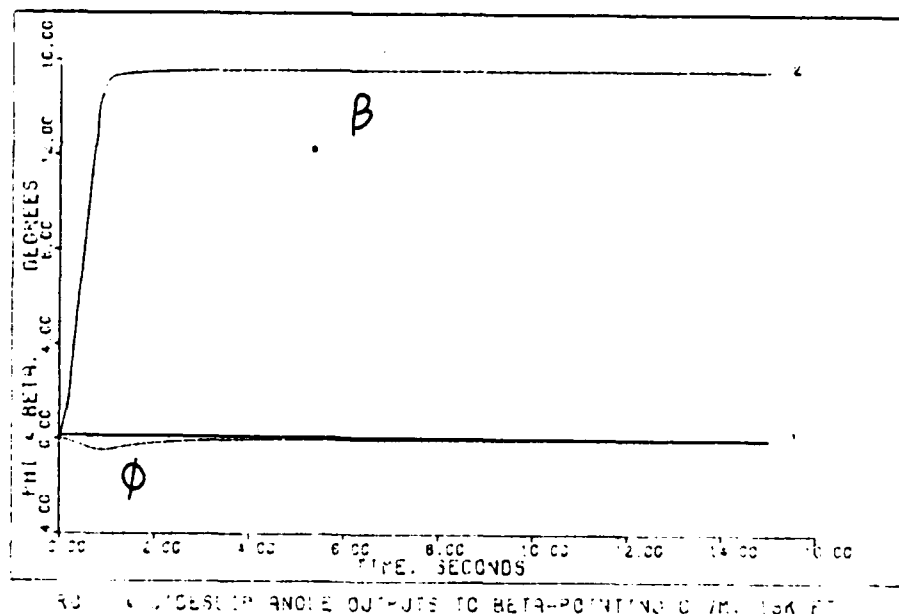


PHI & BETA OUTPUTS TO BETA-POINTING: L-C. 9M. 50K FT

FIGURE C - 4



COMMANDED BETA INPUT TO BETA-POINTING C.7M. 15K FT



PITCH & ROLL ANGLE OUTPUTS TO BETA-POINTING C.7M. 15K FT

FIGURE C - 5

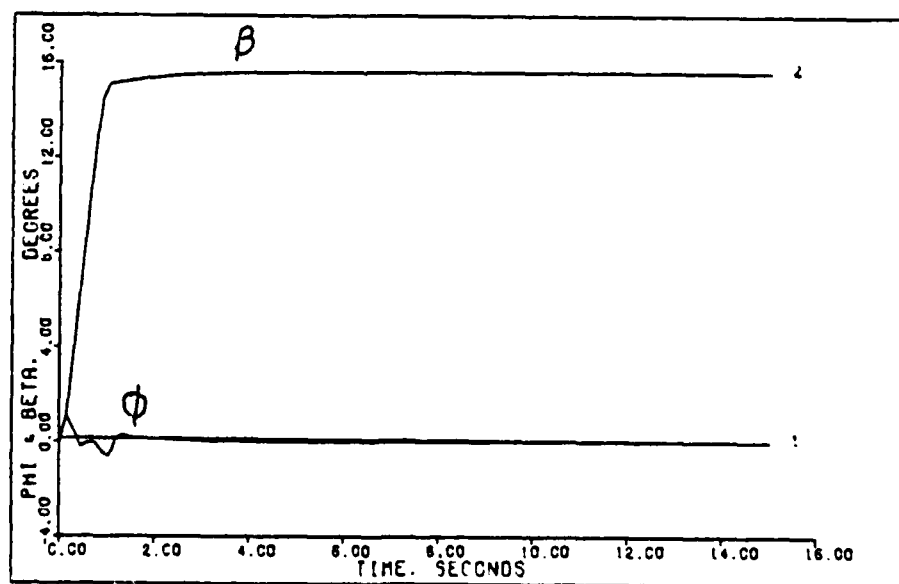
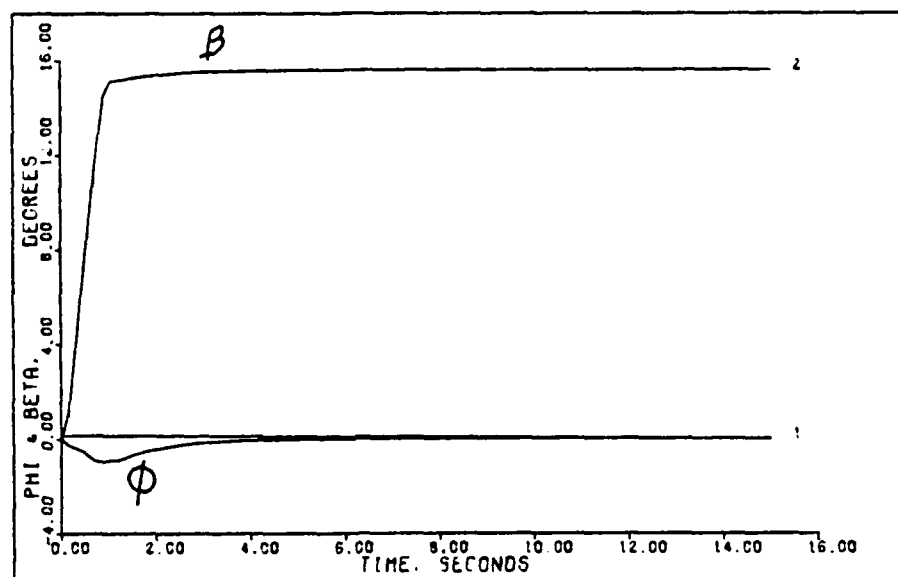
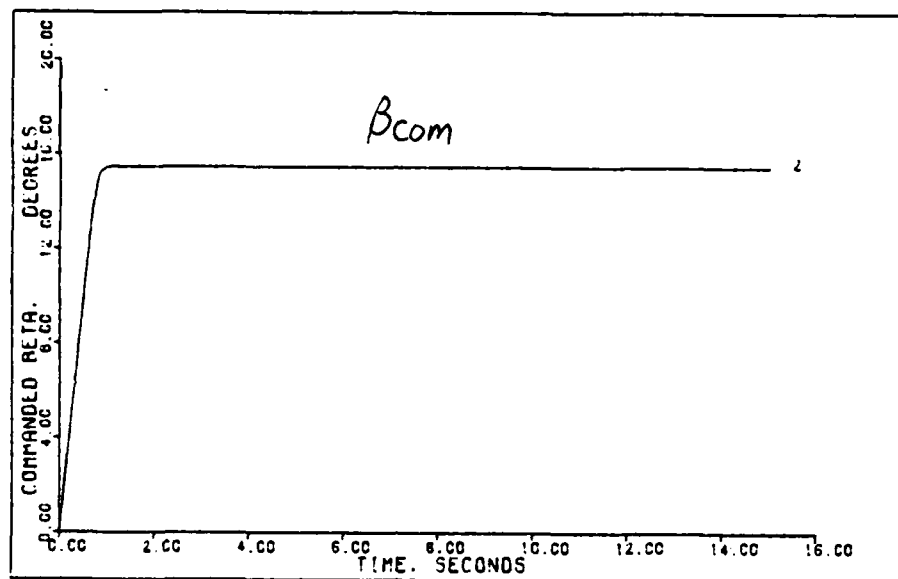
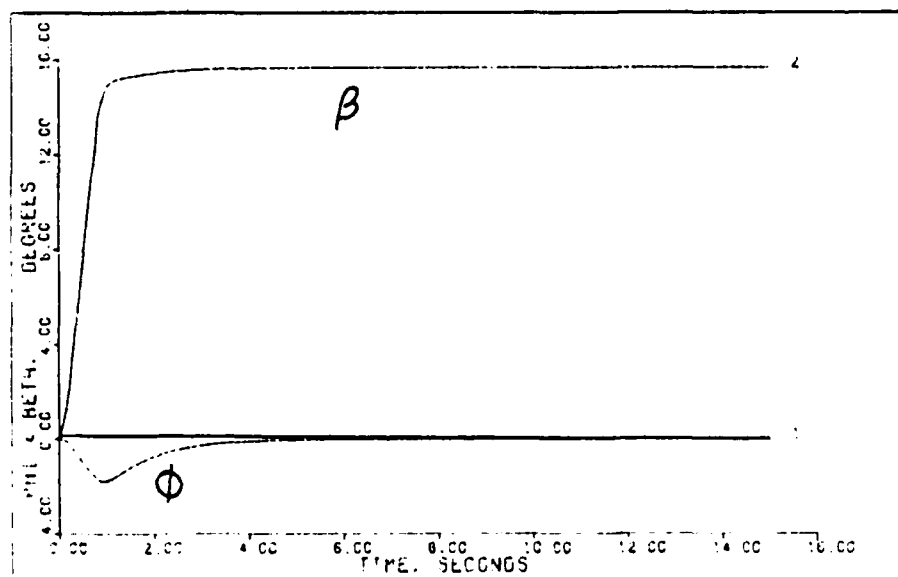


FIGURE C - 6

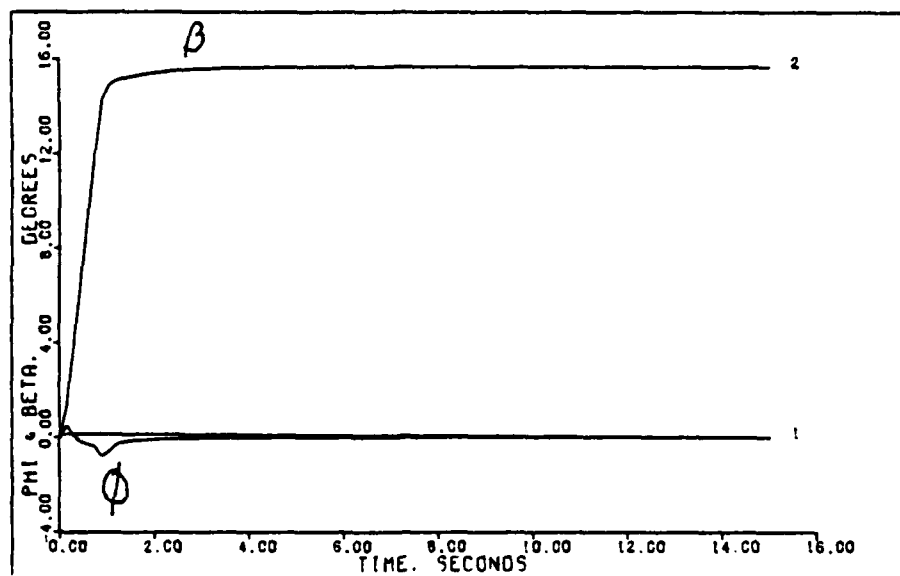


COMMANDED BETA INPUT TO BETA-POINTING G. 9M. OK FT

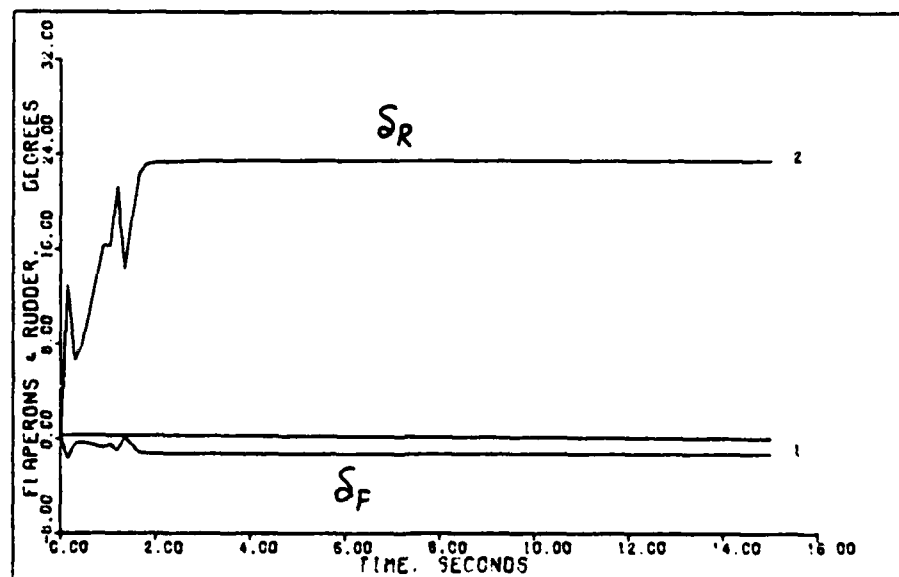


ROLL & SIDESLIP ANGLE OUTPUTS TO BETA-POINTING G. 9M. OK FT

FIGURE C - 7

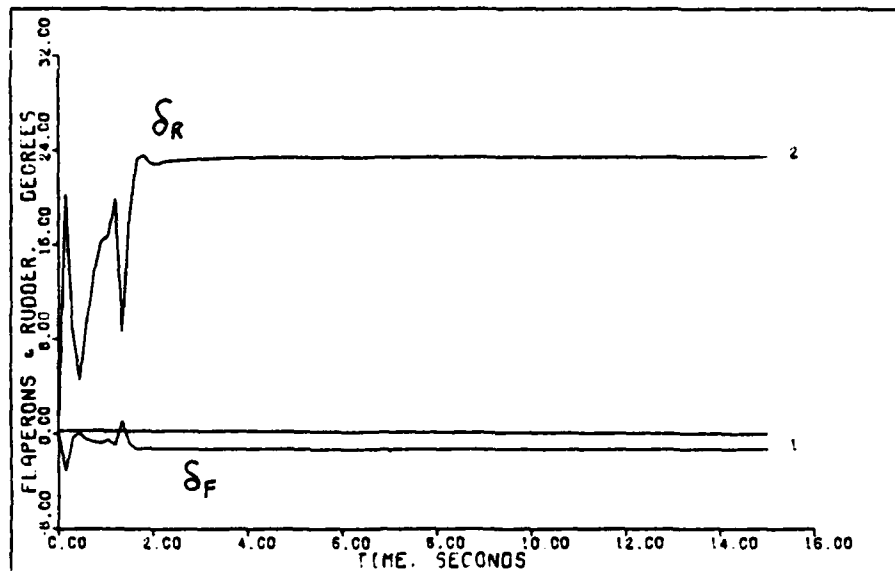


PHI & BETA OUTPUTS TO BETA-POINTING: Z: C.9M. OK FT

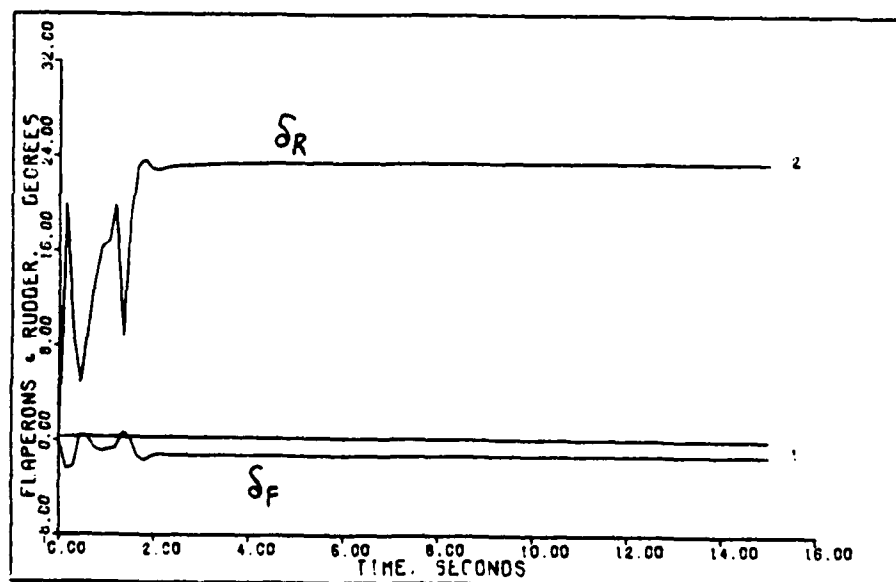


FLAPERON & RUDDER INPUTS TO BETA-POINTING: C.4M. OK FT

FIGURE C - 8



FLAPERON & RUDDER INPUTS TO BETA-POINTING: U:G. 4M. 0K FT



FLAPERON & RUDDER INPUTS TO BETA-POINTING: L:G. 4M. 0K FT

FIGURE C - 9

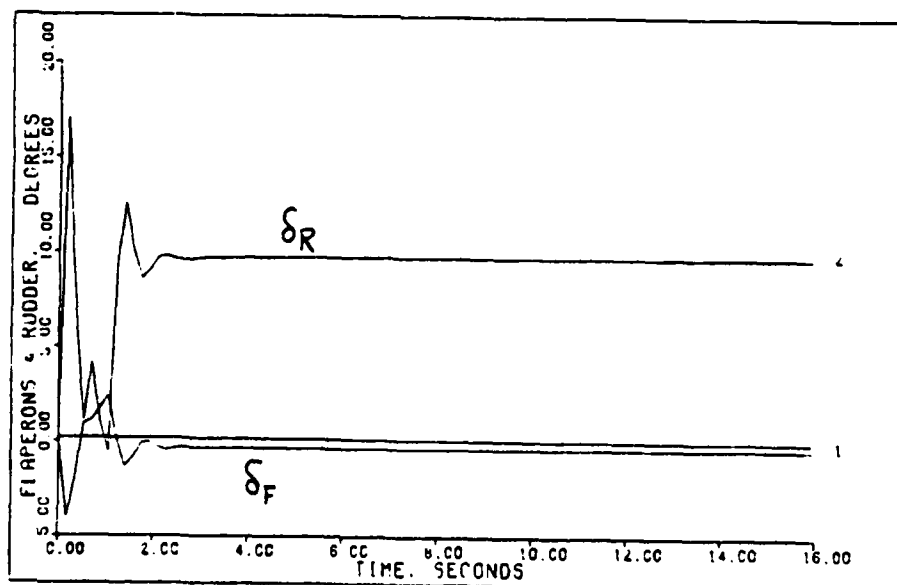
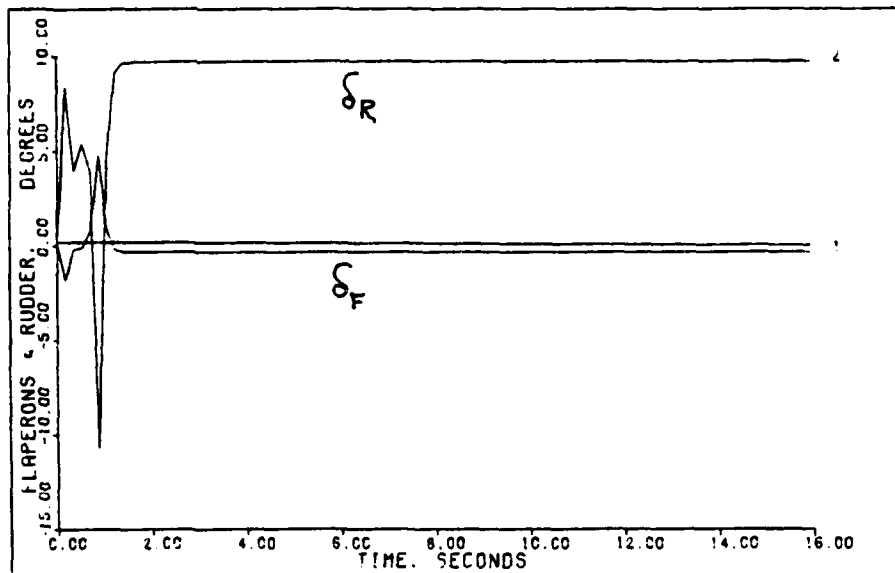
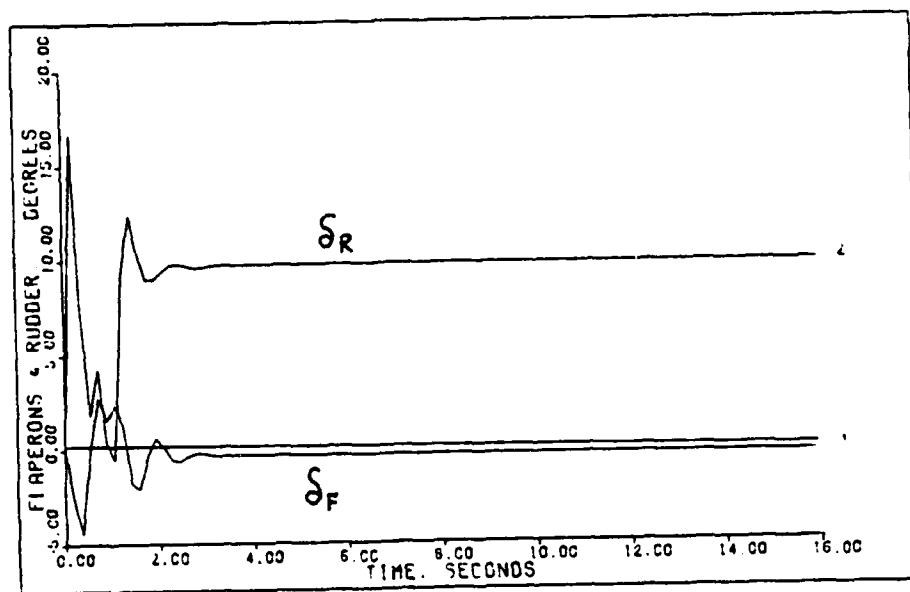
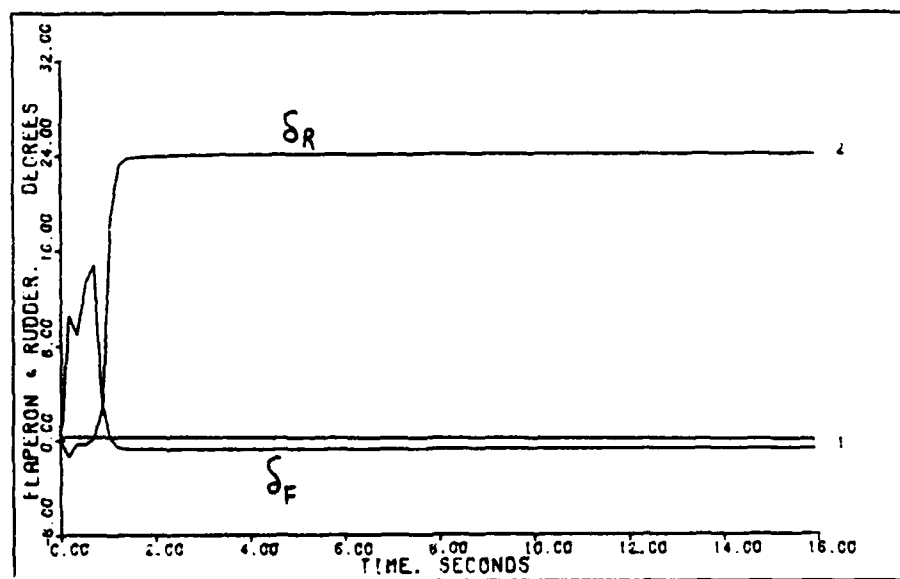


FIGURE C - 10

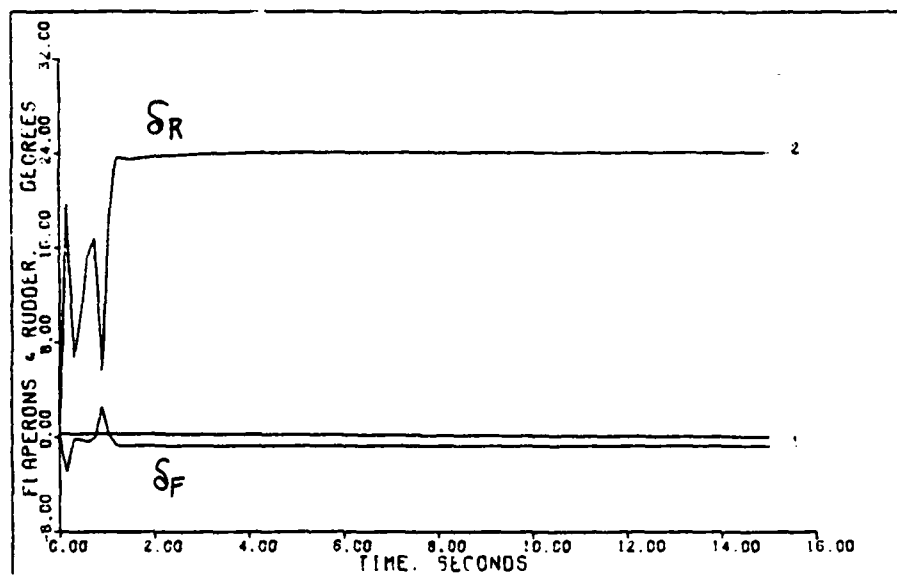


FLAPERONS & RUDDER INPUTS TO BETA-POINTING: 200.9M, 50K FT

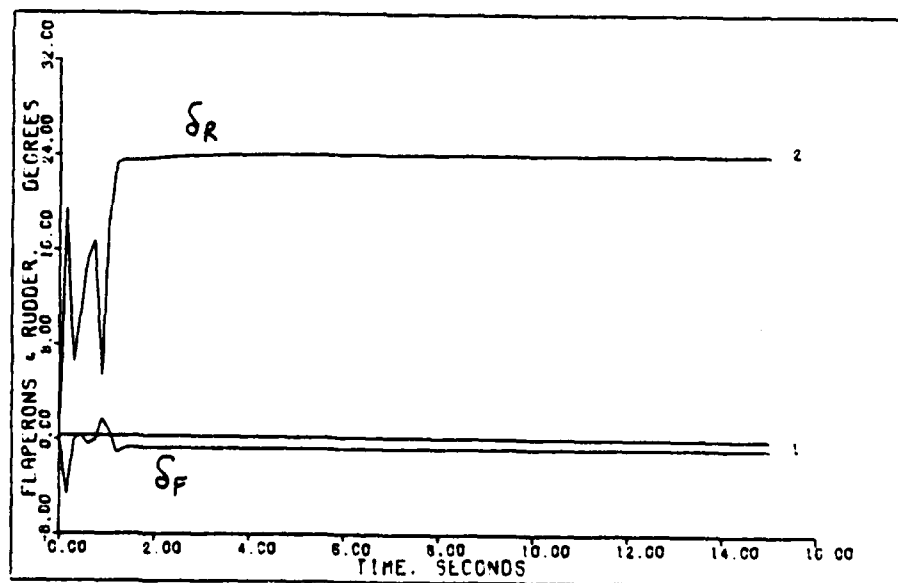


FLAPERON & RUDDER INPUTS TO BETA-POINTING: 0.7M, 15K FT

FIGURE C - 11

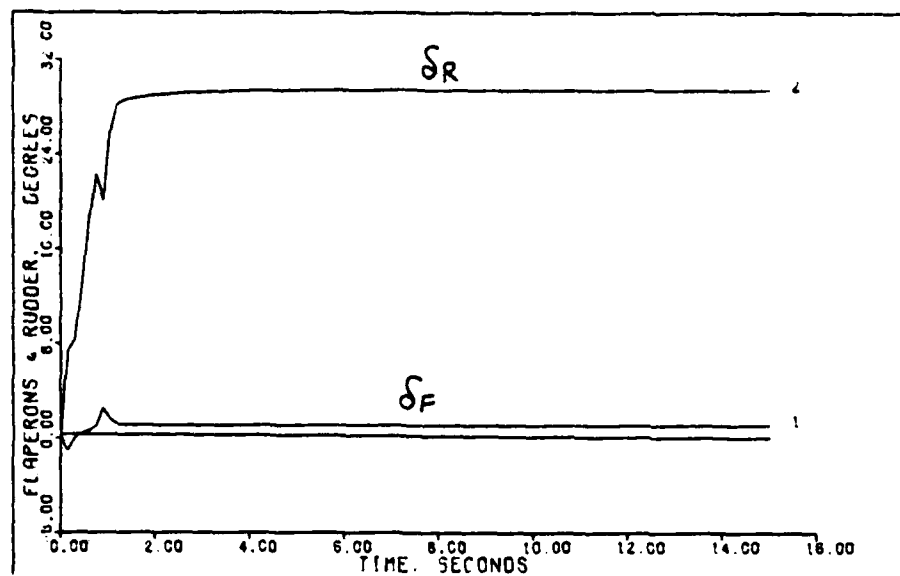


FLAPERON & RUDDER INPUTS TO BETA-POINTING: J:G. 7M. 15K FT

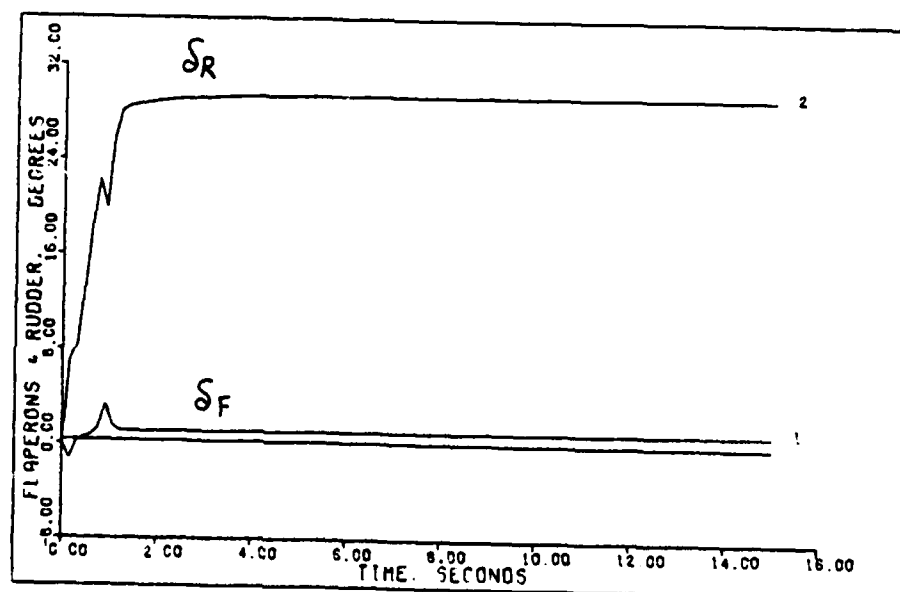


FLAPERONS & RUDDER INPUTS TO BETA-POINTING: Z:G. 7M. 15K FT

FIGURE C - 12

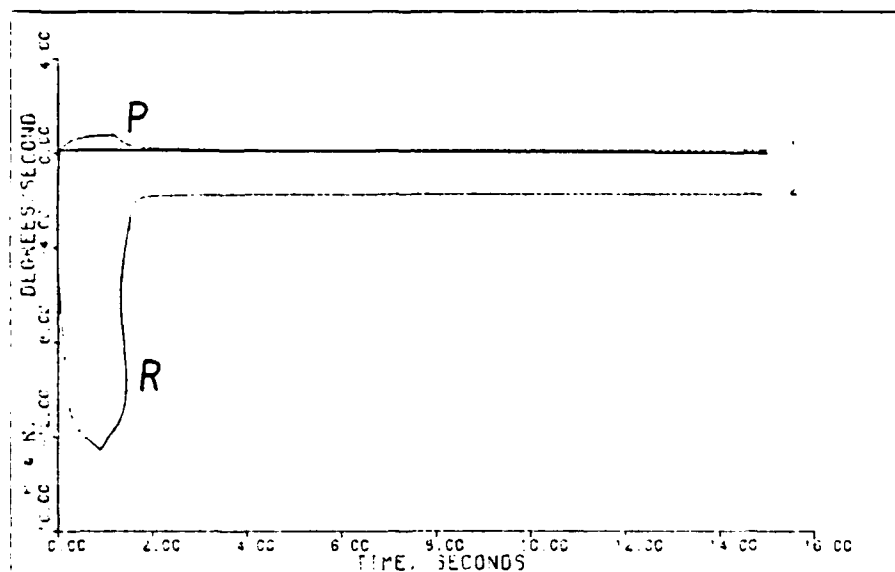


FLAPERON & RUDDER INPUTS TO BETA-POINTING: 0.9M. OK FT

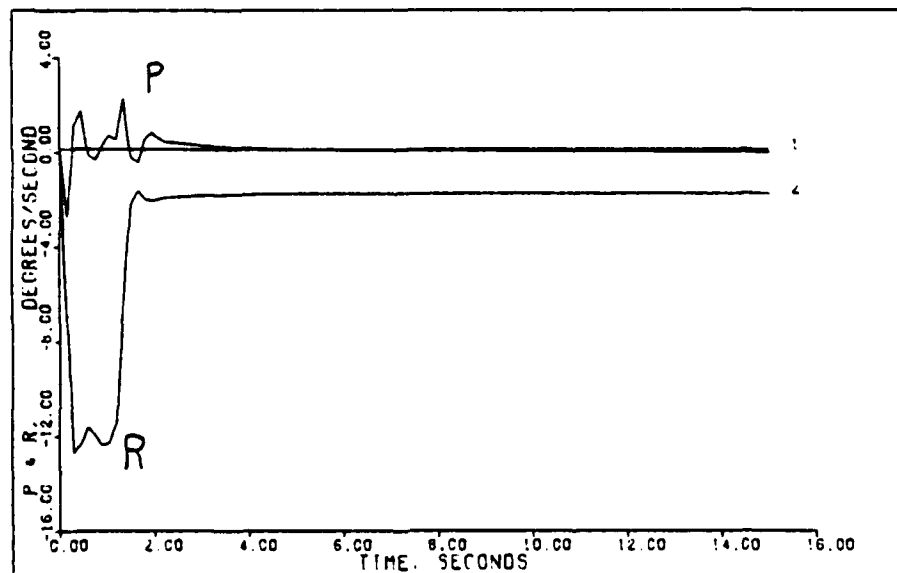


FLAPERON & RUDDER INPUTS TO BETA-POINTING: 2:0.9M. OK FT

FIGURE C - 13

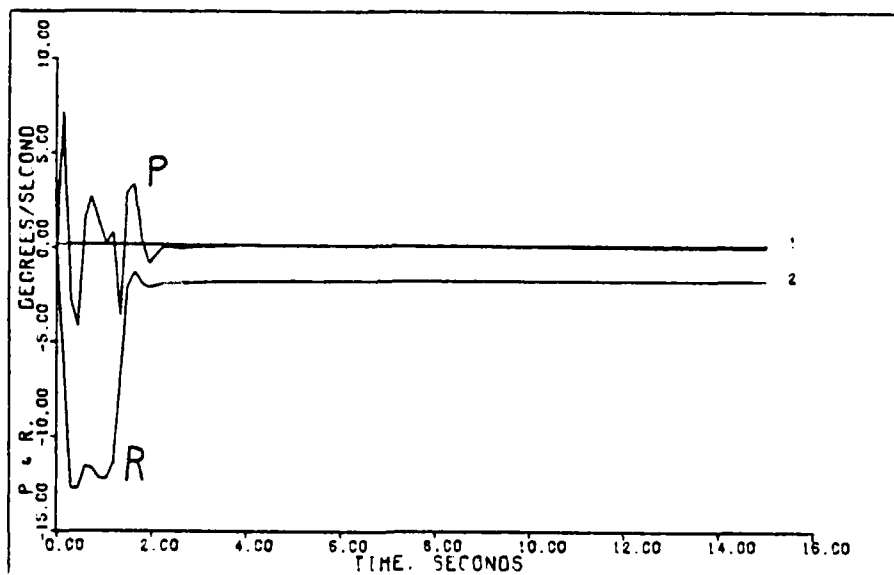


ROLL & YAW RATES FROM BETA-POINTING: 0.4M, OK FT

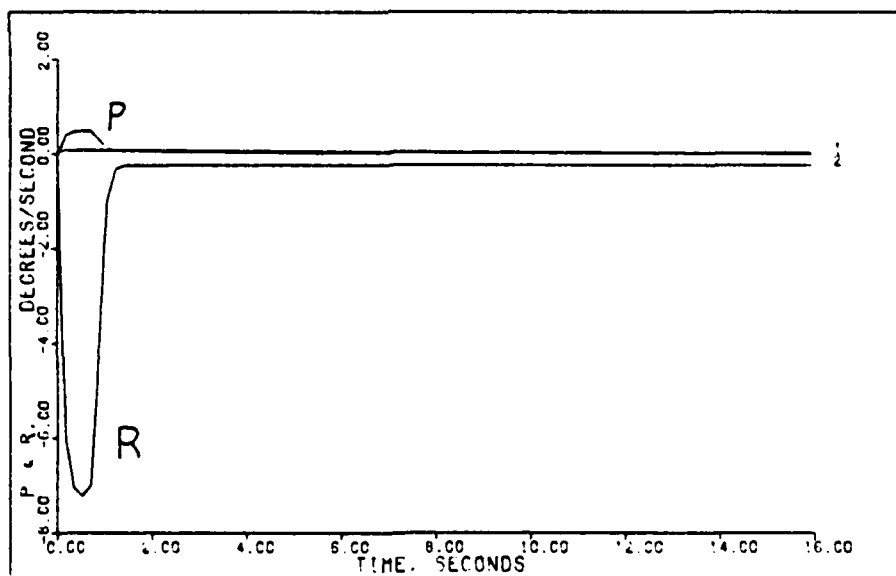


ROLL & YAW RATES FROM BETA-POINTING: 0.4M, OK FT

FIGURE C - 14

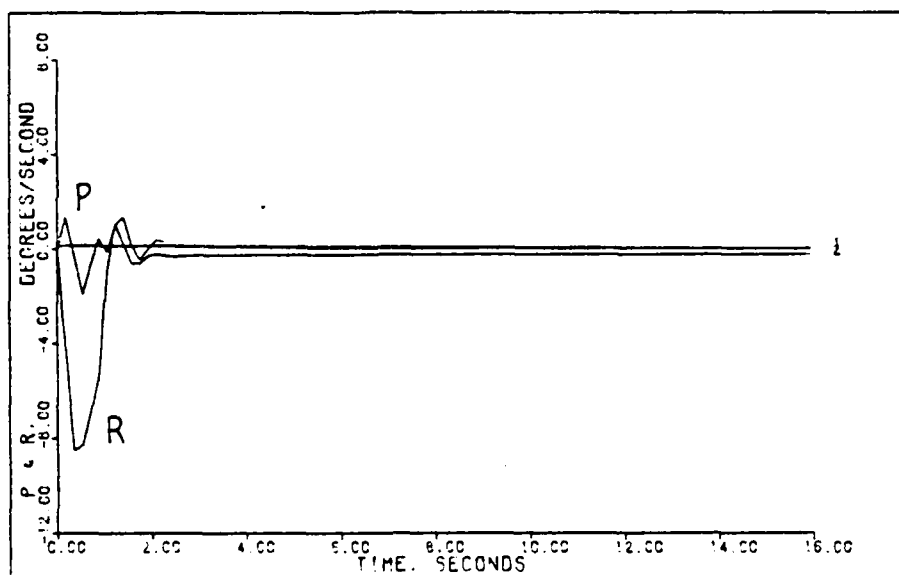


ROLL & YAW RATES FROM BETA-POINTING: 0.4M, 0K FT

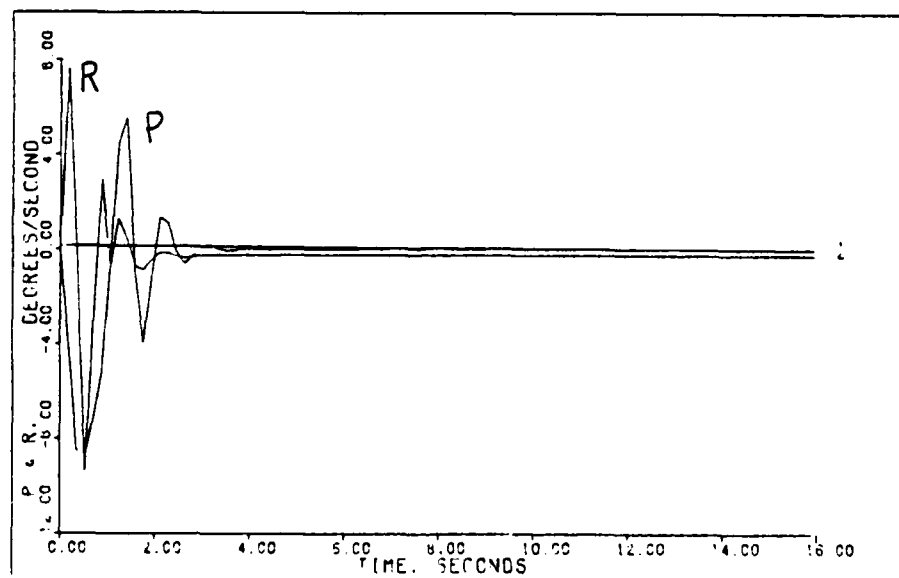


ROLL & YAW RATES FROM BETA-POINTING: 0.9M, 50K FT

FIGURE C - 15



ROLL & YAW RATES FROM BETA-POINTING 0.9M, 50K FT



ROLL & YAW RATES FROM BETA-POINTING 2.0M, 50K FT

FIGURE C - 16

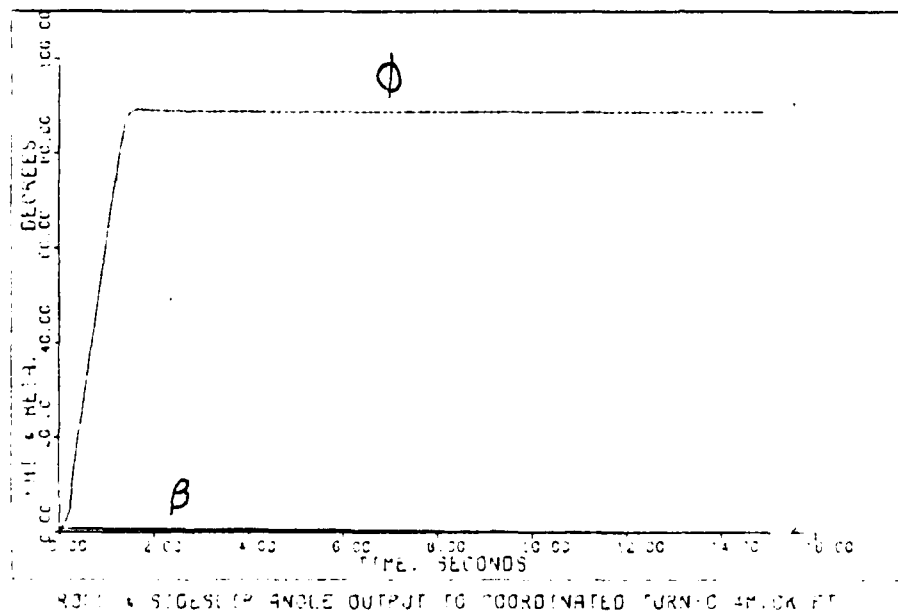
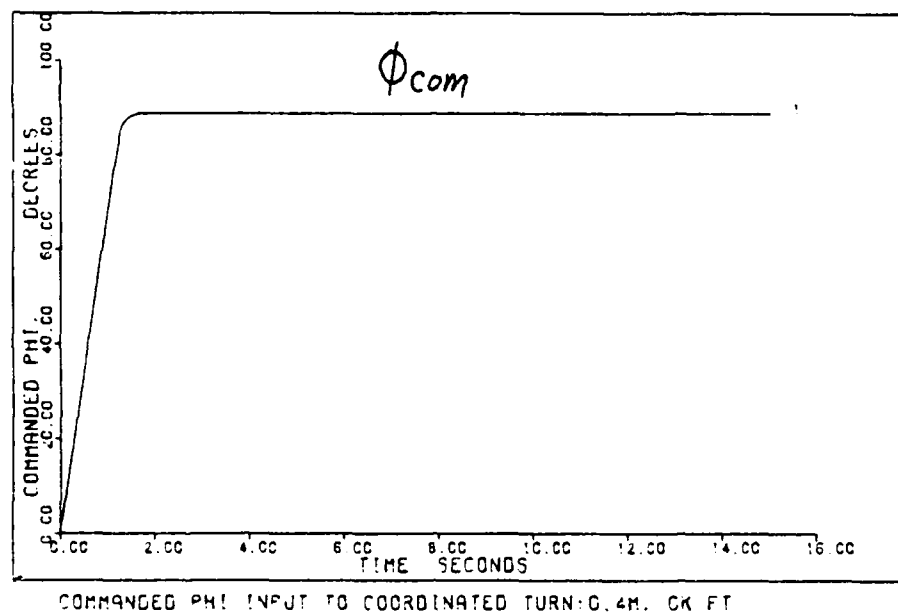
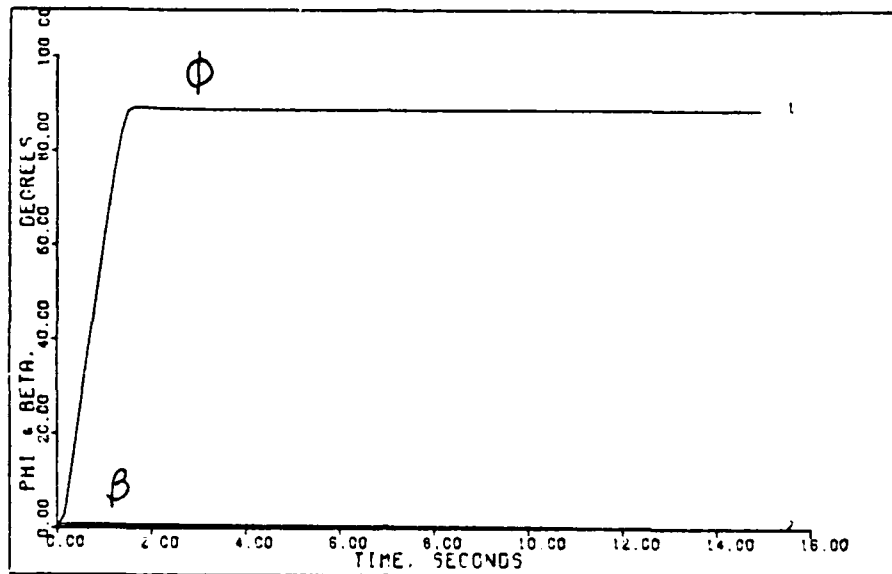
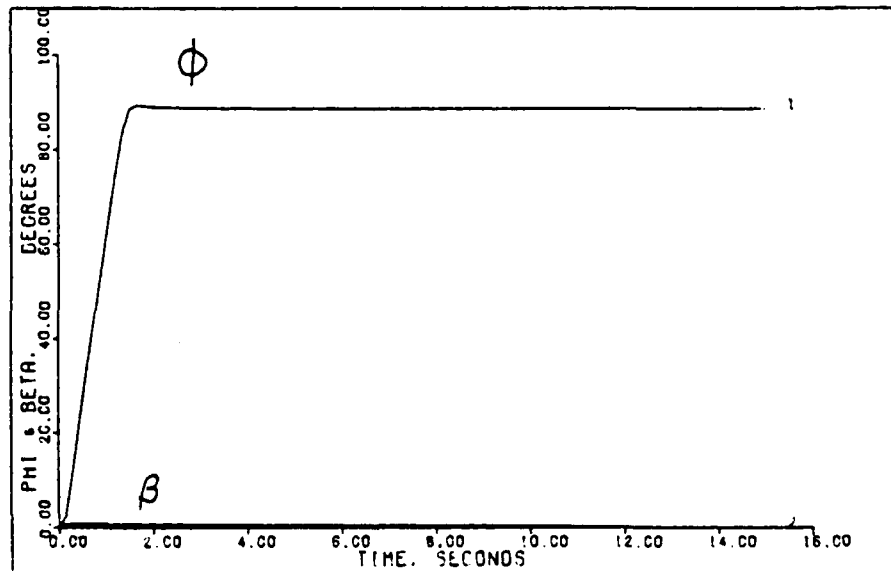


FIGURE C - 17

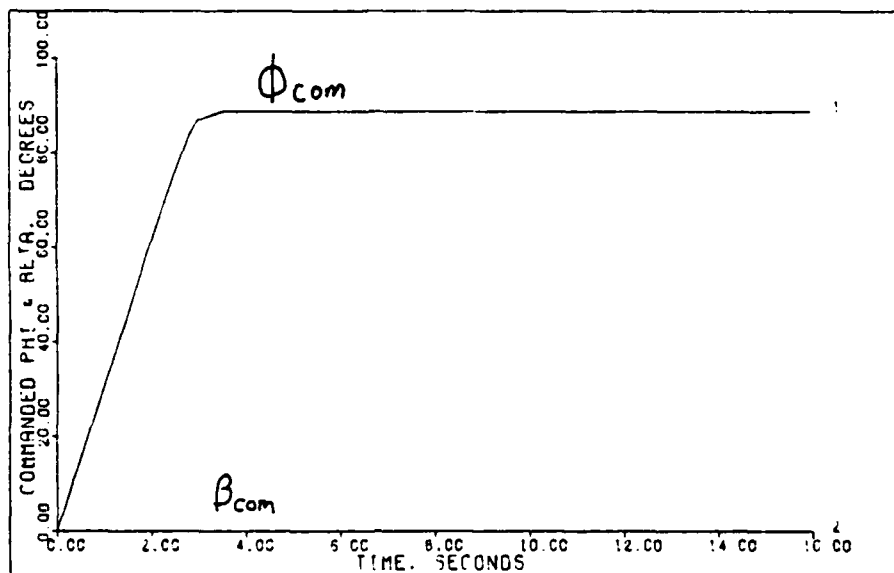


PHI & BETA OUTPUTS TO COORDINATED TURN: J: C. 4M. OK FT

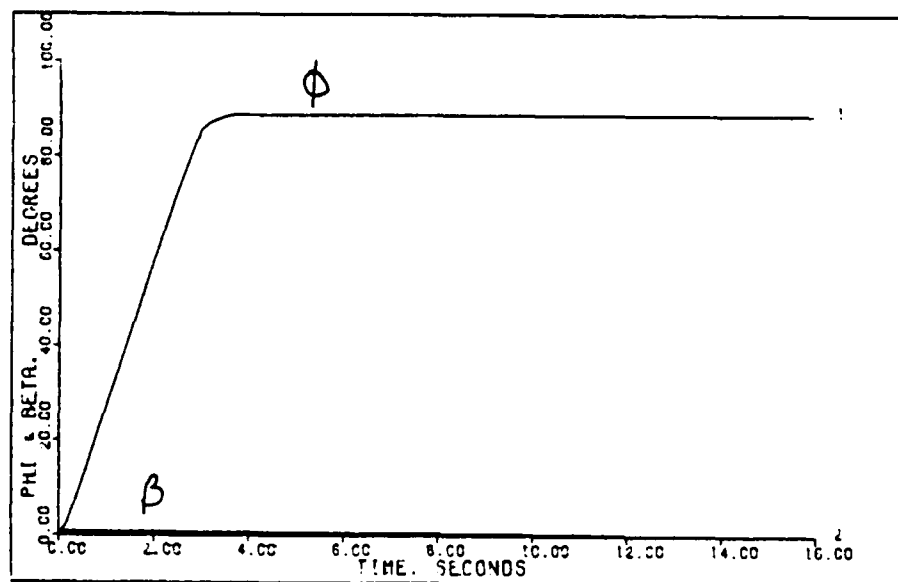


PHI & BETA OUTPUTS TO COORDINATED TURN: Z: C. 4M. OK FT

FIGURE C - 18



COMMANDED PHI & BETA INPUTS TO COORDINATED TURN: 9M. SCK FT



PHI & BETA OUTPUTS TO COORDINATED TURN: 0.9M. SCK FT

FIGURE C - 19

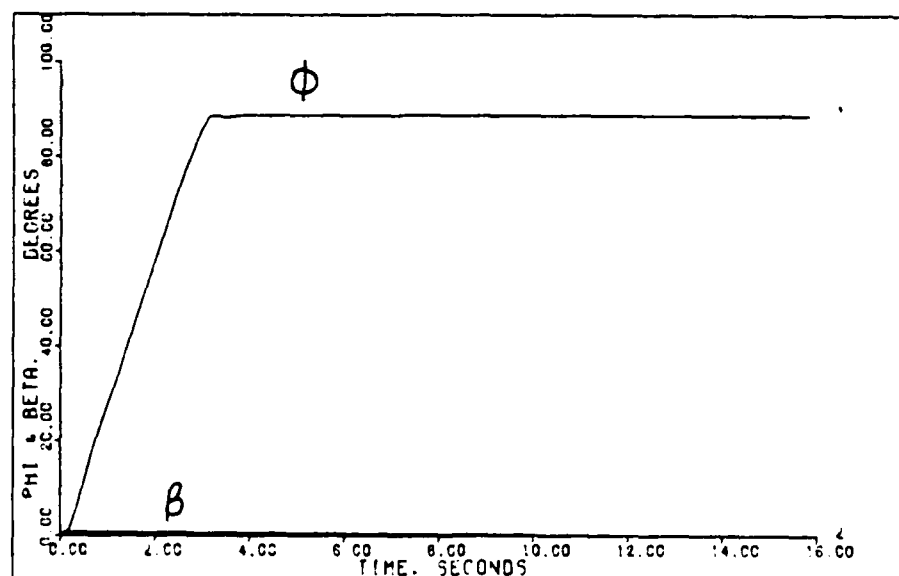
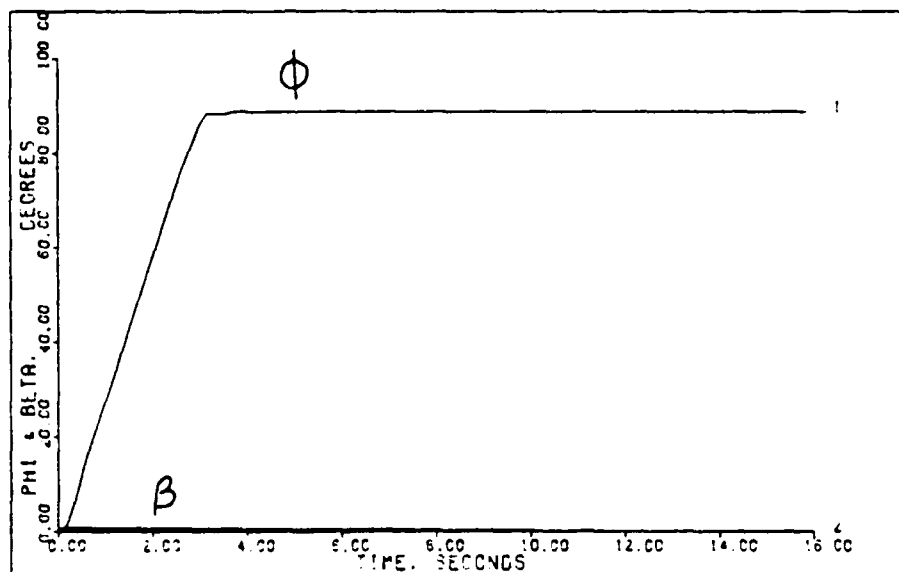
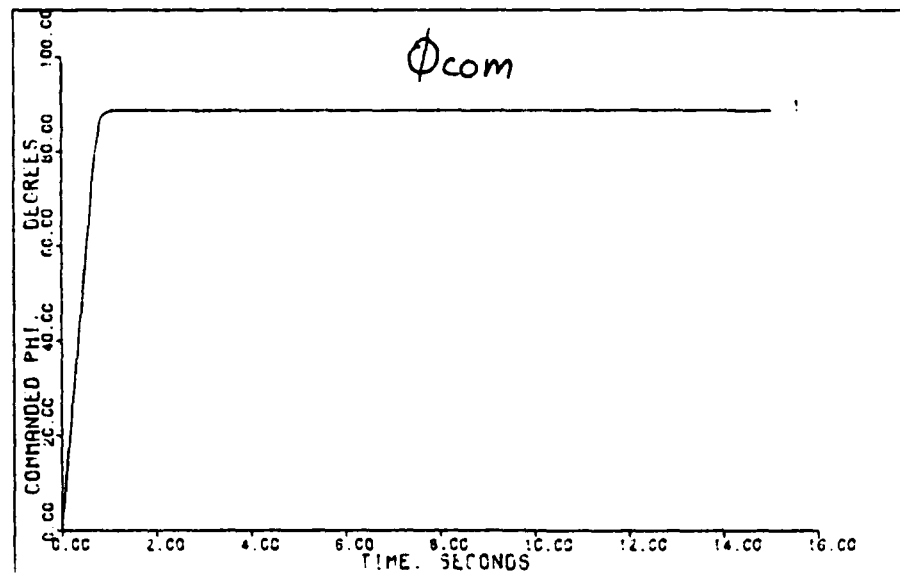
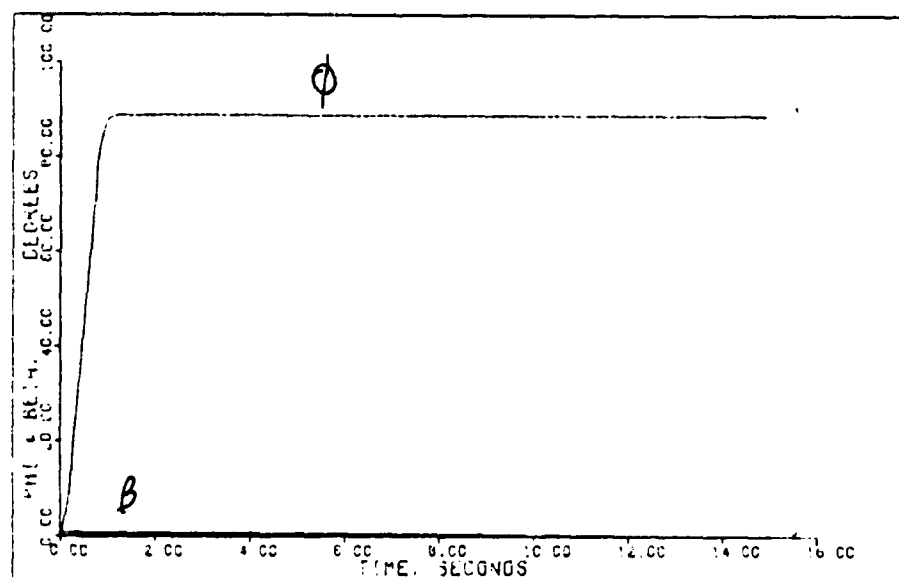


FIGURE C - 20

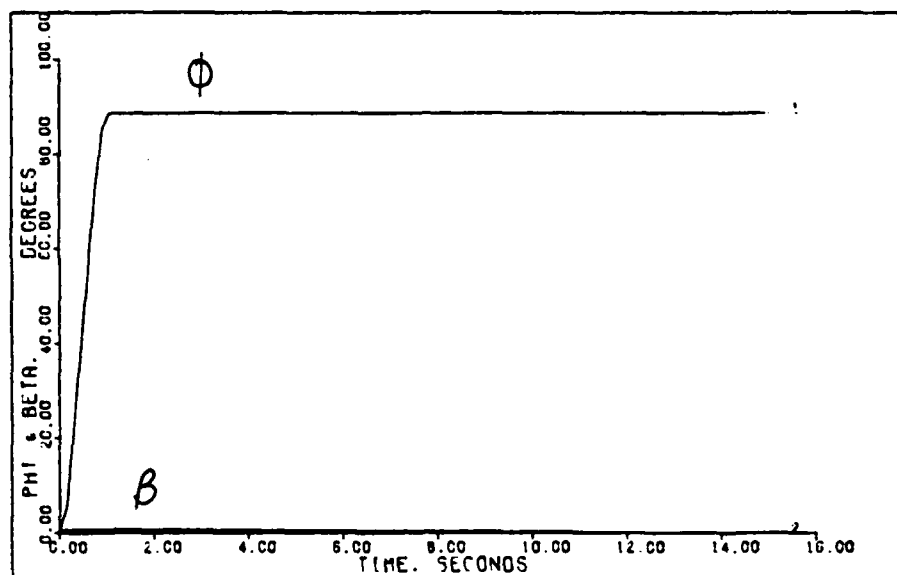


COMMANDED PHI INPUT TO COORDINATED TURN: 0.7M, 15K FT

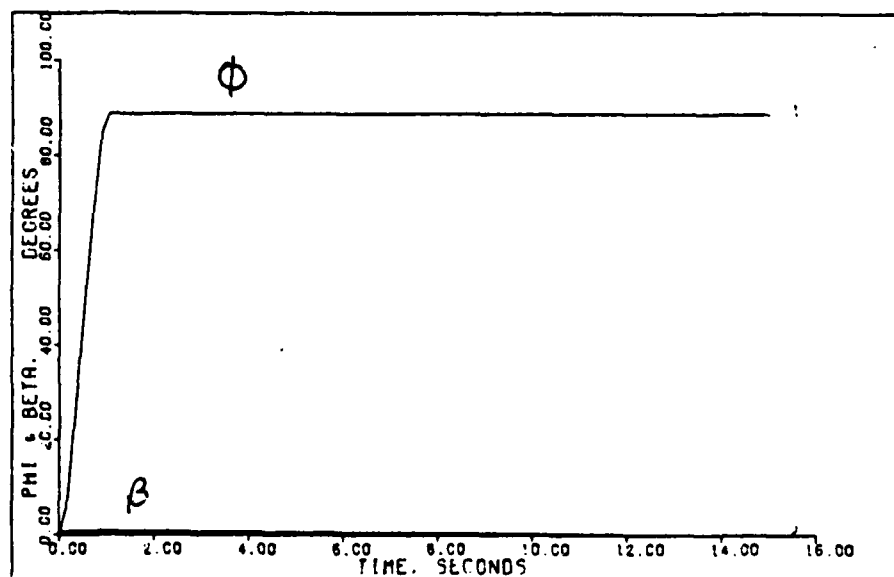


PHI & ROLL ANGLE OUTPUTS TO COORDINATED TURN: 0.7M, 15K FT

FIGURE C - 21

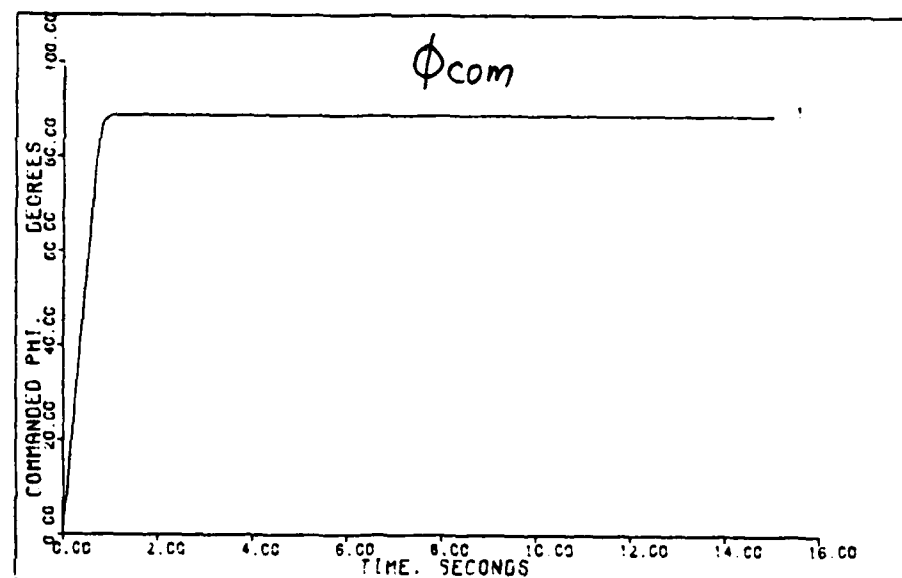


PHI & BETA OUTPUTS TO COORDINATED TURN: J:G 7M.15K FT

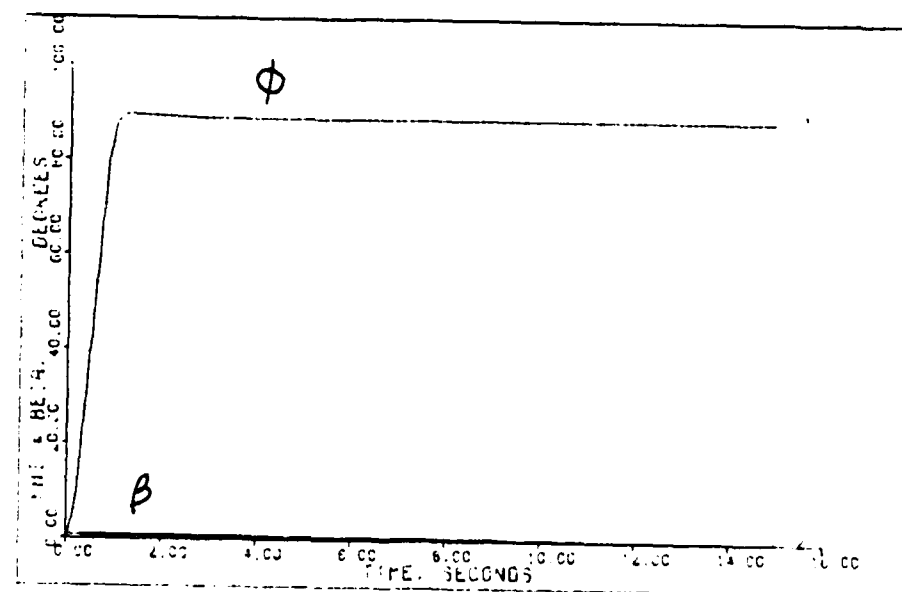


PHI & BETA OUTPUTS TO COORDINATED TURN: L:G 7M.15K FT

FIGURE C - 22

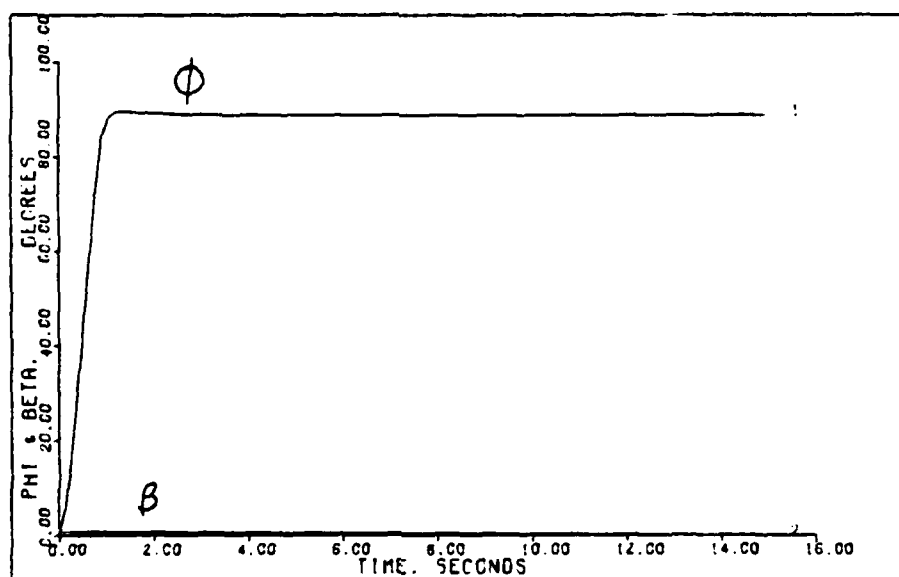


COMMANDED PHI INPUT TO COORDINATED TURN-C. AM. OK FT

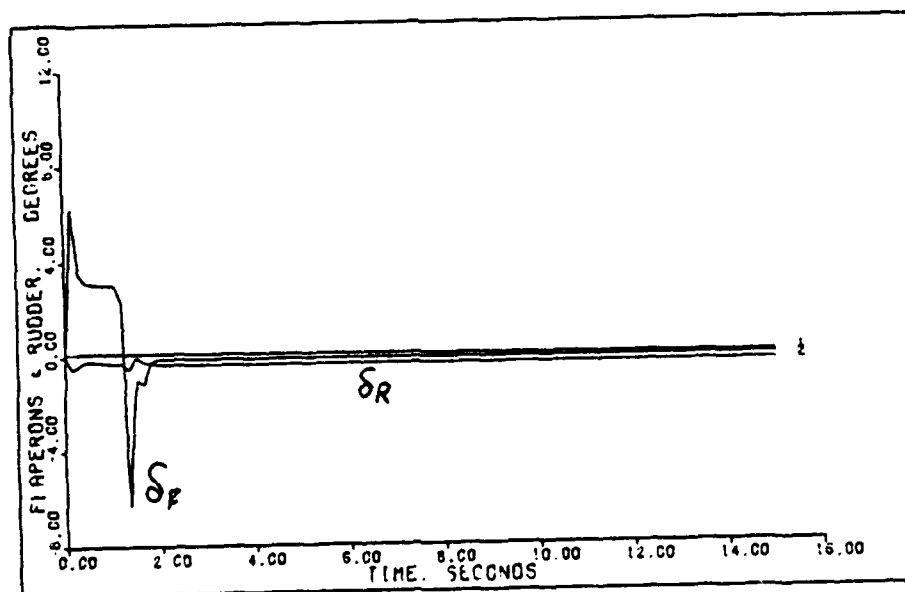


PHI & SIDESLIP ANGLES TO COORDINATED TURN-C. AM. OK FT

FIGURE C - 23

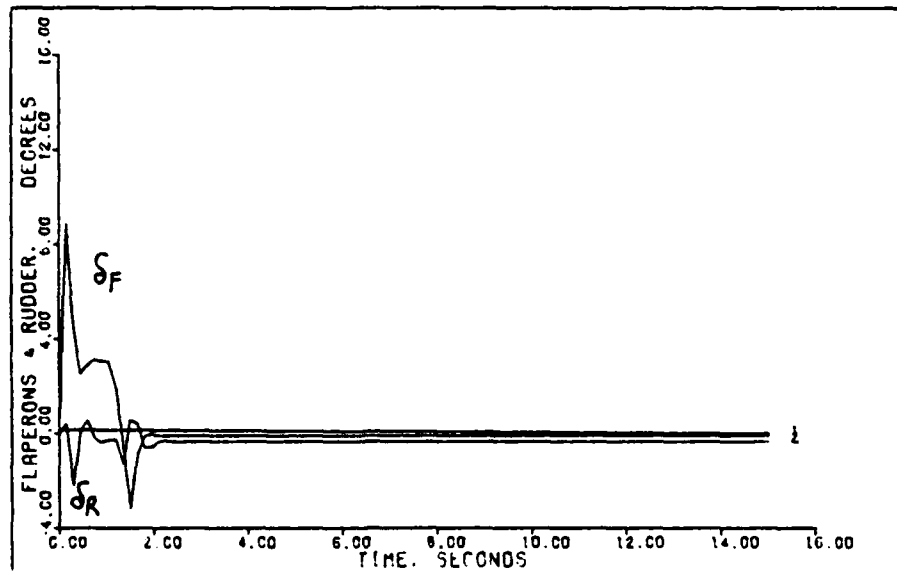


PHI & BETA OUTPUTS TO COORDINATED TURN: 2:0.9M. OK FT

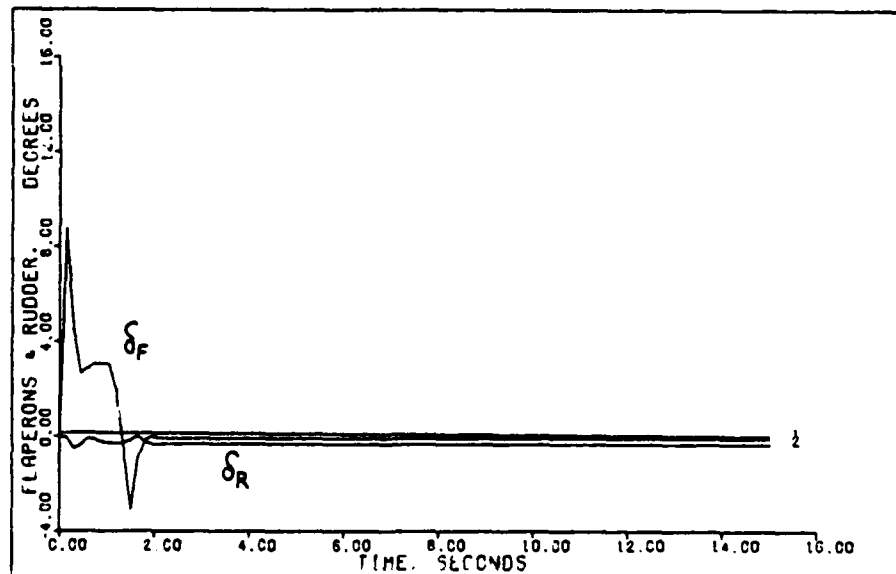


FLAPERON & RUDDER INPUTS TO COORDINATED TURN: 0.4M. OK FT

FIGURE C - 24

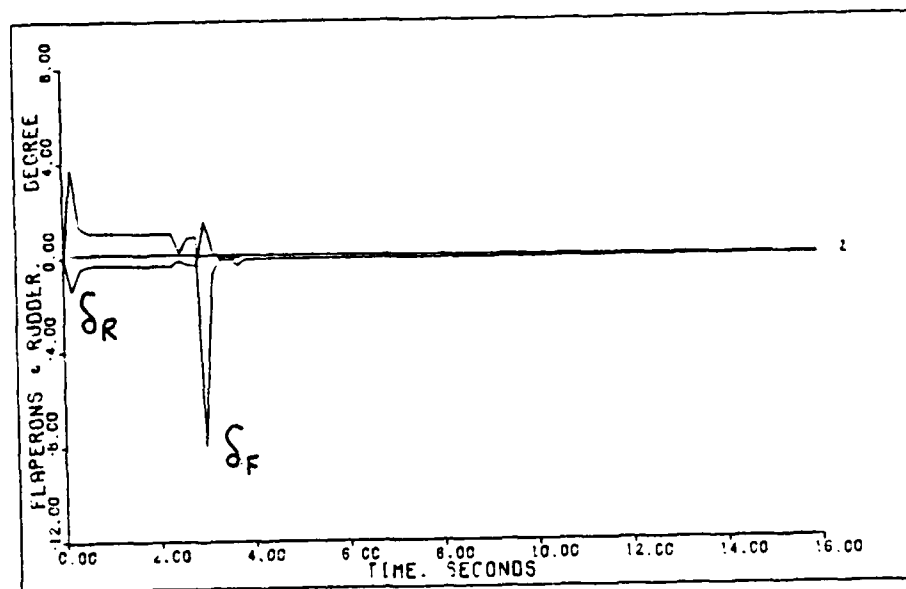


FLAPERON & RUDDER INPUTS TO COORDINATED TURN: J.C. 4M. OK FT

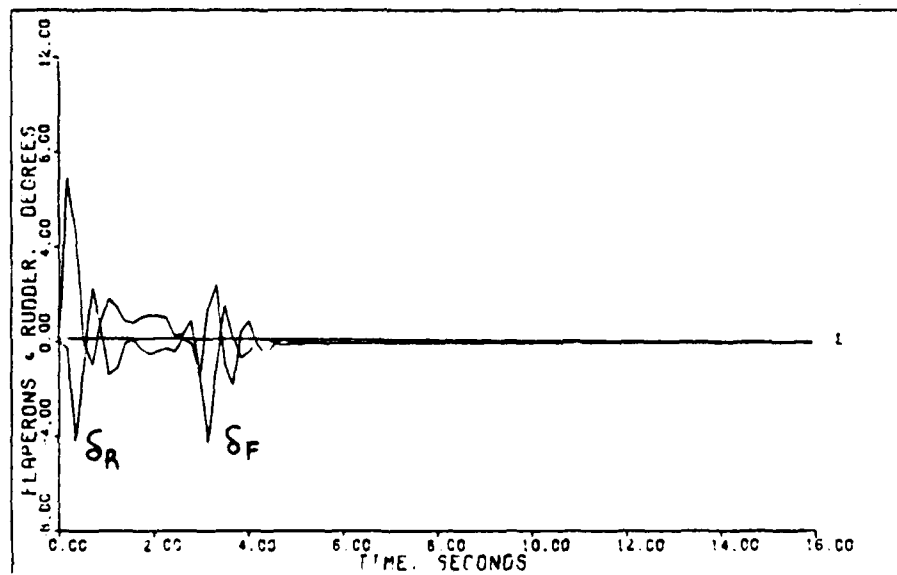


FLAPERON & RUDDER INPUTS TO COORDINATED TURN: Z.C. 4M. OK FT

FIGURE C - 25

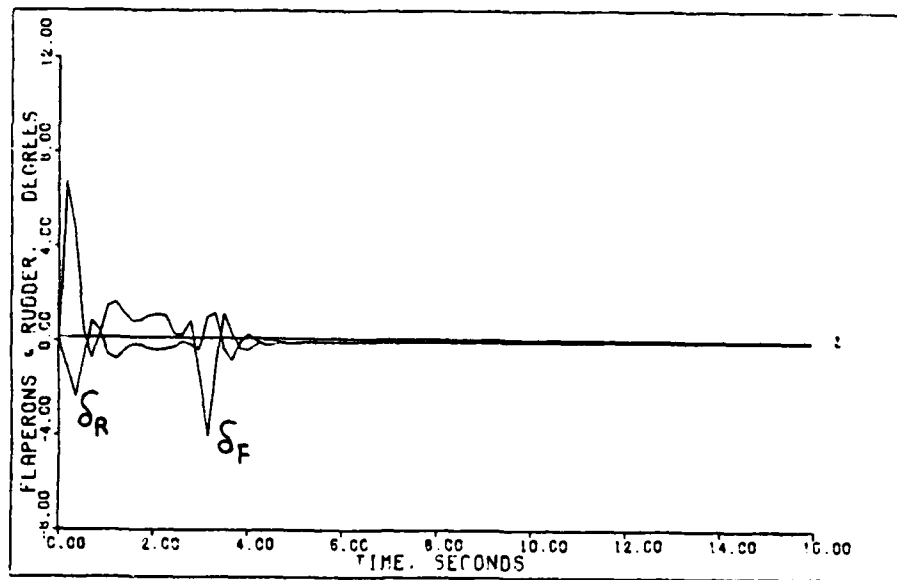


FLAPERON & RUDDER INPUTS TO COORDINATED TURN: 0.9M, 50K FT

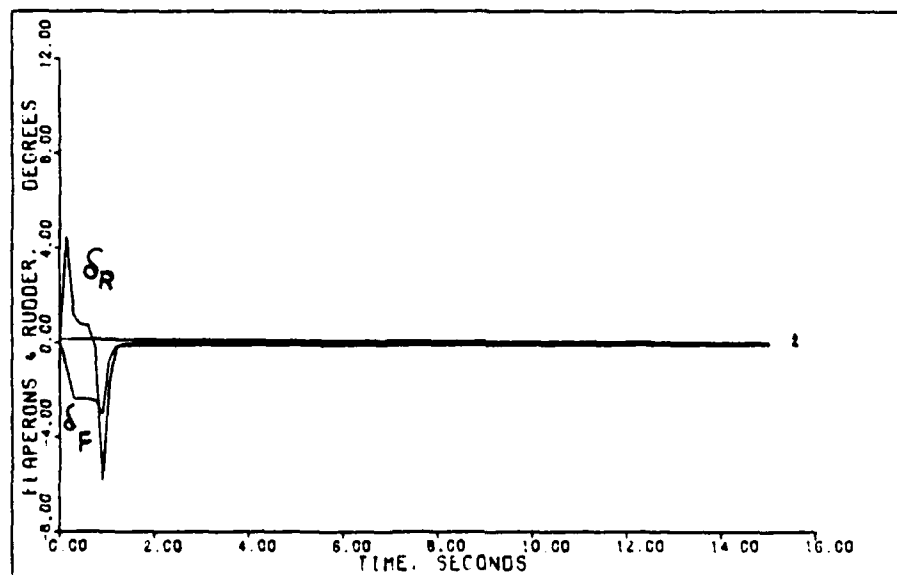


FLAPERON & RUDDER INPUTS TO COORDINATED TURN: 0.9M, 50K FT

FIGURE C - 26

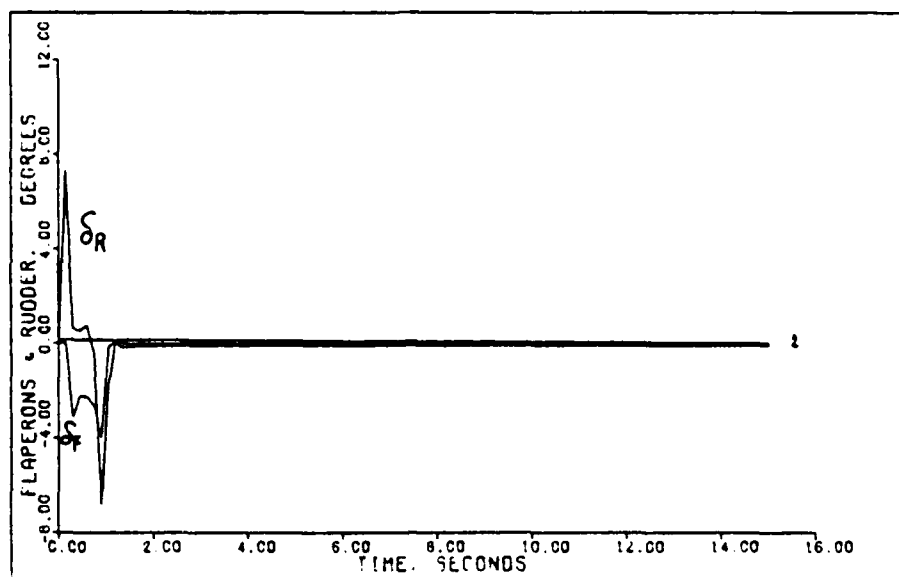


FLAPERON & RUDDER INPUTS TO COORDINATED TURN: 2:0.9M, 50K FT

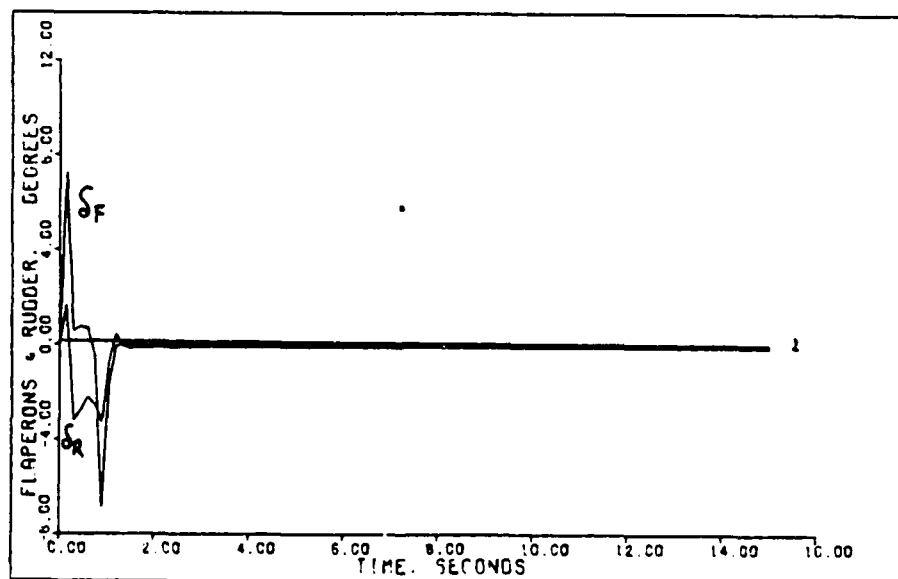


FLAPERON & RUDDER INPUTS TO COORDINATED TURN: 0.7M, 15K FT

FIGURE C - 27

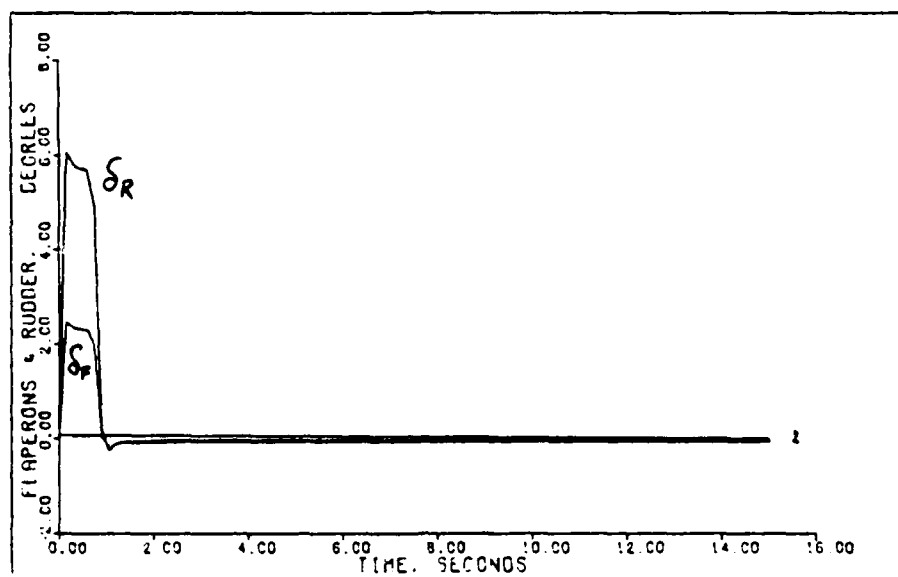


FLAPERON & RUDDER INPUTS TO COORDINATED TURN: J.C. 7M.15K FT

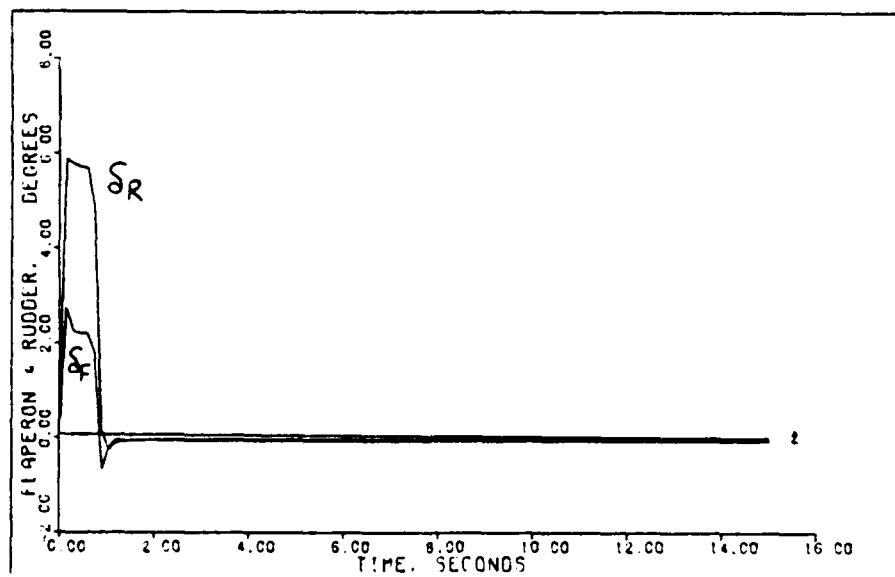


FLAPERON & RUDDER INPUTS TO COORDINATED TURN: Z.C. 7M.15K FT

FIGURE C - 28



FLAPERON & RUDDER INPUTS TO COORDINATED TURN: 0.9M, OK FT



FLAPERON & RUDDER INPUTS TO COORDINATED TURN: 2.0M, OK FT

FIGURE C - 29

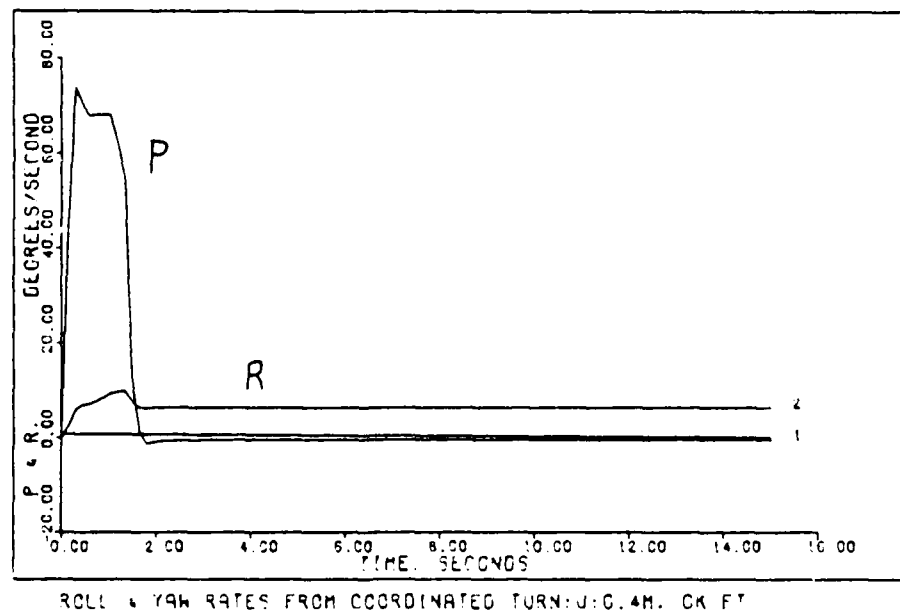
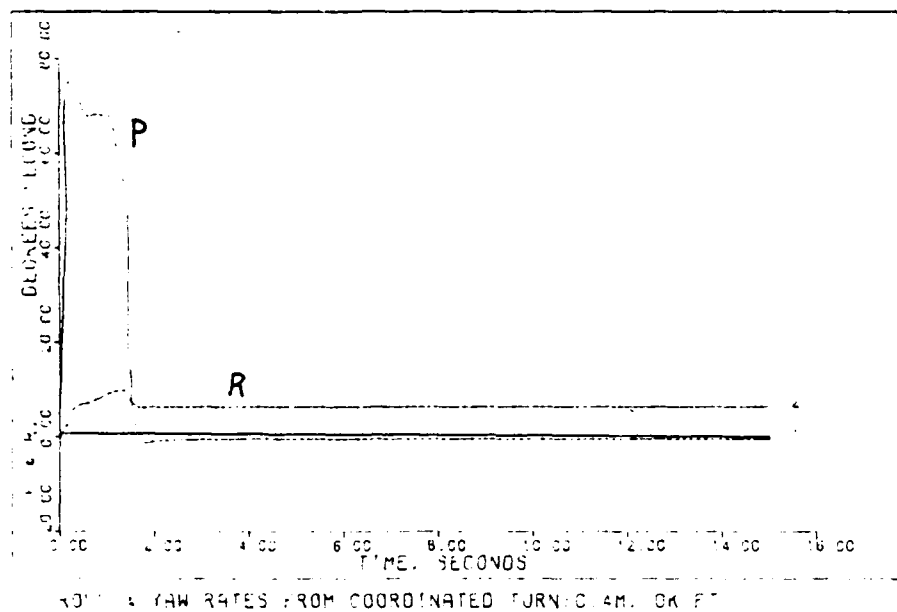
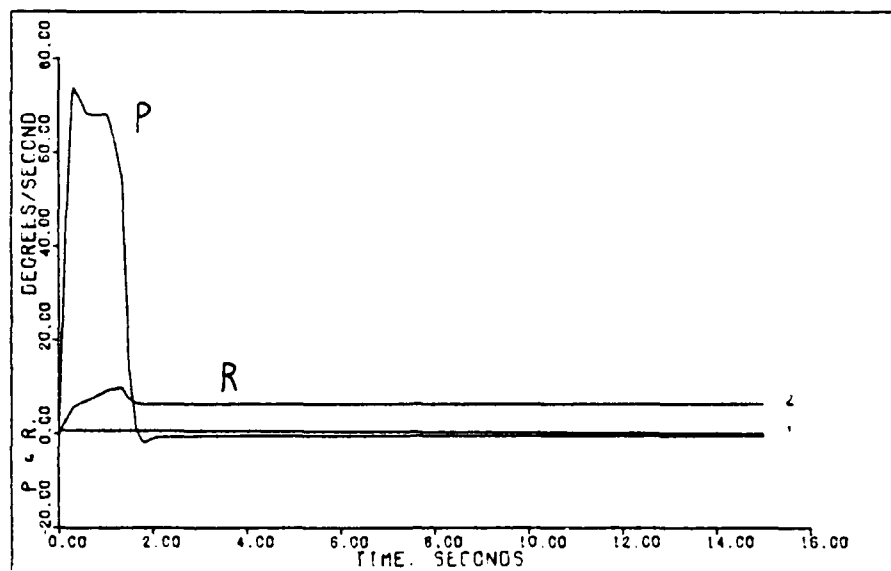
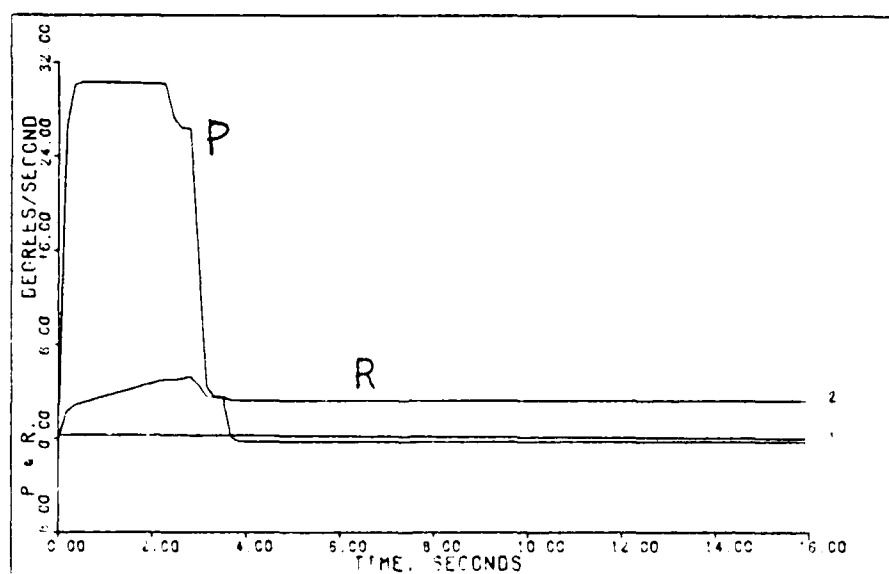


FIGURE C - 30

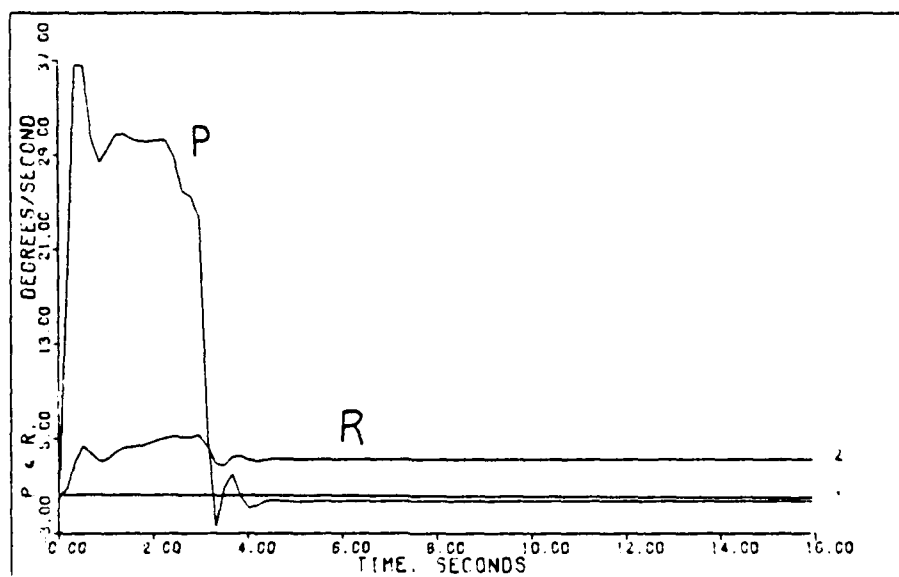


ROLL & YAW RATES FROM COORDINATED TURN: 20,000 FT

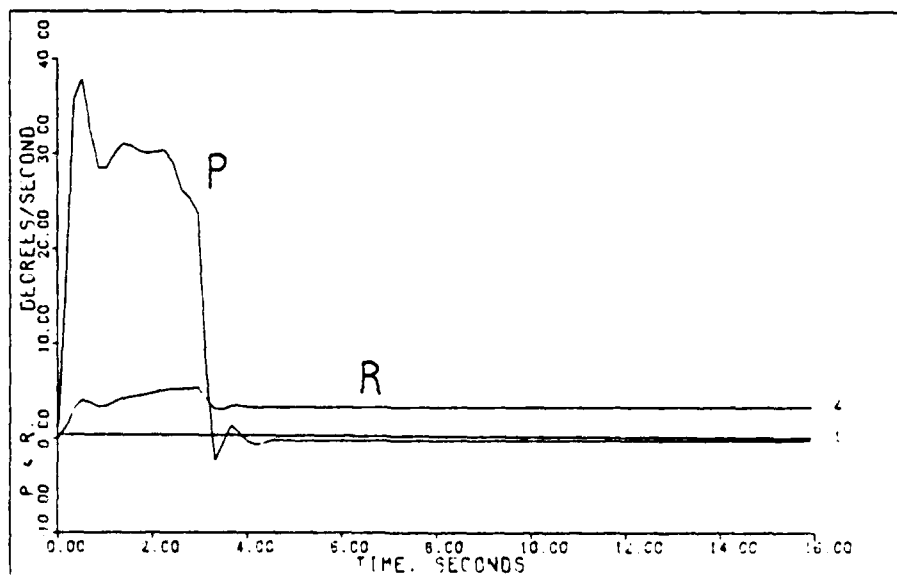


ROLL & YAW RATES FROM COORDINATED TURN: 60,000 FT

FIGURE C - 31

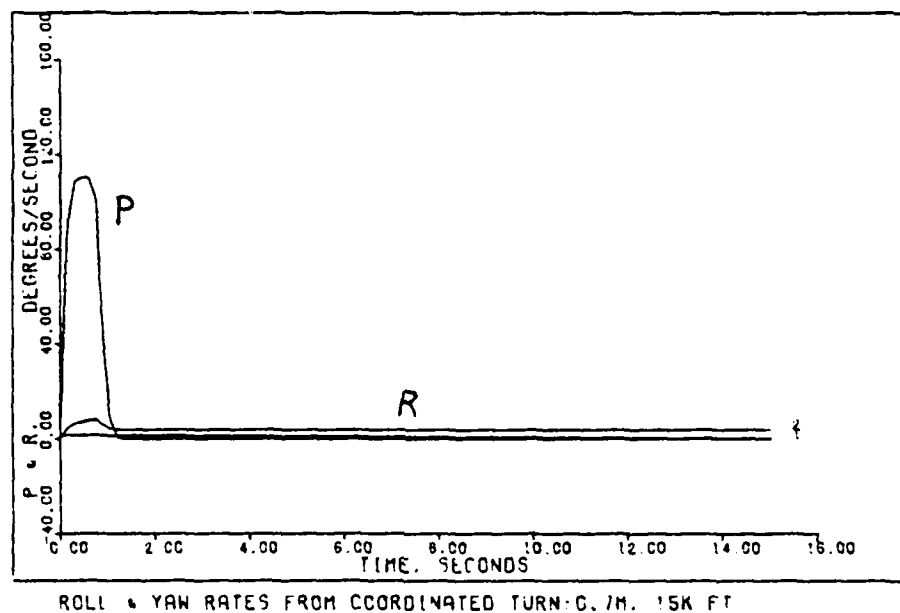


ROLL & YAW RATES FROM COORDINATED TURN: 0.9M, 50K FT

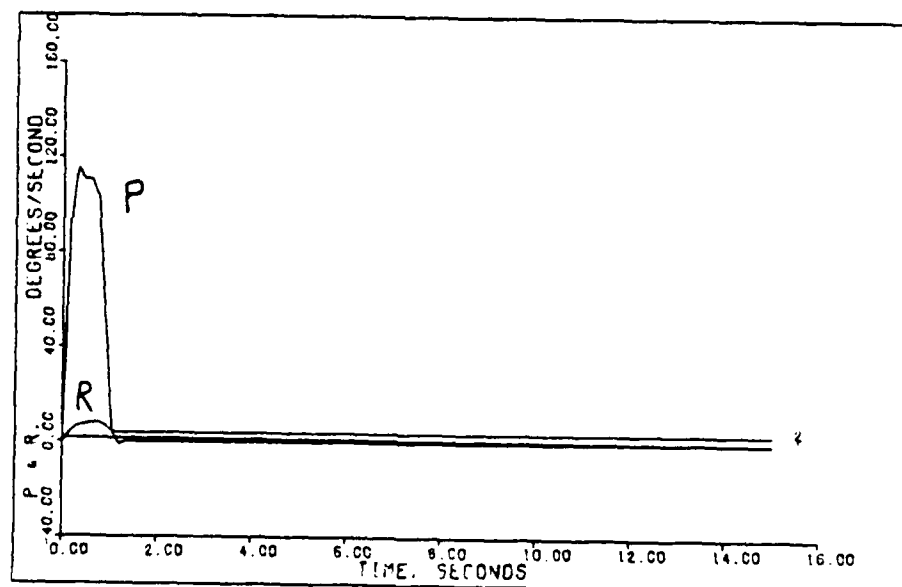


ROLL & YAW RATES FROM COORDINATED TURN: 2.0M, 50K FT

FIGURE C - 32

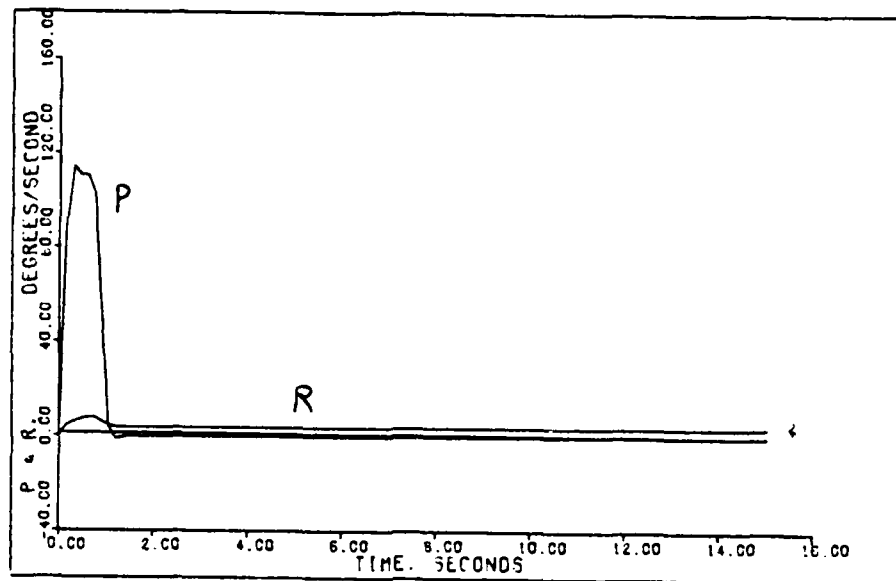


ROLL & YAW RATES FROM COORDINATED TURN: C. 7M. 15K FT

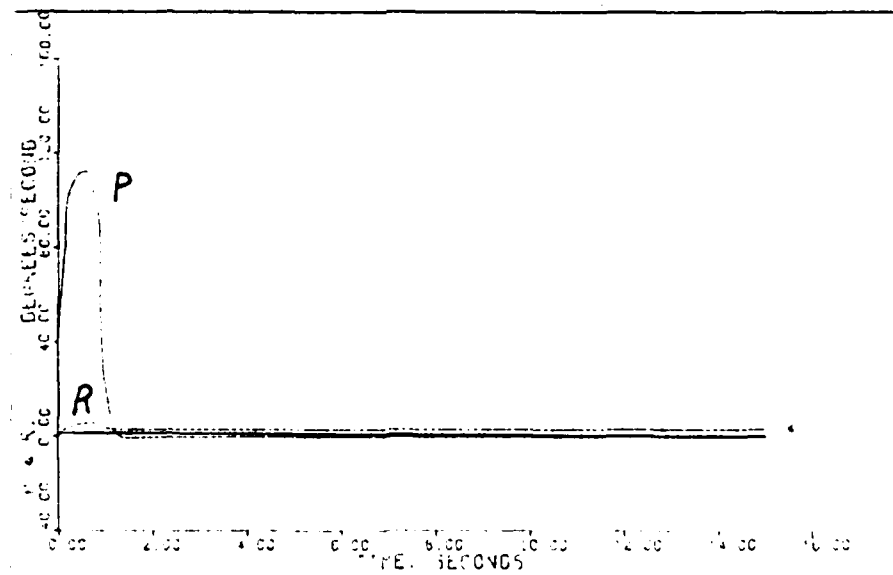


ROLL & YAW RATES TO COORDINATED TURN: C. 7M. 15K FT

FIGURE C - 33



ROLL & YAW RATES FROM COORDINATED TURN: 2-G, 7M, 15K FT



ROLL & YAW RATES FROM COORDINATED TURN: 0.4M, 0K FT

FIGURE C - 34

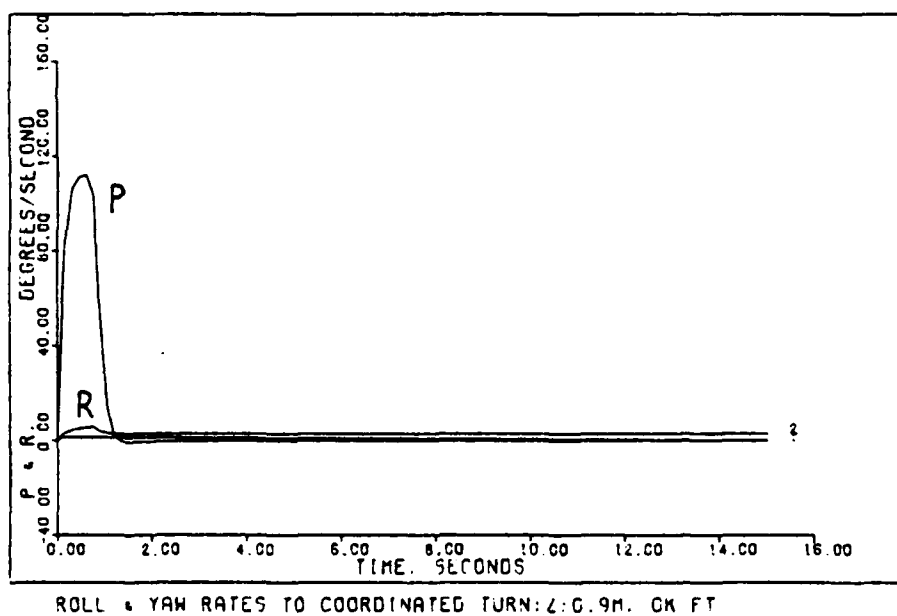


FIGURE C - 35

TABLE D-1

LONGITUDINAL STATE-SPACE MATRICES

Flight Condition - 0.4 Mach, sea level

	<u>A</u> (PLANT MATRIX)			

	0	0	0	1
	-32.17	-.01692	-1.89	-0.3742
	.000001876	-.0003094	-.9991	0.9880
	0	.0005282	10.37	-0.4340

	<u>B</u> (CONTROL INPUT MATRIX)			

	0	0	0	
	-.1179	-.002723	37.82	
	-.0009614	-.0007841	-.00592	
	.0926	-.03481	-.2680	

	<u>C</u> (OUTPUT MATRIX)			

	0	0	0	1
	0	1	0	0
	0	0	1	0

Note: the states are (listed in order) - pitch angle, change in forward velocity, angle-of-attack, and pitch rate.

Note: the control inputs are (listed in order) - horizontal canards, strake-flaperons, and thrust.

Note: the outputs are (listed in order) - pitch rate, change in forward velocity, and angle-of-attack.

TABLE D-2

LONGITUDINAL STATE-SPACE MATRICES

Flight Condition - 0.9 Mach, 50 000 feet

<u>A</u> (PLANT MATRIX)				
0	0	0	1	
-32.02	-.01536	-17.76	-.1665	
0	-.00008461	-.3942	.9978	
0	-.0009140	7.143	-.1584	
<u>B</u> (CONTROL INPUT MATRIX)				
0	0	0		
-.1124	-.01618	6.443		
-.0002668	-.0002067	-.0006428		
.05860	-.01878	-.04575		
<u>C</u> (OUTPUT MATRIX)				
0	0	0	1	
0	1	0	0	
0	0	1	0	

Note: the states are (listed in order) - pitch angle, change in forward velocity, angle-of-attack, and pitch rate.

Note: the control inputs are (listed in order) - horizontal canards, strake-flaperons, and thrust.

Note: the outputs are (listed in order) - pitch rate, change in forward velocity, and angle-of-attack.

TABLE D-3

LONGITUDINAL STATE-SPACE MATRICES

Flight Condition - 0.7 Mach, 15 000 feet

<u>A</u> (PLANT MATRIX)				
0	0	0	1	
-32.13	-.01548	.5001	-.3035	
-.000001132	-.0001218	-1.152	.9917	
0	.0002201	20.17	-.4928	
<u>B</u> (CONTROL INPUT MATRIX)				
0	0	0		
-.1877	-.005027	27.25		
-.001136	-.0007193	-.001819		
.1708	-.05466	-.1930		
<u>C</u> (OUTPUT MATRIX)				
0	0	0	1	
0	1	0	0	
0	0	1	0	

Note: the states are (listed in order) - pitch angle, change in forward velocity, angle-of-attack, and pitch rate.

Note: the control inputs are (listed in order) - horizontal canards, strake-flaperons, and thrust.

Note: the outputs are (listed in order) - pitch rate, change in forward velocity, and angle-of-attack.

TABLE D-4
LONGITUDINAL STATE-SPACE MATRICES
Flight Condition - 0.9 Mach, sea level

<u>A</u> (PLANT MATRIX)				
0	0	0	1	
-32.17	-.0637	4.044	-.5743	
0	-.0002263	-3.542	.9856	
0	.0002669	72.18	-1.189	
<u>B</u> (CONTROL INPUT MATRIX)				
0	0	0		
-.6987	-.03225	32.98		
-.003985	-.0009334	-.001305		
.6060	-.1008	-.2334		
<u>C</u> (OUTPUT MATRIX)				
0	0	0	1	
0	1	0	0	
0	0	1	0	

Note: the states are (listed in order) - pitch angle, change in forward velocity, angle-of-attack, and pitch rate.

Note: the control inputs are (listed in order) - horizontal canards, strake-flaperons, and thrust.

Note: the outputs are (listed in order) - pitch rate, change in forward velocity, and angle-of-attack.

TABLE D-5

LATERAL STATE-SPACE MATRICES

Flight Condition - 0.4 Mach, sea level

<u>A</u> (PLANT MATRIX)				
0	0	1	.06997	
.07187	-.2162	.0698	-.9976	
0	-9.349	-2.621	1.045	
0	5.145	-.08368	-.1034	
<u>B</u> (CONTROL INPUT MATRIX)				
0	0			
-.0008002	.0008783			
.9806	.1514			
.06228	-.04981			
<u>C</u> (OUTPUT MATRIX)				
1	0	0	0	
0	1	0	0	

Note: the states are (listed in order) - roll angle, sideslip angle, roll rate, and yaw rate

Note: the control inputs are (listed in order) - differential flaperons and rudder.

Note: the outputs are (listed in order) - roll angle and sideslip angle.

TABLE D-6

LATERAL STATE-SPACE MATRICES

Flight Condition - 0.9 Mach, 50 000 feet

<u>A</u> (PLANT MATRIX)				
0	0	1	.08690	
.03661	-.07105	.08658	-.9962	
0	-9.59	-.8622	.4814	
0	3.306	-.03038	-.01828	
<u>B</u> (CONTROL INPUT MATRIX)				
	0	0		
	-.0003309	.0002964		
	.4374	.1144		
	.02538	-.03312		
<u>C</u> (OUTPUT MATRIX)				
1	0	0	0	
0	1	0	0	

Note: the states are (listed in order) - roll angle, sideslip angle, roll rate, and yaw rate

Note: the control inputs are (listed in order) - differential flaperons and rudder.

Note: the outputs are (listed in order) - roll angle and sideslip angle.

TABLE D-7

LATERAL STATE-SPACE MATRICES

Flight Condition - 0.7 Mach, 15 000 feet

<u>A</u> (PLANT MATRIX)				
0	0	1	.04944	
.04335	-.2229	.04938	-.9988	
0	-19.48	-.2976	1.008	
0	7.912	-.09287	-.09788	
<u>B</u> (CONTROL INPUT MATRIX)				
0	0			
-.0008422	.0009084			
1.497	.2680			
.09646	-.08652			
<u>C</u> (OUTPUT MATRIX)				
1	0	0	0	
0	1	0	0	

Note: the states are (listed in order) - roll angle, sideslip angle, roll rate, and yaw rate

Note: the control inputs are (listed in order) - differential flaperons and rudder.

Note: the outputs are (listed in order) - roll angle and sideslip angle.

TABLE D-8

LATERAL STATE-SPACE MATRICES

Flight Condition - 0.9 Mach, sea level

<u>A</u> (PLANT MATRIX)				
0	0	1	.03979	
.03199	-.4704	.03976	-.9992	
0	-74.83	-8.95	2.094	
0	18.93	-.2587	-.1653	
<u>B</u> (CONTROL INPUT MATRIX)				
	0	0		
	-.002488	.001397		
	2.789	.6026		
	.1802	-.1831		
<u>C</u> (OUTPUT MATRIX)				
1	0	0	0	
0	1	0	0	

Note: the states are (listed in order) - roll angle, sideslip angle, roll rate, and yaw rate

Note: the control inputs are (listed in order) - differential flaperons and rudder.

Note: the outputs are (listed in order) - roll angle and sideslip angle.

TABLE E-1

DESIGN PARAMETERS AND COMMANDED INPUTS FOR LONGITUDINAL CONTROLLER

Flight Condition - 0.4 Mach, sea level

Maneuver	Command Vector \underline{v} *	ALPHA	EPSILON	SIGMA (Diagonal values)
Direct Climb	1.2,.4,2,3.2 1.2,135,16,16 0,0,0,0	0.9	1.15	1.9,.7,0
Direct Lift1	.2,.27,.5,.7 0,0,0,0 0,0,0,0			
Direct Lift2	1.6,.37,2.4,3.2 0,0,0,0 0,0,0,0			
Pitch-Pointing	.8,.036,1.2,1.6 0,0,0,0 .8,.036,16,16			
Vertical Translation1	0,0,0,0 0,0,0,0 1.8,.03,3.2,4.5	0.5	3.3	1.2,.9,.016
Vertical Translation2	0,0,0,0 0,0,0,0 0.8,.024,16,16			

*Note: Each pulse entry in \underline{v} has four parts:

- 1) The time (seconds) the input reached steady-state,
- 2) steady-state value (angles are in radians),
- 3) the time the input leaves steady-state and starts to return to zero,
- 4) and the time the input returns to zero.

WD-R140 983

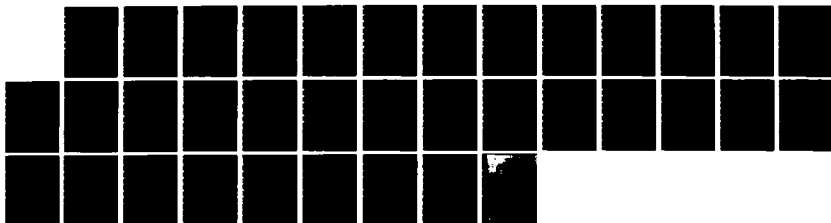
MULTIVARIABLE DIGITAL FLIGHT CONTROL DESIGN OF THE
X-29A(U) AIR FORCE INST OF TECH WRIGHT-PATTERSON AFB OH
SCHOOL OF ENGINEERING R S FELDMANN MAR 84
AFIT/GE/EE/84M-3

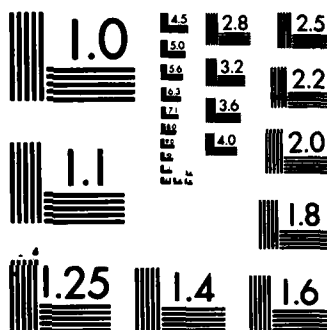
4/4

UNCLASSIFIED

F/G 1/3

NL





MICROCOPY RESOLUTION TEST CHART
NATIONAL BUREAU OF STANDARDS-1963-A

TABLE E-2

DESIGN PARAMETERS AND COMMANDED INPUTS FOR LONGITUDINAL CONTROLLER

Flight Condition - 0.9 Mach, 50 000 feet

Maneuver	Command Vector <u>v</u> *	ALPHA	EPSILON	SIGMA (Diagonal values)
Direct Climb	1.2,.25,2,3.2 1.2,50,16,16 0,0,0,0	1.1	0.9	1.75,.5,0
Direct Lift1	.2,.19,.5,.7 0,0,0,0 0,0,0,0			
Direct Lift2	1.6,.22,2.4,3.2 0,0,0,0 0,0,0,0			
Pitch-Pointing	.8,.012,1.2,1.6 0,0,0,0 .8,.012,16,16			
Vertical Translation1	0,0,0,0 0,0,0,0 1.8,.012,3.2,4.5	1.1	0.9	2,1.5,.05
Vertical Translation2	0,0,0,0 0,0,0,0 0.8,.0075,16,16			

*Note: Each pulse entry in v has four parts:

- 1) The time (seconds) the input reached steady-state,
- 2) steady-state value (angles are in radians),
- 3) the time the input leaves steady-state and starts to return to zero,
- 4) and the time the input returns to zero.

TABLE E-3

DESIGN PARAMETERS AND COMMANDED INPUTS FOR LONGITUDINAL CONTROLLER

Flight Condition - 0.7 Mach, 15 000 feet

Maneuver	Command Vector \underline{v} *	ALPHA	EPSILON	SIGMA (Diagonal values)
Direct Climb	1.2,.32,2,3.2 1.2,165,16,16 0,0,0,0	1	0.9	2.2,2,0
Direct Lift1	.2,.30,.5,.7 0,0,0,0 0,0,0,0			
Direct Lift2	1.6,.29,2.4,3.2 0,0,0,0 0,0,0,0			
Pitch-Pointing	.8,.032,1.2,1.6 0,0,0,0 .8,.032,16,16	.9	0.85	2.65,2,.08
Vertical Translation1	0,0,0,0 0,0,0,0 1.8,.032,3.2,4.5			2.55,2,.0158
Vertical Translation2	0,0,0,0 0,0,0,0 0.8,.032,16,16			

*Note: Each pulse entry in \underline{v} has four parts:

- 1) The time (seconds) the input reached steady-state,
- 2) steady-state value (angles are in radians),
- 3) the time the input leaves steady-state and starts to return to zero,
- 4) and the time the input returns to zero.

TABLE E-4

DESIGN PARAMETERS AND COMMANDED INPUTS FOR LONGITUDINAL CONTROLLER

Flight Condition - 0.9 Mach, sea level

Maneuver	Command Vector <u>v</u> *	ALPHA	EPSILON	SIGMA (Diagonal values)
Direct Climb	1.2,.4,2,3.2 1.2,325,16,16 0,0,0,0	1	0.9	2.2,2,0
Direct Lift1	.2,.28,.5,.7 0,0,0,0 0,0,0,0			
Direct Lift2	1.6,.33,2.4,3.2 0,0,0,0 0,0,0,0			
Pitch-Pointing	.8,.015,1.2,1.6 0,0,0,0 .8,.015,16,16			2.2,2,.4
Vertical Translation1	0,0,0,0 0,0,0,0 1.8,.02,3.2,4.5	0.4	3.6	1.4,1.2,.016
Vertical Translation2	0,0,0,0 0,0,0,0 0.8,.015,16,16			

*Note: Each pulse entry in v has four parts:

- 1) The time (seconds) the input reached steady-state,
- 2) steady-state value (angles are in radians),
- 3) the time the input leaves steady-state and starts to return to zero,
- 4) and the time the input returns to zero.

TABLE E-5

DESIGN PARAMETERS AND COMMANDED INPUTS
FOR LATERAL CONTROLLERS

Flight Condition - 0.4 Mach, sea level

Maneuver	Command Vector \underline{v}	ALPHA	EPSILON	SIGMA (Diagonal values)
Beta- Pointing (IRC)				
Beta- Pointing (FGRC)	0,0,0,0 1.2,.24,16,16			
Beta- Pointing (MGRC)				
		1.0	1.0	1.0,1.0
Coordinated Turn (IRC)	1.3,1.55,16,16 0,0,0,0			
Coordinated Turn (FGRC)				
Coordinated Turn (MGRC)				

Note: (IRC) - Individual Robust Controller
(FGRC) - Full Gain Robust Controller
(MGRC) - Minimum Gain Robust Controller

Note: The measurement (M) matrix is a (2 x 2) diagonal matrix
with diagonal entries (0.1,0.1) for all lateral controllers

TABLE E-6

DESIGN PARAMETERS AND COMMANDED INPUTS
FOR LATERAL CONTROLLERS

Flight Condition - 0.9 Mach, 50 000 feet

Maneuver	Command Vector \underline{v}	ALPHA	EPSILON	SIGMA (Diagonal values)
Beta- Pointing (IRC)				
Beta- Pointing (FGRC)	0,0,0,0 0.8,0.1,16,16			
Beta Pointing (MGRC)				
		1.0	1.0	1.0,1.0
Coordina- ted Turn (IRC)	2.9,1.55,16,16 0,0,0,0			
Coordina- ted Turn (FGRC)				
Coordina- ted Turn (MGRC)				

Note: (IRC) - Individual Robust Controller
(FGRC) - Full Gain Robust Controller
(MGRC) - Minimum Gain Robust Controller

Note: The measurement (M) matrix is a (2 x 2) diagonal matrix
with diagonal entries (0.1,0.1) for all lateral controllers

TABLE E-7
DESIGN PARAMETERS AND COMMANDED INPUTS
FOR LATERAL CONTROLLERS

Flight Condition - 0.7 Mach, 15 000 feet

Maneuver	Command Vector \underline{v}	ALPHA	EPSILON	SIGMA (Diagonal values)
Beta-Pointing (IRC)				
Beta-Pointing (FGRC)	0,0,0,0 0.8,0.27,16,16			
Beta-Pointing (MGRC)		1.0	1.0	1.0,1.0
Coordinated Turn (IRC)	0,8,1.55,16,16 0,0,0,0			
Coordinated Turn (FGRC)				
Coordinated Turn (MGRC)				

Note: (IRC) - Individual Robust Controller
(FGRC)- Full Gain Robust Controller
(MGRC)- Minimum Gain Robust Controller

Note: The measurement (M) matrix is a (2 x 2) diagonal matrix with diagonal entries (0.1,0.1) for all lateral controllers

TABLE E-8

DESIGN PARAMETERS AND COMMANDED INPUTS
FOR LATERAL CONTROLLERS

Flight Condition - 0.9 Mach, sea level

Maneuver	Command Vector v	ALPHA	EPSILON	SIGMA (Diagonal values)
Beta-Pointing (IRC)				
Beta-Pointing (FGRC)	0,0,0,0 0.8,0.27,16,16			
Beta-Pointing (MGRC)		1.0	1.0	1.0,1.0
Coordinated Turn (IRC)	0,8,1.55,16,16 0,0,0,0			
Coordinated Turn (FGRC)				
Coordinated Turn (MGRC)				

Note: (IRC) - Individual Robust Controller
(FGRC)- Full Gain Robust Controller
(MGRC)- Minimum Gain Robust Controller

Note: The measurement (M) matrix is a (2 x 2) diagonal matrix with diagonal entries (0.1,0.1) for all lateral controllers

TABLE F-1

LONGITUDINAL CONTROLLER MATRICES

Flight Condition - 0.4 Mach, sea level

Maneuver	Command Vector \underline{v}	ALPHA	** K_0
	*		
Direct Climb	1.2,.4,2,3.2 1.2,135,16,16 0,0,0,0	0.9	
Direct Lift1	.2,.27,.5,.7 0,0,0,0 0,0,0,0		.1454E+02 .7336E-03 0 -.1816E+02 -.1455E-00 0 .4401E-01 .1915E-01 0
Direct Lift2	1.6,.37,2.4,3.2 0,0,0,0 0,0,0,0		
Pitch-Pointing	.8,.036,1.2,1.6 0,0,0,0 .8,.036,16,16		
Vertical Translation1	0,0,0,0 0,0,0,0 1.8,.03,3.2,4.5	0.5	.1464E+2 .1504E-2 -.8665E1 -.1828E2 -.2982E+0 -.2283E2 .4432E-1 .3925E-1 -.2866E-1
Vertical Translation2	0,0,0,0 0,0,0,0 0.8,.024,16,16		

*Note: Each pulse entry in \underline{v} has four parts:

- 1) The time (seconds) the input reached steady-state,
- 2) steady-state value (angles are in radians),
- 3) the time the input leaves steady-state and starts to return to zero,
- 4) and the time the input returns to zero.

**Note: $K_0 = \text{ALPHA} * K_1$

TABLE F-2

LONGITUDINAL CONTROLLER MATRICES

Flight Condition - 0.9 Mach, 50 000 feet

Maneuver	Command Vector \underline{v} *	ALPHA	** K_0		
Direct Climb	1.2,.25,2,3.2 1.2,50,16,16 0,0,0,0	1.1			
Direct Lift1	.2,.19,.5,.7 0,0,0,0 0,0,0,0		21.0796	-0.0118	0
			-28.1325	-0.2238	0
			0.2976	0.0769	0
Direct Lift2	1.6,.22,2.4,3.2 0,0,0,0 0,0,0,0				
Pitch-Pointing	.8,.012,1.2,1.6 0,0,0,0 .8,.012,16,16				
Vertical Translation1	0,0,0,0 0,0,0,0 1.8,.012,3.2,4.5		24.0910	-0.0470	0
			-32.1514	-0.6714	0
			0.3396	0.2306	0
Vertical Translation2	0,0,0,0 0,0,0,0 0.8,.0075,16,16				

*Note: Each pulse entry in \underline{v} has four parts:

- 1) The time (seconds) the input reached steady-state,
- 2) steady-state value (angles are in radians),
- 3) the time the input leaves steady-state and starts to return to zero,
- 4) and the time the input returns to zero.

**Note: $K_0 = \text{ALPHA} * K_1$

TABLE F-3

LONGITUDINAL CONTROLLER MATRICES

Flight Condition - 0.7 Mach, 15 000 feet

Maneuver	Command Vector \underline{v}	ALPHA	** K_0		
	*				
Direct Climb	1.2,.32,2,3.2 1.2,165,16,16 0,0,0,0	1			
Direct Lift1	.2,.30,.5,.7 0,0,0,0 0,0,0,0		.7711E1 .1408E-1 0 -.1231E2 -.1894 0 .5085E-1 .6612E-1 0		
Direct Lift2	1.6,.29,2.4,3.2 0,0,0,0 0,0,0,0				
Pitch- Pointing	.8,.032,1.2,1.6 0,0,0,0 .8,.032,16,16	.9	.7895E1 .1197E-1 -.1812E2 -.1260E2 -.1610 -.5613E2 .5206E-1 .5620E-1 -.1351		
Vertical Transla- tion1	0,0,0,0 0,0,0,0 1.8,.032,3.2,4.5				
Vertical Transla- tion2	0,0,0,0 0,0,0,0 0.8,.032,16,16		.7597E1 .1197E-1 -.3578E1 -.1213E2 -.1610 -.1109E2 .5009E-1 .5620E-1 -.2669E-1		

*Note: Each pulse entry in \underline{v} has four parts:

- 1) The time (seconds) the input reached steady-state,
- 2) steady-state value (angles are in radians),
- 3) the time the input leaves steady-state and starts to return to zero,
- 4) and the time the input returns to zero.

**Note: $K_0 = \text{ALPHA} * K_1$

TABLE F-4

LONGITUDINAL CONTROLLER MATRICES

Flight Condition - 0.9 Mach, sea level

Maneuver	Command Vector \underline{v} *	ALPHA	** K_0		
Direct Climb	1.2,.4,2,3.2 1.2,325,16,16 0,0,0,0	1			
Direct Lift1	.2,.28,.5,.7 0,0,0,0 0,0,0,0		.1913E1	.4871E-2	0
			-.8215E1	-.9711E-1	0
			.3250E-1	.5459E-1	0
Direct Lift2	1.6,.33,2.4,3.2 0,0,0,0 0,0,0,0	1			
Pitch- Pointing	.8,.015,1.2,1.6 0,0,0,0 .8,.015,16,16		.1913E1	.4871E-2	-.3760E2
			-.8215E1	-.9711E-1	-.2237E3
			.3250E-1	.5459E-1	-.1015E1
Vertical Transla- tion1	0,0,0,0 0,0,0,0 1.8,.02,3.2,4.5	0.4			
Vertical Transla- tion2	0,0,0,0 0,0,0,0 0.8,.015,16,16		.1948E1	.4676E-2	-.2407E1
			-.8364E1	-.9323E-1	-.1432E2
			.3310E-1	.5240E-1	-.6499E-1

*Note: Each pulse entry in \underline{v} has four parts:

- 1) The time (seconds) the input reached steady-state,
- 2) steady-state value (angles are in radians),
- 3) the time the input leaves steady-state and starts to return to zero,
- 4) and the time the input returns to zero.

**Note: $K_0 = \text{ALPHA} * K_1$

TABLE F-5

LATERAL CONTROLLER MATRICES

Flight Condition - 0.4 Mach, sea level

Maneuver	Command Vector \underline{v}	ALPHA	$* K_0$	
Beta-Pointing (IRC)	0,0,0,0 1.2,.24,16,16	1.0		
Coordinated Turn (IRC)	1.3,1.55,16,16 0,0,0,0		10.12 .2225	-21.74 144.8
Beta-Pointing (FGRC)	0,0,0,0 1.2,.24,16,16			
Coordinated Turn (FGRC)	1.3,1.55,16,16 0,0,0,0		3.282 1.384	-8.871 41.67
Beta-Pointing (MGRC)	0,0,0,0 1.2,.24,16,16			
Coordinated Turn (MGRC)	1.3,1.55,16,16 0,0,0,0		3.282 0	0 41.67

*Note: $K_0 = \text{ALPHA} * K_1$

Note: (IRC) - Individual Robust Controller
 (FGRC) - Full Gain Robust Controller
 (MGRC) - Minimum Gain Robust Controller

Note: The measurement (M) matrix is a (2 x 2) diagonal matrix
 with diagonal entries (0.1,0.1) for all lateral controllers

TABLE F-6

LATERAL CONTROLLER MATRICES

Flight Condition - 0.9 Mach, 50 000 feet

Maneuver	Command Vector \underline{v}	ALPHA	* K_0	
Beta-Pointing (IRC)	0,0,0,0 0.8,0.1,16,16	1.0		
Coordinated Turn (IRC)	2.9,1.55,16,16 0,0,0,0			
Beta-Pointing (FGRC)	0,0,0,0 0.8,0.1,16,16			
Coordinated Turn (FGRC)	2.9,1.55,16,16 0,0,0,0		3.282 1.384	-8.871 41.67
Beta-Pointing (MGRC)	0,0,0,0 0.8,0.1,16,16			
Coordinated Turn (MGRC)	2.9,1.55,16,16 0,0,0,0		3.282 0	0 41.67

*Note: $K_0 = \text{ALPHA} * K_1$

Note: (IRC) - Individual Robust Controller
 (FGRC) - Full Gain Robust Controller
 (MGRC) - Minimum Gain Robust Controller

Note: The measurement (M) matrix is a (2 x 2) diagonal matrix
 with diagonal entries (0.1,0.1) for all lateral controllers

TABLE F-7

LATERAL CONTROLLER MATRICES

Flight Condition - 0.7 Mach, 15 000 feet

Maneuver	Command Vector \underline{v}	ALPHA	* K_0	
Beta-Pointing (IRC)	0,0,0,0 0.8,0.27,16,16	1.0	6.344 1.792	-15.42 87.78
Coordinated Turn (IRC)	0.8,1.55,16,16 0,0,0,0			
Beta-Pointing (FGRC)	0,0,0,0 0.8,0.27,16,16		3.282 1.384	-8.871 41.67
Coordinated Turn (FGRC)	0.8,1.55,16,16 0,0,0,0			
Beta-Pointing (MGRC)	0,0,0,0 0.8,0.27,16,16		3.282 0	0 41.67
Coordinated Turn (MGRC)	0.8,1.55,16,16 0,0,0,0			

*Note: $K_0 = \text{ALPHA} * K_1$

Note: (IRC) - Individual Robust Controller
 (FGRC) - Full Gain Robust Controller
 (MGRC) - Minimum Gain Robust Controller

Note: The measurement (M) matrix is a (2 x 2) diagonal matrix
 with diagonal entries (0.1,0.1) for all lateral controllers

TABLE F-8

LATERAL CONTROLLER MATRICES

Flight Condition - 0.9 Mach, sea level

Maneuver	Command Vector \underline{v}	ALPHA	$* K_0$	
Beta-Pointing (IRC)	0,0,0,0 0.8,0.27,16,16	1.0		
Coordinated Turn (IRC)	0.8,1.55,16,16 0,0,0,0			
Beta-Pointing (FGRC)	0,0,0,0 0.8,0.27,16,16			
Coordinated Turn (FGRC)	0.8,1.55,16,16 0,0,0,0		3.282 1.384	-8.871 41.67
Beta-Pointing (MGRC)	0,0,0,0 0.8,0.27,16,16			
Coordinated Turn (MGRC)	0.8,1.55,16,16 0,0,0,0			

*Note: $K_0 = \text{ALPHA} * K_1$

Note: (IRC) - Individual Robust Controller
 (FGRC)- Full Gain Robust Controller
 (MGRC)- Minimum Gain Robust Controller

Note: The measurement (M) matrix is a (2 x 2) diagonal matrix
 with diagonal entries (0.1,0.1) for all lateral controllers

TABLE G-1

LONGITUDINAL FIGURES OF MERIT

Flight Condition - 0.4 Mach, sea level

Maneuver	Command Vector \underline{y}	t_s^*	t_p^{**}	M_p^{***}
Direct Climb	1.2,.4,2,3.2	15	1.65	.4165
	1.2,135,16,16	1.35	1.5	136.9
	0,0,0,0	6.90	2.25	.2816
Direct Lift1	.2,.27,.5,.7	15	.45	.2783
	0,0,0,0	15	.6	-.1186
	0,0,0,0	14.7	.6	.1005
Direct Lift2	1.6,.37,2.4,3.2	15	1.95	.3862
	0,0,0,0	15	2.55	-.3265
	0,0,0,0	15	2.55	.3002
Pitch- Pointing	.8,.036,1.2,1.6	15	1.05	.0381
	0,0,0,0	15	1.35	-.0087
	.8,.036,16,16	4.05	1.35	.0383
Vertical Transla- tion1	0,0,0,0	15	4.80	-.0012
	0,0,0,0	15	4.95	.0005
	1.8,.03,3.2,4.5	15	3.15	.0314
Vertical Transla- tion2	0,0,0,0	15	1.2	.0011
	0,0,0,0	15	1.5	-.0005
	0.8,.027,16,16	3.9	2.55	.0288

*Note: settling time in seconds

**Note: peak time in seconds

***Note: peak value (greatest magnitude), angles in radians

Note: commanded inputs are smoothed

Note: commanded inputs in order are - pitch rate, change in velocity, and angle-of-attack

TABLE G-2

LONGITUDINAL FIGURES OF MERIT

Flight Condition - 0.9 Mach, 50 000 feet

Maneuver	Command Vector \underline{v}	t_s^*	t_p^{**}	M_p^{***}
Direct Climb	1.2,.25,2,3.2	15.92	1.75	.2681
	1.2,50,16,16	1.40	1.575	50.30
	0,0,0,0	15.40	2.625	.3226
Direct Lift1	.2,.19,.5,.7	15.92	.35	.1932
	0,0,0,0	15.92	.7	-.2042
	0,0,0,0	15.92	.7	.0857
Direct Lift2	1.6,.22,2.4,3.2	15.92	2.275	.2379
	0,0,0,0	15.92	2.80	-.6226
	0,0,0,0	15.92	2.8	.2975
Pitch- Pointing	.8,.012,1.2,1.6	15.92	1.05	.0129
	0,0,0,0	15.92	1.40	-.0082
	.8,.012,16,16	7.00	1.40	.0141
Vertical Transla- tion1	0,0,0,0	15.92	2.275	.0006
	0,0,0,0	15.92	2.275	-.0024
	1.8,.012,3.2,4.5	15.92	3.15	.0120
Vertical Transla- tion2	0,0,0,0	15.92	1.4	.0004
	0,0,0,0	15.92	1.575	-.0016
	0.8,.0075,16,16	1.925	2.80	.0076

*Note: settling time in seconds

**Note: peak time in seconds

***Note: peak value (greatest magnitude), angles in radians

Note: commanded inputs are smoothed

Note: commanded inputs in order are - pitch rate, change in velocity, and angle-of-attack

TABLE G-3

LONGITUDINAL FIGURES OF MERIT

Flight Condition - 0.7 Mach, 15 000 feet

Maneuver	Command Vector v	t_s^*	t_p^{**}	M_p^{***}
Direct Climb	1.2,.32,2,3.2	15.00	1.65	.3464
	1.2,165,16,16	1.35	1.50	165.82
	0,0,0,0	9.6	2.25	.2245
Direct Lift1	.2,.30,.5,.7	15.00	.45	.3185
	0,0,0,0	15.00	.6	-.0525
	0,0,0,0	15.00	.6	.1107
Direct Lift2	1.6,.29,2.4,3.2	15.00	1.95	.3143
	0,0,0,0	15.00	2.55	-.1106
	0,0,0,0	15.00	2.55	.2227
Pitch- Pointing	.8,.032,1.2,1.6	15.00	1.05	.0371
	0,0,0,0	15.00	1.35	-.0106
	.8,.032,16,16	4.5	1.35	.0342
Vertical Transla- tion1	0,0,0,0	15.00	2.4	.0018
	0,0,0,0	15.00	3.3	-.0007
	1.8,.032,3.2,4.5	15.00	3.6	.0222
Vertical Transla- tion2	0,0,0,0	15.00	1.8	.0020
	0,0,0,0	15.00	2.7	-.0007
	0.8,.032,16,16	9.3	14.85	.0319

*Note: settling time in seconds

**Note: peak time in seconds

***Note: peak value (greatest magnitude), angles in radians

Note: commanded inputs are smoothed

Note: commanded inputs in order are - pitch rate, change in velocity, and angle-of-attack

TABLE G-4

LONGITUDINAL FIGURES OF MERIT

Flight Condition - 0.9 Mach, sea level

Maneuver	Command Vector \underline{v}	t_s^*	t_p^{**}	M_p^{***}
Direct Climb	1.2,.4,2,3.2	15.00	1.5	.4449
	1.2,325,16,16	1.35	1.5	326.6
	0,0,0,0	6.6	1.8	.0993
Direct Lift1	.2,.28,.5,.7	15.00	.45	.3232
	0,0,0,0	15.00	.6	-.0507
	0,0,0,0	15.00	.6	.0677
Direct Lift2	1.6,.33,2.4,3.2	15.00	1.95	.3683
	0,0,0,0	15.00	7.65	-.1288
	0,0,0,0	15.00	2.25	.0999
Pitch- Pointing	.8,.015,1.2,1.6	15.00	0.9	.0231
	0,0,0,0	15.00	1.35	-.0196
	.8,.015,16,16	3.75	15.00	.0150
Vertical Transla- tion1	0,0,0,0	15.00	1.95	.0024
	0,0,0,0	15.00	2.4	-.0003
	1.8,.02,3.2,4.5	15.00	3.45	.0154
Vertical Transla- tion2	0,0,0,0	15.00	1.05	.0023
	0,0,0,0	15.00	1.65	-.0002
	0.8,.02,16,16	7.05	15.00	.0150

*Note: settling time in seconds

**Note: peak time in seconds

***Note: peak value (greatest magnitude), angles in radians

Note: commanded inputs are smoothed

Note: commanded inputs in order are - pitch rate, change in velocity, and angle-of-attack

TABLE G-5

LATERAL FIGURES OF MERIT

Flight Condition - 0.4 Mach, sea level

Maneuver	Command Vector \underline{v}	t_s^*	t_p^{**}	M_p^{***}
Beta-Pointing (IRC)		15 1.5	1.2 15	-.0030 .2422
Beta-Pointing (FGRC)	0,0,0,0 1.2,.24,16,16	15 2.1	1.2 15	-.0127 .2422
Beta-Pointing (MGRC)		15 2.1	0.3 15	.0150 .2422
Coordinated Turn (IRC)		1.5 6.0	1.95 .15	1.5522 -.0004
Coordinated Turn (FGRC)	1.3,1.55,16,16 0,0,0,0	1.5 7.8	1.65 0.3	1.5591 .0012
Coordinated Turn (MGRC)		1.5 7.5	1.65 .15	1.5620 -.0004

*Note: settling time in seconds

**Note: peak time in seconds

***Note: peak value (greatest magnitude), angles in radians

Note: commanded inputs are smoothed

Note: commanded inputs in order are - roll angle, and sideslip angle

TABLE G-6

LATERAL FIGURES OF MERIT

Flight Condition - 0.9 Mach, 50 000 feet

Maneuver	Command Vector \underline{v}	t_s *	t_p **	M_p ***
Beta-Pointing (IRC)		15.92 1.05	1.05 15.92	-.0018 .1003
Beta-Pointing (FGRC)	0,0,0,0 .8,.1,16,16	15.92 2.8	1.05 1.05	-.0127 .1004
Beta-Pointing (MGRC)		15.92 2.98	0.35 15.92	.0258 .1003
Coordinated Turn (IRC)		3.15 15.05	4.025 .175	1.5502 -.0002
Coordinated Turn (FGRC)	2.9,1.55,16,16 0,0,0,0	3.15 15.92	3.85 0.35	1.5536 .0026
Coordinated Turn (MGRC)		3.15 15.78	4.025 .35	1.5532 .0008

*Note: settling time in seconds

**Note: peak time in seconds

***Note: peak value (greatest magnitude), angles in radians

Note: commanded inputs are smoothed

Note: commanded inputs in order are - roll angle, and sideslip angle

TABLE G-7

LATERAL FIGURES OF MERIT

Flight Condition - 0.7 Mach, 15 000 feet

Maneuver	Command Vector \underline{v}	t_S *	t_P **	M_P ***
Beta-Pointing (IRC)		15.00 1.2	0.9 15.00	-.0082 .2722
Beta-Pointing (FGRC)	0,0,0,0 .8,.27,16,16	15.00 1.65	0.9 15.00	-.0172 .2723
Beta-Pointing (MGRC)		15.00 1.8	0.15 15.00	.0188 .2723
Coordinated Turn (IRC)		1.05 9	15.00 1.35	1.5500 -.0002
Coordinated Turn (FGRC)	0.8,1.55,16,16 0,0,0,0	1.05 9.9	15 0.3	1.5500 .0011
Coordinated Turn (MGRC)		1.05 10.05	1.2 .45	1.5504 .0011

*Note: settling time in seconds

**Note: peak time in seconds

***Note: peak value (greatest magnitude), angles in radians

Note: commanded inputs are smoothed

Note: commanded inputs in order are - roll angle, and sideslip angle

TABLE G-8

LATERAL FIGURES OF MERIT

Flight Condition - 0.9 Mach, sea level

Maneuver	Command Vector \underline{v}	t_s *	t_p **	M_p ***
Beta-Pointing (IRC)		15.00 1.8	0.9 15.00	-.0310 .2738
Beta-Pointing (FGRC)	0,0,0,0 .8,.27,16,16			
Beta-Pointing (MERC)		15.00 1.95	0.9 15.00	-.0137 .2738
Coordinated Turn (IRC)		1.05 6.6	1.35 0.6	1.5648 -.0011
Coordinated Turn (FGRC)	0.8,1.55,16,16 0,0,0,0			
Coordinated Turn (MERC)		1.05 10.95	1.35 .30	1.5647 .0022

*Note: settling time in seconds

**Note: peak time in seconds

***Note: peak value (greatest magnitude), angles in radians

Note: commanded inputs are smoothed

Note: commanded inputs in order are - roll angle, and sideslip angle

TABLE H-0

CONTROL INPUT DEFLECTIONS AND RATES

All Flight Conditions

Control Surface	Maximum Deflection (degrees) *	Maximum Deflection Rate (degrees/sec)	Limit Hinge Movement per side (in-lbs) **
Canard	-60 to +30	100	+ 79110 -
Flaperon (IB)	-19.5 to +13	50	+24857
Flaperon (OB)	-19.5 to +13	50	+22197
Strake-Flap	-30 to +30	30	+16356
Rudder	-30 to +30	105	+26867

- * Note (+) Canard - trailing edge down
 (+) Right Flaperon - trailing edge up
 (+) Left Flaperon - trailing edge down
 (+) Strake-flap - trailing edge down
 (+) Rudder - trailing edge left

Information on thrust dead-zone, time-lags, rates, and maximum output at various flight conditions is available from the Grumman reduced-state simulation program. Also, the limits on the inboard and outboard flaperons have been changed and are different for the digital and analog reversion mode.

TABLE H-1

LONGITUDINAL CONTROL INPUT RATES

Flight Condition - 0.4 Mach, sea level

Maneuver	Command Vector \underline{v}	* $\dot{\delta}_c$	** $\dot{\delta}_s$	*** $\dot{\delta}_t$
Direct Climb	1.2,.4,2,3.2 1.2,135,16,16 0,0,0,0	46	-191	21
Direct Lift1	.2,.27,.5,.7 0,0,0,0 0,0,0,0	143	176	0.5
Direct Lift2	1.6,.37,2.4,3.2 0,0,0,0 0,0,0,0	59	-74	.31
Pitch-Pointing	.8,.036,1.2,1.6 0,0,0,0 .8,.036,16,16	-17	-39	-.05
Vertical Translation1	0,0,0,0 0,0,0,0 1.8,.03,3.2,4.5	12	27	.04
Vertical Translation2	0,0,0,0 0,0,0,0 0.8,.027,16,16	-16	-37	-.05

*Note: maximum canard rate (magnitude) in degrees/second

**Note: maximum strake rate (magnitude) in degrees/second

***Note: maximum thrust rate (magnitude) in hundreds of lbs./second

Note: commanded inputs are smoothed

Note: commanded inputs in order are - pitch rate, change in velocity, and angle-of-attack

TABLE H-2

LONGITUDINAL CONTROL INPUT RATES

Flight Condition - 0.9 Mach, 50 000 feet

Maneuver	Command Vector \underline{v}	* $\dot{\delta}_c$	** $\dot{\delta}_s$	*** $\dot{\delta}_t$
Direct Climb	1.2,.25,2,3.2 1.2,50,16,16 0,0,0,0	-29	-122	37
Direct Lift1	.2,.19,.5,.7 0,0,0,0 0,0,0,0	-80	103	1.3
Direct Lift2	1.6,.22,2.4,3.2 0,0,0,0 0,0,0,0	-38	46	1.43
Pitch-Pointing	.8,.012,1.2,1.6 0,0,0,0 .8,.012,16,16	-24	79	.72
Vertical Translation1	0,0,0,0 0,0,0,0 1.8,.012,3.2,4.5	14	41	.34
Vertical Translation2	0,0,0,0 0,0,0,0 0.8,.0075,16,16	-16	-49	-.40

*Note: maximum canard rate (magnitude) in degrees/second

**Note: maximum strake rate (magnitude) in degrees/second

***Note: maximum thrust rate (magnitude) in hundreds of lbs./second

Note: commanded inputs are smoothed

Note: commanded inputs in order are - pitch rate, change in velocity, and angle-of-attack

TABLE H-3

LONGITUDINAL CONTROL INPUT RATES

Flight Condition - 0.7 Mach, 15 000 feet

Maneuver	Command Vector \underline{v}	* $\dot{\delta}_c$	** $\dot{\delta}_s$	*** $\dot{\delta}_t$
Direct Climb	1.2, .32, 2, 3.2 1.2, 165, 16, 16 0, 0, 0, 0	-29	-144	44
Direct Lift1	.2, .30, .5, .7 0, 0, 0, 0 0, 0, 0, 0	-92	145	.66
Direct Lift2	1.6, .29, 2.4, 3.2 0, 0, 0, 0 0, 0, 0, 0	59	-74	.31
Pitch-Pointing	.8, .032, 1.2, 1.6 0, 0, 0, 0 .8, .032, 16, 16	-17	-38	.05
Vertical Translation1	0, 0, 0, 0 0, 0, 0, 0 1.8, .032, 3.2, 4.5	12	27	.04
Vertical Translation2	0, 0, 0, 0 0, 0, 0, 0 0.8, .032, 16, 16	-16	-37	-.05

*Note: maximum canard rate (magnitude) in degrees/second

**Note: maximum stroke rate (magnitude) in degrees/second

***Note: maximum thrust rate (magnitude) in hundreds of lbs./second

Note: commanded inputs are smoothed

Note: commanded inputs in order are - pitch rate, change in velocity, and angle-of-attack

TABLE H-4

LONGITUDINAL CONTROL INPUT RATES

Flight Condition - 0.9 Mach, sea level

Maneuver	Command Vector \underline{v}	* $\dot{\delta}_c$	** $\dot{\delta}_s$	*** $\dot{\delta}_t$
Direct Climb	1.2,.4,2,3.2 1.2,325,16,16 0,0,0,0	-12	-141	71
Direct Lift1	.2,.28,.5,.7 0,0,0,0 0,0,0,0	-29	124	.53
Direct Lift2	1.6,.33,2.4,3.2 0,0,0,0 0,0,0,0	14	-58	.35
Pitch-Pointing	.8,.015,1.2,1.6 0,0,0,0 .8,.015,16,16	-13	-73	-.34
Vertical Translation1	0,0,0,0 0,0,0,0 1.8,.02,3.2,4.5	4	16	.09
Vertical Translation2	0,0,0,0 0,0,0,0 0.8,.02,16,16	-4	-17	-.09

*Note: maximum canard rate (magnitude) in degrees/second

**Note: maximum strake rate (magnitude) in degrees/second

***Note: maximum thrust rate (magnitude) in hundreds of lbs./second

Note: commanded inputs are smoothed

Note: commanded inputs in order are - pitch rate, change in velocity, and angle-of-attack

TABLE H-5

LATERAL CONTROL INPUT RATES

Flight Condition - 0.4 Mach, sea level

Maneuver	Command Vector \underline{v}	* $\dot{\delta}_f$	** $\dot{\delta}_r$
Beta-Pointing (IRC)		-11	87
Beta-Pointing (FGRC)	0,0,0,0 1.2,.24,16,16	-21	136
Beta-Pointing (MGRC)		18	134
Coordinated Turn (IRC)		-57	3
Coordinated Turn (FGRC)	1.3,1.55,16,16 0,0,0,0	59	-17
Coordinated Turn (MGRC)		59	-3

*Note: maximum differential flaperon rate in degrees/second

**Note: maximum rudder rate in degrees/second

Note: commanded inputs are smoothed

Note: commanded inputs in order are - roll angle, and sideslip angle

Note: rates presented are the greatest magnitude

TABLE H-6

LATERAL CONTROL INPUT RATES

Flight Condition - 0.9 Mach, 50 000 feet

Maneuver	Command Vector \underline{v}	* $\dot{\delta}_f$	** $\dot{\delta}_r$
Beta-Pointing (IRC)		23	88
Beta-Pointing (FGRC)	0,0,0,0 .8,.1,16,16	-22	95
Beta-Pointing (MGRC)		23	93
Coordinated Turn (IRC)		-50	11
Coordinated Turn (FGRC)	2.9,1.55,16,16 0,0,0,0	38	-21
Coordinated Turn (MGRC)		37	8

*Note: maximum differential flaperon rate in degrees/second

**Note: maximum rudder rate in degrees/second

Note: commanded inputs are smoothed

Note: commanded inputs in order are - roll angle, and side-slip angle

Note: rates presented are the greatest magnitude

TABLE H-7

LATERAL CONTROL INPUT RATES

Flight Condition - 0.7 Mach, 15 000 feet

Maneuver	Command Vector \underline{v}	* $\dot{\delta}_f$	** $\dot{\delta}_r$
Beta-Pointing (IRC)		-15	86
Beta-Pointing (FGRC)	0,0,0,0 .8,.27,16,16	-20	132
Beta-Pointing (MGRC)		-32	130
Coordinated Turn (IRC)		-37	16
Coordinated Turn (FGRC)	0.8,1.55,16,16 0,0,0,0	49	26
Coordinated Turn (MGRC)		49	-33

*Note: maximum differential flaperon rate in degrees/second

**Note: maximum rudder rate in degrees/second

Note: commanded inputs are smoothed

Note: commanded inputs in order are - roll angle, and side-slip angle

Note: rates presented are the greatest magnitude

TABLE H-8

LATERAL CONTROL INPUT RATES

Flight Condition - 0.9 Mach, sea level

Maneuver	Command Vector \underline{v}	* $\dot{\delta}_f$	** $\dot{\delta}_r$
Beta-Pointing (IRC)		10	49
Beta-Pointing (FGRC)	0,0,0,0 .8,.27,16,16		
Beta-Pointing (MERC)		14	46
Coordinated Turn (IRC)		40	16
Coordinated Turn (FGRC)	0.8,1.55,16,16 0,0,0,0		
Coordinated Turn (MERC)		39	18

*Note: maximum differential flaperon rate in degrees/second

**Note: maximum rudder rate in degrees/second

Note: commanded inputs are smoothed

Note: commanded inputs in order are - roll angle, and sideslip angle

Note: rates presented are the greatest magnitude

VITA

Roger S. Feldmann was born in Stillwater, Oklahoma on 10 May 1961. He attended Vanderbilt University, Nashville, TN, from August 1978 to May 1982, with a four-year Air Force ROTC scholarship. He was graduated cum laude with the degree of Bachelor of Science in Electrical Engineering and received his reserve commission in the United States Air Force on 14 May 1982.

He enrolled in the School of Engineering, Air Force Institute of Technology, in May 1982 as a direct accession selectee. His next assignment is with the Test Wing, Air Force Systems Command, Eglin AFB, FL.

UNCLASSIFIED

SECURITY CLASSIFICATION OF THIS PAGE

REPORT DOCUMENTATION PAGE

1. REPORT SECURITY CLASSIFICATION UNCLASSIFIED			1b. RESTRICTIVE MARKINGS				
2a. SECURITY CLASSIFICATION AUTHORITY			3. DISTRIBUTION/AVAILABILITY OF REPORT Approved for public release; distribution unlimited.				
2b. DECLASSIFICATION/DOWNGRADING SCHEDULE							
4. PERFORMING ORGANIZATION REPORT NUMBER(S) AFIT/GE/EE/83D-21			5. MONITORING ORGANIZATION REPORT NUMBER(S)				
6a. NAME OF PERFORMING ORGANIZATION School of Engineering		6b. OFFICE SYMBOL (If applicable) AFIT/ENG		7a. NAME OF MONITORING ORGANIZATION			
6c. ADDRESS (City, State and ZIP Code) Air Force Institute of Technology Wright-Patterson AFB, Ohio 45433				7b. ADDRESS (City, State and ZIP Code)			
8a. NAME OF FUNDING/SPONSORING ORGANIZATION		8b. OFFICE SYMBOL (If applicable)		9. PROCUREMENT INSTRUMENT IDENTIFICATION NUMBER			
8c. ADDRESS (City, State and ZIP Code)				10. SOURCE OF FUNDING NOS.			
				PROGRAM ELEMENT NO.		PROJECT NO.	
11. TITLE (Include Security Classification) See Box 19				WORK UNIT NO.			
12. PERSONAL AUTHOR(S) Roger S. Feldmann, B. E., 2Lt, USAF							
13a. TYPE OF REPORT MS Thesis		13b. TIME COVERED FROM _____ TO _____		14. DATE OF REPORT (Yr., Mo., Day) 1983 December		15. PAGE COUNT 319	
16. SUPPLEMENTARY NOTATION							
Approved for public release: LAW AFR 190-17, LYNN E. WOLAVER Dean for Research and Professional Development Air Force Institute of Technology (AFIT) 2 MAY 84							
17. COSATI CODES			18. SUBJECT TERMS (Continue on reverse if necessary and identify by block number) Flight Control, Digital Flight Control, Multivariable Control, Proportional Plus Integral Control				
FIELD	GROUP	SUB. GR.					
19. ABSTRACT (Continue on reverse if necessary and identify by block number) Title: Multivariable Digital Flight Control Design of the X-29A Thesis Chairman: Dr. John J. D'Azzo Deputy Department Head Electrical Engineering Department Air Force Institute of Technology							
20. DISTRIBUTION/AVAILABILITY OF ABSTRACT UNCLASSIFIED/UNLIMITED <input checked="" type="checkbox"/> SAME AS RPT. <input type="checkbox"/> DTIC USERS <input type="checkbox"/>				21. ABSTRACT SECURITY CLASSIFICATION UNCLASSIFIED			
22a. NAME OF RESPONSIBLE INDIVIDUAL Dr. John J. D'Azzo		22b. TELEPHONE NUMBER (Include Area Code) 513-255-3576		22c. OFFICE SYMBOL AFIT/ENG			

END

FILMED

6-84

DTIC

